



**Maynooth
University**
National University
of Ireland Maynooth

Biodistribution and Modes of Action of Multipotent Adult Progenitor Cell therapy in Murine Models of Transplant Rejection

Fiona Carty B. Sc.

A thesis submitted to

The National University of Ireland, Maynooth for the degree of

Doctor of Philosophy

in the Department of Biology, National University of Ireland Maynooth

Research Supervisor: Dr. Karen English

Industrial Partner: ReGenesys BVBA

Head of Department: Prof. Paul Moynagh

August 2017

Table of Contents

Table of Contents	i
Declaration of Authorship	viii
Abstract	ix
Publications	x
Abbreviations	xi
Acknowledgements	xvi
Chapter 1 Introduction	i
1.1 Transplant Rejection.....	2
1.1.1 The innate immune system in transplant rejection.....	3
1.1.2 Antigen Presentation	5
1.1.3 T cell differentiation.....	7
1.1.4 B cells in Transplantation.....	9
1.2 Therapeutic interventions to prevent allograft rejection and GvHD	10
1.2.1 Lymphodepletion.....	10
1.2.2 Homeostatic Expansion after lymphodepletion	11
1.2.3 Maintenance Immunosuppression.....	14
1.2.4 Problems associated with immunosuppressive regimens.....	15
1.3 Animal Models of Transplant Rejection.....	16
1.3.1 GvHD	16
1.3.2 Models of Homeostatic Proliferation	21
1.4 Adult Stromal Cells	24
1.4.1 Mesenchymal Stromal Cells.....	24
1.4.2 Multipotent Adult Progenitor Cells.....	25
1.5 Immunomodulation by MSC and MAPC [®] cells.....	28

1.5.1	Innate immunity	28
1.5.2	B cells	32
1.5.3	T cells	32
1.6	Mechanisms of MSC and MAPC cells immunomodulation	34
1.6.1	IFN- γ signalling in MSC and MAPC cells	34
1.6.2	PGE2 production by MSC and MAPC cells	38
1.7	Biodistribution of MSC and MAPC cells	40
1.7.1	Methods of tracking MSC and MAPC cells <i>in vivo</i>	40
1.7.2	Overcoming the lung barrier	42
1.7.3	MSC are short-lived <i>in vivo</i>	44
1.8	MSC & MAPC cells for Transplantation	46
1.8.1	MSC & MAPC cells for GvHD	46
1.9	MSC & MAPC cells for SOT Rejection	49
1.10	Aims and Objectives	51
	Chapter 2 Materials and Methods	53
2.1	Regulatory Issues	54
2.1.1	Ethical Approval and HPRA compliance	54
2.1.2	Compliance with GMO and Safety Guidelines	54
2.1.3	Animal Strains	54
2.2	MAPC Cell Culture	54
2.2.1	Thawing Procedure	55
2.2.2	Culturing Procedure	55
2.2.3	Cryopreservation Procedure	56
2.2.4	Generation of conditioned media	56
2.3	MSC Culture	56
2.3.1	Thawing Procedure	56
2.3.2	Culturing Procedure	57
2.3.3	Cryopreservation Procedure	57

2.3.4	Generation of conditioned media	57
2.4	HUVEC Cell Culture	57
2.4.1	Thawing Procedure.....	57
2.4.2	Culturing Procedure	58
2.4.3	Cryopreservation Procedure	58
2.4.4	Maintenance	58
2.5	PBMC cell culture	60
2.5.1	PBMC Isolation.....	60
2.5.2	Cryopreservation	60
2.5.3	Thawing Procedure.....	60
2.6	Methods of cell characterization.....	61
2.6.1	Characterisation of MAPC cells morphology	61
2.6.2	Characterisation of surface markers expressed by MAPC cells and MSC. .	61
2.6.3	Tube formation assay	61
2.6.4	Differentiation assay.....	63
2.6.5	CFSE assay.....	64
2.7	<i>In vitro</i> assays:	65
2.7.1	Stimulation of MAPC cells and MSC with IFN- γ	65
2.7.2	Treatment of MAPC cells with PPAR δ agonist and antagonist.....	65
2.7.3	ATG <i>in vitro</i> assay:	65
2.8	<i>In vivo</i> models.....	66
2.8.1	Humanised model of acute graft versus host disease	66
2.8.2	Murine model of IL-7 driven homeostatic proliferation	66
2.8.3	Murine model of lymphopenia driven homeostatic proliferation	67
2.9	Western Blotting.....	71
2.9.1	Protein Extraction.....	71
2.9.2	SDS-Polyacrylamide Gel Electrophoresis.....	71
2.9.3	Immunoblotting.....	71
2.10	Flow Cytometry	72

2.10.1	Analysis of immunomodulatory protein expression by MAPC cells.....	72
2.10.2	Surface staining of murine cell populations.....	73
2.10.3	Intracellular transcription factor staining.....	73
2.10.4	Intracellular cytokine staining.....	76
2.10.5	Immunophenotyping study.....	76
2.11	Cryo-imaging.....	76
2.11.1	Qtracker [®] labelling of MAPC cells.....	76
2.11.2	Cryopreservation of Tissue.....	80
2.11.3	Sample Sectioning and imaging using CryoViz [™] Technology.....	80
2.11.4	Image Processing.....	81
2.11.5	Cell Quantification.....	81
2.11.6	Image Reconstruction.....	81
2.12	Histology.....	83
2.12.1	Tissue Processing.....	83
2.12.2	H&E Staining.....	83
2.12.3	Histological Scoring.....	83
2.13	Statistical Methods.....	84
Chapter 3 Biodistribution and Modes of Action of MAPC cells in a humanised model of aGvHD		86
3.1	Introduction.....	87
3.2	Characterisation of surface markers expressed by human MAPC cells.....	89
3.3	MAPC cells and MSC CM induces tube formation of HUVEC.....	90
3.4	MAPC cells differentiate into adipocytes and osteocytes.....	95
3.5	MAPC cells suppress T cell proliferation induced by CD3/CD28 activation beads in a dose-dependent manner.....	95
3.6	Human MAPC cells administered on day 7 but not day 0 significantly increase survival and reduce pathology in aGvHD mice.....	98

3.7	Human MAPC cells administered on day 7 decrease the pathology in target organs of aGvHD.	99
3.8	The number of MAPC cells detected in target organs following IV injection is higher in mice that have received PBMC than healthy controls.	105
3.9	IFN- γ stimulation improves the immunosuppressive capacity of MAPC cells <i>in vitro</i> ...	114
3.10	IFN- γ stimulated MAPC cells administered on day 0 prolong survival in aGvHD.	114
3.11	γ MAPC cells reduce the pathology of target organs in aGvHD.	116
3.12	The number of MAPC cells detected in aGvHD target organs is increased when cells were pre-stimulated with IFN- γ	121
3.13	PPAR δ agonism inhibits the efficacy of MAPC cells administered on day 7 to the aGvHD model.	124
3.15	PPAR δ agonism reduces the biodistribution of day 7 MAPC cells in aGvHD.	131
3.15	PPAR δ agonism inhibits the efficacy of IFN- γ stimulated MAPC cells administered on day 0 to the aGvHD model.	131
3.17	PPAR δ agonism reduces the biodistribution of γ MAPC cells administered on day 0 to aGvHD.	136
3.18	PPAR δ agonism inhibits IFN- γ induced STAT1 signalling.	136
3.19	PPAR δ agonism does not affect IFN- γ driven expression of IDO, PDL1 or ICAM1 by MAPC cells <i>in vitro</i>	137
3.20	PPAR δ modulates expression of COX-2 by MAPC cells.	142
3.21	Summary.	144
Chapter 4 MAPC cells suppress IL-7 driven stimulation of T cells <i>in vivo</i>.		146
4.1	Introduction.	147
4.2	Optimisation of IL-7 driven homeostatic proliferation <i>in vivo</i> model.	147
4.3	MAPC cells administered IV reduce proliferation and production of IFN- γ by T cells in response to IL-7 in the spleen but not the lymph nodes.	152
4.4	MAPC cells administered IP reduce proliferation and production of IFN- γ by T cells in response to IL-7 in the spleen and lymph nodes.	158

4.5	IL-7 and MAPC cells alter the frequency and number of the immune cell compartments in the spleen.	161
4.6	MAPC cells suppress the number and frequency of monocytes, eosinophils and granulocytes in the spleen.	162
4.7	IL-7 reduces the number and frequency of macrophages in the spleen, and MAPC cells suppress their expression of MHC class II.	166
4.8	IL-7 and MAPC cells have no effects on the number or frequency of DC in the spleen but the populations within the dendritic cell compartment are altered.	170
4.9	MAPC cells IP enhance the frequency and alter the phenotype of CD4 ⁺ CD25 ⁺ GITR ⁺ cells in the spleen.	173
4.10	MAPC cells enhance the number of B2 cells and alter the subsets within this population	174
4.11	MAPC cells IV enhance the number and frequency of B1a and plasma cells.	177
4.12	MAPC cells IV and MAPC cells IP exhibit differential biodistribution patterns.	178
4.13	Summary.	185
Chapter 5 MAPC cells suppress pro-inflammatory T cells following lymphodepletion		187
5.1	Introduction.	188
5.2	100 mg of ATG administered IP depletes the number of CD4 and CD8 T cells in the spleen and lymph nodes.	189
5.3	T cells in the spleen are depleted at day 4, while in the lymph nodes they're depleted at day 7.	191
5.4	T cells in the spleen and lymph nodes are undergoing proliferation on day 7 of the lymphodepletion model.	195
5.5	MAPC cells IP suppress T cell proliferation in the spleen but not in the lymph nodes ...	195
5.6	MAPC cells IP enhance the frequency of Treg in the lymph nodes following lymphodepletion.	198
5.7	MAPC cells suppress the frequency of CD8 ⁺ IFN- γ producing cells in the spleen and lymph nodes following lympho-depletion.	201

5.8	Suppression of IFN- γ production by CD8 ⁺ T cells by MAPC cells is dependent on PGE ₂	201
5.9	Summary.....	205
	Chapter 6 Discussion	207
	Chapter 7 Bibliography	259

Declaration of Authorship

I certify that the work presented herein is, to the best of my knowledge, original, resulting from research performed by me, except where acknowledged otherwise (Work carried out in Chapter 4 was done in collaboration with Dr. James Reading and the 3i team at Kings College London). This work has not been submitted in whole, or in part, for a degree at this or any other University.

Fiona Carty B. Sc

Date

Abstract

T cell homeostatic proliferation (HP) and Graft versus Host Disease (GvHD) are major barriers to the success of transplantation. Multipotent Adult Progenitor Cells (MAPC cells) have demonstrated promising safety and therapeutic profiles in experimental models and small clinical trials of transplantation and acute GvHD (aGvHD), however, the mechanisms by which MAPC cells mediate these effects is not entirely clear. Thus, the aim of this thesis was to develop our understanding of the modes of action and biodistribution of MAPC cells in *in vivo* models of GvHD and HP.

MAPC cells were capable of delaying aGvHD onset when delivered 7 days after peripheral blood mononuclear cell (PBMC) delivery. MAPC cells were not significantly effective when administered along with PBMC, however interferon (IFN)- γ licensing improved this, and increased the biodistribution of MAPC cells towards GvHD target organs. PPAR δ was identified as a key modulator of MAPC cell function, as activation of PPAR δ hampered the efficacy of MAPC cells in the aGvHD model, while antagonism of PPAR δ had the opposite effect. *In vitro* studies suggest that PPAR δ may impart an inhibitory effect on COX-2 expression in MAPC cells

In an IL-7 driven HP model MAPC cells suppressed T cell proliferation and function and modulated splenic myeloid and B cell populations, however their effects were dependent on the administrative route applied (intravenously (IV) or intraperitoneally (IP)). Whole animal biodistribution studies demonstrated that MAPC cells delivered IP persisted *in vivo* for longer than MAPC cells delivered IV, and accumulated in the omentum, while MAPC cells IV accumulated predominantly in the lung. In a lymphodepletion driven model of HP, MAPC cells delivered IP suppressed IFN- γ production by T cells and enhanced Treg. Importantly, MAPC cells mediated their suppressive effects on HP through production of PGE₂.

The data presented herein contributes to a broader understanding regarding the activity of MAPC cells during transplant rejection. These findings provide a platform for future studies regarding the use and optimisation of MAPC cells for transplant rejection.

Publications

Carty F and English K. The immune response to the allograft in: *Kidney Transplantation, Bioengineering and Regeneration*. Elsevier, 2017 pp:235-247

Carty F, Mahon BP and English K. The influence of macrophages on mesenchymal stromal cell therapy: Passive or aggressive agents? *Clinical and Experimental Immunology*. 2017 April; 188(1):1-11.

Cahill E*, Kennelly H*, **Carty F***, Mahon BP and English K. Hepatocyte Growth Factor Is Required for Mesenchymal Stromal Cell Protection Against Bleomycin-Induced Pulmonary Fibrosis. *Stem Cells Translational Medicine*. 2016(5):1307-1318. *Joint first authors

McClellan S, Healy ME, Collins C, Carberry S, O'Shaughnessy L, Dennehy R, Adams Á, Kennelly H, Corbett JM, **Carty F**, Cahill LA, Callaghan M, English K, Mahon BP, Doyle S, Shinoy M. Linocin and OmpW Are Involved in Attachment of the Cystic Fibrosis-Associated Pathogen *Burkholderia cepacia* Complex to Lung Epithelial Cells and Protect Mice against Infection. *Infection and Immunity*. 2016 April; 84(5):1424-37.

Reading JL, Vaes B, Hull C, Sabbah S, Hayday T, Wang NS, DiPiero A, Lehman NA, Taggart JM, **Carty F**, English K, Pinxteren J, Deans R, Ting AE, and Tree T. Suppression of IL-7-dependent effector T cell expansion by Multipotent Adult Progenitor Cells and PGE2. *Molecular Therapy*. 2015 November; 23(11):1783-93.

Cahill EF, Tobin LM, **Carty F**, Mahon BP and English K. Jagged-1 is required for the expansion of CD4⁺ CD25⁺ FoxP3⁺ regulatory T cells and tolerogenic dendritic cells by murine mesenchymal stromal cells. *Stem Cells Research and Therapy*. 2015 March; 11; 6(1):19.

Abbreviations

3D	Three dimensional
aGvHD	Acute Graft versus Host Disease
AT	Adipose tissue
ATG	Anti-thymocyte globulin
APC	Antigen presenting cells
BAFF	B-cell activating factor
BCL-2	B-cell lymphoma 2
BCR	B-cell receptor
BLI	Bioluminescence imaging
BM	Bone Marrow
Breg	Regulatory B cells
BSA	Bovine serum albumin
CD45.1	C57/B16-CD45.1
cDC	Conventional DC
CFSE	Carboxyfluorescein succinimidyl ester
cGvHD	Chronic Graft versus Host Disease
CM	Conditioned media
CNIs	Calcineurin inhibitors
COPD	Chronic obstructive pulmonary disease
COX-2	Cyclooxygenase 2
cRPMI	Complete Roswell Park Memorial Institute medium
CsA	Cyclosporine A
CTLA-4	Cytotoxic T-lymphocyte-associated protein 4
DAMPs	Danger associated molecular patterns
DC	Dendritic cells
DMEM	Dulbecco's Modified Eagle's Medium

DMSO	Dimethyl sulfoxide
DSA	Donor specific antibodies
DSS	Dextran sulfate sodium
EBAO	Ethidium bromide/acridine orange
EBM	Endothelial basal media
EDTA	Ethylenediaminetetraacetic acid
EGF	Epidermal growth factor
EGM	Endothelial growth media
FACs	Fluorescence-activated cell sorting
FasL	Fas ligand
FBS	Fetal bovine serum
FGF	Fibroblast growth factor
FN	Fibronectin
GI	Gastrointestinal
GITR	Glucocorticoid-induced TNFR family related gene
GM-CSF	Granulocyte macrophage-colony stimulating factor
GvHD	Graft versus Host Disease
GvL	Graft-versus-leukaemia
Gy	Gray
H&E	Haematoxylin and eosin Y
HGF	Hepatocyte growth factor
HI	Heat inactivated
HI-FBS	Heat inactivated Fetal bovine serum
HLA	Human leukocyte antigen
HP	Homeostatic proliferation
HPRA	Health Products Regulatory Authority
HSC	Hematopoietic stem cell
HSCT	Hematopoietic stem cell transplantation

HUVEC	Human umbilical vein endothelial cells
IBD	Inflammatory bowel disease
IBMX	3-isobutyl-1-methylxanthine
IBTS	Irish Blood Transfusion Service
ICAM1	Intercellular adhesion molecule 1
ICOS	Inducible T-cell Co-stimulator
IDO	Indoleamine 2,3-dioxygenase
IFN- γ	Interferon- γ
Ig	Immunoglobulin
IGF	Insulin-like growth factor
IL-	Interleukin-
IL-1RA	IL-1 receptor antagonist
Indo	Indomethacin
IP	Intraperitoneal
IRI	Ischemia reperfusion injury
ISCT	International Society of Cellular Therapies
ISDs	Immunosuppressive drugs
IV	Intravenous
KLRG1	Killer cell lectin-like receptor subfamily G member 1
LA-BSA	Linoleic acid- bovine serum albumin
L-glut	L-glutamine
LPS	Lipopolysaccharide
mAb	Monoclonal antibody
MAPC cells [®]	Multipotent Adult Progenitor Cells
MDSC	Myeloid derived suppressor cell
MFI	Mean fluorescence intensity
MHA	Minor histocompatibility antigen
MHC	Major histocompatibility complexes

MLR	Mixed lymphocyte reaction
MRI	Magnetic resonance imaging
MSC	Mesenchymal Stromal Cells
mTOR	Mammalian target of rapamycin
NF- κ B	Nuclear factor- κ B
NK cell	Natural killer cell
NKT cell	Natural killer T cell
NOD-SCID	Non-obese diabetic-severe combined immunodeficiency
NOS	Nitric oxide synthase
NSG	NOD-SCID IL-2 γ^{null} mice
OCT	Optimal cutting temperature compound
OVA	Ovalbumin
PAMPs	Pathogen associated molecular patterns
PBMC	Peripheral blood mononuclear cells
PBS	Phosphate-buffered saline
PD	Population doublings
pDC	Plasmacytoid DC
PDL	Programmed death ligand
PDGF	Platelet derived growth factor
PGE2	Prostaglandin E2
PHA	Phytohaemagglutinin
PMA	Phorbol-myristate-acetate
PPAR δ	Peroxisome proliferator-activated receptor δ
PRRs	Pattern recognition receptors
P/S	Penicillin-streptomycin
PVDF	Polyvinylidene fluoride
qPCR	Quantitative Polymerase Chain Reaction
RBC	Red blood cells

rh	Recombinant human
RIPA	Radioimmunoprecipitation assay
RPMI	Roswell Park Memorial Institute medium
shRNA	Short hairpin RNA
SOD	Superoxide dismutase
SOT	Solid Organ Transplantation
STAT	Signal transducer and activator of transcription
TAE	Tris-acetate-EDTA
TBS	Tris-buffered saline
TBST	Tris-buffered saline containing 0.1% Tween 20
TCR	T-cell receptor
TGF- β	Transforming growth factor β
TLR	Toll like receptor
TNF- α	Tumour necrosis factor- α
TNBS	Trinitrobenzene sulfonic acid
Treg	Regulatory T cells
TSG-6	TNF-inducible gene 6
UC	Umbilical Cord
VCAM1	vascular cell adhesion molecule 1
VEGF	vascular endothelial growth factor

Acknowledgements

First I'd like to express my thanks to my supervisor Dr. Karen English. Thank you for all of the motivation, support and advice over the past 4 years. It's been such a pleasure to work under your guidance and I doubt I would've pursued research if you hadn't encouraged me and given me so much of your time when I was an undergrad. I am sincerely grateful to have had the opportunity to work in your lab – Thank you.

I'd also like to thank our collaborators in ReGenesys and Athersys, as well as Dr. James Reading and Dr. Tim Tree in KCL. I've really enjoyed working with you all over the years, and your support and encouragement is greatly appreciated.

To all past and present members of the Cellular lab, thank you for everything. I've been extremely lucky to work with such great people. I've learnt so much from you all, and I wouldn't have gotten through without all those cups of tea or your help on harvest days. I'd also like to thank everyone in the Biology Dept. who helped me all the way through, particularly Gillian and Deirdre for keeping the BRU running smoothly and Noel and Nick for all of your help with the CryoViz.

To my wonderful PhD pals, Helen, Jen, Susan, Siobhan, Therese and Aine, you made the past few years so enjoyable. Thank you for all of the LOL's and for helping keep the imposter syndrome at bay!

To all of my friends especially Michelle, Rich and the LCC gals, thank you for always being there for me and understanding my occasional periods of radio silence! To my extended family and all of the Rigneys, your kindness and support has meant the world to me. I can't leave out my four-legged sisters, Bonnie, Holly, and Molly - thank you for always giving me a laugh.

Niall, I'm not sure you quite knew what you were getting yourself in for when you chose to move in with a final year PhD student! Thank you for keeping me hydrated this past year with copious amounts of tea (or beer!), and putting up with my bouts of insomnia. You have kept me

sane and laughing. You are the kindest person I know, thank you for your positivity and for always helping me celebrate the small stuff!

I'm incredibly fortunate to have such a supportive family who act as cheer leaders, life coaches and problem solvers. Bren, thanks for your love always, you may be over 5,000 miles away but your calls and texts are always a welcome distraction. To my parents Martin and Hilary, you are so encouraging. Thank you for always being there and believing in me. I'm very lucky to have such fantastic parents – Thank you!

Chapter 1

Introduction

1.1 Transplant Rejection

Since the first successful transplant over 50 years ago, the field of transplantation has grown exponentially. Solid organ transplantation (SOT) is now the treatment of choice for end stage kidney, liver, heart and lung disease with over 21,000 patients a year receiving transplants in the United States (McDonald-Hyman, Turka & Blazar, 2015). Similarly, allogeneic hematopoietic stem cell (HSC) transplantation (HSCT) has become a common therapy to restore the immune system in patients with immune deficiencies, or in those who have lost bone marrow (BM) function following myeloablative doses of radiation or chemotherapy (Jenq & van den Brink, 2010). HSCs give rise to a replacement immune system in these individuals, with innate immune cells typically recovering in the first month after transplantation, while reconstitution of the adaptive immune system may take up to two years (Chaudhry *et al.*, 2017). Engraftment of this new immune system allows patients to fight infection and future malignancies.

There has been significant progress made in both SOT and HSCT over the past century, however allo-immunity remains the greatest barrier to successful graft survival. Allo-recognition is a key facet of the immune system; it is the recognition of ‘non-self’ which allows the body to protect itself from invading pathogens while maintaining tolerance to ‘self’. In the case of SOT, the recipient recognizes donor tissue as foreign, while in HSCT the graft can generate an allo-response to the host. Rejection of the solid organ can be acute or chronic, and culminates with graft failure, and ultimately another transplant is required (McDonald-Hyman, Turka & Blazar, 2015).

Graft versus Host Disease (GvHD), which can also manifest as either acute or chronic is a common side effect of HSCT. It affects roughly 50% of allogeneic HSCT recipients and has fatality rates of 20%. Acute GvHD (aGvHD) appears in the first 100 days after HSCT and is characterised by a strong T cell response and systemic destruction of organs, particularly the gastrointestinal (GI) tract, skin, and liver. Chronic GvHD (cGvHD) on the other hand develops from day 100 post HSCT onwards and features involvement of B cells and antibody mediated tissue fibrosis. GvHD is a systemic disease, with symptoms such as fever, diarrhoea

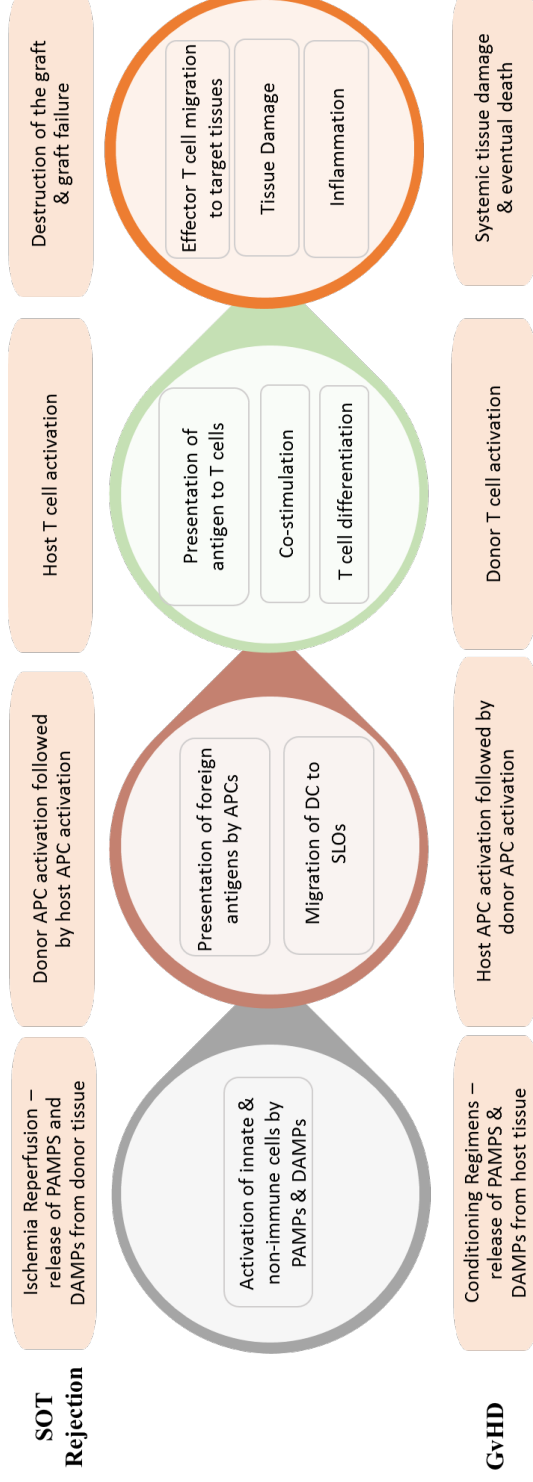
and tissue destruction ultimately leading to death in patients who don't respond to therapy (Mcdonald-Hyman, Turka & Blazar, 2015; Sung & Chao, 2013).

Allo-rejection in both solid organ graft rejection and GvHD share many of the same key steps (Fig. 1.1). The innate immune system is quickly activated in both cases in response to damaged tissue. The innate system then activates adaptive cells which carry out a targeted attack on foreign tissue through production of cytokines, contact mediated killing, or production of allo-antibodies (Wood & Goto, 2012). In both instances, regulatory cells produce tolerogenic signals which can suppress the immune response to the graft (Wood, Bushell & Hester, 2012).

1.1.1 The innate immune system in transplant rejection

The innate immune response in transplantation is initiated by the release of danger stimuli by damaged tissue. Ischemia reperfusion injury (IRI) is an unavoidable side effect of SOT which occurs when blood supply to tissue is interrupted, and the organ is subsequently exposed to hypoxic conditions. Reperfusion upon transplantation then triggers the release of free oxygen radicals causing further damage to the donor tissue (Cravedi & Heeger, 2014; Ponticelli, 2014). In contrast, in HSCT danger signals are host derived, produced by damaged tissue following harsh myeloablative therapies (Toubai *et al.*, 2016). In both cases, injuries initiate the release of danger associated molecular patterns (DAMPs) and pathogen associated complexes (PAMPS), which can activate the complement system and innate immune cells of both donor and host through pattern recognition receptors (PRRs). DAMPs in this context typically include necrotic cells, cellular debris, heat shock proteins, tissue factor and high mobility group box 1, while PAMPS are provided by bacterial components such as lipopolysaccharide (LPS) which passes from the GI tract following damage to the intestinal barrier by conditioning regimens (Eltzschig & Eckle, 2011; Zeiser, Socié & Blazar, 2016).

This stimulation of the innate system causes a cascade of pro-inflammatory cytokine and chemokine production, and recruitment of leukocytes to damaged tissue (Itoh *et al.*, 2010; Li *et al.*, 2010; Shen *et al.*, 2013). Neutrophils and monocytes are among the first populations to accumulate in damaged tissue, followed by natural killer (NK) cells which have been shown



➤ **Figure 1.1 Commonalities and differences in progression of SOT rejection and GvHD.** In both SOT rejection and GvHD PAMPs and DAMPs released by damaged tissue activate innate immune cells and non-immune cells. In SOT PAMPs and DAMPs are produced by the donor graft which has undergone ischemia reperfusion. In GvHD PAMPs and DAMPs are host derived, and are released by damaged tissue following condition regimens. Activated non-haematopoietic APCs upregulate MHC molecules, while DC process antigen and migrate to SLOs. In SOT rejection donor APC are activated before host APC, and this is reversed in GvHD. APC present foreign antigen to T cells and stimulate or inhibit T cell activity via co-stimulatory molecules. T cells then differentiate into various subsets depending on the cytokine milieu. This process is similar in both SOT rejection and GvHD. Activated T cells migrate to target tissue, produce pro-inflammatory cytokines, and mediate tissue destruction. In SOT rejection host T cells mediate destruction of the donor graft, whereas in GvHD donor T cells target host tissue particularly GvHD target organs. SOT: solid organ transplantation, GvHD: Graft versus Host Disease PAMPs: Pathogen associated molecular patterns DAMPs: Danger associated molecular patters, SLOs: Secondary lymphoid organs

to further contribute to tissue damage by mediating death of tubular epithelial cells (Zhang *et al.*, 2008). Furthermore, NK cells are major producers of interferon- γ (IFN- γ), which leads to priming of antigen presenting cells (APC) (Robb & Hill, 2012; Harmon *et al.*, 2016). Dendritic cells (DC) provide the bridge between the innate and adaptive response, and their activation by PAMPs, DAMPs and other innate immune cells stimulates their maturation and migration to T cell priming sites (Koyama *et al.*, 2015; Zeiser *et al.*, 2016).

1.1.2 Antigen Presentation

The first step in the adaptive immune response to the allograft is mediated by interactions between APC and T cells. Allogeneic tissue expresses foreign major histocompatibility complexes (MHC) which are the predominant targets of the recipient immune system. CD8⁺ and CD4⁺ T cells recognise either MHC I or MHC II respectively on the surface of APC through the direct, indirect, and semi-direct pathways (Jiang *et al.*, 2004; Safinia *et al.*, 2010). The direct pathway occurs when T cells recognise foreign MHC molecules on allogeneic DC, while the indirect pathway recognition occurs when DC process and present allogeneic MHC as peptides to syngeneic T cells (Afzali *et al.*, 2013; Archbold *et al.*, 2008a, 2008b; Lechler and Batchelor, 1982; Safinia *et al.*, 2010). The third and final pathway for allo-recognition is the ‘semi-direct’ pathway, which exploits the ability of immune cells to exchange surface molecules. In this case, MHC-peptide complexes are acquired by allogeneic DC via cell-cell contact, exosomes or nanotubes in a process referred to as ‘cross dressing’ (Denzer *et al.*, 2000; Montecalvo *et al.*, 2008; Robbins and Morelli, 2014). The now chimeric APC present intact allogeneic MHC complexes to T cells via the semi direct pathway, while simultaneously presenting allogeneic MHC as peptides via the indirect pathway (Afzali *et al.*, 2013; Marino *et al.*, 2016a; Safinia *et al.*, 2010).

GvHD presents an unusual and complex scenario whereby HSCT recipients are chimeric for both host and donor APC. Extrapolation of the exact process by which antigen presentation occurs is difficult due to disparities between experimental and clinical GvHD, and it is likely that differences in antigen presentation processes exist depending on the degree of MHC mismatch. In general, it is thought that host APC initiate GvHD by activating donor T

cells via the direct pathway (Shlomchik *et al.*, 1999). Donor DC then perpetuate the condition by processing and presenting host antigen to donor T cells via the indirect and semi-direct pathways (Socie & Blazar, 2009). It was originally assumed that professional APC were responsible for GvHD initiation. Surprisingly, non-haematopoietic APC such as fibroblasts and epithelial cells which are activated to express MHC and co-stimulatory molecules following conditioning regimens are now thought to be responsible for this effect (Koyama *et al.*, 2011; Koyama and Hill, 2017; Li *et al.*, 2012; Shlomchik *et al.*, 1999; Weber *et al.*, 2014). Moreover, recent studies have actually shown that depletion of host DC, particularly CD8⁺ conventional DC (cDC), exacerbates aGvHD (Toubai *et al.*, 2015; Weber *et al.*, 2014). With regards to donor APC, CD103⁺ cDC are thought to be the predominant drivers of GvHD progression. CD103⁺ cDC are initially activated by PAMPs and DAMPs, and then go on to present peptide indirectly to donor T cells primarily in the lymph nodes (Koyama *et al.*, 2015; Markey *et al.*, 2009). While donor DC have been shown to cross dress in GvHD, the semi-direct pathway does not induce proliferation of T cells. The expression of host MHC by donor DC does however instigate contact between the DC and T cell, which allows the TCR to bind to syngeneic MHC. Thus, cross dressed DC promote T cell activation through the indirect pathway (Markey *et al.*, 2014).

In SOT it has been demonstrated that all three pathways of allo-recognition play a role in T cell activation. Initially upon transplantation, donor APC activate recipient T cells through the direct pathway. This pathway eventually subsides however, due to the limited number of donor leukocytes within the graft (Boardman *et al.*, 2016). Thus, long term allo-reactivity requires the other pathways of recognition. The indirect and semi-direct pathways are responsible for T cell activation in models of skin, islet and cardiac transplantation (Harper *et al.*, 2015; Marino *et al.*, 2016b; Smyth *et al.*, 2017). Taken together, these studies suggest that recipient APC acquire intact MHC from donor derived vesicles to activate T cells through the semi-direct pathway. It is through this semi-direct method that CD8⁺ T cells are activated by donor MHC I. Furthermore, the indirect pathway is used to activate CD4⁺ T cells, which subsequently promote the activity of CD8⁺ cells. This suggests that a single DC can activate a CD8⁺ T cell through the semi-direct pathway, while at the same time activating a CD4⁺ T cell

through the indirect pathway, and so the CD8⁺ cell is in close proximity to the CD4⁺ cell from which it requires help. In the case of skin transplantation, suppression of host CD8⁺ cDC which are the main cross-presenters slows down graft rejection, which is comparable to the GvHD studies mentioned above (Smyth, Lechler & Lombardi, 2017).

1.1.3 T cell differentiation

Following interactions between MHC complexes and the T-cell receptor (TCR), naïve T cells require co-stimulation through accessory molecules. T cells exposed to allo-antigen in the absence of co-stimulation are only partially activated. This renders T cells anergic, or hypo responsive upon subsequent exposure to their cognate antigen (Anderson *et al.*, 2005; Wood, Bushell & Hester, 2012). Thus, inhibition of co-stimulatory pathways has been explored as a strategy to prevent allo-activity (Kinnear *et al.*, 2013). The outcome of interactions between APC and T cells depends on the activity of co-stimulatory molecules. For example, CD80/CD86 expressed by DC can stimulate naïve T cells via CD28 or cytotoxic T-lymphocyte-associated protein 4 (CTLA-4). CD28 ligation induces interleukin (IL)-2 production by T cells, promoting T cell proliferation, while CTLA-4 ligation on the other hand decreases IL-2 production and increases the inhibitory activity of Treg. Other stimulatory pathways include the Inducible T-cell Co-stimulator (ICOS) and OX40 pathways which stimulate T cell differentiation and survival, while the inhibitory programmed death ligand (PDL) pathway suppresses cytokine production and TCR signalling in activated T cells (Kinnear, Jones & Wood, 2013).

Next, T cells are differentiated into their various subsets depending on the cytokine environment in which antigen presentation occurs (Liu *et al.*, 2013). IFN- γ and tumour necrosis factor- α (TNF- α) producing type 1 CD4⁺ (Th1) and CD8⁺ (Tc1) cells are induced by NK and DC derived IFN- γ and IL-12 (Henden and Hill, 2015; Koyama *et al.*, 2015; Robb and Hill, 2012; Sad *et al.*, 1995). Both Th1 and Tc1 cells are key contributors to acute rejection and GvHD, and mediate tissue destruction directly via IFN- γ and perforin production, and the Fas/ Fas ligand (FasL) pathway (Burman *et al.*, 2007; Grazia *et al.*, 2010; Liu *et al.*, 2013; Sleater *et al.*, 2007; Wong *et al.*, 2016).

While Th1/Tc1 subsets are considered to be the drivers of allograft rejection, Th2 and Th17 cells have also been implicated. Th2 differentiation is promoted in the presence of IL-4, and Th2 cells produce IL-4 and IL-10. These cytokines can suppress Th1 activity which originally lead investigators to believe that Th2 cells may be protective in transplantation. However this is not the case, as depletion of Th2 cells prevents murine GvHD (Nikolic *et al.*, 2000). IL-6 and IL-23 production by APC induces Th17 differentiation, while the addition of IL-1 β results in the production of Th1/17 cells (Fábrega *et al.*, 2009, 2007; Koyama *et al.*, 2015). Th17 cells are present during acute rejection, however the role of Th17 in chronic rejection remains unclear (Liu *et al.*, 2013). Chronic allograft rejection which is associated with the indirect pathway of antigen presentation has been linked to donor specific Th1/17 cell populations producing IL-17 and IFN- γ (Sullivan, Adams & Burlingham, 2014).

Following differentiation, the vast majority of T cells become effector T cells which migrate to target tissues and attack allogeneic cells. Pre-existing effector and central memory T cells also threaten graft survival, as these cell types have lower activation thresholds than naïve T cells, are quicker to kill target cells, and promote the production of donor specific antibodies (DSA) by B cells (Benichou *et al.*, 2017). Allo-reactive effector and memory T cells can be generated prior to transplantation due to ‘antigen mimicry’ induced by commensal bacteria and infection, or previous exposure to allo-antigen due to a blood transfusion, pregnancy or previous transplant (Wong *et al.*, 2016). The vigorous response of memory T cells to the allograft is exacerbated by the fact that memory T cells are resistant to many immunosuppressive therapies, and have a competitive advantage over naïve cells during homeostatic proliferation (HP) (Benichou *et al.*, 2017). This is discussed in further detail later in this chapter.

In the context of allograft rejection, it is thought that the outcome of the immune reaction may depend on the ratio of allo-reactive T cells to regulatory T cells (Treg). Nguyen *et al.* (2014) have shown that the suppressive capacity of Treg in transplant recipients prior to transplantation correlates with the success of immediate graft function. Higher levels of CD45RO expression and reduced levels of CD27 expression on Treg cells are associated with better graft outcome, suggesting that the effector memory Treg subpopulation in particular

may contribute to the immunosuppressive micro-environment (Giaretta *et al.*, 2013). Treg mediate their protective effects in a number of ways; they express CTLA-4, acting as a negative regulator for T cell activation, and Treg derived indoleamine 2,3-dioxygenase (IDO) and IL-10 also dampens inflammation by inhibiting APC activity, suppressing T cell proliferation and promoting the conversion of conventional T cells to Treg type 1 cells (Wood, Bushell & Hester, 2012).

1.1.4 B cells in Transplantation

B cells are not the predominant mediator of allograft rejection, however they do contribute to the rejection process. B cells can capture allo-antigen via the B-cell receptor (BCR) and present this to T cells via the indirect pathway (Noorchashm *et al.*, 2006; Shiu *et al.*, 2015). Following presentation of allo-antigen to T cells, B cells produce high affinity allo-antibody (Taylor *et al.*, 2007) which can bind to foreign tissue, disrupting the function of graft endothelial cells and further enhance cellular uptake by APC (Chong & Sciammas, 2015; Wood, 2005). DSAs are produced by two types of memory B cells; the quiescent memory B cells and the long lived plasma cell. (Chong & Sciammas, 2015; Crespo *et al.*, 2001; Mauiyyedi *et al.*, 2001). Patients can develop allo-antibodies against MHC molecules, ABO blood group antigens, or foreign antigens expressed by endothelium. In those who have been sensitized by a previous transplant, blood transfusion or pregnancy, allo-antibodies can cause hyper-acute rejection immediately after graft reperfusion (Ahern *et al.*, 1982; Racusen & Haas, 2006; Trpkov *et al.*, 1996). In patients who haven't been sensitized, these antibodies can be produced from 6 months post transplantation and have been shown to contribute to chronic rejection and allograft failure in renal transplantation (Lionaki *et al.*, 2013).

B cell reconstitution is slow following HSCT, and both aGvHD and cGvHD are associated with B cell lymphopenia (Glauzy *et al.*, 2014). This phenomenon could be due to a number of factors including poor B-cell generation from the BM, T cell mediated death, or the use of immunosuppressants. The role of B cells in aGvHD is unclear and mostly based on observations from the clinic. Rituximab (a B-cell depleting antibody) has been shown to improve aGvHD outcomes in small clinical studies, while high levels of B cells in the stem

cell graft is linked to increased incidences of aGvHD (Shimabukuro-Vornhagen *et al.*, 2009). This suggests that B cells are pathogenic in aGvHD, however they may also play a protective role which is discussed in further detail below. The role of B cells in cGvHD is better characterised. High levels of B-cell activating factor (BAFF) are detected in cGvHD patients, and this is thought to cause the activation and proliferation of auto-reactive B cells. Similar to SOT, in cGvHD B cells can present antigen, produce allo-antibody and mediate tissue destruction (Sarantopoulos *et al.*, 2014).

In recent years exciting progress has been made in the identification and characterisation of IL-10 producing regulatory B cells (Breg). Breg are not restricted to just one subset, as a number of B cell subsets have been shown to have the capacity to produce IL-10. In both mice and humans IL-10 producers are commonly enriched within the CD5⁺ B1 subset, while in humans, immature B cells characterised by high expression levels of CD38 and CD24 are also consistently shown to demonstrate Breg function (Mauri and Menon, 2015; Rosser and Mauri, 2015; Saxena *et al.*, 2017). Breg have been shown to promote tolerance in a number of murine models of allograft rejection (Durand *et al.*, 2015; Durand & Chiffolleau, 2015). Similarly, total body irradiation induces IL-10 producing B cells which suppress donor CD4⁺ T cell proliferation in GvHD (Rowe *et al.*, 2006; Markey *et al.*, 2009), and patients with cGvHD demonstrate suppressed Breg function (Masson *et al.*, 2015).

1.2 Therapeutic interventions to prevent allograft rejection and GvHD

1.2.1 Lymphodepletion

In order to prevent rejection episodes in both SOT and HSCT, host T cells are depleted using induction therapy. This is usually administered along with other immunosuppressants or conditioning regimens prior to transplantation. The most commonly used induction therapies are the lymphocyte depleting antibodies anti-thymocyte globulin (ATG) and alemtuzumab (traded as Campath) (Zwang & Turka, 2014). Campath is an anti-CD52 monoclonal antibody (mAb), which depletes T cells, NK cells, B cells and monocytes, while ATG is an anti-CD3 antibody which predominantly targets T cells, but is also thought to affect B cells and DC (Lowenstein *et al.*, 2006; Ruzek *et al.*, 2009; Mohty, 2007). These therapies deplete their

target cells by inducing complement or antibody dependent cytotoxicity, and apoptosis (Valdez-Ortiz *et al.*, 2015). The effects of Campath varies between the different T cell subsets, with CD8⁺ cells being the least sensitive and CD4⁺ CD25⁺ cells being the most sensitive to depletion (Lowenstein *et al.*, 2006; Grimaldi *et al.*, 2016). On the other hand, ATG binds more efficiently to CD8⁺ T cells than CD4⁺ T cells resulting in more rapid depletion of the CD8⁺ T cell population (Ruzek *et al.*, 2009). Despite this difference, the CD4⁺ populations which remain following both Campath and ATG depletion are rich in regulatory and memory T cells with naïve T cells being preferentially depleted (Gallon *et al.*, 2006; Havari *et al.*, 2014; Noris *et al.*, 2007; Ruzek *et al.*, 2009; Xia *et al.*, 2012).

1.2.2 Homeostatic Expansion after lymphodepletion

In both humans and mice, the size and heterogeneity of the T cell pool is tightly regulated by homeostatic stimuli. Thymic production of new T cells diminishes with age, and so, survival of the peripheral T cell pool is critical to maintain immunocompetence (Plas, Rathmell & Thompson, 2002). Survival signals are delivered to T cells through contact with self-peptide loaded MHC complexes expressed by APC, and exposure to gamma chain cytokines, primarily IL-7. IL-7 is constitutively produced by stromal cells in lymphoid tissue, and upon binding to IL-7R α , signal transducer and activator of transcription (STAT)5 is activated leading to expression of the anti-apoptotic protein B-cell lymphoma (Bcl)-2. Thus, IL-7 promotes T cell survival, and T cells starved of IL-7 undergo apoptosis. Under normal lymphoreplete conditions, access to IL-7 is limited and competition for the cytokine is high (Tchao & Turka, 2012) (Fig. 1.2). Consumption of the cytokine is governed by expression of IL-7R, with naïve and central memory T cells expressing high levels of IL-7R, while effector and regulatory T cell subsets have lower IL-7R expression (Mazzucchelli & Durum, 2007).

Under lymphopenic conditions there are less T cells competing for and consuming IL-7. Thus, the availability of IL-7 increases and T cells which have escaped depletion undergo accelerated HP (Moxham *et al.*, 2008; Wu *et al.*, 2004). Furthermore, under these conditions, T cells acquire effector/memory functions and skew towards a Th1 phenotype

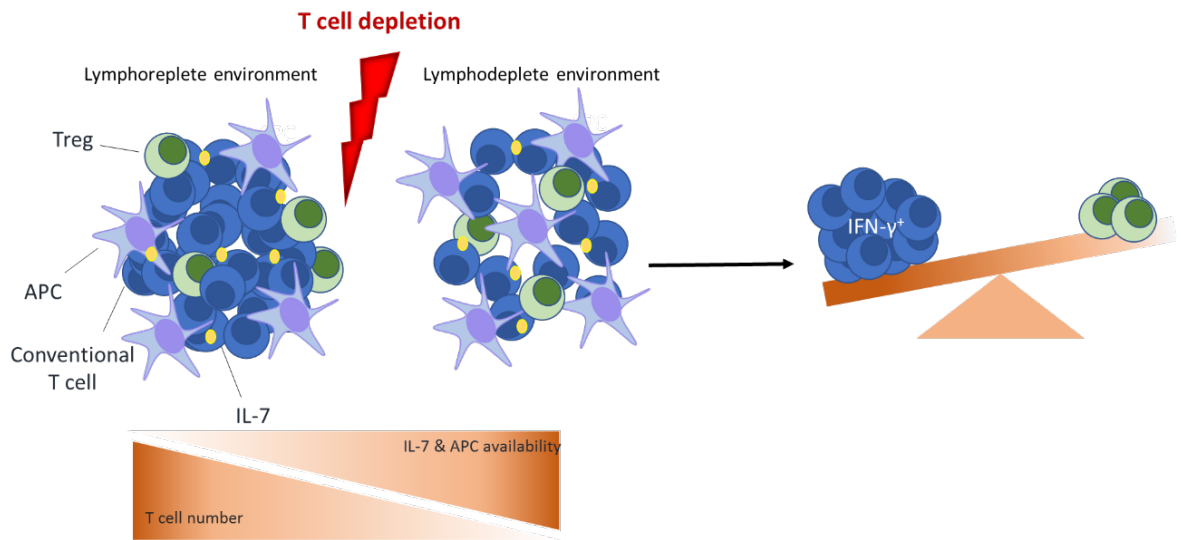


Figure 1.2 Homeostatic expansion of T cells following lymphodepletion. T cells require IL-7 and contact with self-MHC peptide expressed by APC in order to survive and proliferate. In the normal lymphoreplete environment T cell numbers are high, and availability of these stimuli is low. Following T cell depletion, T cell number is lower, and the availability of these stimuli is increased. The abundance of IL-7 causes the skew of the T cell department towards a pro-inflammatory IFN- γ producing population. MHC: Major histocompatibility complex, APC: Antigen presenting cells, IL-7: Interleukin-7, IFN- γ : Interferon- γ

(Neujahr *et al.*, 2006; Moxham *et al.*, 2008). With regards to Treg, the effects of lymphopenia are not as clear, and depends on the depletive strategy used. Treg numbers are increased following HP in immunodeficient, ATG or anti-CD25 treated hosts, while treatment with Campath or CD4⁺/CD8⁺ antibodies has the opposite effect (Ruzek *et al.*, 2009; Macedo *et al.*, 2012; Neujahr *et al.*, 2006; Moxham *et al.*, 2008; Vignali *et al.*, 2016). *In vitro*, IL-7 has been shown to abrogate Treg suppressive function, while memory Treg treated with IL-7 acquire a Th17 phenotype (Younas *et al.*, 2013; Heninger *et al.*, 2012). Overall, it is thought that HP in lymphopenic conditions promotes the expansion of a pro-inflammatory T cell pool which is likely to cause allograft rejection and autoimmunity (Neujahr *et al.*, 2006; Moxham *et al.*, 2008; Wu *et al.*, 2004; Grimaldi *et al.*, 2016) (Fig 1.2). For example, Wu *et al.* (2004) found that HP can render T cells resistant to co-stimulatory blockade, and secondary autoimmune disorders are commonly reported following lymphodepletion with Campath (Grimaldi *et al.*, 2016). Furthermore, blockade of the IL-7R has been shown to prevent GvHD and allograft rejection in murine models (Mai *et al.*, 2014; Chung, Dudl & Min, 2007).

As alluded to above, reconstitution of the T cell pool varies depending on the depletive strategy used. For example, the expansion of regulatory and memory T cells following ATG therapy is extensively reported (Boenisch *et al.*, 2012; Broady *et al.*, 2009; Feng *et al.*, 2008; Meyer *et al.*, 2015; Ruzek *et al.*, 2009; Valdez-Ortiz *et al.*, 2015; Xia *et al.*, 2012). Interestingly, the expansion of the Treg compartment following ATG mediated depletion is thought to be dependent on T cell/monocyte interactions (Boenisch *et al.*, 2012; Broady, Yu & Levings, 2009; Crepin *et al.*, 2015; Gurkan *et al.*, 2010). This expansion of Treg may not result in favourable graft outcomes however, as Crepin *et al.* (2015) have shown that ATG administration in renal transplantation results in an increase in late stage differentiated T cells which are linked to acute rejection. Following induction therapy with Campath, CD8⁺ T cells predominate and both CD4⁺ and CD8⁺ cells skew towards an effector profile. (Grimaldi *et al.*, 2016; Marco *et al.*, 2013; Macedo *et al.*, 2012). When Campath is added to conditioning regimens prior to HSCT, NK cells have been shown to dominate lymphocytes at early time points, with high levels of NK cells correlating with GvHD incidence (Matthews *et al.*, 2009).

Furthermore, Campath therapy is linked to impaired Treg reconstitution in renal transplant recipients (Macedo *et al.*, 2012).

1.2.3 Maintenance Immunosuppression

To prevent the acute rejection which may occur once HP replenishes the T cell pool, 'maintenance' immunosuppression regimens are employed. The earliest immunosuppressive drugs (ISDs) used in transplantation were corticosteroids, which are still the most commonly used therapy for GvHD (McDonald, 2016; Deeg, 2007; Flowers & Martin, 2015). Corticosteroids suppress systemic inflammation by inhibiting leukocyte migration, and suppressing DC maturation, and T cell proliferation (Franchimont, 2004). Mild GvHD of the skin can be treated with topical steroids, while in more severe cases systemic delivery is required (Ferrara *et al.*, 2009). Steroids successfully treat roughly 50% of GvHD patients, however severe cases tend to be refractory to corticosteroids. Prognosis rates are dismal (up to 85% mortality) (Westin *et al.*, 2011) for those with steroid refractory GvHD, and second line therapies are rarely successful (Jaglowski & Devine, 2014). Steroids have many adverse effects, and so to keep doses as low as possible they are often used in conjunction with other immunosuppressants, and their use is eventually tapered once they are no longer required (Martin *et al.*, 2015).

The discovery of calcineurin inhibitors (CNIs) in the 1980s revolutionised transplantation. Both cyclosporine A (CsA) and tacrolimus are CNIs, that mediate their action by binding to the cytoplasmic enzyme calcineurin (Azzi, Sayegh & Mallat, 2013). The main consequence of calcineurin inhibition is blockade of IL-2 signalling which potently suppresses T cell proliferation. Thus, CNIs are more selective suppressors of the immune system than steroids. This strategy of immunosuppression effectively inhibits inflammatory T cell activity, however, since Treg also require IL-2 to proliferate, their activity is also restricted (Gallon *et al.*, 2015; Miroux *et al.*, 2009, 2012). Nevertheless, CNIs are the most commonly used immunosuppressant for SOT, and are commonly used to prevent or treat GvHD (Azzi, Sayegh & Mallat, 2013; Ferrara *et al.*, 2009). Similar to steroids, CNIs can be highly toxic, thus their use needs to be minimized. Moreover, since both steroids and CNIs are 'blanket'

immunosuppressants, patients have a very poor immune response and are vulnerable to infection and malignancies (Fishman *et al.*, 2013; Chapman, Webster & Wong, 2013; Ferrara *et al.*, 2009). There is an unmet need for safe immunosuppressants for the treatment of both GvHD and SOT. In recent years mammalian target of rapamycin (mTOR) inhibitors have been added to immunosuppressive regimens. mTOR inhibitors block IL-2 production but not T cell activation, and are not as nephrotoxic as CNIs. Furthermore, they have an encouraging effect on Treg (Adams, Sanchez-Fueyo & Samuel, 2015; Shan *et al.*, 2015). Though safer than CNIs, mTOR inhibitors are not entirely safe, thus, efforts to develop novel strategies to induce tolerance are ongoing. Other strategies currently being investigated to prevent GvHD and allograft rejection are cellular therapies, neutralizing antibodies against IL-6 and TNF- α , and inhibitors of T cell co-stimulation, however these therapies require further investigation before becoming first line therapies (McDonald-Hyman, Turka & Blazar, 2015).

1.2.4 Problems associated with immunosuppressive regimens

As previously mentioned, rejection remains to be a major hurdle to the success of both SOT and HSCT. Despite major advances in the prophylactic and therapeutic strategies to prevent or cure allograft rejection or GvHD, these therapies often have unwanted secondary consequences. The first major concern regarding the use of lympho-ablative therapies and long-term immunosuppressants is the risks associated with immune-deficiency. Patients who receive ATG prior to HSCT or SOT have increased incidences of Epstein-Barr virus and cytomegalovirus (Kekre & Antin, 2017; van den Hoogen, Hoitsma & Hilbrands, 2012; Hardinger, Brennan & Klein, 2013), while opportunistic infections such as *Aspergillus* are commonly associated with blanket immunosuppressants (Azzi, Sayegh & Mallat, 2013; Hernandez, Martin & Simkins, 2015). To minimize infection, patients are commonly given preventative antimicrobial drugs, however infections do still occur and are a substantial cause of fatality among transplant recipients (Patel & Paya, 1997; Tomblyn *et al.*, 2009).

The development of malignancies in immunocompromised patients is also a major cause of death following transplantation, and SOT recipients have 2-3 times the risk of developing cancer compared to the general population. This may be due to increased

vulnerability to carcinogenic viral infections, or the reduced ability of immune cells to detect and destroy abnormal cells (Chapman, Webster & Wong, 2013). SOT is generally avoided in patients who have survived previous malignancies, however HSCT can sometimes be the only curative treatment for those with haematological cancers such as leukaemia or multiple myeloma (van den Brink, Alpdogan & Boyd, 2004). In these patients, clinicians must consider the graft-versus-leukaemia (GvL) effect before administering high doses of immunosuppressants. The GvL effect refers to the process by which donor T cells and NK cells eradicate tumours (Bleakley & Riddell, 2004). Though depletive and maintenance therapies are needed to prevent GvHD in HSCT recipients, unfortunately these therapies inhibit the GvL effect of donor cells, thus over-use of immunosuppression in HSCT can lead to disease relapse (Kekre & Antin, 2017).

Apart from their immunosuppressive effects, the long-term use of maintenance immunosuppressants also leads to debilitating side effects. Steroids can cause diabetes, muscle weakness and osteoporosis while CNIs have severely nephrotoxic effects (Ferrara *et al.*, 2009). These morbidities leave patients with a poor quality of life, and can lead to death through the development of secondary conditions. Transplant recipients and clinicians face an ongoing balancing act to achieve a 'sweet spot' of immunosuppression which prevents rejection, but limits infection and malignancies. Taken together, these unwanted consequences of long-term immunosuppressive therapies highlight the requirement for novel strategies to prevent graft rejection and GvHD.

1.3 Animal Models of Transplant Rejection

1.3.1 GvHD

Pre-clinical studies of disease most commonly employ mouse models, as mice are relatively easy and cheap to maintain, and the mouse genome is similar to that of humans. For GvHD studies the mouse is particularly suitable, as transgenic strains are readily available which can develop the usefulness of many models. Protocols used to generate GvHD *in vivo* vary, and experimental conditions determine the mechanisms and severity of disease progression. The

two most important conditions to consider are the conditioning regimen, and the degree of mismatch between donor and recipient.

In terms of conditioning regimens, most murine GvHD models begin with a total body irradiation step to mimic the damage caused by myeloablative conditioning and improve engraftment of donor cells. Generally, higher doses of irradiation correlate with increased donor cell engraftment and severity of disease (Parmar *et al.*, 2014). In recent years however, the relevance of this irradiation step has been questioned, as present day clinical regimens are more likely to involve chemotherapeutic drugs. Thus, some studies have used alternative conditioning regimens including administration of busulfan or cyclophosphamide (Sadeghi *et al.*, 2008; Ferrara, 2009; Riesner *et al.*, 2016). Furthermore, to develop less acute models of GvHD conditioning regimens can be avoided altogether (Reddy, Negrin & Hill, 2008; Chu & Gress, 2008).

Conditioning regimens are usually followed by the transfer of donor BM and splenic T cells to the recipient. The mouse strains chosen for this step determine the degree of mismatch between donor and recipient as outlined in table 1.1. Murine models of GvHD are most frequently established using an MHC mismatch. The simplest way to achieve an MHC mismatch is by transplanting donor cells from one strain to another with a disparate haplotype, for example from a C57/Bl6 (H2^b) to a Balb/C (H2^d) mouse. These fully MHC mismatched models are typically very acute, and are predominantly driven by interactions between host APC and donor CD4⁺ T cells, with CD8⁺ cells only playing a minor role in pathology (Reddy, Negrin & Hill, 2008). A second method of achieving a full mismatch is by cross breeding two strains, and transplanting cells from one of the parent strains into the off-spring (i.e. C57/Bl6 into C57/Bl6 X DBA2 F1). This approach is favoured in some cases as donor cells can engraft in the absence of conditioning regimens (Murphy, 2000). The effects of this type of mismatch can vary depending on the protocol used for experiment set up. For example, a high dose of irradiation followed by transfer of BM cells and splenic T cells from C57/Bl6 to a C57/Bl6 X DBA2 F1 causes CD4⁺ T cell driven aGvHD, whereas using the same two strains in reverse, but without irradiation or BM transfer leads to the development of cGvHD (Reddy, Negrin & Hill, 2008; Chu & Gress, 2008). The cGvHD model is also driven by CD4⁺ T cells, however

in this case disease progression resembles that of systemic lupus erythematosus, arising from the generation of auto-antibodies by B cells (Chu & Gress, 2008).

A second method of replicating GvHD *in vivo* is through the use of MHC matched, but minor histocompatibility antigen (MHA) mismatched models. In contrast to MHC mismatched models, these systems can require one or both of the CD4⁺ and CD8⁺ compartments depending on the combination of strains used. For example, when B10.D2 is used as a donor to the DBA/2 strain, aGvHD development is dependent on CD4⁺ cells, however when donor and recipient are reversed, CD8⁺ cells drive the disease (Reddy, Negrin & Hill, 2008). MHA mismatched models can also be used to develop cGvHD models, such as the B10.D2 to Balb/C model (Chu & Gress, 2008; Reddy, Negrin & Hill, 2008). MHA mismatched models are typically less severe than those with a full MHC mismatch and more closely resemble clinical GvHD (Riesner *et al.*, 2016).

Table 1.1 Commonly used murine GvHD models

Donor Strain	Donor Haplotype	Recipient Strain	Recipient Haplotype	Irradiation
Acute models				
C57/B16	b	Balb/C	d	Yes
Balb/C	d	C57/B16	b	Yes
C57/B16	b	C57/B16 X DBA2 F1	b/d	Yes
B.10D2	d	DBA2	d	Yes
DBA2	d	B.10D2	d	Yes
Chronic models				
C57/B16 X DBA2 F1	b/d	C57/B16	b	No
B.10D2	d	Balb/C	d	Yes
DBA2	d	C57/B16 X DBA2 F1	b/d	No
C57/B16	b	C57/B16 X Balb/C F1	b/d	No

In order to improve the translational relevance of animal models of GvHD, xenogeneic or humanised models have been developed. These models are particularly valuable for testing human specific therapeutics such as antibodies and cellular therapies, where the effects of the therapy in question is specific to human cells. Optimisation of humanised models of GvHD began 30 years ago, with the administration of human peripheral blood mononuclear cells (PBMC) to immunodeficient mice lacking B and T cells, however engraftment of human cells to these mice was very low, and so GvHD was rare (Hoffmann-Fezer *et al.*, 1993). Advances were made in the development of immunodeficient mice throughout the 90's, however it wasn't until Shultz *et al.* (2005) reported robust engraftment of human cells in a nonobese diabetic/severe combined immunodeficiency (NOD/SCID) IL-2R γ^{null} (NSG) strain that a suitable model could be developed. This strain required less PBMC to induce GvHD than its predecessors, and while conditioning regimens accelerated engraftment, GvHD was also observed in non-irradiated hosts (King *et al.*, 2009; Ito *et al.*, 2009; Parmar *et al.*, 2014). This model develops acute disease driven by CD4 $^{+}$ T cells, though CD8 $^{+}$ T cells do contribute once supported by CD4 $^{+}$ cells (Ito *et al.*, 2017), and recognition of both MHC I and MHC II host molecules by donor cells progresses disease, as knock out of either molecule delays disease onset (King *et al.*, 2009). Furthermore, TNF- α plays a role in disease progression in this system, highlighting a role for Th1 cells (King *et al.*, 2009). Humanised models of cGvHD are not as robust, and are still in development using fetal liver and thymus transplantation, CD34 $^{+}$ cells, or granulocyte macrophage-colony stimulating factor (GM-CSF) treated PBMC (Fujii *et al.*, 2015; Lockridge *et al.*, 2013; Sonntag *et al.*, 2015).

The humanised model of aGvHD is now commonly used by many groups, including the English lab, and previous members of our group worked to refine the model set out by Pearson *et al.* (2008) (Tobin *et al.* 2013, M. Healy, 2015, PhD Thesis). The model requires total body irradiation of NSG mice, and intravenous (IV) injection of PBMC isolated from buffy packs 4-6 hours later. Pearson *et al.* initially suggested that 2×10^7 PBMC per mouse should induce GvHD, however our group found that this lead to irreproducible results. Consistency of experiments was improved by administrating PBMC using weight based dosing, and 8×10^5 cells/gram was found to reliably cause aGvHD. Transient weight loss is

observed in the first few days after irradiation, presumably caused by stress or mild inflammation (M. Healy, 2015, PhD Thesis, J. Corbett, 2016, PhD Thesis). In general, all animals return to their original weight within 4 or 5 days, until weight loss and other symptoms of GvHD manifest between days 10-16 (Tobin *et al.* 2013 M. Healy, 2015, PhD Thesis, J. Corbett, 2016, PhD Thesis). This type of bi-phasic pattern of pathogenesis is consistent with other models of GvHD that use conditioning regimens (Sadeghi *et al.*, 2008). While the model is quite robust, it does have some weaknesses. Some PBMC donors induce aGvHD faster than others, and some PBMC donors have been demonstrated to be completely ineffective at inducing aGvHD for unknown reasons (M. Healy, 2015, PhD Thesis). Furthermore, NSG do not have functional DC, and human T cells cannot directly recognise murine MHC molecules. Thus, this aGvHD model is driven by donor APC presenting antigen to donor T cells (Ito *et al.*, 2017) which may not accurately represent the clinical scenario. Nevertheless, this humanised model is a very valuable tool to examine the efficacy of human specific therapies for GvHD.

1.3.2 Models of Homeostatic Proliferation

As described previously, excess IL-7 in the lymphopenic environment is an important stimulus for the HP of T cells after transplantation. The effects of the increased availability of IL-7 is usually studied in one of two ways; using transgenic mice with increased IL-7 signalling, or by delivering exogenous IL-7. A number of transgenic mice have been developed with increased IL-7R expression or over-production of IL-7. While these models have been useful to study the function of IL-7, they are not entirely relevant to study the role of IL-7 in transplantation. For example, IL-7R expression is tightly regulated, and expression is decreased following TCR engagement. Thus, constitutive expression of IL-7R is not representative of the situation in transplantation, and has been shown to lead to death of CD8⁺ cells (Kimura *et al.*, 2013). Similarly, in models where IL-7 is overproduced, thymocyte development is augmented, and lymphoproliferative disorders and autoimmune disorders develop (Mertsching, Burdet & Ceredig, 1995). Again, this is not translationally relevant, as IL-7 signalling is usually normal in transplant recipients up until the point of lymphodepletion. Ideally, a murine model where

over expression of IL-7 can be induced at an appropriate time point could be used to examine the effects of a sudden increase in IL-7 levels, however this type of model has not yet been developed.

The first reports of administration of exogenous IL-7 to murine models was reported by Morrissey *et al.* (1991a, 1991b), who found that twice daily injections of recombinant IL-7 transiently increased the frequency of CD4⁺ and CD8⁺ T cells in the spleen and lymph nodes of immunocompetent mice, and accelerated T cell reconstitution in lymphopenic hosts. Interestingly, IL-7 had more potent effects on the CD8⁺ compartment than the CD4⁺ compartment in the immunocompetent model. In a similar model of IL-7 induced proliferation, administration of human IL-7 increases the ratio of CD8⁺ to CD4⁺ cells in the spleen of immunocompetent mice, and splenocytes from IL-7 treated mice demonstrated enhanced proliferative responses to a range of stimuli *ex vivo*. Furthermore, the increase in T cell numbers following IL-7 administration is primarily due to peripheral T cell expansion rather than increased thymic emigration, as this expansion occurred even in the absence of the thymus (Komschlies *et al.*, 1994). While the models used in these studies demonstrate robust expansion of the T cell pool following IL-7 administration, they require frequent injections of high concentrations of IL-7 which is costly.

This issue was addressed by Boyman *et al.* (2008) who conjugated recombinant IL-7 to an anti-IL-7 antibody (M25) by incubating the two reagents together for 30 minutes prior to administration. Administration of the recombinant human (rh) IL-7/M25 complex three times at 2-day intervals was superior at promoting pre-B cell and T cell numbers in lymphoid tissues compared to rhIL-7 alone. Similarly, Lundstrom *et al.* (2013) demonstrated that injection of soluble IL-7R α increased the expansive effects of rhIL-7 on adoptively transferred T cells. It is thought that these molecules improve the potency of IL-7 by increasing the stability and half-life of the cytokine *in vivo* (Boyman *et al.*, 2008; Martin *et al.*, 2013). Upregulation of the activation marker CD44 by T cells following IL-7/M25 treatment suggests that this model resembles spontaneous HP that occurs in response to lymphopenia, while blockade of either IL-7R or TCR demonstrated that T cells are proliferating in this model in response to both IL-7 signalling and contact with self MHC-peptide complexes (Boyman *et al.*, 2008). Thus, this

method of administering three IL-7/M25 complexes on alternate days is a suitable method for mimicking lymphopenia induced proliferation *in vivo* without requiring extensive lymphodepletive regimens or immunocompromised mice (Simonetta *et al.*, 2012; Arbelaez *et al.*, 2015).

Of course, the administration of recombinant IL-7 does not accurately reflect HP in the lymphopenic environment which exists following induction therapy. Immunodeficient mice have been used for many years to examine the HP of adoptively transferred T cells in lymphopenic settings (Singh & Schwartz, 2006). In the clinic however, transplants are generally given to lymphoreplete individuals, and so lympho-depleting antibodies are commonly used to prevent graft rejection. These depletive therapies do not completely eliminate host immune cells, and residual non-depleted cells can undergo homeostatic expansion (Wu *et al.*, 2004) (Fig. 1.2). Thus, the homeostatic expansion of T cells in an immunocompetent mouse following treatment with T cell depleting antibodies is usually a more relevant method to study HP in the context of transplantation than the use of immunodeficient mice.

Laurence Turka's group were the first to show that T cells that escaped lympho-depletive therapies undergo HP *in vivo* (Wu *et al.*, 2004). While ATG is commonly used to deplete T cells in the clinic, the effects of lymphodepletion are not fully understood due to the difficulties associated with examining immune-reconstitution in human lymphoid tissues. Thus, murine models have generated much of what we know about the mechanism of action of ATG and HP following induction therapies. Murine models typically administer two doses of ATG intraperitoneally (IP), 3 days apart (Ruzek *et al.*, 2009; Xia *et al.*, 2012; Ayasoufi *et al.*, 2016). Proliferation of T cells is then usually measured using BrdU incorporation, adoptive transfers with proliferation dyes or by measuring expression of the nuclear antigen Ki67 (protein associated with cell proliferation).

1.4 Adult Stromal Cells

1.4.1 Mesenchymal Stromal Cells

Mesenchymal Stromal Cells (MSC) are a heterogeneous population of non-haematopoietic multipotent cells which can be isolated from the BM and other postnatal tissues such as adipose tissue (AT) and umbilical cord (UC) (Caplan, 2009). *In vitro*, MSC adhere to plastic and differentiate into osteocytes, adipocytes and chondrocytes (Dominici *et al.*, 2006). Thus, MSC first garnered interest due to their potential to differentiate into functional committed cells within injured tissue. For example, Horwitz *et al.* demonstrated that BM-MSC can engraft into bone and differentiate into functional osteoblasts, leading to clinical benefits in children with severe brittle bone disease (Horwitz *et al.*, 2002, 1999). Later it was found that although small numbers of MSC can engraft into damaged tissue, the therapeutic benefits observed following MSC administration in many disorders was probably due to the release of pro-reparative and anti-inflammatory soluble factors from the cells *in vivo* (Prockop & Olson, 2009). For instance, human BM-MSC produce TNF-inducible gene 6 (TSG-6) *in vivo* which contributes to improved infarct size and cardiac function in a murine model of acute myocardial infarction, while our group has shown using both murine and human BM-MSC that hepatocyte growth factor (HGF) production by MSC is required for their protective effect in murine models of pulmonary fibrosis and chronic obstructive pulmonary disease (COPD) (Cahill *et al.*, 2016; Kennelly, Mahon & English, 2016).

Later on it was discovered that many of the soluble factors produced by MSC are anti-inflammatory, thus in recent years there has been much interest into the use of these cells in a range of inflammatory disorders (English & Mahon, 2011). In seminal studies, Le Blanc *et al.* demonstrated that allogeneic human BM-MSC could suppress lymphocyte proliferation *in vitro*, and later successfully treated a child with steroid refractory GvHD using haploidentical MSC (Le Blanc *et al.*, 2004, 2003). These findings sparked hundreds of pre-clinical and clinical trials using MSC for the treatment of a range of inflammatory conditions including rheumatoid arthritis, Crohn's disease, and SOT (www.clinicaltrials.gov). Various formulations of 'off the shelf' MSC or MSC-like products have since been developed by corporations, with the first being Prochymal[®], developed by Osiris Therapeutics Inc. These

are referred to as ‘off-the-shelf’ as one MSC culture can be expanded in culture, cryo-preserved, and thawed and infused when required at the point of care. The expansive capacity and low immunogenicity of MSC allows for the production of thousands of doses from one donor, such that lot to lot variation is limited. In 2005, the FDA approved the use of Prochymal[®] for a subset of patients with aGvHD under the compassionate use program, while in 2012, Prochymal[®] was approved for aGvHD in Canada and New Zealand (Caplan, Mason & Reeve, 2017; Dodson & Levine, 2015). However, despite promising data from pre-clinical trials, Osiris has struggled to bring Prochymal[®], to the US market due to poor results in clinical trials for GvHD (Galipeau, 2013).

1.4.2 Multipotent Adult Progenitor Cells

Like MSC, Multipotent Adult Progenitor Cells (MAPC cells[®]) are also an adherent cell population isolated from the BM with regenerative and immunomodulatory capacities. Despite their similarities, MSC and MAPC cells are distinct populations which adopt disparate characteristics due to differences in their expansion protocols. MSC are typically cultured to 80-90% confluency in the absence of recombinant growth factors at 21% O₂, while MAPC cells are maintained at low density on fibronectin coated flasks in hypoxic conditions. Furthermore, the medium used to culture MAPC cells is supplemented with growth factors and dexamethasone. These different methods of cell culture lead to differences in the expansion capacities, cell surface phenotype and mRNA expression profiles between the two cell types (Vaes *et al.*, 2012). Compared to MSC, MAPC cells demonstrate an increase in expansion capacity before senescence, which is advantageous for clinical manufacturing of large cell banks. In terms of morphology and phenotype, MAPC cells are smaller than MSC, and express lower levels of HLA ABC on their surface. Moreover, MSC and MAPC cells exhibit unique mRNA and miRNA expression profiles, with MAPC cells generally expressing higher levels of genes involved in cell cycle and DNA repair, and MSC expressing higher levels of genes involved in tissue development and cell to cell signalling (Crabbe *et al.*, 2016; Reading *et al.*, 2013; Roobrouck *et al.*, 2011). In terms of immunomodulatory capacities, MAPC cells

demonstrate comparable inhibitory effects to MSC in *in vivo* T cell proliferation assays (Reading *et al.*, 2013; Jacobs *et al.*, 2013) (Table 1.2).

Like MSC, MAPC cells have been investigated for their therapeutic potential in a range of conditions including stroke, GvHD and inflammatory bowel disease (IBD). Both MSC and MAPC cells demonstrate similar therapeutic effects, *in vitro* and *in vivo* (Lehman *et al.*, 2012; Reading *et al.*, 2013). While few studies have directly compared the efficacy of MSC and MAPC cells from the same donors, it has been shown that compared to MSC, MAPC cells are superior at promoting angiogenesis and suppressing inflammation in stroke (Lehman *et al.*, 2012; Mora-Lee *et al.*, 2012; Roobrouck *et al.*, 2011). Similar to MSC, MAPC cells have also been developed into a clinical grade ‘off the shelf’ product (MultiStem[®]) by Athersys Inc., who have co-ordinated a number of trials to demonstrate the safety and efficacy of the product. A phase I trial demonstrated the safety profile of MultiStem[®] for GvHD prophylaxis and MultiStem[®] was granted Orphan Drug Status by the FDA for GvHD prevention (Maziarz *et al.*, 2015). A phase II trial found that ischemic stroke patients who received MultiStem[®] had improved recovery rates compared to placebo treated groups (Mays & Deans, 2016; Busch *et al.*, 2011; DePaul *et al.*, 2015; Walker *et al.*, 2012) , however a disappointing phase II trial reported poor efficacy of MultiStem[®] in patients with chronic, advanced ulcerative colitis (Athersys Inc., 2014). Thus, like MSC, promising pre-clinical studies using MAPC cells for various indications have not always been reproducible in the clinic. For both cell types, poor clinical efficacy could be attributed to many factors including timing of administration, variables in the potency of cells derived from different donors, and interactions between the cellular therapy and other drugs. Thus, in order to maximise the therapeutic potential of MSC and MAPC cells in the clinic, more knowledge is required on their modes of action *in vivo*.

Table 1.2 Similarities and differences between MSC and MAPC cells

Feature	MSC	MAPC cells	Reference
Adherence to plastic	Yes	Yes	(Dominici <i>et al.</i> , 2006)
Shape	Fibroblast-like	Smaller, spindle shape	(Roobrouck <i>et al.</i> , 2011)
Tri-lineage Differentiation	Yes	Yes	(Roobrouck <i>et al.</i> , 2011)
Proliferative capacity	20-25 population doublings	>70 population doublings	(Roobrouck <i>et al.</i> , 2011)
Immunosuppressive capacity	Yes	Yes	(Reading <i>et al.</i> , 2013)
Gene expression profile	Higher expression of genes involved in tissue development and cell to cell signalling	Higher expression of genes involved in cell cycle and DNA repair	(Roobrouck <i>et al.</i> 2011; Crabbe <i>et al.</i> 2016)
Pro-angiogenic	Yes	More-so than MSC	(Lehman <i>et al.</i> , 2012; Mora-Lee <i>et al.</i> , 2012)
HLA expression	ABC >90%	<25%	(Reading <i>et al.</i> , 2013)

1.5 Immunomodulation by MSC and MAPC cells

The use of MSC and MAPC cells in inflammatory conditions exploits the ability of these cells to influence the innate and adaptive immune response through both contact-dependent and independent mechanisms. MSC and MAPC cells respond to inflammatory cues by upregulating expression of immunomodulatory surface molecules such as PD ligand 1 (PDL1), and secreting anti-inflammatory mediators such as IDO and prostaglandin E2 (PGE2). The mechanisms by which MSC and MAPC cells modulate the immune response are complex, and differ depending on the surrounding environment (Bernardo & Fibbe, 2013; English, 2013). It is thought that MSC and MAPC cells predominantly mediate their anti-inflammatory effects through the release of soluble factors which act on both a local and systemic level (Choi *et al.*, 2011). The therapeutic soluble factors implicated in MSC and MAPC cell therapy are summarised in Table 1.3.

1.5.1 Innate immunity

The innate immune system is the first line of defence against foreign antigens, and triggers the inflammatory reaction in allograft rejection and GvHD. There is a substantial body of literature reporting the effects of MSC and MAPC cells on innate cells (Le Blanc & Davies, 2015), and it is likely that this contributes to the therapeutic effect of these cells *in vivo*. Accumulation of innate cells at sites of tissue damage is well characterised, and these cells are the first to contribute to transplant associated inflammation. MSC and MAPC cells may dampen the cytokine cascade associated with activation of the innate immune system via several mechanisms. For example, human BM-MSC suppress proliferation and IFN- γ production by NK cells via the production of IDO and PGE2 (Spaggiari *et al.*, 2008; Noone *et al.*, 2013; Aggarwal & Pittenger, 2005), while BM derived MAPC cells have been shown to suppress IL-2 driven proliferation, but not cytotoxic activity, of NK cells in an IDO dependent fashion (Jacobs *et al.*, 2014). MAPC cells don't express HLA ABC, while MSC expression of HLA ABC is low to intermediate.

Table 1.3 Soluble factors released by MSC and MAPC cells

Soluble Factor	Function	Cells affected	Reference
IDO	Depletes tryptophan which is required for immune cell activity	NK cells Macrophages T cells B cells	(Noone <i>et al.</i> , 2013; Meisel <i>et al.</i> , 2004; Peng <i>et al.</i> , 2014b; François <i>et al.</i> , 2012b)
PGE2	Can promote or dampen inflammatory cells – Usually anti-inflammatory when produced by MSC or MAPC cells	NK cells Macrophages T cells	(Noone <i>et al.</i> , 2013; Chiossone <i>et al.</i> , 2016; Reading <i>et al.</i> , 2015; English <i>et al.</i> , 2009)
TSG-6	Inhibits cytokine production & repairs damaged tissue	Macrophages	(Choi <i>et al.</i> , 2011)
IL-6	Can promote or inhibit inflammation – Usually anti-inflammatory when produced by MSC	Neutrophils DC	(Munir <i>et al.</i> , 2016; Djouad <i>et al.</i> , 2007)
VEGF	Promotes cell survival & angiogenesis	B cells	(Healy <i>et al.</i> , 2015)
Lactate	Reprograms metabolism	Macrophages	(Selleri <i>et al.</i> , 2016)
TGF- β	Resolves inflammation and promotes tissue repair	Macrophages T cells	(Noh <i>et al.</i> , 2016; English <i>et al.</i> , 2009)
IL-1 receptor antagonist (IL-1RA)	Competes with IL-1R to bind IL-1, sequestering IL-1 mediated activation of immune cells	Macrophages	(Luz-Crawford <i>et al.</i> , 2016a)

Since NK cells are known to target HLA ABC negative cells for lysis, it is possible that MSC and MAPC cells *in vivo* are killed in this manner. *In vitro* studies show that MSC and MAPC cells can be lysed by activated, but not resting NK cells. IFN- γ stimulated MSC and MAPC cells upregulate HLA ABC expression, and activation with IFN- γ has been shown to protect both cell types from NK cell mediated lysis *in vitro* (Jacobs *et al.*, 2014; Noone *et al.*, 2013; Spaggiari *et al.*, 2006). Theoretically, inactivated MSC or MAPC cells would not encounter activated NK cells *in vivo*, as activated NK cells produce IFN- γ . Nevertheless, there may be a lag time between IFN- γ stimulation and HLA ABC expression, which may provide opportunity for NK cells to lyse MSC or MAPC cells. The crosstalk between NK cells and MSC or MAPC cells *in vivo* is not yet clear, and its elucidation may provide strategies by which MSC or MAPC cell persistence *in vivo* can be improved.

Despite being the most abundant fraction of the innate immune system, the effects of MSC and MAPC cells on granulocytes has not been well characterised. Human BM-MSC have been shown to inhibit adhesion of neutrophils to inflamed endothelial cells *in vitro* in an IL-6 dependent manner (Munir *et al.*, 2016), while human AT-MSC suppress the oxidative burst of activated neutrophils in a co-culture system (Jiang *et al.*, 2016). The English lab has also demonstrated that BM-MSC can inhibit IL-8 induced activation, expansion, function (elastase activity) and migration of human neutrophils *in vitro* (H. Kennelly, 2015, PhD thesis). Interestingly Jiang *et al.* demonstrated that human AT-MSC are capable of engulfing neutrophils *in vitro* in an intercellular adhesion molecule 1 (ICAM1) dependent manner. It is thought that this uptake by MSC prevents the release of tissue-destructive proteases from activated neutrophils, contributing to the regulatory effects of MSC. Furthermore, MSC were shown to produce superoxide dismutase (SOD) which is known to suppress neutrophil driven inflammation by preventing the expulsion of destructive proteases from dying cells. MSC were shown to prevent neutrophil death and subsequent protease release in a murine model of vasculitis, however knockdown of SOD destroyed this effect.

The effects of MSC and MAPC cells on the innate system is not exclusively inhibitory, as MSC and MAPC cells have been shown to promote regulatory macrophage and dendritic cell populations. For example, MSC derived PGE₂, IDO, lactate and TSG-6 promote

the shift of macrophages and monocytes into anti-inflammatory M2 like populations (Chiossone *et al.*, 2016; Choi *et al.*, 2011; François *et al.*, 2012a; Kim and Hematti, 2009; Maggini *et al.*, 2010; Melief *et al.*, 2013; Németh *et al.*, 2009; Selleri *et al.*, 2016) and *in vivo*, a number of studies have shown that IV administered MSC incite the skew of pulmonary macrophages towards M2 phenotypes. For example, human BM-MSCs promote regulatory monocytes/macrophages in the lung in a murine model of autoimmune uveitis (Ko *et al.*, 2016), while in an experimental colitis model, murine BM-MSCs promote transforming growth factor (TGF)- β production by pulmonary macrophages (Liu *et al.*, 2015). Similarly, following IP injection, murine BM-MSCs form aggregates with macrophages, B cells and T cells in the peritoneal cavity, and mRNA levels suggest that M2 macrophages are present within these aggregates (Sala *et al.*, 2015).

Similarly, MSCs have been shown to inhibit DC migration and maturation while simultaneously promoting tolerogenic DC (Cahill *et al.*, 2015; Chiesa *et al.*, 2011; English *et al.*, 2008; Spaggiari *et al.*, 2009; Zhang *et al.*, 2009). For example, Chiesa *et al.* (2011), demonstrated that murine BM-MSCs inhibited DC maturation, which impeded their ability to activate both CD4⁺ and CD8⁺ T cells. Furthermore, this study went on to show that IV administration of MSCs impairs migration of DC to lymph nodes, and thus, priming of antigen specific T cells. Likewise, BM-MSCs blocked CD11c⁺ DC maturation in a murine model of kidney transplantation, and splenic DC harvested from MSC treated transplant recipients had a lower stimulatory effect on allogeneic CD4⁺ T cells than untreated transplant recipients in an *ex vivo* mixed lymphocyte reaction (MLR) (Ge *et al.*, 2010). On the other hand, MSCs can promote regulatory populations of DC. For example, DCs cultured with human BM-MSCs induce T cell anergy and generate Treg *in vitro* (Zhao *et al.*, 2012), while our group have shown that murine BM-MSCs promote tolerogenic DC which can induce Treg in a co-culture system (Cahill *et al.*, 2015). The effects of MSCs on DC have been attributed to the production of IL-6 by MSCs (Djouad *et al.*, 2007), and Notch signalling (Cahill *et al.*, 2015; Li *et al.*, 2008).

1.5.2 B cells

The influence of MSC on B cells has generated much confusion in the field. While Corcione *et al.* (2006) have shown that human BM-MSCs suppress proliferation of purified peripheral B cells, Healy *et al.* (2015) have since reported the contrary, showing that human BM-MSCs derived vascular endothelial growth factor (VEGF) promotes survival and expansion of peripheral B cells in a contact dependent manner. Similarly, Franquesa *et al.* (2015) have shown that human AT-MSCs promote the survival of tonsil derived B cells, however they do not increase their proliferation, whereas Rosado *et al.* (2014) found that human BM-MSCs promoted proliferation of CpG stimulated peripheral B cells. Discrepancies in findings between different groups may be due to the source of MSC, source and purity of B cell populations and agents used to induce proliferation. Interestingly, despite both Franquesa *et al.* (2015) and Rosado *et al.* (2014) finding differences in the effects of MSC on purified B cells, both found that in a mixed culture of B cells and T cells, B cell proliferation was reduced by MSC.

As mentioned previously in this chapter, IL-10 producing Breg demonstrate tolerogenic roles *in vivo*. *In vitro* BM-MSCs have been shown to promote IL-10 producing CD38⁺, CD24⁺ B cells (Franquesa *et al.*, 2015), and an increase in peripheral CD5⁺ IL-10⁺ cells has been reported in human GvHD patients following MSC infusions (Peng *et al.*, 2014b). Similarly, IP delivered UC-MSCs increased the frequency of CD5⁺ B Cells in the spleen, lymph nodes and peritoneal cavity in an experimental model of colitis (Chao *et al.*, 2016). The exact mechanisms by which MSC mediate this effect remains unclear, however a partial role for IDO has been implicated (Peng *et al.*, 2014).

1.5.3 T cells

Perhaps the most appreciated feature of MSC immunomodulation to date is their ability to preferentially suppress proliferation and activation of pro-inflammatory T cells, while simultaneously promoting anti-inflammatory Treg (Ghannam *et al.*, 2010; Luz-Crawford *et al.*, 2013; Reading *et al.*, 2013). MSC and MAPC cells can indirectly modulate T cell populations through the suppression of APC and induction of tolerogenic populations described above,

however it is clear that T cells can also be modulated in a direct fashion. It is generally accepted that MAPC cells and MSC suppress proliferation of Th1 cells via the secretion of IDO (Chinnadurai *et al.*, 2015; Reading *et al.*, 2013). While the suppressive effects of MSC on Th1 cells are maintained in the absence of cell contact, MSC require contact to suppress Th17 cells, with a number of studies showing that MSC suppress IL-17 production by T cells in a PGE2 and PDL1 dependent fashion (Duffy *et al.* 2011; Ghannam *et al.* 2010; Luz-Crawford *et al.* 2012; Obermajer *et al.* 2014; Reading *et al.* 2015). MSC and MAPC cells demonstrate similar inhibitory effects on CD8⁺ T cells. Human BM-MSCs suppress cytotoxic activity via the production of soluble factors (Rasmusson *et al.*, 2003), while MAPC cells carry out this effect in a contact-dependent manner (Plessers *et al.*, 2016).

In contrast to blanket immune-suppressants such as CsA, MSC do not completely abrogate the proliferation of all T cells, but rather modulate the population towards a regulatory phenotype (Ghannam *et al.*, 2010). The exact mechanisms employed by MSC to expand Treg are not fully understood (Najar *et al.*, 2016). According to Luz-Crawford *et al.* murine BM-MSCs can directly induce an IL-10 producing CD4⁺ CD25⁺ FoxP3⁺ population during the differentiation of CD4⁺ cells into Th1 and Th17 populations *in vitro* (Luz-Crawford *et al.*, 2013). On the other hand, Cahill *et al.*, found that murine BM-MSCs could expand, but not induce Treg under basal conditions (Cahill *et al.*, 2015). This expansion of the Treg population was dependent on MSC expression of Jagged 1. With regards to human MSC, co-culture of purified CD4⁺ cells with BM-MSCs results in increased expression of CD25 and FoxP3 in a cell contact dependent manner. Furthermore, PGE2 and TGF- β production by MSC are also required for this expansion of Treg (English *et al.*, 2009).

While *in vitro* studies have shown that MSC promote Treg through the production of paracrine factors, *in vivo*, the promotion of Treg by MSC requires an intermediate cell type. In a murine model of cardiac allo-transplantation MAPC cells induce Treg in a myeloid derived suppressor cell (MDSC) dependent fashion (Eggenhofer *et al.*, 2013). Furthermore, in a similar allograft model it has been shown that MSC stimulate MDSC to induce Th17 which are consequently converted to Treg (Obermajer *et al.*, 2014). Discrepancies between Treg data *in vitro* and *in vivo* emphasise the complexities of MSC and MAPC cell mediated

immunomodulation, and caution against over-interpretation of data derived from experimental models.

1.6 Mechanisms of MSC and MAPC cells immunomodulation

1.6.1 IFN- γ signalling in MSC and MAPC cells

Neither MSC or MAPC cells are constitutively immunosuppressive, and they both require activation by pro-inflammatory stimuli to adopt an anti-inflammatory phenotype (Bernardo & Fibbe, 2013; English, 2013). There is a cross-talk which exists between MSC and MAPC cells and the immune cells on which they mediate their effects, and the mediators they produce or express are dependent on the signals they are exposed to. For example, MAPC cells produce IDO in response to IFN- γ , or PGE2 in response to IL-1 β (Reading *et al.*, 2013, 2015), and so, the mechanisms by which MSC or MAPC cells mediate their immunomodulation can differ depending on the disease and cytokine milieu. The interplay between IFN- γ and MSC or MAPC cells is perhaps the most well characterised facet of MSC/MAPC cells mediated immunosuppression, and is translationally relevant across many disease systems.

In vivo, IFN- γ is produced by an array of immune cells including macrophages, NK cells, DC and T cells. Exposure of both human and mouse MSC to IFN- γ results in STAT1 induction and phosphorylation. In murine BM-MSC, STAT1 knockdown inhibits mRNA levels of PDL1, nitric oxide synthase (NOS)2 and IL-18bp, and reduces the immunosuppressive capacity of murine MSC in a T cell proliferation assay (Vigo *et al.*, 2016). In human UC-MSC, STAT1 knock down reduces IDO production, and STAT1 overexpression improves the suppressive capacity of MSC in a T cell proliferation assay (Mounayar *et al.*, 2015). IFN- γ stimulation of MSC induces IDO production, and cyclooxygenase (COX)-2, ICAM1 and PDL1 expression (Raghavan Chinnadurai *et al.*, 2014; Davies *et al.*, 2016; English *et al.*, 2007a; M. François, *et al.*, 2012a; 2012b; Hermankova *et al.*, 2016; Ren *et al.*, 2010). Furthermore IDO production and COX-2 mRNA expression in response to IFN- γ and TNF- α stimulation directly correlates to the suppressive capacity in a T cell proliferation assay (François *et al.*, 2012; Kota *et al.*, 2017). The importance of IFN- γ activation of MSC has been demonstrated in a number of *in vitro* and *in vivo* studies, where blockade of the IFN- γ

signalling axis destroys the immunosuppressive effect of MSC therapy (Krampera *et al.*, 2006; Meisel *et al.*, 2004; Polchert *et al.*, 2008; Ren *et al.*, 2008).

Since MSC require IFN- γ stimulation to mediate immunosuppression, many groups hypothesised that reduced efficacy of MSC in some disease systems may be due to low levels of IFN- γ at that time. For example, our group found that administration of human BM-MSC to a humanised GvHD model was therapeutic when MSC were delivered on day 7, but not day 0. Presumably the levels of IFN- γ *in vivo* at day 0 are very low, and since MSC are generally cleared within a few days of administration it is logical to assume that MSC weren't effective at this stage as there was no activation of the cells with IFN- γ . Thus, MSC were stimulated with IFN- γ prior to administration on day 0, and this significantly improved their efficacy (Tobin *et al.*, 2013). Similarly, Polchert *et al.* (2008) reported the same trend in a murine model of GvHD using murine BM-MSC, while Duijvestein *et al.* (2011) found that IFN- γ stimulated human BM-MSC were more effective at ameliorating colitis in both dextran sulfate sodium (DSS) and 2,4,6-trinitrobenzenesulfonic acid (TNBS) murine models.

It is clear that MSC and MAPC cells require IFN- γ responsiveness to achieve maximal therapeutic effects. Thus, it is important that we understand the molecular steps involved in the generation of the IFN- γ response by MSC and MAPC cells. In a recent study by Luz-Crawford *et al.* (2016b) peroxisome proliferator-activated receptor (PPAR) δ was found to inhibit the response of murine MSC to inflammatory cytokines. PPAR δ is a ligand-inducible transcription factor which can be activated by unsaturated fatty acids and eicosanoids such as linoleic acid, arachidonic acid and Prostaglandins A1, D2 and I2, (PGA1, PGD2, PGI2) (Forman, Chen & Evans, 1997; Schumann *et al.*, 2015; Ricciotti & Fitzgerald, 2011; Daynes & Jones, 2002). PPAR δ is expressed in many cell types, and in addition to its role in lipid metabolism and homeostasis, it is thought to play a role in immunoregulation through repression of nuclear factor (NF)- κ B and STAT1 (Daynes & Jones, 2002). The role of PPAR δ in immune regulation is still not entirely clear, however a number of studies have shown that PPAR δ activation can modify the macrophage phenotype.

Like MSC and MAPC cells, macrophages can alter their immunoregulatory profile depending on the cytokine milieu in which they differentiate. M1 macrophages are 'classically

activated' by Toll like receptor (TLR) ligands and IFN- γ , whereas M2 macrophages are 'alternatively activated' by IL-4 and IL-13 (Mills & O'Neill, 2016). M1 macrophages are considered to be pro-inflammatory, while M2 macrophages are a regulatory-like population associated with production of IL-10. Macrophages derived from PPAR δ ^{-/-} mice are unable to shift towards an M2 profile when stimulated with IL-4 or IL-13 (Odegaard *et al.*, 2008; Kang *et al.*, 2008). According to Kang *et al.* (2008), stimulation of macrophages with IL-4 and IL-13 activates PPAR δ via a STAT6 mechanism, while Odegaard *et al.* (2008) suggest that PPAR δ is activated by fatty acids which accumulate following stimulation. Furthermore, PPAR δ agonism hinders COX-2 induction in murine macrophages infected with *Leishmania mexicana* (Diaz-Gandarilla *et al.*, 2013). Similarly, in human monocyte derived macrophages PPAR δ agonism represses the expression of NF- κ B and STAT1 target genes such as IDO and PDL1, and PPAR δ agonist treated macrophages were superior at activating CD8⁺ T cells *in vitro* (Adhikary *et al.*, 2015) (Fig. 1.3).

The previously mentioned study by Luz-Crawford *et al.* demonstrated that PPAR δ is expressed by human BM, menstrual blood, and UC derived MSC. Menstrual blood derived cells expressed higher mRNA levels of PPAR δ than the other cell types, and higher PPAR δ expression inversely correlated with immunosuppressive efficacy in a T cell proliferation assay. Antagonism of PPAR δ in human BM-MSC improved their immunosuppressive ability in a T cell proliferation assay, while BM-MSC derived from PPAR δ ^{-/-} mice similarly demonstrated superior immunosuppressive capacities *in vitro* compared to their wild type counterparts. Moreover, PPAR δ ^{-/-} MSC showed improved therapeutic efficacy in a murine model of collagen induced arthritis, and higher expression of vascular cell adhesion molecule (VCAM)1, ICAM1 and nitric oxide in response to IFN- γ and TNF- α stimulation. The increased potency of MSC when PPAR δ was inhibited was attributed to increased NF- κ B activity (Luz-Crawford *et al.*, 2016b)(Fig 1.3). To date, this is the only study outlining the effects of PPAR δ signalling on the immunomodulatory profile of MSC or MAPC cells, thus further investigations should be

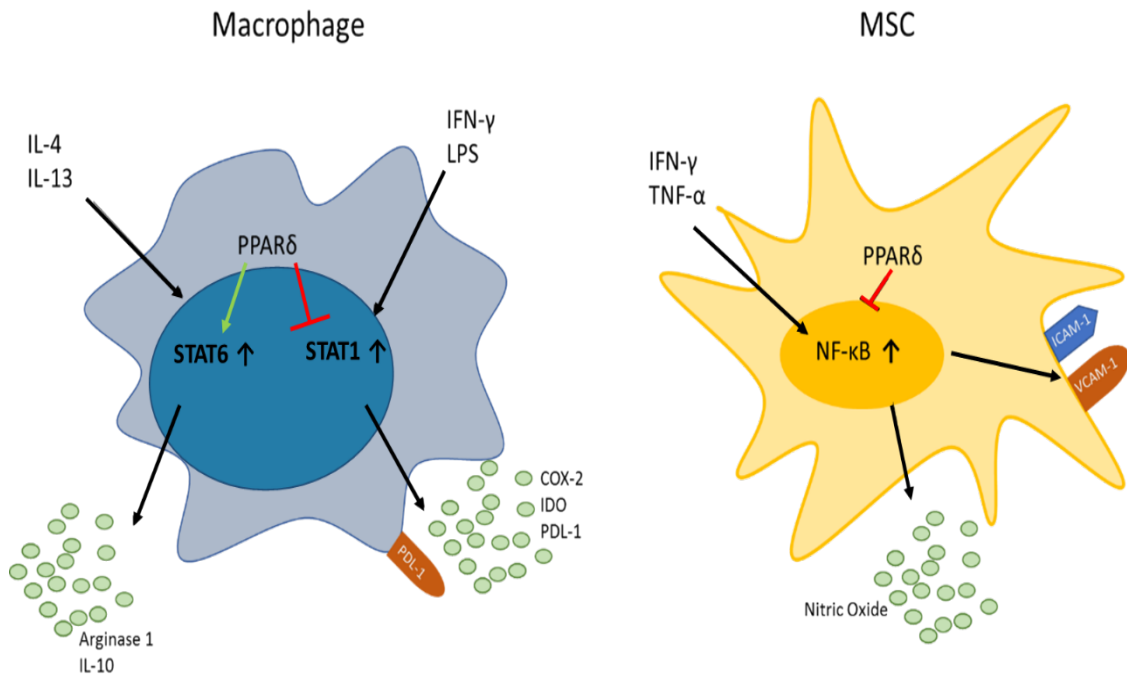


Figure 1.3 Role of PPAR δ in macrophage and MSC inflammatory pathways. In macrophages PPAR δ promotes differentiation towards the M2 phenotype following stimulation with IL-4 and IL-3. PPAR δ activation inhibits macrophages from differentiating into M1 populations following stimulation with IFN- γ and LPS. In MSC PPAR δ inhibits NF- κ B activation in response to IFN- γ and TNF- α stimulation, which negatively affects their expression of immunomodulatory factors (nitric oxide, ICAM1 and VCAM1). PPAR δ : Peroxisome proliferator -activated receptor δ , IL-4: interleukin-4, IL-3: interleukin-3, IFN- γ : interferon- γ , LPS: lipopolysaccharide, NF- κ B: Nuclear factor - κ B, TNF- α : Tumour necrosis factor- α , ICAM1: Intercellular adhesion molecule 1, VCAM1: vascular cell adhesion molecule 1

done to elucidate the effects PPAR δ ligands on MSC or MAPC cells such that their therapeutic effects are not abrogated in the clinic.

1.6.2 PGE2 production by MSC and MAPC cells

PGE2 is a lipid molecule which can be produced by many cell types, but particularly by immune cells following induction of the enzyme COX-2 by pro-inflammatory stimuli. COX-2 converts arachidonic acid, which is released from the membrane, to Prostaglandin G2 (PGG2), and then Prostaglandin H2 (PGH2). Next PGH2 is converted to PGE2 by microsomal PGE synthase 1, which like COX-2 is induced by pro-inflammatory cytokines. PGE2 binds to the PGE2 receptors EP1-4, and is a potent regulator of inflammation (Zhang *et al.*, 2015). In acute inflammation, PGE2 can be pro-inflammatory, as it contributes to vasodilation, which allows innate cells to migrate to sites of injury, and has been shown to promote the activation of Th17 cells. On the other hand, PGE2 contributes to the resolution of inflammation by hindering DC maturation and T cell proliferation. Moreover, PGE2 is involved in immunosuppression associated with liver cirrhosis and colon cancers (Nakanishi & Rosenberg, 2013).

PGE2 and COX-2 are constitutively expressed by both murine and human MSC, however their expression is further increased by stimulation with IFN- γ , IL-1 β or TNF- α (English *et al.*, 2007b; Aggarwal & Pittenger, 2005; Hermankova *et al.*, 2016; Rozenberg *et al.*, 2016; Bartosh *et al.*, 2013; Kota *et al.*, 2017; Vasandan *et al.*, 2016). Similarly, human BM-MAPC cells have been shown to increase PGE2 production following IL-1 β stimulation (Reading *et al.*, 2015). While PGE2 has both pro and anti-inflammatory effects, MSC and MAPC cells derived PGE2 is generally agreed to be anti-inflammatory and COX-2 mRNA levels in various human BM-MSC donors following IFN- γ or TNF- α stimulation correlates with their suppressive capacity *in vitro* (Kota *et al.*, 2017). However, paradoxical roles have been reported. For example, a number of studies have shown that MSC suppress IL-17 production by T cells in a contact and PGE2 dependent fashion (Duffy *et al.*, 2011; Ghannam *et al.*, 2010). In the absence of cell contact, murine AT-MSC enhance IL-17 production by CD3⁺ splenocytes, while human BM-MSC supernatants increase IL-17 production by T cells (Darlington *et al.*, 2010; Rozenberg *et al.*, 2016; Nataša Obermajer *et al.*, 2014). Interestingly,

there is a direct correlation between the amount of PGE2 in MSC supernatants and IL-17 production by T cells, and MSC supernatants from which PGE2 is removed fail to promote IL-17 production (Rozenberg *et al.*, 2016). Therefore, the contribution of cell contact may be vital in orchestrating the PGE2 mediated suppressive effects of MSC on Th17 cells.

Overall, the majority of studies suggest an anti-inflammatory role for MSC or MAPC cells derived PGE2. *In vitro*, suppression of T cell proliferation and activation by murine BM-MAPC cells, human BM-MAPC cells, and human BM-MSC requires PGE2 (Highfill *et al.*, 2009; Reading *et al.*, 2015; Auletta *et al.*, 2015). Furthermore, cell contact, PGE2 and TGF- β are involved in the induction of Treg by human BM-MSC (English *et al.*, 2009). With regards to the innate system, murine BM-MSC require PGE2 to promote IL-10 production by monocytes/macrophages (Németh *et al.*, 2009), while the capacity of human BM-MSC to skew the differentiation of macrophages towards an immunosuppressive population is lost in the presence of a COX-2 inhibitor (Chiossone *et al.*, 2016). Overexpression of COX-2 improved the immunosuppressive capacity of human UC-MSC in a co-culture with phytohaemagglutinin (PHA)-stimulated PBMC, while human BM-MSC treated with tetrandrine, an alkaloid which increases PGE2 secretion, are superior at suppressing TNF- α production by LPS stimulated macrophages (Li *et al.*, 2015; Yang *et al.*, 2016).

In vivo, murine BM-MAPC cells and human BM-MSC require PGE2 to prevent GvHD (Highfill *et al.*, 2009; Auletta *et al.*, 2015), while COX-2 short hairpin RNA (shRNA) knockdown in human BM-MSC abrogates their immunomodulatory capacity in a rodent model of traumatic brain injury (Kota *et al.*, 2017). In an *in vivo* MLR, murine BM-MAPC cells which had been pre-treated with the COX inhibitor indomethacin lost the ability to enhance expression of the inhibitory co-stimulatory regulators CTLA-4 and PD1, and suppress expression of the stimulatory molecules OX40 and 41BB on T cells (Highfill *et al.*, 2009). Furthermore, BM-MSC treated with tetrandrine to induce PGE2 production are superior at suppressing TNF- α levels in a murine ear inflammation model than untreated MSC (Yang *et al.*, 2016). Thus, the immunomodulatory capacities of MSC and MAPC cells in many conditions can be ascribed to the induction of COX-2 and subsequent production of PGE2. Therefore, it is important that the

mechanisms behind COX-2 induction, and PGE2 mediated immunomodulation is fully elucidated in order to fully exploit this aspect of MSC or MAPC cells biology in the clinic.

1.7 Biodistribution of MSC and MAPC cells

Despite many proof of concept studies displaying therapeutic efficacy of MSC in pre-clinical models of disease, the mechanisms by which MSC carry out this activity is not fully understood. The fate of MSC following administration *in vivo* is one example of this. There are two important considerations to make regarding the life of MSC *in vivo*; how long do the cells survive, and where do they go? Early studies suggested that MSC engraft, differentiate and replace damaged cells (Horwitz *et al.*, 2002). However, researchers now tend to agree that the majority of MSC are cleared quickly after administration, thus are left with a very short window of opportunity to achieve their immunosuppressive effects *in vivo*. Overall, it is thought that the effects of MSC and MAPC cells *in vivo* are due to a ‘hit and run’ mechanism whereby MSC and MAPC cells modulate the immune system quickly before being cleared. While this is clearly having a therapeutic effect in a range of disease models, many groups believe that prolonging the persistence of MSC *in vivo* would increase their efficacy (Ankrum, Ong & Karp, 2014). Moreover, while MSC and MAPC cells mediate many of their effects through soluble factors such as IDO and PGE2, they also mediate immunosuppression via contact dependent mechanisms, thus migration to the sites of inflammation would improve the capacity for MSC and MAPC cells to carry out these juxtacrine effects (Sohni & Verfaillie, 2013).

1.7.1 Methods of tracking MSC and MAPC cells *in vivo*

In vivo tracking of transplanted cells allows researchers to identify cells of interest, track their biodistribution, visualise their co-localization with other cell types, and eventually understand cell behaviour (Karp & Leng Teo, 2009). Quantitative Polymerase Chain Reaction (qPCR) and histological methods are the cheapest and simplest methods of tracking the fate of cells *in vivo*. In xenogeneic models MSC can be tracked by examining tissues for species specific genes, while in syngeneic or allogeneic MSC can be labelled fluorescently or transduced with reporter genes prior to administration, or sex-specific genes can be measured (Chapel *et al.*,

2003; Creane *et al.*, 2017; François *et al.*, 2014). For example, Horwitz *et al.* (2002) detected human transduced BM-MSC 4-6 weeks after administration to patients using PCR. Similarly, Le Blanc *et al.* (2004) detected the presence of donor MSC in the colon of a GvHD patient using FISH on tissue sections for detection of cells with XX chromosomes, as donor was female and recipient male. In a xenogeneic model, Auletta *et al.* (2015) identified human MSC by staining mouse tissue for the presence of human β -2-Microglobulin.

While PCR can detect the presence or absence of MSC in each tissue, the number of cells cannot be quantified, nor is it possible to tell whether the cells detected are live or dead (Creane *et al.*, 2017). Most studies using PCR to trace MSC report that MSC are present for months after administration, however according to Leibacher *et al.* (2017) human DNA is undetectable 24 hours after MSC administration, and fluorescently labelled MSC counter stained with Hoescht dye show no nuclear signal, demonstrating that most MSC are no longer intact after transplantation. Differences between studies may be due to the delivery routes, protocols used or sensitivity of the products used for mRNA detection. Similarly, quantification is difficult with histological techniques, as only a small number of sections from each tissue can be examined, and variation between sections can be high. Furthermore, the detection of donor specific genes *in vivo* using either PCR or histology may not always represent the presence of viable MSC. It has recently emerged that MSC can transfer mRNA and miRNAs to adjacent cells (Ng, Kunczewicz & Karp, 2015), for example, human BM-MSC can transfer insulin-like growth factor (IGF)-1R gene to murine tubular cells lacking this gene, and this can be detected *in vitro* using PCR (Tomasoni *et al.*, 2013). Thus, detection of MSC derived genes could theoretically be the detection of mRNA transferred to host cells.

Traditional *in vivo* imaging instruments such as magnetic resonance imaging (MRI) and bioluminescence imaging (BLI) have been used to detect radiolabelled or fluorescently transduced MSC and MAPC cells *in vivo* (Barbash *et al.*, 2003; Eggenhofer *et al.*, 2012; Jackson *et al.*, 2010; Wang *et al.*, 2015). These techniques are indispensable for live animal imaging, however they are restricted with regards to their field of view, depth of view, contrast, resolution, and quantification abilities. Furthermore, the viability of directly labelled cells is unclear, as Eggenhofer *et al.* (2012) detected radioactively labelled MSC in the liver at

24 hours post administration, however when these MSC were isolated they were shown to be dead. While fluorescence due to reporter genes should be more reliable as it requires viable cells, it is unclear at this point whether phagocytes could express these reporter genes acquired from MSC (Nguyen *et al.* 2014).

In the past number of years a number of studies have utilised CryoViz™ technology to detect fluorescently labelled MSC *in vivo* (Auletta *et al.*, 2015; Luk *et al.*, 2016; Schmuck *et al.*, 2016; DePaul *et al.*, 2015; Saat *et al.*, 2016). While imaging with this system cannot be carried out on live animals, the instrument meets many of the limitations which other systems are unable to accomplish. Cryo-imaging provides contrast rich, brightfield anatomical, and fluorescence cellular imaging of an entire mouse with micron-scale resolution (Roy *et al.*, 2009). The CryoViz™ consists of a motorized cryo-micro-tome with a brightfield/fluorescent microscope, and a robotic imaging system positioner, all of which are fully automated by a control system. An organ or whole mouse within a block of optimal cutting temperature compound (OCT) is sectioned and subsequently imaged, allowing the system to acquire three-dimensional (3D), high-resolution, large field of view, brightfield anatomy, and fluorescence image volumes from sequential images of the sample block. These features make the CryoViz™ an ideal tool for tracking the biodistribution of fluorescently labelled MAPC cells in inflammatory disease models. Studies using the CryoViz™ generally label transferred cells with Qtracker® beads which can only be detected when they are concentrated in the MSC. Thus, lysed or phagocytosed MSC do not have a fluorescent signal (Luk *et al.*, 2016).

1.7.2 Overcoming the lung barrier

The vast majority of *in vivo* studies administer MSC IV, as this is the most practical delivery route in the clinic. An inevitable consequence of systemic delivery however, is the entrapment of the cells in the lungs (Eggenhofer *et al.*, 2014; Fischer *et al.*, 2009; Lee *et al.*, 2014). The size of MSC and MAPC cells is a contributor to this entrapment, as MSC and MAPC cells are larger in diameter than capillaries, and MSC have also been shown to express adhesion molecules that attach to the lung endothelium (Kerkela *et al.*, 2013). IV infusion of human MSC to murine models can cause the formation of microemboli in pulmonary tissue (Lee *et*

al., 2009), and this damage can activate MSC to produce trophic factors such as TSG-6 (Lee *et al.*, 2014). While a number of studies have reported that MSC migrate towards damaged tissue *in vivo* (Sasaki *et al.* 2008; Jackson *et al.* 2010), most studies have reported that very few MSC escape the lungs (Eggenhofer *et al.*, 2012; Luk *et al.*, 2016; Schmuck *et al.*, 2016; Toupet *et al.*, 2015; Barbash *et al.*, 2003)(Table 1.4). Those MSC that do pass the lung barrier are found mainly in the liver, followed by the spleen and kidneys (Schmuck *et al.*, 2016; Saat *et al.*, 2016). In general, researchers tend to agree that the production of trophic factors by MSC in the lung, and their effects on local cells are responsible for their systemic immunomodulatory activity.

For example, in a rat model of type 2 diabetes, IV delivered UC-MSC alleviate insulin resistance and skew macrophages in the stromovascular fraction towards the M2 phenotype, despite no MSC being detected in the adipose tissue. MSC were however detected in the liver, and an increase in M2 macrophages was observed there (Xie *et al.*, 2016). Thus, polarization of leukocytes at sites of MSC distribution following IV delivery may amplify the systemic response to MSC. This is supported by a model of corneal allo-transplantation which showed that IV administered MSC were ineffective when lung monocytes and macrophages were depleted (Ko *et al.*, 2016). Similarly, in a murine model of ovalbumin (OVA) induced asthma, depletion of alveolar macrophages abrogated the therapeutic effects of IV delivered MSC. In this study, overall IL-10 protein levels were higher in the lung homogenates of MSC treated mice compared to untreated mice, or MSC treated mice in which alveolar macrophages were depleted. Therefore, this study suggests that MSC treatment increases IL-10 production by cell populations in the asthmatic lung (Mathias *et al.*, 2013).

Thus, it is likely that MSC and MAPC cells mediate their effects by causing the polarization of local immune cells towards regulatory populations, while simultaneously producing soluble factors which are dispersed systemically. This however can be problematic in some instances. For example, in a murine model of GvHD murine MAPC cells are ineffective when administered IV, but are efficacious when delivered intrasplenically. The mode of action of MAPC cells in this model is due to their production of PGE2 which has a

short half-life *in vivo*. Thus, in this case MAPC cells may need to be in close proximity to target cells in order for PGE2 to have its desired effect (Highfill *et al.*, 2009).

Since IV infusion is the most translationally relevant mode of delivery in the clinic, a number of groups have attempted to improve the efficacy of MSC by improving their capacity to cross the lung barrier. Kerkela *et al.* (2013) sub-cultured human UC-MSC and BM-MSC with pronase rather than trypsin, and found lower expression levels of fibronectin (FN) and the FN receptors on the cell surface. Furthermore, migration of rat BM-MSC to inflamed areas in a model of carrageenan-induced inflammation was superior when cells were detached using pronase rather than trypsin. Similarly, blockade of integrin expression by human placenta derived MSC improved lung clearance and migration to damaged tissue in a murine model of LPS induced ear inflammation (Wang *et al.* 2015). Thus, further clarification of the causes of lung entrapment may allow us to maximise the potential of MSC and MAPC cells by improving their biodistribution *in vivo*.

1.7.3 MSC are short-lived *in vivo*

MSC were originally thought to be immune privileged, able to escape rejection by the host immune system. However, it is now clear that allogeneic MSC are recognised by the host immune system, though not to the same extent as other cell types. Recognition of MSC and MAPC cells by the recipient, as well as the harsh conditions encountered *in vivo* are likely to contribute to the death and clearance of MSC and MAPC cells (Ankrum, Ong & Karp, 2014). Many studies have reported that MSC disappear within a few days of IV administration (Eggenhofer *et al.*, 2012; Karp & Leng Teo, 2009; Saat *et al.*, 2016), however others have reported detection of MSC weeks after transplantation (Wang *et al.*, 2015; Tolar *et al.*, 2011) (Table 1.4). Studies which have reported migration of IV administered MSC outside the lungs, or long-term persistence of MSC have been questioned of late, as research has looked into the viability of detected cells being examined. For example, Eggenhofer *et al.* (2012) detected radioactively labelled MSC in the liver at 24 hours post administration, however when these MSC were isolated they were shown to be dead. In this study, lung, liver, spleen, kidney and BM were examined for the presence of viable MSC, however viable cells were only detected

in the lung. Similarly, a recent study examining the biodistribution of human BM-MSc in naive mice has shown that MSC reduce in size and lose nuclear integrity shortly after injection. Furthermore, within 30 minutes of administration more than half of the detected MSC in the lung expressed calreticulin which is an inducer of phagocytosis (Leibacher *et al.*, 2017). Thus, detection methods used for analysis may be inaccurate, as it has been argued that fluorescent signals *in vivo* can sometimes represent debris or phagocytosed MSC, while we now know that MSC can transfer mRNA and miRNA to adjacent cells (Eggenhofer *et al.*, 2014; Ng, Kunczewicz & Karp, 2015).

Nevertheless, it is evident from the many pre-clinical studies that despite their short window of opportunity *in vivo*, MSC and MAPC cells manage to provide a long lasting therapeutic effect. It is likely that even after death MSC and MAPC cells can induce tolerogenic populations. This has been shown in a recent study by Luk *et al.* (2016) wherein heat inactivated AT-MSc (HI-MSc) are as potent as normal MSC in a murine model of sepsis. Interestingly, HI-MSc were not cleared as quickly as normal MSC in either healthy mice or mice with injured kidneys. There were twice as many HI-MSc as normal MSC detected at 2 hours post administration, and four times as many at 24 hours. Similarly, in the injured mice, at 2 hours post administration 90% of the heat inactivated cells administered were detected compared to only 25% of normal MSC. At 24 hours, the number of HI-MSc detected in injured mice was four times that of the normal MSC. It's unclear why there is such a shift in clearance rates, perhaps HI-MSc are slower to be recognised by the host immune system.

Furthermore, a number of recent studies have reported that dying or dead MSC can modulate macrophage populations. In a murine model of dust mite induced asthma, MSC were phagocytosed by some lung macrophages. The macrophages which phagocytosed MSC expressed higher mRNA levels of TGF- β and IL-10 and lower mRNA levels of IL-6 than macrophages that didn't phagocytose MSC (Braza *et al.*, 2016). Furthermore, Phinney *et al.* recently described a process by which MSC undergoing mitophagy secrete miRNA containing exosomes and transfer their mitochondria to macrophages. Uptake of MSC derived exosomes by macrophages also increases their expression of transcripts of cytokines associated with NF- κ B signalling such as IL-1 β , PGE2, TNF and IL-10. Production of these cytokines by

macrophages may prolong the effects MSC therapy long after MSC have been cleared (Phinney *et al.*, 2015).

Overall, the therapeutic efficacy of MSC and MAPC cells is probably hindered by their limited biodistribution and persistence *in vivo*. Culture conditions, timing of administration, and the health of MSC prior to delivery may impact their fate *in vivo*, and the optimal delivery method for one condition may not suit another. Thus, it is crucial that the biodistribution of MSC and MAPC cells is fully understood in order to optimise and tailor their administration to each condition.

1.8 MSC & MAPC cells for Transplantation

While traditional immunosuppressants have revolutionised transplantation and significantly improved the short-term success of the allograft, unwanted side effects lead to the development secondary conditions and fatalities. In the past decade, MSC and MAPC cells have shown great promise as facilitators of successful transplantation due to their immunomodulatory properties (English & Wood, 2013; McDonald-Hyman, Turka & Blazar, 2015; Griffin *et al.*, 2013). Unlike blanket immunosuppressants, MSC and MAPC cells simultaneously suppress pro-inflammatory immune cell activity without hindering the frequency or activity of regulatory populations, and demonstrate a positive safety profile (Auletta *et al.*, 2015; Eggenhofer *et al.*, 2014; Highfill *et al.*, 2009; Hoogduijn *et al.*, 2013; Popp *et al.*, 2011; Mudrabettu *et al.*, 2015). Thus, MSC and MAPC cells are being investigated as alternative strategies to prevent transplant rejection and GvHD.

1.8.1 MSC & MAPC cells for GvHD

The most common use of MSC to date has been for the treatment of steroid refractory GvHD. Both MSC and MAPC cells have been shown to suppress GvHD in murine models, with efficacy being linked to suppression of T cell proliferation, protection of damaged tissue and migration of MSC to GvHD target organs (Amarnath *et al.*, 2015; Auletta *et al.*, 2015; Highfill *et al.*, 2009; Kovacsovics-Bankowski *et al.*, 2008; Luz-Crawford *et al.*, 2016c; Tobin *et al.*, 2013). Both Highfill *et al.* (2010) and Auletta *et al.* (2015) found a role for PGE2 in MSC and

Table 1.4 MSC and MAPC cell biodistribution studies

MSC source	Recipient	Delivery Route	Detection Method	Persistence	Migration to damaged sites	Reference
Murine AT	Murine model of kidney IRI	IV	CryoViz™	99% disappeared at 24hrs	No but overall higher number in injured mice	(Luk <i>et al.</i> , 2016)
Human BM	Rat model of lung injury	IV	CryoViz™	<0.06% left by day 2	No but higher overall number in injured mice	(Schmuck <i>et al.</i> , 2016)
Murine BM	Murine ischemic liver injury	IV	Radiolabeling & ex vivo culture	Small number of live cells in lung only at 24hrs	No	(Eggenhofer <i>et al.</i> , 2012)
Human BM	Murine GvHD	IV	BLI with luciferase reporter	Still detectable at 52 days	Yes & higher retention in diseased mice	(Wang <i>et al.</i> , 2015)
Murine MAPC	Immunocompetent vs. immunodeficient mice	IV	BLI with luciferase reporter	day 4 in immunocompetent vs. day 30 in immunodeficient mice	ND	(Tolar <i>et al.</i> , 2011)
Human BM	Immunocompetent mouse	IV	FACs & PCR	Undetectable at 24hrs	ND	(Leibacher <i>et al.</i> , 2017)
Human BM	Irradiated mouse	IV	PCR	Detected up until 60 days	Yes	(François <i>et al.</i> , 2014)
Human MAPC	Rat model of Spinal cord injury	IV	CryoViz™	Small amount detected at 48hrs	Yes	(DePaul <i>et al.</i> , 2015)
Human UC	Murine liver injury model	IV	CryoViz™	50% or less detected at 4hrs	ND	(de Witte <i>et al.</i> , 2017)

All cells are MSC unless otherwise stated. MAPC cells are BM-derived in each case. ND = not determined

MAPC cell mediated suppression of murine GvHD, while Amarnath *et al.* (2015) implicated a role for MSC derived adenosine in a xenogeneic GvHD model. In a humanised model, IP injected menstrual blood derived MSC were more effective at prolonging survival than BM-MSC, and this increased efficacy correlated with an increased number of MSC reaching the spleen (Luz-Crawford *et al.*, 2016c). Similarly, Highfill *et al.* (2010) found that MAPC cells were only effective in a murine GvHD model when injected intrasplenically. Thus, contact with T cells at this site may be necessary for MSC and MAPC cells to mediate their effects, or the short half-life of MSC/MAPC cells derived factors may require MSC/MAPC cells to be in close contact with target cells for optimal efficacy.

Another important consideration to make is the timing of administration of MSC/MAPC cells. Neither murine or human MSC are effective at suppressing GvHD when administered on day 0 of murine or humanised models (Sudres *et al.*, 2006; Tobin *et al.*, 2013; Bruck *et al.*, 2013; Tisato *et al.*, 2007). Our group and others have shown that pre-stimulation of MSC with IFN- γ before administration rescues the therapeutic effect of MSC, thus, the lack of efficacy of MSC given at this time is probably due to a lack of pro-inflammatory stimuli *in vivo* (Tobin *et al.*, 2013; Polchert *et al.*, 2008). In support of this, Polchert *et al.* found that murine BM-MSC were ineffective at treating murine GvHD when donor splenocytes were incapable of producing IFN- γ . Interestingly, Tisato *et al.* (2007) also found that administration of UC-MSC to a humanised mouse model on day 0 had no therapeutic effect, but on the other hand MSC delivered once symptoms of GvHD had already presented were also ineffective. Thus, delivery of MSC must be after an inflammatory response has developed, but not too late when the response can't be inhibited.

In 2004 the first report of successful MSC therapy in a paediatric case of steroid refractory GvHD was published. In this case, two infusions of BM-MSC donated by the patients mother ameliorated GvHD (Le Blanc *et al.*, 2004). Next Ringden *et al.* (2006) treated eight patients with steroid refractory GvHD with allogeneic BM-MSC and reported that 6 of the patients had a complete response. Survival was significantly improved in this group compared to patients who did not receive MSC. Since these initial studies, a large number of human trials have proven the safety profile of MSC and MAPC cells for GvHD. The effects of

MSC in human GvHD are similar to those of the murine models. UC-MSC significantly reduce NK cells in cGvHD (Gao *et al.*, 2016), while Treg and Breg numbers have been shown to be increased (Gao *et al.*, 2016; Peng *et al.*, 2014b). The majority of academic-led trials show a response rate of 50-60% (Ball *et al.*, 2013; Kurtzberg *et al.*, 2014), however, in order to develop MSC or MAPC cells into a clinical product, a homogeneous ‘off the shelf’ product is required. Prochymal[®] has shown promise in phase II trials treating aGvHD, with 50-80% response rates depending on disease severity (Kurtzberg *et al.*, 2014; Kebriaei *et al.*, 2009). However, two larger placebo controlled studies treating either steroid refractory GvHD with MSC, or using MSC as a prophylactic therapy failed to meet their primary end points (Allison, 2009). A phase I aGvHD trial using MAPC cells reported a positive safety profile, and MultiStem[®] has been granted Orphan Drug Status by the FDA for the prophylaxis of GvHD (Bokkelen, 2011).

1.9 MSC & MAPC cells for SOT Rejection

Following the success of MSC in preclinical trials for GvHD, research progressed on MSC for the treatment of SOT. In animal models of transplantation, MSC inhibit lymphocyte infiltration and fibrosis in the graft, subsequently promoting long term graft survival (Eggenhofer *et al.*, 2011; Popp *et al.*, 2008; Sivanathan *et al.*, 2014). The efficacy of MSC in this setting is associated with the induction of regulatory cell populations (Casiraghi *et al.*, 2008; Eggenhofer *et al.*, 2013; Wei Ge *et al.*, 2010; Li *et al.*, 2010; Obermajer *et al.*, 2014a; Popp *et al.*, 2008). For example, in a murine model of allogeneic islet transplantation, locally delivered autologous BM-MSC create an immune-privileged site preventing graft rejection. In the spleen of transplanted animals, MSC reduce IFN- γ and IL-17 production by CD4⁺ T cells while simultaneously promoting Treg and IL-10 production (Ben Nasr *et al.*, 2015). Similarly, in a model of renal transplantation, the frequency of Treg in the spleen correlates with distribution of murine MSC to this site (Casiraghi *et al.*, 2012). In the clinic, allogeneic MAPC cells have been shown to enhance Treg numbers in the periphery of a patient who received a liver transplant (Soeder *et al.*, 2015), while in a small pilot study autologous MSC have been shown to increase Treg in the graft following renal transplantation compared to the

non-MSC treated group (Perico *et al.*, 2011). Furthermore, the combination of MSC and rapamycin promotes Treg frequency and graft survival in murine models of transplantation compared to either therapy alone (Cheng *et al.*, 2015; Ge *et al.*, 2009). The effects of MSC and MAPC cells are not restricted to Treg however; in a murine model of corneal allograft IV administered human BM-MSC promote regulatory IL-10 producing monocytes/macrophages in a TSG-6 dependent manner (Ko *et al.*, 2016), and two cardiac allograft studies show that the induction of Treg by murine AT-MSC and rat BM-MAPC cells is dependent on regulatory MDSC (Obermajer *et al.* 2014; Eggenhofer *et al.* 2013).

In the clinic it is thought that MSC may allow for a reduction in the use of toxic immunosuppressive drugs. A recent pilot study carried out by Pan *et al.* investigated the use of MSC in combination with low dose tacrolimus as a therapy for renal transplantation. In this study 16 patients were administered low dose tacrolimus along with MSC therapy, while a control group of 16 patients received a standard dose of tacrolimus alone. Interestingly, 2 years after transplantation there was no difference in renal function or graft survival between the 2 groups (Pan *et al.*, 2016). Similarly, a larger randomized controlled study showed that administration of autologous BM-MSC in combination with CNIs were more effective at preventing acute rejection in kidney allo-transplantation than IL-2 receptor blockade in combination with CNIs. Moreover, MSC showed similar efficacy when administered with standard or low dose CNIs (Tan *et al.*, 2012). In a phase I-II controlled trial however, one IV infusion of third party BM-MSC demonstrated no therapeutic benefit in liver transplant recipients. The goal of this trial was to wean MSC recipients off toxic immunosuppressants however this was unachievable (Detry *et al.*, 2017). Thus, the mechanisms of MSC and MAPC cells therapy require further elucidation before being introduced into the clinic. The timing of administration and the unknown interactions that MSC may have with immunosuppressive drugs are facets of MSC biology which are particularly relevant to the SOT field.

In terms of the effect of MSC/MAPC cells on HP, little is known. While it is well known that MSC and MAPC cells suppress T cell proliferation *in vivo*, this has not been examined in the context of induction therapies or HP. As mentioned previously, human

MAPC cells suppress IL-7 driven proliferation and cytokine production by T cells in a PGE2 dependent manner *in vitro* (Reading *et al.*, 2015). This however has not been examined *in vivo* to date.

1.10 Aims and Objectives

This chapter has outlined our current knowledge on the suitability of MSC and MAPC cells as therapies for the treatment of GvHD and transplant rejection. While preclinical studies have demonstrated the efficacy of MSC and MAPC cells in rodent models, in the clinic the performance of MSC has been underwhelming (Galipeau, 2013). Poor clinical efficacy demonstrates that more knowledge regarding the modes of action of these cell types is required in order to exploit their therapeutic effects. Thus, the aim of this thesis is to build on existing knowledge regarding the efficacy and modes of action of MAPC cells in pre-clinical models of transplantation, and to provide data which can be used to optimise their efficacy in the clinic.

The goals addressed herein can be divided into two strands; elucidating the modes of action used by MAPC cells *in vivo* to suppress inflammation, and identifying optimal protocols for the improved biodistribution and efficacy of MAPC cells in murine models of GvHD and HP.

These goals can be summarised as:

- (1) To optimise the biodistribution and efficacy of MAPC cells in a humanised model of aGvHD (Chapter 3)
- (2) To demonstrate the efficacy and define the optimal administrative route of MAPC cells in a murine model of IL-7 driven homeostatic proliferation (Chapter 4).
- (3) To demonstrate the efficacy and elucidate the mode of action of MAPC cells in a murine model of lymphopenia driven homeostatic proliferation (Chapter 5).

Overall, the aim of this thesis is to demonstrate the therapeutic efficacy of MAPC cells in murine models of transplantation, and improve our understanding of MAPC biodistribution and suppression of inflammation *in vivo*. The data presented herein will contribute to a

broader understanding of the *in vivo* fate and activity of MAPC cells which can be applied to future studies and the use of MAPC cells therapy in the clinic.

Chapter 2

Materials and Methods

2.1 Regulatory Issues

2.1.1 Ethical Approval and HPRA compliance

All procedures involving the use of animals or human materials were carried out by licensed personnel. Ethical approval for all work was granted by the ethics committee of Maynooth University. Animal experiments adhered to the project authorisations received from the Health Products Regulatory Authority (HPRA) (AE19124/p004) and (AE19124/p006).

2.1.2 Compliance with GMO and Safety Guidelines

All GMO/GMM work was performed according to approved standard operation procedures and recording protocols approved by the Environmental Protection Agency (Ireland). Safe working practices were employed throughout this study as documented in the Maynooth University Biology Department Safety manual.

2.1.3 Animal Strains

Experiments were performed using either NSG, CD45.1 or C57BL/6 mice aged between 6 and 24 weeks. All mice were housed according to the Dept. of Health (Ireland) guidelines and used with ethical approval under the terms of project authorization from the HPRA. Sample sizes for animal experiments were determined by statistical power calculation using SISA software found online at <http://home.clara.net/sisa/power.html>.

2.2 MAPC Cell Culture

Human MAPC cells used in this study were clinical grade MultiStem[®] cells isolated from the BM of healthy donors by enterprise partners in ReGenesys and Athersys Inc. BM aspirates were obtained with consent from healthy donors and cultured at low density, on plastic tissue culture flasks coated with 1X FN (Sigma-Aldrich, St. Louis, USA) in MAPC cell media (Table

2.1). MAPC cell cultures were maintained under low oxygen tension in a humidified atmosphere of 5% CO₂.

2.2.1 Thawing Procedure

Culture flasks were coated with 1X FN and incubated at 37°C/ 5%CO₂/ 20% O₂ for 30 minutes before 1X FN was removed. A vial of MAPC cells was removed from liquid nitrogen and placed in a water bath at 37°C to thaw. When the vial was almost completely thawed, the cell suspension was transferred to a 15 ml conical tube and topped up with fresh MAPC cell medium (Table 2.1) in a laminar flow cabinet. The cell suspension was centrifuged at 350 g for 5 minutes. Supernatant was discarded and the pellet was resuspended in 1 ml MAPC cell medium. Cells were stained with ethidium bromide/acridine orange (EBAO) (Sigma-Aldrich) and counted using a haemocytometer and fluorescent microscope. Cells were seeded at a density of 2000 MAPC cells/cm² in 1X FN coated culture flasks in MAPC cell medium and incubated at 37°C/5%CO₂/5% O₂.

2.2.2 Culturing Procedure

Cells were cultured every 2-3 days. To culture cells, medium was removed and cells were washed with phosphate buffered saline (PBS) (Sigma-Aldrich). 0.05% Trypsin-ethylenediaminetetraacetic acid (EDTA) (Sigma-Aldrich) was added to each flask (2 ml for T75, 5 ml for T175). Flasks were incubated for 2-5 minutes in a 37°C/ 5.5%CO₂/ 20% O₂ incubator. To stop the trypsin reaction, MAPC cell medium was added to each flask at a volume equal to the volume of trypsin used. Cells were transferred to 15 ml tubes and centrifuged at 350 g for 5 minutes. Supernatant was discarded and the pellet was resuspended in 1 ml MAPC cell medium. Cells were counted and seeded as described in section 2.2.1 and the number of population doublings (PD) that each culture had undergone was calculated by adding the initial PD to the binary logarithm of (the number of cells harvested/the number of cells seeded).

2.2.3 Cryopreservation Procedure

MAPC cells were collected and counted as described in section 2.2.2. and cooled on ice. Cells to be frozen down were resuspended in cold Dulbecco's Modified Eagle's Medium (DMEM) (Lonza, Basel, Switzerland) containing 20% fetal bovine serum (FBS) (Atlas Biologicals, CO, USA), and 10% dimethyl sulfoxide (DMSO) (Sigma-Aldrich). Each cryovial was put in a Nalgene container filled with 100% isopropanol (Sigma-Aldrich) which was stored at -80°C. The vials were transferred to liquid nitrogen after a minimum of 6 hours.

2.2.4 Generation of conditioned media

Cells were thawed and seeded in MAPC cell media and incubated at 37°C/ 5.5%CO₂/5% O₂ as described in section 2.2.1. The next day media was removed, cells were rinsed twice with PBS and serum free media (Table 2.2) was added to cells. 4 days later serum free media was removed and spun down at 900 g for 10 minutes to pellet debris. Supernatant was aliquoted and stored at -80°C. This media is now referred to as MAPC cells conditioned media (MAPC cells CM).

2.3 MSC Culture

Human MSC were isolated by enterprise partners in ReGenesys and Athersys Inc. from the same BM aspirates as MAPC cells. MSC were cultured on plastic tissue culture flasks and were maintained at normal oxygen tension in a humidified atmosphere of 5% CO₂.

2.3.1 Thawing Procedure

A vial of cells was removed from liquid nitrogen and put into a water bath at 37°C to thaw. When the vial was almost completely thawed, the cell suspension was transferred to a 15 ml conical tube and topped up with fresh MSC medium (Table 2.3). The cell suspension was centrifuged at 350 g for 5 minutes. Supernatant was discarded and the pellet was resuspended in 1 ml MSC medium. Cells were stained with EBAO and counted using a haemocytometer and fluorescent microscope. Cells were seeded at a density of 4000 cells/cm² in MSC media and incubated at 37°C/5%CO₂/ 20% O₂.

2.3.2 Culturing Procedure

To culture cells, medium was removed and cells were washed with PBS. 0.05% Trypsin-EDTA was added to each flask (4 ml for T75, 8 ml for T175). Flasks were incubated for 2-5 minutes in a 37°C/5%CO₂/ 20% O₂ incubator. To stop the trypsin reaction, MSC medium was added to each flask at a volume equal to the volume of trypsin used. Cells were transferred to 15 ml tubes and centrifuged at 350 g for 5 minutes. Supernatant was discarded and the pellet was resuspended in 1 ml MSC medium. Cells were counted as described in section 2.3.1. and PD were calculated in the same way as MAPC cells.

2.3.3 Cryopreservation Procedure

Cells were collected and counted as described in 2.3.2. Cryopreservation was carried out using the procedure outlined in 2.2.3 and freeze down media contained 70% DMEM (Lonza), 20% FBS (Lonza) and 10% DMSO.

2.3.4 Generation of conditioned media

Cells were thawed and seeded in MSC media and incubated at 37°C/5%CO₂/ 20% O₂. The next day media was removed, cells were rinsed twice with PBS and serum free media (Table 2.2) was added to cells. 4 days later serum free media was removed and spun down at 900 g for 10 minutes to pellet debris. Supernatant was aliquoted and stored at -80°C. This media was referred to as MSC conditioned media (MSC CM).

2.4 HUVEC Cell Culture

2.4.1 Thawing Procedure

Cryopreserved vials of human umbilical vein endothelial cells (HUVEC) were purchased from Lonza. A vial of cells was removed from liquid nitrogen and put into a water bath at 37°C to thaw, being careful not to submerge the entire vial. When the vial was almost completely thawed, the cell suspension was transferred to a 15 ml conical tube and topped up with fresh

endothelial growth media (EGM) (Lonza) (Table 2.4). Cells were counted using EBAO and a haemocytometer, and seeded at a density of 3000 cells/cm² in EGM and incubated in a 37°C/ 5.5%CO₂/ 20% O₂ incubator.

2.4.2 Culturing Procedure

Cells were cultured when they were 70-80% confluent. To culture cells, medium was removed and cells were rinsed with PBS. 0.05% Trypsin-EDTA was added to each flask (2 ml for T75, 4 ml for T175) and removed immediately. The cell layer was examined microscopically, allowing the trypsinisation process to continue until 90% of the cells had detached from the flask. To stop the trypsin reaction, PBS was added to each flask at a volume equal to the volume of trypsin used. Cells were transferred to 15 ml tubes and centrifuged at 220 g for 5 minutes. Supernatant was discarded and the pellet was resuspended in 1 ml EGM. Cells were counted and seeded as described in section 2.4.1.

2.4.3 Cryopreservation Procedure

Cells were collected and counted as described in 2.4.2. Cryopreservation was carried out using the procedure outlined in 2.2.3; however, in this case, freeze down media is composed of with 70% endothelial basal medium (EBM) (Lonza), 20% FBS (Lonza) and 10% DMSO.

2.4.4 Maintenance

Growth medium was changed the day after seeding and every second day thereafter.

Table 2.1: MAPC cells Medium

Reagents	Supplier
60% DMEM, low glucose	Lonza
40% MCDB-201	Sigma-Aldrich
1x Insulin-Transferrin-Selenium	Lonza
0.5x linoleic acid-bovine serum albumin (LA-BSA)	Sigma-Aldrich
1x Pen-Strep	Lonza
10 ⁻⁴ M L-Ascorbic acid-2-phosphate	Sigma-Aldrich
18% FBS	Atlas Biologicals
10 ng/ml human platelet derived growth factor (hPDGF-BB)	R&D systems
10 ng/ml human endothelial growth factor (hEGF)	Sigma-Aldrich
50 nM Dexamethasone	Sigma-Aldrich

Table 2.2: Serum Free Medium

Reagents	Supplier
60% DMEM, low glucose	Lonza
40% MCDB-201	Sigma-Aldrich
1x Insulin-Transferrin-Selenium	Lonza
0.5x LA-BSA	Sigma-Aldrich
1x Pen-Strep	Lonza
10 ⁻⁴ M L-Ascorbic acid-2-phosphate	Sigma-Aldrich

2.5 PBMC cell culture

2.5.1 PBMC Isolation

Whole blood buffy coat packs, which contained red blood cells, white blood cells and platelets, were supplied by the Irish Blood Transfusion Service (IBTS). PBMC were isolated from whole blood by density gradient centrifugation. The contents of buffy coat packs were diluted 1 in 2 with sterile PBS. 25 ml diluted blood was carefully layered on top of 15 ml Lymphoprep™ (Stem Cell Technologies, Cambridge, UK) in a 50 ml centrifugation tube. Tubes were centrifuged at 400 g for 25 minutes with no brake and low acceleration. After centrifugation, the white buffy coat layer containing PBMC was removed into a new sterile 50 ml tube, leaving red blood cells (RBC) and remaining plasma behind. PBMC were centrifuged at 800 g for 10 minutes, and washed in sterile PBS and centrifuged at 800 g for 5 minutes twice. Residual RBC were lysed by resuspending the PBMC pellet in 5 ml 1X RBC lysis buffer (Biolegend, San Diego, USA) for 5 minutes. RBC lysis buffer was quenched by adding 20 ml complete Roswell Park Memorial Institute medium (cRPMI) (Table 2.5). PBMC were centrifuged at 350 g for 5 minutes and resuspended in 10 ml of cRPMI for counting.

2.5.2 Cryopreservation

PBMC were counted as described in 2.2.1. Cryopreservation was carried out as described 2.2.3; however, PBMC were frozen in RPMI containing 20% heat inactivated FBS (HI-FBS), and 10% DMSO.

2.5.3 Thawing Procedure

A vial of PBMC was removed from liquid nitrogen and placed in a -80°C freezer for 30 minutes. The vial was then carried on ice to a water bath at 37°C, and thawed. When the vial was thawed, 4 µM DNase I (Roche Diagnostics, Germany) was added directly to the vial in a laminar flow cabinet and mixed using a p1000 pipette. The cell suspension was transferred to a 15 ml conical tube and topped up with fresh cRPMI before being centrifuged at 350 g for 5 minutes. Supernatant was discarded and the pellet was resuspended in 15 ml cRPMI. Cells were counted as described in section 2.2.1.

2.6 Methods of cell characterization

2.6.1 Characterisation of MAPC cells morphology

The morphology of undifferentiated MAPC cells was examined by light phase microscopy before each passage. Pictures were taken at 10X magnification. The morphology of MAPC cells was compared to that of MSC isolated from the same donors. Olympus CK40-SLP inverted microscope and photos taken using an Optika digital camera with Optika Vision Pro software.

2.6.2 Characterisation of surface markers expressed by MAPC cells and MSC.

MAPC cells and MSC were trypsinised and resuspended in PBS containing 2% HI-FBS (FACs buffer) at approximately 1×10^6 /ml. 100 μ l of this suspension was added to each well of a v-bottomed 96 well plate. Cells were washed twice in FACs buffer and then labelled with a panel of anti-human monoclonal antibodies and the appropriate isotype controls listed in Table 2.6. Cells were incubated at 4°C for 30 minutes and washed in FACs buffer. The cells were resuspended in FACs buffer and acquired on an Accuri C6 flow cytometer (BD Biosciences, Oxford, UK). MSC were used as a control to compare the surface marker expression by MAPC cells.

2.6.3 Tube formation assay

MAPC cell and MSC CM was generated as described in sections 2.2.4 and 2.3.4. HUVEC were cultured as described in section 2.4. Matrigel™ (BD Biosciences) was thawed on ice over 2 days in the fridge and kept on ice for the duration of the experiment. PBS and plates were chilled on ice prior to starting the assay. Matrigel™ was gently mixed and diluted in pre-chilled PBS to a working concentration of 6.5 mg/ml. 400 μ l of the diluted Matrigel™ was added to each well of a 24 well plate. The plate was incubated at 37°C for 1 hour. 5.5×10^4 HUVEC cells were added to each well in 1 ml of the appropriate CM and

Table 2.3: MSC Medium

Reagents	Supplier
MSC Basal Medium	Lonza
MSC Growth Supplement	Lonza
L-Glutamine	Lonza
Gentamicin	Lonza

Table 2.4: HUVEC Media

Reagents	Supplier
Endothelial Basal Medium (EBM)	Lonza
hEGF	Lonza
Hydrocortisone	Lonza
GA-1000	Lonza
BBE	Lonza
FBS	Lonza
Ascorbic Acid	Lonza

Table 2.5: Complete RPMI

Reagents	Supplier
80% RPMI	Sigma-Aldrich
10% HI FBS	GE Healthcare Life Sciences (Utah, USA)
1% P/S	Sigma-Aldrich
1% L-Glut	Sigma-Aldrich
0.1% β -mercaptoethanol	Sigma-Aldrich

Table 2.6.: Antibodies used to characterise the surface markers on MAPC cells

Antibody	Fluorochrome	Isotype	Supplier	Clone
		Control		
CD44	FITC	IgG2b	eBioscience	IM7
CD45	FITC	IgG1	eBioscience	2D1
CD90	APC	IgG1	eBioscience	eBIO5E10
CD105	APC	IgG1	eBioscience	SN6
HLA ABC	APC	IgG1	eBioscience	W6/32
HLA DR	PE	IgG2a	eBioscience	L243

incubated at 37°C/ 5.5%CO₂/ 20% O₂ for 18 hours. The assay was carried out in triplicate. EGM was used as a positive control for the assay, with EBM being used as a negative control. Serum free media which had never been exposed to cells was used as a negative control for the samples being tested. Images were taken of 4 random fields in each well at 5X magnification using a light microscope and the number of tubes formed between cells was counted.

2.6.4 Differentiation assay

MAPC cells (5×10^4 /well) were seeded into 6 well plates on day 0. On day 1, high glucose DMEM (Sigma-Aldrich) with 10% FBS, 1% penicillin-streptomycin (P/S) (Sigma-Aldrich) and 1% L-glutamine (L-glut) (Sigma-Aldrich) was added to control wells. Control media containing 100 nM dexamethasone (Sigma-Aldrich), 200 μ M L-ascorbic acid (Sigma-Aldrich), 10 mM β -glycerophosphate (Sigma-Aldrich), and 0.1 mg/ml L-thyroxine (Sigma-Aldrich) were added to bone differentiation wells. Control media containing 1 μ M dexamethasone, 5 μ g/ml insulin (Sigma-Aldrich), 0.5 mM 3-isobutyl-1-methylxanthine (IBMX) (Sigma-Aldrich) and 0.2 mM indomethacin (Sigma-Aldrich) were added to adipocyte differentiation wells. Media was changed every 2 days for one week. On day 8, cells were fixed with 10% formalin

(Sigma-Aldrich). Osteocytes and adipocytes were stained with Oil Red O stain (Sigma-Aldrich) and Alizarin Red S stain (Sigma-Aldrich) respectively for 20 minutes. Excess stain was washed using distilled H₂O for osteocytes and PBS for adipocytes. Cells were examined using an Olympus CK40-SLP inverted microscope and images taken using an Optika digital camera with Optika Vision Pro software.

2.6.5 CFSE assay

The proliferation of T cells in the presence of MAPC cells at ratios 1:5, 1:10, 1:20 and 1:40 MSC: PBMC was determined using a carboxyfluorescein succinimidyl ester (CFSE) dilution assay. CFSE is taken up into the cytoplasm of cells, and is divided between daughter cells following cell division. Thus, the proliferation of cells can be measured by flow cytometry by analysing the fluorescence intensity of individual cells. MAPC cells were seeded into 4 rows of a 96 well round bottom plate at decreasing densities (1×10^4 , 5×10^3 , 2.5×10^3 , 1.25×10^3) and incubated in MAPC cell media overnight. PBMC were thawed as described in section 2.5.3 and labelled with 10 μ M CFSE (Sigma-Aldrich), in warm PBS for 10 minutes before being washed with cold PBS. MAPC cell media was removed from 96 well plates, and PBMC (5×10^4 /well) and anti-CD3/CD28 beads (Thermo Fisher, MA, USA) (1×10^4 /well) were added to each well in 200 μ l complete RPMI. PBMC cultured alone and PBMC cultured with activation beads were used as negative and positive controls respectively. Cells were co-cultured in 20% O₂ for 4 days. On day 4, cells were harvested and washed twice in FACS buffer before being stained with antibodies for CD3 (eBioscience) and 7AAD (eBioscience) (Table 2.10) for 30 minutes at 4°C. Cells were washed in FACS buffer and CFSE dilution of CD3⁺ 7AAD⁻ cells was analysed by flow cytometry, to include viable T cells only. The absolute number of CFSE dividing cells was calculated by adding a known number of counting beads which were used for quantitation (BD Biosciences) (1.5×10^4 /well).

2.7 *In vitro* assays:

2.7.1 Stimulation of MAPC cells and MSC with IFN- γ

MAPC cells were thawed and seeded into 6 well plates at a density of 2000 cells/cm². When MAPC cells reached confluency, 50 ng/ml IFN- γ (Peprotech, Rocky Hill, NJ) was added. 24 hours later cells were sub cultured and used for subsequent experiments.

2.7.2 Treatment of MAPC cells with PPAR δ agonist and antagonist

To activate PPAR δ , MAPC cells were treated with the highly selective PPAR δ agonist GW0742 (Tocris Bioscience, Bristol, UK) at a concentration of 1 μ M for 24 hours prior to exposure to pro-inflammatory cytokines, or introduction to the humanised aGvHD model. To antagonise PPAR δ , MAPC cells were treated with the selective PPAR δ antagonist GSK3787 (Tocris Bioscience) at a concentration of 1 μ M for 24 hours prior to exposure to pro-inflammatory cytokines, or introduction to the humanised aGvHD model.

2.7.3 ATG *in vitro* assay:

Spleens were dissected from CD45.1/Bl6 mice (Jackson Laboratories, Bar Harbour, ME, USA), put into 10 ml cRPMI and kept on ice. Spleens were then passed through a 70 μ m filter and resuspended in 10 ml cRPMI, followed by centrifugation at 350 g for 5 minutes. The pellet was resuspended in 2ml 1X RBC lysis buffer for 2 minutes. 10 ml of cRPMI was added and cells were centrifuged at 350 g for 5 minutes. Supernatant was removed and splenocytes were counted using EBAO. 1×10^5 cells were seeded per well of a round bottom 96 well plate in triplicate in cRPMI supplemented with or without 10 μ g/ml, 50 μ g/ml or 250 μ g/ml ATG (Cedarlane Laboratories, Burlington, CA) or rabbit serum (Cedarlane Laboratories) as a control. Cells were harvested after 16, 24, and 48 hours and washed twice in FACs buffer before being surface stained with anti-mouse CD4 PerCP (eBioscience) and CD8 FITC (eBioscience) for 30 minutes. Cells were washed in FACs buffer and acquired on an Accuri C6. Counting beads were used to enumerate total cell numbers.

2.8 *In vivo* models

2.8.1 Humanised model of acute graft versus host disease

NSG mice (Jackson Laboratories, Bar Harbour, ME, USA) aged between 6 and 24 weeks were exposed to a conditioning dose of 2.4 Gray (Gy) whole-body gamma irradiation. Human PBMC were isolated by Ficoll-density centrifugation as described in 2.5.1 and washed 3 times in PBS before being administered to irradiated NSG mice ($8 \times 10^5/g$) via IV injection. Negative control mice received PBS. In some groups, sub-cultured MAPC cells ($6.4 \times 10^5/g$) were administered IV on either day 0 or day 7 (Fig. 2.1).

Signs of aGvHD typically manifested between days 10 and 16 post-PBMC transfusion. Mice were monitored every second day up to day 9, and then on a daily basis until the end of the experiment on day 28. aGvHD scores were assigned to mice based on the appearance of symptoms such as weight loss, appearance, and activity levels as outlined in Table 2.7. For each category animals were scored between 0 and 4 based on the severity of symptoms. The scores given based on each of these categories was combined to give an overall aGvHD score. When mice lost over 15% of their total body weight, reached a cumulative aGvHD score of 5 or scored 4 in a single category they were humanely euthanised by cervical dislocation. For imaging experiments, mice were culled 4, 24, or 48 hours after MAPC cell administration, and for tissue analysis mice were culled on day 12.

2.8.2 Murine model of IL-7 driven homeostatic proliferation

Congenic strains are commonly used to track the fate of adoptively transferred cells. C57/Bl6 and C57/Bl6-CD45.1 (CD45.1) strains (Jackson Laboratories) exhibit differential expression of the pan leukocyte marker CD45. Leukocytes derived from C57/Bl6 can be identified by expression of CD45.2, while CD45.1 mice are identified by expression of CD45.1. For adoptive transfer experiments CD4⁺ T cells were isolated from the spleen of C57/Bl6 mice using a negative selection kit (R&D systems, Abingdon, UK). Briefly, spleens were passed through a 40 µm filter and cells were washed in cRPMI before being treated for 2 minutes with 1X RBC lysis buffer. Cells were washed in cRPMI, counted, and washed in PBS before being resuspended in 1X MagCollect™ buffer to a cell density of 2×10^8 cells/ml. For every 1×10^8

cells processed, 100 μ l of CD4⁺ T cell biotinylated antibody cocktail was added and cells were incubated for 15 minutes at 4°C. After incubation, 100 μ l of streptavidin ferrofluid per 1×10^8 cells was added and cells were further incubated for 15 minutes at 4°C. Following the incubations, the mixture was brought to a final volume of 3ml with 1X MagCollect™ buffer. The tubes were placed into a magnetic stand for 6 minutes. Magnetically labelled cells migrated towards the magnet, leaving the desired CD4⁺ T cells behind in suspension. This incubation was repeated for another 6 minutes to ensure that a pure population was obtained. The CD4⁺ T cell suspension was centrifuged at 300 g for 5 minutes then resuspended in cRPMI and counted. CD4⁺ cells were then resuspended at 2×10^7 cells/ml in PBS and incubated with 10 μ M APC eFluor proliferation dye (eBioscience) for 10 minutes in the dark. Labelling was stopped by adding cold media and incubating the cell suspension on ice for 5 minutes. Cells were washed three times with complete media and three times with PBS.

4×10^6 CD45.2⁺, CD4⁺ cells were administered IV to CD45.1 mice on day -2. 1 μ g or 2 μ g recombinant murine IL-7 (Peprotech) was incubated with 5 μ g or 10 μ g of the IL-7 antibody M25 (BioXcell, NH, USA) for 30 minutes at 37°C in PBS. This complex was then administered via IP injection on days 0, 2 and 4. MAPC cells were thawed as described in section 2.2.1 and washed three times in PBS. 1×10^6 MAPC cells in PBS were administered via IP injection or IV injection on day 1. Mice were humanely euthanised by cervical dislocation on day 5 and spleens and lymph nodes were harvested for processing (Fig. 2.2).

2.8.3 Murine model of lymphopenia driven homeostatic proliferation

For preliminary experiments either 25 mg/kg or 50 mg/kg ATG was administered IP or IV to CD45.1 mice on days 0 and 3. Following preliminary experiments, the ATG model was set up by administering 50 mg/kg ATG IP on days 0 and 3, with administration of 1×10^6 MAPC cells either IP or IV on day 4 (Fig. 2.3). Mice were humanely euthanized by cervical dislocation on day 5 and spleens and lymph nodes were harvested for flow cytometry. In experiments where indomethacin was introduced, 30 μ g indomethacin (Indo) (Sigma-

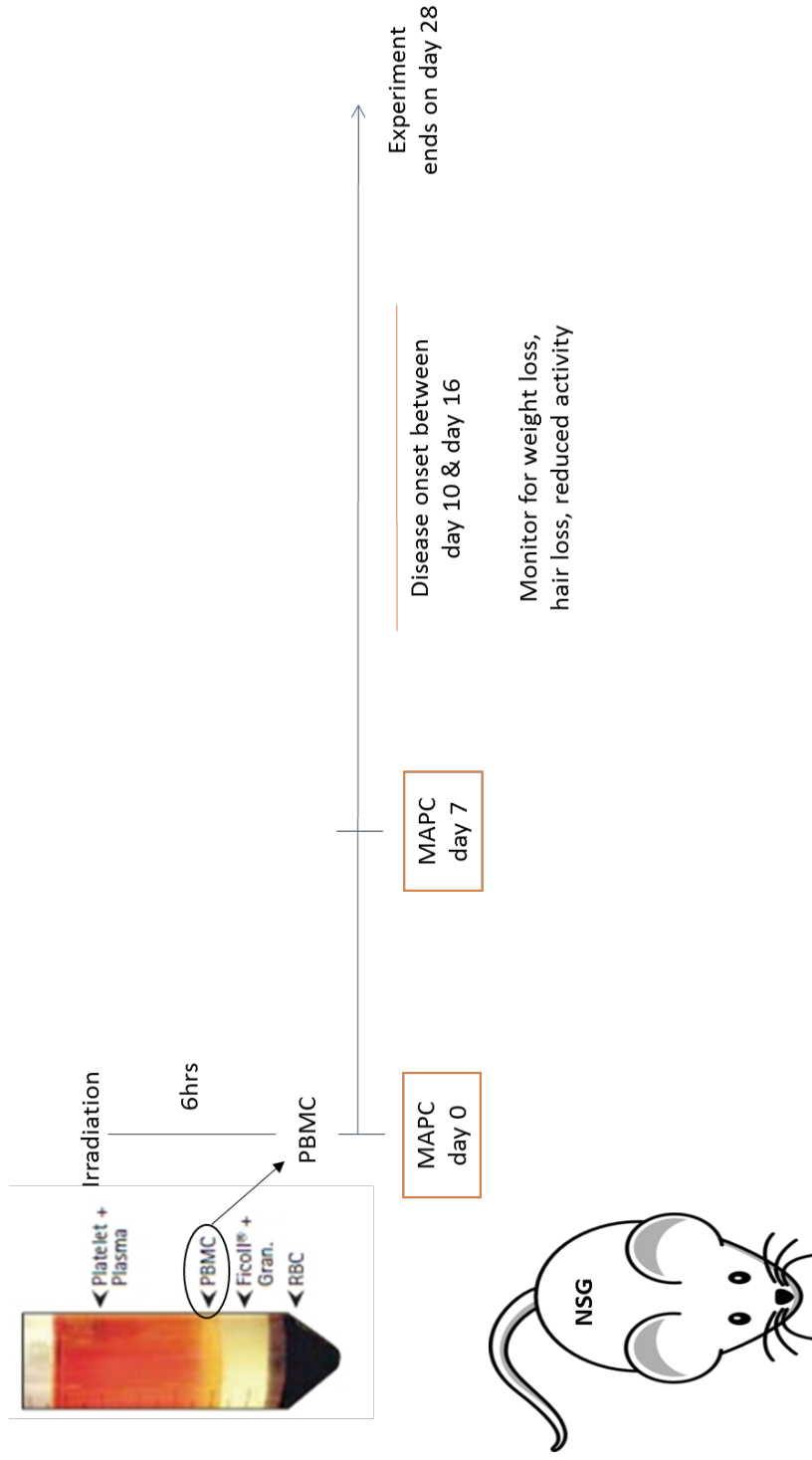


Figure 2.1 Schematic timeline of humanised aGvHD model. NSG mice were irradiated and PBMC isolated from buffy coats were administered approximately 6 hours later. Some mice were administered MAPC cells on day 0 or day 7 IV. Symptoms presented between days 10 and 16, and mice were assigned aGvHD scores based on the severity of these symptoms as outlined in table 2.7. Mice that reached a score of 5 or lost >15% of total body weight were humanely euthanised. All mice were humanely euthanised on day 28. aGvHD: acute GvHD, PBMC: Peripheral blood mononuclear cells

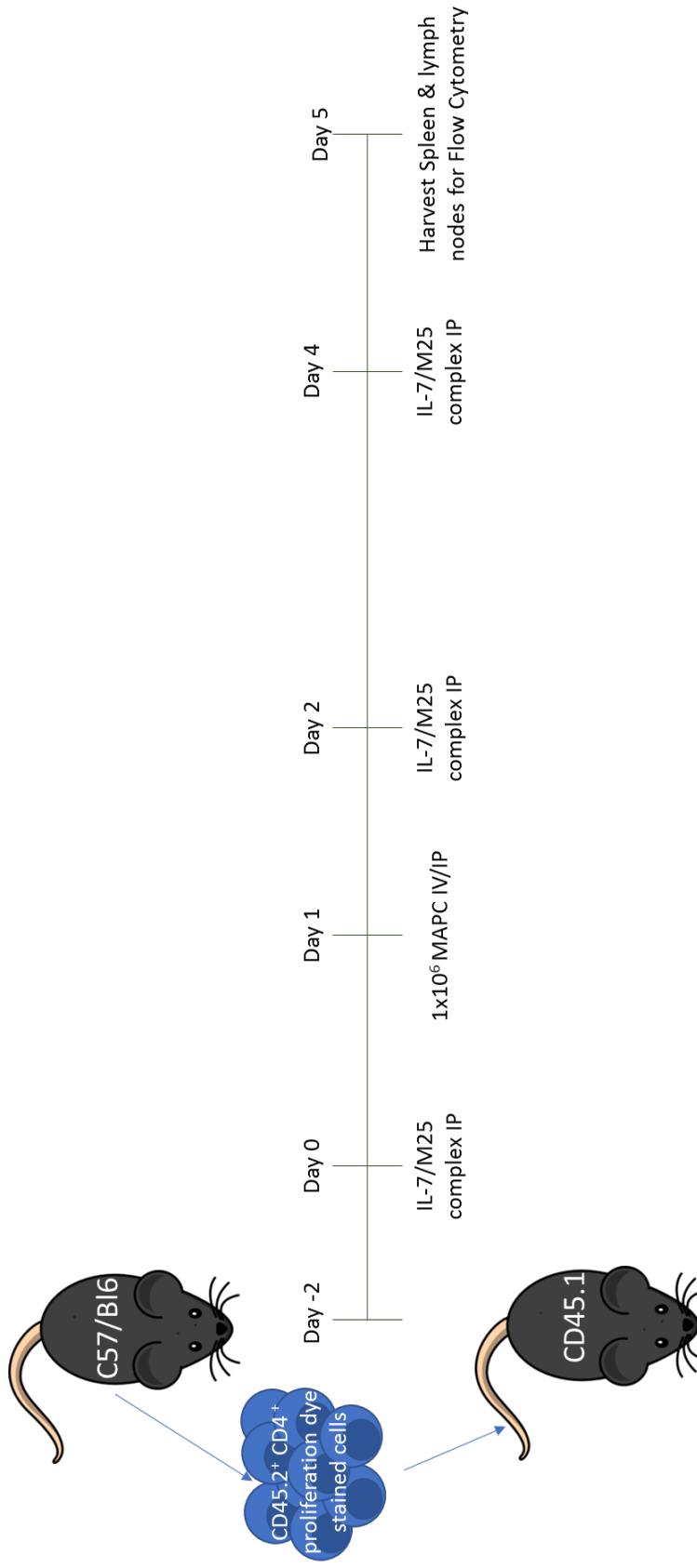


Figure 2.2 Schematic timeline of IL-7 driven HP model. CD4⁺ splenocytes were isolated from C57/Bl6 mice and stained with an APC efluor proliferation dye. 4x10⁶ CD4⁺ cells were adoptively transferred to CD45.1 mice on day -2 via IV injection. Recombinant murine IL-7 was incubated with the IL-7 antibody M25 for 30 minutes before being injected IP on days 0, 2 and 4. MAPC cells were administered either IV or IP on day 1. Mice were humanely sacrificed on day 5, and spleens and lymph nodes were harvested for flow cytometry. IV: intravenous, IP: intraperitoneal, IL-7/M25: interleukin-7/interleukin-7 antibody complex, HP: homeostatic proliferation.

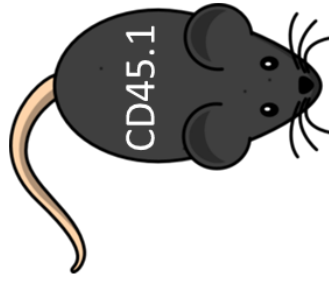
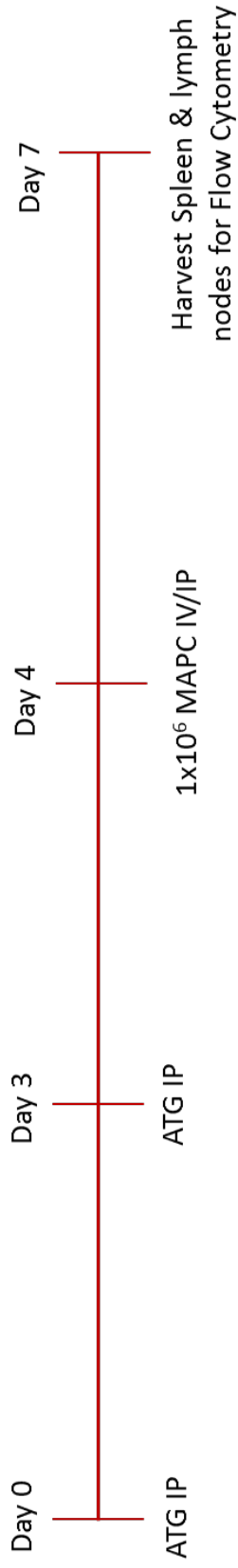


Figure 2.3 Schematic timeline of lymphopenia driven HP model. 50 mg/kg ATG was administered to CD45.1 mice on days 0 and 3. On day 4 MAPC cells were administered either IV or IP. Mice were humanely euthanized on day 7 and spleens and lymph nodes were harvested for flow cytometry. ATG: anti-thymocyte globulin, IV: intravenous, IP: intraperitoneal, HP: homeostatic proliferation.

Aldrich) was administered IP on days 4, 5 and 6, with diluent (1% ethanol in PBS) being used as a control.

2.9 Western Blotting

2.9.1 Protein Extraction

MAPC cells from 2 wells of a six well plate were trypsinised and pooled before being resuspended in 1 ml ice cold PBS. Samples were centrifuged at 12,000 g for 5 minutes twice at 4°C and resuspended in 100 µl radioimmunoprecipitation assay (RIPA) buffer (Sigma-Aldrich) containing 1X protease inhibitor cocktail (Roche) for 10 minutes. Lysates were then centrifuged at 12,000 g for 10 minutes at 4°C and the supernatant was collected and stored at -20°C. Prior to loading, samples were mixed with 6X sample buffer and boiled for 5 minutes.

2.9.2 SDS-Polyacrylamide Gel Electrophoresis

MagicMark™ XP Western Protein Standard and samples were loaded into separate 0.75mm wells. Electrophoresis was performed at 60 V through a 5% polyacrylamide stacking gel (Table 2.8) and a 10% polyacrylamide resolving gel (Table 2.8) at 80 V for up to 2 hours.

2.9.3 Immunoblotting

Following separation by electrophoresis, polyvinylidene fluoride (PVDF) membranes (GE Healthcare, Buckinghamshire, UK) were prepared by activating in methanol (Sigma-Aldrich) for 30 seconds, washing in dH₂O for 2 minutes, followed by a 10 minute wash in transfer buffer (Table 2.8). 2 pieces of extra thick Whatman blotting paper (Bio-Rad, Hertfordshire, UK) were soaked in transfer buffer. Resolving gels were then placed in transfer buffer for 10 minutes before being transferred to PVDF membranes in a Hoefer TE 70 Semiphor semi-dry transfer unit (GE Healthcare) at 100 mA for 30 minutes. For the transfer, 1 piece of soaked blotting paper was placed on the bottom surface of the transfer unit followed by the PVDF membrane. The resolving gel was placed on top with care and air bubbles removed. Another piece of Whatman blotting paper was added and the unit closed and set to run. Following transfer, membranes were removed from the unit and incubated in blocking buffer (Table 2.9)

for 1 hour at room temperature. Membranes were then incubated with primary antibodies for STAT1 and pSTAT1 (Table 2.9) under agitation at 4°C overnight followed by 3x5 minute washes in Tris-buffered saline containing 0.1% Tween 20 (TBST) (Table 2.8). Membranes were then incubated in a rabbit secondary antibody (Table 2.9) for 1 hour at room temperature before being washed again 3 times in TBST. Membranes were developed by covering in 3ml of BM Chemiluminescence Western Blotting Substrate (POD) (Roche) for 1 minute and imaged using a G:BOX (Syngene, Cambridge, UK). To ensure that loading of each sample was equal, membranes were washed in TBST three times and incubated with an antibody for Actin (Table 2.9) which was chosen as a house keeping protein, before being washed again in TBST three times and incubated with a mouse secondary antibody (Table 2.9). The membrane was developed again and imaged using the G:BOX. Densitometry was carried out using Image J open source software (National Institutes of Health, USA).

2.10 Flow Cytometry

2.10.1 Analysis of immunomodulatory protein expression by MAPC cells

MAPC cells were cultured and stimulated with IFN- γ as described in sections 2.2 and 2.7.1, before being transferred to v bottom 96 well plates washed twice in FACs buffer. Cell pellets were dissociated briefly by vortexing and antibodies for CD105, ICAM1 or PDL1 were added (Table 2.10). Cells were incubated with surface antibodies for 30 minutes at 4°C, and then washed in FACs buffer. Cells were then ready to acquire by flow cytometry on an Accuri C6. For analysis of IDO, cells were incubated with 1X Brefeldin A (eBioscience) for 4 hours before being sub cultured to prevent the release of IDO into supernatant. Cells being analysed for IDO or COX-2 levels were surface stained with CD105 antibody as described, and then treated with the intracellular FoxP3 kit as per manufacturer's instructions (eBioscience) to prepare cells for intracellular staining. Briefly, surface stained cells were incubated with 200 μ l fixation buffer for 30-60 minutes at 4°C. 100 μ l 1X permeabilisation buffer was added and cells were then centrifuged at 350 g for 5 minutes. Cells were blocked with 2% rat serum (eBioscience) for 15 minutes to prevent non-specific staining, and either IDO or COX-2

antibodies (Table 2.7) were then added for 45 minutes. Cells were then washed in FACs buffer and acquired using the Accuri C6.

2.10.2 Surface staining of murine cell populations

Spleens, and mesenteric, inguinal and axillary lymph nodes were harvested from CD45.1 mice and a single cell suspension was prepared by dissociating the organs and passing through a 40 µm pore cell strainer. Spleens and lymph nodes were centrifuged at 350 g and splenocytes were treated with 1 ml 1X RBC lysis buffer for 2 minutes before being quenched with cRPMI and centrifuged again at 350 g. Cells were seeded into 96 well v bottom plates for flow cytometry. For analysis of CD4⁺ and CD8⁺ T cells, B1a cells, and eosinophils, cells were washed twice in FACs buffer, treated with CD16/32 (eBioscience) for 15 minutes to prevent non-specific staining, and stained with appropriate antibodies (Table 2.11) for 30 minutes. Cells were then washed with FACs buffer and acquired on the Accuri C6, with counting beads used to quantify cell populations.

2.10.3 Intracellular transcription factor staining

Spleens and lymph nodes were prepared for flow cytometry as described in the previous section, and surface stained for expression of CD4, CD8 and CD25 (Table 2.11). Cells were then treated with the intracellular FoxP3 kit as per manufacturer's instructions (eBioscience) to prepare cells for intracellular staining. Briefly, surface stained cells were incubated with 200 µl fixation buffer overnight at 4°C. 100 µl 1X permeabilisation buffer was added and cells were then centrifuged at 350 g for 5 minutes. Cells were blocked with 2% rat serum (eBioscience) for 15 minutes to prevent non-specific staining, and either Ki67 or FoxP3 antibodies (Table 2.11) were then added for 45 minutes. Cells were then washed in FACs buffer and acquired using the Accuri C6, with counting beads used to quantify cell populations.

Table 2.7: aGvHD scoring scale

	Symptom			
Score	Weight Loss	Posture	Fur texture	Activity Levels
0	0%	Normal	Normal	Normal
1	0-10%	Mild hunching	Mild ruffling	Mild reduction in activity
2	10-15%	Moderate hunching	Moderate ruffling and hair loss	Moderate reduction in activity
3	15-20%	Severe hunching	Severe ruffling and moderate hair loss	Stationary unless stimulated
4	>20%	Severe hunching and impaired movement	Severe ruffling and hair loss	Extreme lethargy and paralysis

Table 2.8: Reagents used for Western Blotting

Buffer	Composition
10X TBS (Tris buffered saline)	25 mM Tris, pH 7.4 containing 0.14 M NaCl
TBST (Tris buffered saline with Tween)	25 mM Tris, pH 7.4 containing 0.14 M NaCl (v/v) Tween-20 (Sigma-Aldrich)
Laemmli sample buffer	62.5 mM Tris-HCL, pH 6.8, 10% (w/v) glycerol, 2% (w/v) SDS, 0.7 M β -mercaptoethanol and 0.001% (w/v) bromophenol blue.
TAE (Tris-acetate-EDTA) Buffer	40 mM Tris base, 0.1% (v/v) glacial acetic acid, 1mM EDTA
Transfer Buffer	25 mM Tris, 192 mM glycine, 20% (v/v) methanol
10% separating gel	42% H ₂ O, 0.375 M Tris, 30% Protogel (Thermo-Fisher), 0.0006% TEMED (Sigma-Aldrich), 0.0006% ammonium persulphate (Sigma-Aldrich)
Stacking gel	58% H ₂ O, 0.125M Tris, 17% Protogel, 0.002% TEMED, 0.0005% ammonium persulphate.
Blocking Buffer	TBST with 5% (w/v) non-fat dry Milk or 5% BSA

Table 2.9: Antibodies used for Western Blotting

Antibody	Clone	Dilution Factor	Diluent	Blocking buffer	Secondary Anti-body	Supplier	
Primary Antibodies:							
pSTAT1	Tyr701	1:1000	5% BSA TBST	TBST 5%	with (w/v)	Anti-Rabbit HRP	Cell Signaling
STAT1	D1K9Y	1:1000	5% BSA TBST	TBST 5% non-fat milk	with (w/v) dry	Anti-Rabbit HRP	Cell Signaling
Actin	8H10D10	1:5000	5% Milk TBST	n/a		Anti-mouse HRP	Cell Signaling
Secondary Antibodies:							
Anti-mouse HRP	n/a	1:1000	5% Milk TBST	n/a	n/a		Cell Signaling
Anti-rabbit HRP	n/a	1:1000	5% Milk TBST	n/a	n/a		Cell Signaling

Table 2.10: Human antibodies used for *in vitro* assays

Antibody	Fluorochrome	Supplier	Clone
CD3	APC	eBioscience	UCHT1
7AAD	PerCP	eBioscience	
CD105	APC	eBioscience	SN6
PDL1	PE	eBioscience	MIH1
ICAM1	PE	eBioscience	HA58
COX-2	PE	BD Biosciences	33/Cox-2
IDO	PE	eBioscience	eyedio

2.10.4 Intracellular cytokine staining

Single cell suspensions of spleens and lymph nodes were prepared as described in section 2.10.2. Cells were then transferred to round bottom 96 well plates, and incubated with 100 ng/ml phorbol-myristate-acetate (PMA) (Sigma-Aldrich), 1 µg/ml ionomycin (Sigma-Aldrich) and 1X Brefeldin A (eBioscience) for 4 hours before being prepared for intracellular flow cytometry as described in section 2.10.3. Cells were stained with either IFN- γ or TNF- α antibodies (Table 2.11) for 45 minutes and washed before being acquired using the Accuri C6, with counting beads used to quantify cell populations.

2.10.5 Immunophenotyping study

Spleens and lymph nodes were dissected and shipped (at 4°C temp. controlled) to the 3i team in Kings College London where they were processed for flow cytometry. A single cell solution was then prepared by passing each organ through a mesh filter, and splenocytes were then treated with RBC lysis buffer. Cells were transferred to v bottom 96 well plates, washed in FACs buffer, and surface stained using the panels outlined in Tables 2.12-2.14. Analysis was done using an automated gating pipeline designed by the 3i team.

2.11 Cryo-imaging

2.11.1 Qtracker[®] labelling of MAPC cells

MAPC cells were thawed or sub-cultured as described in section 2.2 and resuspended at 10×10^6 /ml in MAPC cell media. MAPC cells were labelled with the Qtracker[®] 625 labelling kit (Thermo-Fisher) according to manufacturer's instructions. Briefly, 5 µl Qtracker[®] component A was mixed with 5 µl Qtracker[®] component B, and incubated for 5 minutes at room temperature. 1 ml media was added to the Qtracker[®] mixture and 5×10^6 cells were added. Cells were incubated for 1 hour at 37°C on a rocker. Cells were washed twice in MAPC cells media, before being washed twice in PBS and administered to animal models.

Table 2.11: Mouse Panels used for *in vivo* experiments

	Antibody	Fluorochrome	Supplier	Clone
Adoptive Transfer	CD45.1	FITC	eBioscience	A20
	CD45.2	FITC	eBioscience	104
	CD4	PerCP	eBioscience	GK 1.5
	CD8	PE	eBioscience	53-6.7
T cell proliferation:	CD4	PerCP	eBioscience	GK 1.5
	CD8	FITC	eBioscience	53-6.7
	Ki67	PE	eBioscience	SolA15
T cell cytokines:	CD4	PerCP	eBioscience	GK 1.5
	CD8	FITC	eBioscience	53-6.7
	IFN- γ	PE	eBioscience	XMG1.2
	TNF- α	APC	eBioscience	MP6-XT22
Treg:	CD4	FITC	eBioscience	GK 1.5
	CD25	APC	eBioscience	PC61.5
	FOX-P3	PE	eBioscience	FJK-16s
Eosinophils:	MHCII	FITC	eBioscience	M1/70
	F4/80	APC	eBioscience	BM8
	Ly6G	PE	eBioscience	RB6-8C5
	Siglec F	PerCP	eBioscience	1RNM44N
B1a cells	CD19	FITC	eBioscience	eBio1D3
	CD5	APC	eBioscience	53-7.3

Table 2.12: Myeloid Panel used for immunophenotyping study

Antibody	Fluorochrome	Supplier	Clone
CD45	Qdot 605	eBioscience	30-F11
CD11c	BV786	BD Biosciences	HL3
CD11b	BV510	Biolegend	M1/70
F4/80	PerCP	Biolegend	BM8
Ly6C	AF700	BD Biosciences	AL-21
Ly6G	APC	BD Biosciences	1A8
C103	PE	BD Biosciences	M290
CD317	BV510	Biolegend	927
MHCII	FITC	BD Biosciences	2G9
CD86	PE-Cy7	BD Biosciences	GL1
Lin: CD3	BV421	BD Biosciences	145-2C11
CD19		BD Biosciences	1D3
NK1.1		Biolegend	PK136
Live/Dead	NIR	Biolegend	

Table 2.13: T cell Panel used for immunophenotyping study

Antibody	Fluorochrome	Supplier	Clone
CD45	Qdot 605	eBioscience	30-F11
CD5	BV510	BD Biosciences	53-7.3
TCR-d	PE-Cy7	Biolegend	GL3
NK1.1	BV650	Biolegend	PK136
CD4	BV786	BD Biosciences	GK1.5
CD8	AF700	BD Biosciences	53-6.7
CD25	APC	BD Biosciences	PC61
GITR	PE	BD Biosciences	DTA-1
CD44	FITC	BD Biosciences	IM7
CD62L	PerCP	BD Biosciences	MEL-14
KLRG1	BV421	BD Biosciences	2F1
Live/Dead	NIR	Biolegend	

Table 2.14: B cell panel used for immunophenotyping study

Antibody	Fluorochrome	Supplier	Clone
CD45	Qdot 605	eBioscience	300-F11
IgG1	PE	BD Biosciences	A85-1
B220	AF700	BD Biosciences	RA3-6B2
IgM	BV786	BD Biosciences	R6-60.2
IgD	PerCP	Biolegend	11-26C.2A
GL-7	AF647	BD Biosciences	GL7
CD95	PE-Cy7	BD Biosciences	JO2
CD138	BV650	Biolegend	281-2
CD5	BV510	BD Biosciences	53-7.3
CD21/35	FITC	BD Biosciences	7G6
CD23	BV421	BD Biosciences	B3B4
Live/Dead	NIR	Biolegend	

2.11.2 Cryopreservation of Tissue

For imaging of organs, mice were humanely sacrificed by cervical dislocation. Organs of interest were harvested, and put onto a thin layer of black OCT (BioInvision, OH, USA) in Peel-A-Way[®] moulds (Ted Pella Inc., CA, USA) kept on ice. Organs were covered in OCT and frozen on a metal block chilled in liquid nitrogen. Once OCT had solidified samples were transferred to -80°C.

For whole mouse imaging, mice were humanely sacrificed with the lethal injection. OCT was rubbed into the carcass, against the direction of fur to minimize air bubbles. The carcass was put onto a thin layer of OCT in a boat made from heavy duty aluminium foil with the ventral side facing down. Extra OCT was poured over the carcass to cover the mouse. Heavy duty tin foil was wrapped around the aluminium boat and the sample was put into a box containing liquid nitrogen. Once OCT had solidified samples were transferred to -80°C.

2.11.3 Sample Sectioning and imaging using CryoViz[™] Technology

The CryoViz[™] (BioInvision) consists of a motorized cryo-micro-tome with a brightfield/fluorescence microscope, and a robotic imaging system positioner, all of which are fully auto-mated by a control system (Fig. 2.4). An organ or whole mouse within a block of OCT is sectioned and subsequently imaged, allowing the system to acquire three-dimensional (3D), high-resolution, brightfield and fluorescent image volumes from sequential images of the sample block. The CryoViz[™] takes pictures of multiple 'tiles' within each section, thus from each section a number of pictures are generated. These 'tiles' are then combined to generate a full picture of each section, and then each section is combined to generate a 3d image.

Following cryopreservation of tissue, samples were transferred to the CryoViz[™] freezer chamber and left for 2 hours to reach -20°C. Samples which were cube or cuboid shaped were then mounted to the stage using OCT, and left for 30 minutes to stick. Samples were cut until tissue was visible, and then camera and microscope settings were chosen. The microscope was set to a magnification of 1X and an objective of 0.63, and focused on the visible tissue. Brightfield exposures were set to 5.55 ms to image the lung and spleen, and 6.66 ms to image the liver or whole mouse. A wide range of fluorescent exposures were set

and then the optimal exposure chosen. Optimal exposures chosen were 600 ms for lung, 800 ms for liver, and 1000 ms for spleen. The field of view to be imaged within the OCT block was chosen, and the CryoViz™ was then set to alternately slice and image the sample. Organs and whole mice were sectioned at 40 µm.

2.11.4 Image Processing

2D Images were processed using CryoViz™ pre-processor software. This could be done either while images were being acquired or at any stage after imaging had been completed. The pre-processor software combined the 2D images of each section to generate a 3D image of the sample being analysed.

2.11.5 Cell Quantification

CryoViz™ cell detection software was used to automatically detect fluorescent cells within samples. Samples were manually checked and false positives were deleted. In whole mice, autofluorescence in the gut generated many false positives, so all detected cells in the gut were deleted.

2.11.6 Image Reconstruction

Images for presentation of Cryo-imaging data were prepared by creating overlays of detected cells and 3D samples using Amira software.

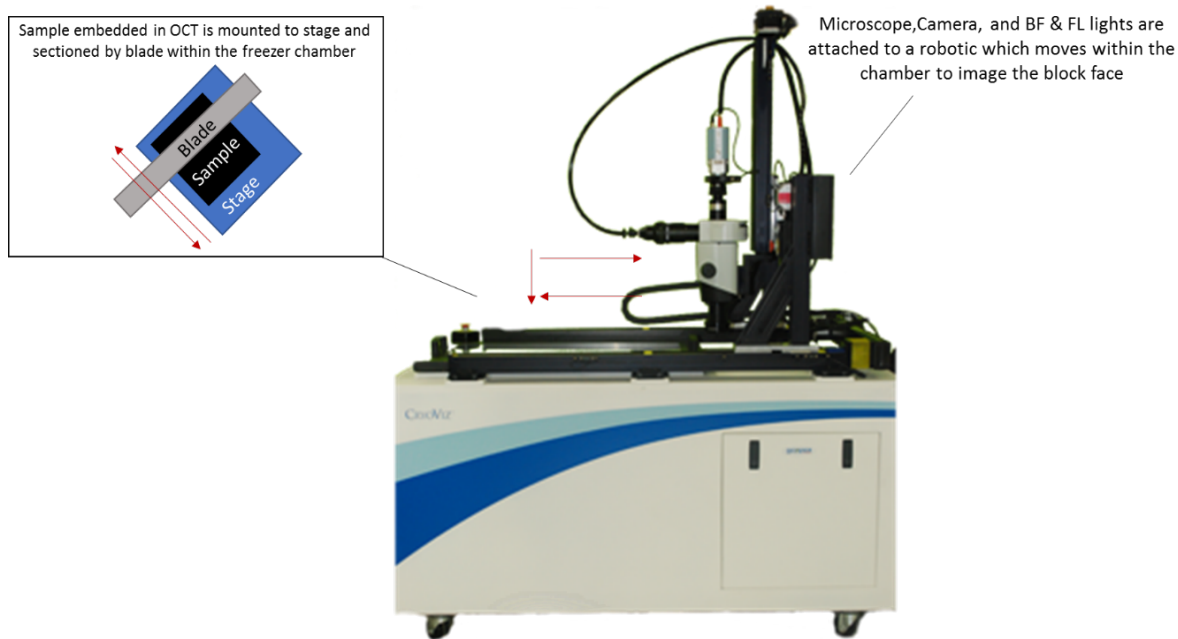


Figure 2.4 Overview of CryoViz™ equipment. Image adapted from photograph sourced on www.bioinvision.com

2.12 Histology

2.12.1 Tissue Processing

Organs were harvested from aGvHD mice on day 12 and placed into 10% neutral buffered formalin (Sigma-Aldrich) for 24 hours at room temperature. Organs were then transferred to 70% ethanol (Sigma-Aldrich) and left at 4°C for 24-72 hours before being processed for histology using an automated processor (Shandon Pathcentre, Runcorn, UK). The automated processor submerged the tissue into containers containing 70%, 80%, 95% and 100% ethanol sequentially in order to dehydrate the samples. Samples were then submerged in xylene (Sigma-Aldrich) and paraffin wax (Sigma-Aldrich). After processing, the samples were embedded in paraffin wax and left to set at 4°C. A Shandon Finesse 325 microtome (Thermo-Shandon, Waltham, MA, USA) was used to cut 5 µm sections of each tissue. After being cut, sections were transferred to a hot water bath and placed onto microscope slides (VWR, Ballycoolin, Ireland) and left to air dry.

2.12.2 H&E Staining

Slides were heated to 56°C for a minimum of 1 hour before being submerged in xylene for 20 minutes. Samples were rehydrated by immersing in 100% ethanol for 10 minutes, followed by 90% ethanol and 80% ethanol for 5 minutes each. Samples were then transferred to dH₂O for 5 minutes before being immersed in Haematoxylin (Sigma-Aldrich) for 3 minutes. Slides were washed under running H₂O for 2 minutes and placed in 1% acid alcohol for 20 seconds. Samples were washed again under running H₂O and immersed in Eosin Y (Sigma-Aldrich) for 3 minutes before washing again. Slides were dehydrated by immersing in 80%, 90% and 100% ethanol for 5 minutes each. Samples were air dried, mounted with DPX mounting media (Sigma- Aldrich) and examined under a light microscope.

2.12.3 Histological Scoring

Following hematoxylin and eosin Y (H&E) staining, slides were examined in a blind manner by covering the labels on each slide prior to examination. A semi-quantitative scoring chart

was used to assess disease progression in the lung, liver, small intestine, and colon (Tobin *et al.*, 2013). Pathological scores were assigned based on the system outlined in Table 2.15.

2.13 Statistical Methods

Statistical analysis was carried out using Graph Pad Prism software. Normality of datasets was tested using the Shapiro-Wilk or D'Agostino-Pearson omnibus normality test methods. Where n numbers were not sufficient for normality testing, non-normal distribution was assumed and non-parametric statistical testing was used. Non-parametrical tests were also used to analyse inherently non-parametric data such as frequency data, and histological scores. All comparisons made between two groups were based on non-parametric data, thus the Mann-Whitney test was used. For parametric data, statistical significance between multiple experimental groups was measured using One-way Anova with post hoc Tukey test. For non-parametric data, statistical significance between multiple experimental groups was measured using Kruskal-Wallis analysis followed by multiple comparisons correction by using the original False Discovery Rate of Benjamini and Hochberg. To compare survival of treatment groups in aGvHD studies, Kaplan Meier curves were generated and statistically analysed using the Mantel-Cox (log rank) test. To compare aGvHD scores between two groups, the Mann Whitney test was used at each time point measured.

Table 2.15: Tissue Scoring System of aGvHD model

Score	Lung	Liver	Small Intestine/Colon
0	Normal	Normal	Normal
1	Scattered areas of mononuclear cells	Scattered areas of mononuclear cells	Mild mononuclear cell infiltration
2	Mild focused areas of mononuclear cell infiltration	Increase in mononuclear cell infiltration and mild endothelialitis	Mild blunting of villi and increased mononuclear cell infiltration
3	Moderate levels of mononuclear cell infiltration and damage to lung architecture	Increase in mononuclear cell infiltration and moderate endothelialitis.	Moderate blunting of villi and increased, cell infiltration and presence of ulceration.
4	Areas of severe mononuclear cell infiltration and damage to lung architecture	Increase in mononuclear cell infiltration and endothelialitis in most vessels	Severe blunting of villi and increased, cell infiltration and presence of ulceration.

Chapter 3
Biodistribution and Modes of Action of MAPC
cells in a humanised model of aGvHD

3.1 Introduction

MSC and MAPC cells are adult progenitor cells with anti-inflammatory and tissue reparative properties (Kennelly, Mahon & English, 2016; Cahill *et al.*, 2016; Reading *et al.*, 2013; Eggenhofer *et al.*, 2013). While both MSC and MAPC cells adhere to plastic *in vitro* and demonstrate similar functions, differences in cell surface phenotype, gene expression, and expansion ability exist (Reading *et al.*, 2013; Crabbe *et al.*, 2016). As a number of cell types can be isolated from the BM, it is important to examine the characteristics of the different cell types using standardised methods to ensure the identity of those cells being used in the current study (Roobrouck *et al.*, 2011). Furthermore, for both ethical and practical reasons, *in vitro* potency assays should be used to validate the functional capacities of MAPC cells before introducing these cells to animal models (Lehman *et al.*, 2012).

With this in mind, a number of groups have shown that the *in vitro* immunosuppressive effects of MAPC cells can be reproduced *in vivo*, demonstrating therapeutic efficacy of MAPC cells in animal models of GvHD (Kovacsovics-Bankowski *et al.*, 2009; Highfill *et al.*, 2009). However, in a murine model, Highfill *et al.* (2010) demonstrated that MAPC cells are only therapeutic in GvHD when injected locally to the spleen. Most *in vivo* studies administer MSC and MAPC cells IV, and it has been widely reported that the vast majority of MSC injected IV to rodent models are trapped in the lungs, with only a small proportion of the cells administered reaching distal organs such as the spleen and liver. Furthermore, MSC are quickly cleared and are no longer detected *in vivo* within a few days of administration (Eggenhofer *et al.*, 2011; Moll & Blanc, 2015). This limited biodistribution and quick clearance of MSC and MAPC cells *in vivo* probably limits the efficacy of cells (Cornelissen *et al.*, 2015). In an effort to overcome these issues regarding limited potency of MAPC cells and MSC, our group and others have manipulated MSC prior to administration to animal models of disease. For example, our group have improved the efficacy of MSC administered to a humanised model of aGvHD by licensing cells with IFN- γ (Tobin *et al.*, 2013). IFN- γ stimulation of human MSC upregulates the expression of HLA ABC and IDO as well as a range of adhesion molecules and chemotactic factors. Thus, it is

possible that IFN- γ stimulation of MSC in this model enhanced the homing capacity or persistence of MSC *in vivo* which subsequently improved their therapeutic effect.

IFN- γ induces STAT1 phosphorylation in MSC which promotes the expression of IFN- γ target genes such as IDO and PDL1. IFN- γ and subsequent STAT1 phosphorylation are required for the therapeutic effects of MSC and MAPC cells in a number of *in vitro* and *in vivo* settings (Krampera *et al.*, 2006; Meisel *et al.*, 2004; Polchert *et al.*, 2008; Ren *et al.*, 2008; Vigo *et al.*, 2016; Mounayar *et al.*, 2015). Thus, MSC and MAPC cells fail to exert immunosuppression when IFN- γ concentrations are low, or when they exhibit poor responsiveness to IFN- γ activation. IFN- γ levels may be low *in vivo* when MSC or MAPC cells are given as a preventative rather than therapeutic treatment, or if given in conjunction with ISDs that suppress IFN- γ production by the host (Sivanathan *et al.*, 2014). Furthermore, IFN- γ responsiveness may vary between donors, or may be impaired following cryopreservation (François *et al.*, 2012b, 2012a).

It is clear that IFN- γ signalling in MSC and MAPC cells is imperative. Thus, the molecular mechanisms by which IFN- γ activates MSC and MAPC cells should be elucidated to identify further strategies of enhancing MSC and MAPC cell efficacy. Recently, Luz-Crawford *et al.* (2016) discovered a role for the nuclear receptor PPAR δ in the responsiveness of murine BM-MSC to concurrent IFN- γ and TNF- α stimulation. PPAR δ ^{-/-} MSC exhibited increased NF- κ B activity in response to these cytokines, and demonstrated superior therapeutic efficacy in an *in vivo* model of arthritis compared to wildtype MSC. Furthermore, PPAR δ expression among human MSC derived from different tissues inversely correlated with T cell suppressive activity *in vitro*. In macrophages PPAR δ is thought to inhibit STAT1 activation (Adhikary *et al.*, 2015), thus it is possible that PPAR δ may also suppress IFN- γ mediated STAT1 signalling in MSC and MAPC cells. This chapter begins by examining the characteristics of human MAPC cells and MSC and validates that the cells being used for this study meet the criteria of MAPC cells as outlined by the international society of cellular therapies (ISCT) (Dominici *et al.*, 2006). Cell surface and morphology were compared with

those of MSC and the functional capacities of MAPC cells were confirmed before moving on to *in vivo* experiments.

While the rodent studies mentioned above have provided us with great insight into the efficacy and modes of action of MSC and MAPC cells in GvHD, for this work the use of humanised models of aGvHD is advantageous as they allow for the study of interactions between human MAPC cells and human immune cells (Tobin *et al.*, 2013). Therefore, the aim of this chapter was to determine the biodistribution of human MAPC cells in a humanised model of aGvHD using CryoViz™ imaging technology. Following on from that I sought to optimise the delivery of MAPC cells to aGvHD target organs by activating MAPC cells with IFN- γ prior to administration, and finally I sought to examine the role of PPAR δ in the efficacy and biodistribution of MAPC cells in aGvHD.

3.2 Characterisation of surface markers expressed by human MAPC cells

While both MSC and MAPC cells are isolated from the BM and have similar functions, phenotypic differences exist between the populations due to differences in culture protocols (Crabbe *et al.*, 2016). The most obvious differences between the cell types are their morphology and cell surface phenotype. In order to ensure cells used in this study displayed the correct morphology, cultures were examined before each passage by light microscopy at 10X magnification. MSC and MAPC cells used in this study were isolated from the same human donor BM samples and both MSC and MAPC cells adhered to plastic as expected (Dominici *et al.*, 2006). MAPC cells exhibited a typical spindle shaped morphology and were smaller than their MSC counterparts which had a ‘fibroblast like’ appearance as previously reported by Roobrouck *et al.* (2011) (Fig. 3.1).

As neither MAPC cells or MSC express a single identifying surface marker, the ISCT have outlined a panel of surface markers which should be positively or negatively expressed by MAPC cells and MSC (Dominici *et al.*, 2006). While both MAPC cells and MSC are heterogeneous cell populations, generally both cell types should express high levels of CD44, CD90 and CD105, and should be negative for expression of CD45 and HLA DR. HLA ABC

is expressed by both cell types, however it is much more highly expressed on MSC than MAPC cells which allows for identification/differentiation between the two cell types (Table 3.1) (Reading *et al.*, 2013; Crabbe *et al.*, 2016). In order to ensure the quality of MAPC cells and MSC used in this study, cultures were examined for the expression of this panel of surface markers. Confluent cultures were trypsinised and prepared for flow cytometry as described in section 2.6.2 and samples were acquired on an Accuri C6. Cells used for this project adhered to the ISCT criteria as shown in Table 3.1 and Fig. 3.2, confirming that MAPC cells and MSC were pure populations, and were not contaminated with haematopoietic cells.

3.3 MAPC cells and MSC CM induces tube formation of HUVEC

Following on from validating the identity and purity of MSC and MAPC cells cultures, it is imperative that functionality of the cells is proven before moving on to *in vivo* experiments. The angiogenic capacity of MAPC cells is an important feature of their therapeutic efficacy (Lehman *et al.*, 2012), and it has previously been shown *in vitro* and *in vivo* that MAPC cells are more effective at promoting angiogenesis than MSC (Roobrouck *et al.*, 2011). Thus, the pro-angiogenic effect of MAPC cells was examined and compared with that of MSC, using a Matrigel™ tube formation assay (Lehman *et al.*, 2012).

HUVEC in MAPC cells or MSC conditioned media (CM) were added to a Matrigel™ matrix and incubated for 18 hours, before the numbers of tubes formed between cells were counted as described in section 2.6.3. HUVEC cultured in EBM were used as a negative control for the assay, and EGM as a positive control. Serum free media which had no contact with cells was used as a negative control for MAPC cells and MSC CM. While both MAPC cells CM and MSC CM significantly increased the number of tubes formed compared to the negative control (6 ± 2.387 , $n = 12$), MAPC cells CM was more effective than that of their MSC counterparts (38.33 ± 3.518 , and 26.92 ± 3.090 respectively, $n = 24$) (Fig 3.3).

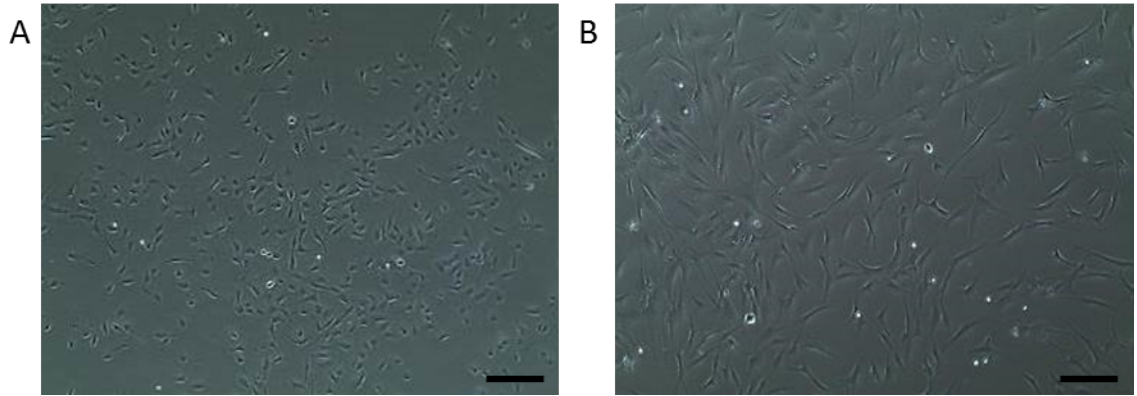


Figure 3.1 Morphology of cultured human MAPC cells compared to human MSC from the same donor. MAPC cells at PD 21 were small spindle shaped cells (A), while MSC from the same donor at PD 17 were also spindle shaped but longer and larger, with fibroblast like morphology (B). Original magnification X10, phase-contrast, light microscopy. Scale bars indicate 100nm.

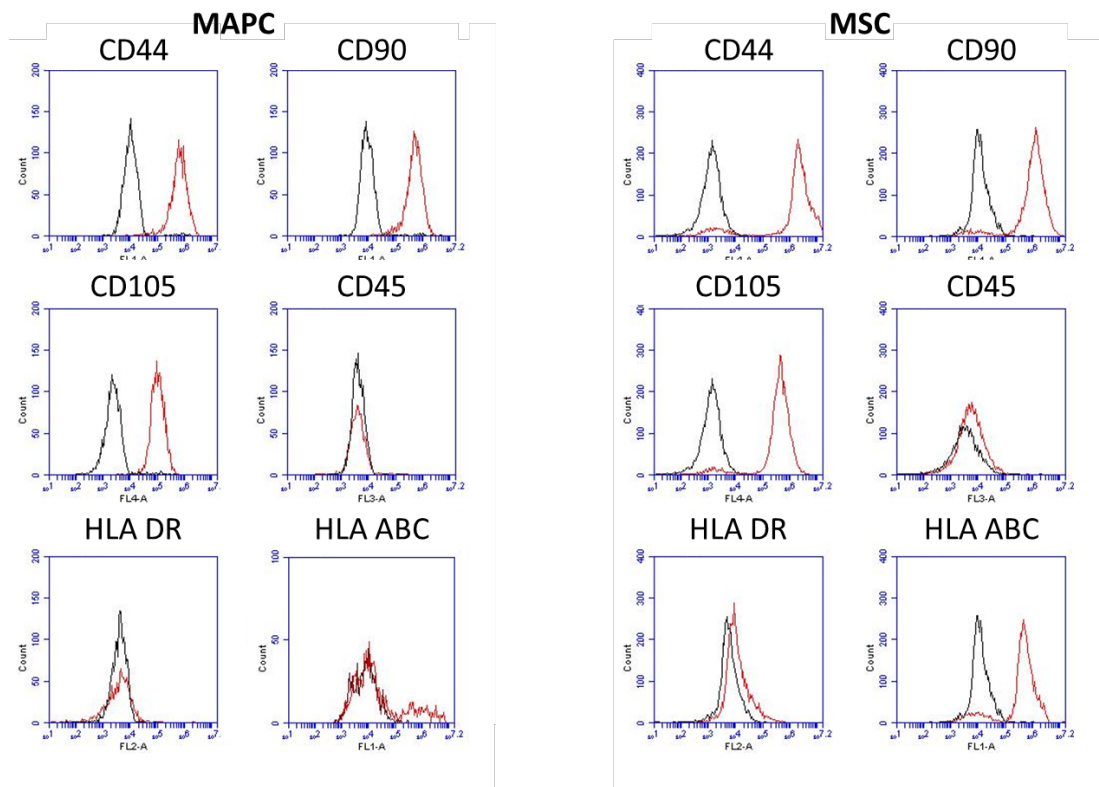


Figure 3.2 Comparison of MAPC cells and MSC surface phenotype. MAPC cells and MSC at PDs 15-30 were examined for surface expression of a range of markers typically used to characterise both cell types using flow cytometry. Both MAPC cells and MSC (red histogram) expressed high levels of CD44, CD90 and CD105 compared to isotype controls (black histogram), while neither cell type expressed CD45 or HLA DR. MAPC cells expressed lower levels of HLA ABC than MSC. This data is representative of 3 MAPC cell and MSC donors.

Table 3.1 Surface Marker Expression by MAPC cells and MSC

Marker	MAPC cells	MSC
CD13	+	+
CD34	-	-
CD44	+	+
CD45	-	-
CD49c	+	+
CD73	+	+
CD80	-	-
CD86	-	-
CD90	+	+
CD105	+	+
HLA ABC	-	+
HLA DR	-	-

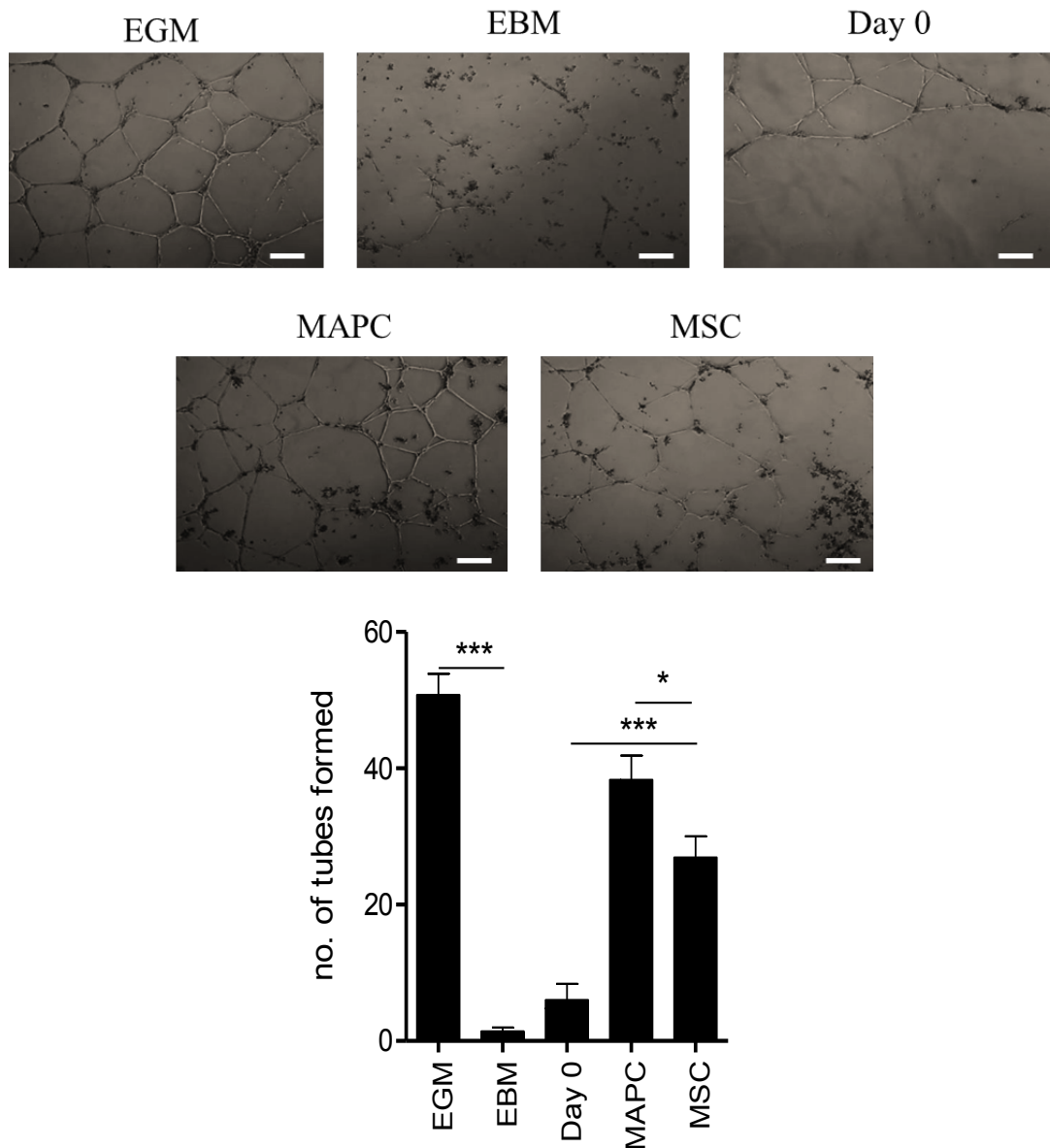


Figure 3.3 MAPC cells and MSC promote tube formation of HUVEC in a Matrigel™ assay. HUVEC in the appropriate media were added to a Matrigel™ matrix for 18 hours and the number of tubes formed between cells was counted. Each condition was compared to HUVEC in serum free media (Day 0). Representative images show that CM collected from MAPC cells cultures were more pro-angiogenic than CM collected from their MSC counterparts. Original magnification X10, phase-contrast, light microscopy. Scale bars indicate 100nm. (A). This assay was done in triplicate for 2 donors, and the number of tubes was counted in 4 random fields in each well (B). Data was tested for normality using a D'Agostino Shapiro test and statistics were determined using ANOVA analysis with a post-hoc Tukey test where * ≤ 0.05 , and *** ≤ 0.001 ; n = 8.

3.4 MAPC cells differentiate into adipocytes and osteocytes.

Another key requirement of MSC and MAPC cells as outlined by the ISCT is their capacity to differentiate into adipocytes and osteocytes (Dominici *et al.*, 2006). Thus, MAPC cells used in this study were assessed for their capacity to differentiate into adipocytes and osteocytes under controlled *in vitro* conditions. Differentiation was induced and examined using the method described in section 2.6.4. MAPC cells which differentiated into adipocytes appeared red following staining with Oil Red O compared to control wells, indicating intracellular lipid vacuoles (Fig. 3.4A). MAPC cells which differentiated into osteocytes appeared red following alizarin red staining compared to control wells indicating mineralisation (Fig. 3.4B). This data demonstrates that MAPC cells used in this study can differentiate along mesenchymal lineages, in line with the criteria outlined by the ISCT (Dominici *et al.*, 2006).

3.5 MAPC cells suppress T cell proliferation induced by CD3/CD28 activation beads in a dose-dependent manner

The most important characteristic of MAPC cells for this project is their ability to suppress inflammation. It has been previously shown that MAPC cells suppress T cell proliferation *in vitro* (Reading *et al.*, 2013, 2015) and I wished to confirm that cells used for this project displayed this capability before advancing on to *in vivo* studies. MAPC cells were seeded into 96 well round bottom plates at a range of densities. 24 hours later MAPC cell medium was removed and 5×10^4 CFSE labelled PBMC in cRPMI were added to each well with 1×10^4 anti CD3/CD28 beads as described in section 2.6.5. 4 days later PBMC were collected and stained with CD3 antibody and 7AAD to examine the proliferation of live T cells by flow cytometry. The number of proliferating CFSE labelled T cells was enumerated using counting beads. The number of T cells proliferating when PBMC were cultured with anti CD3/CD28 beads was significantly increased compared to controls as expected ($n = 8$). MAPC cells were shown to significantly suppress T cell proliferation at each ratio of 1:5, 1:10, 1:20 and 1:40 MAPC cells to PBMC ($n = 8$). This immunosuppression was decreased as the ratio of PBMC to

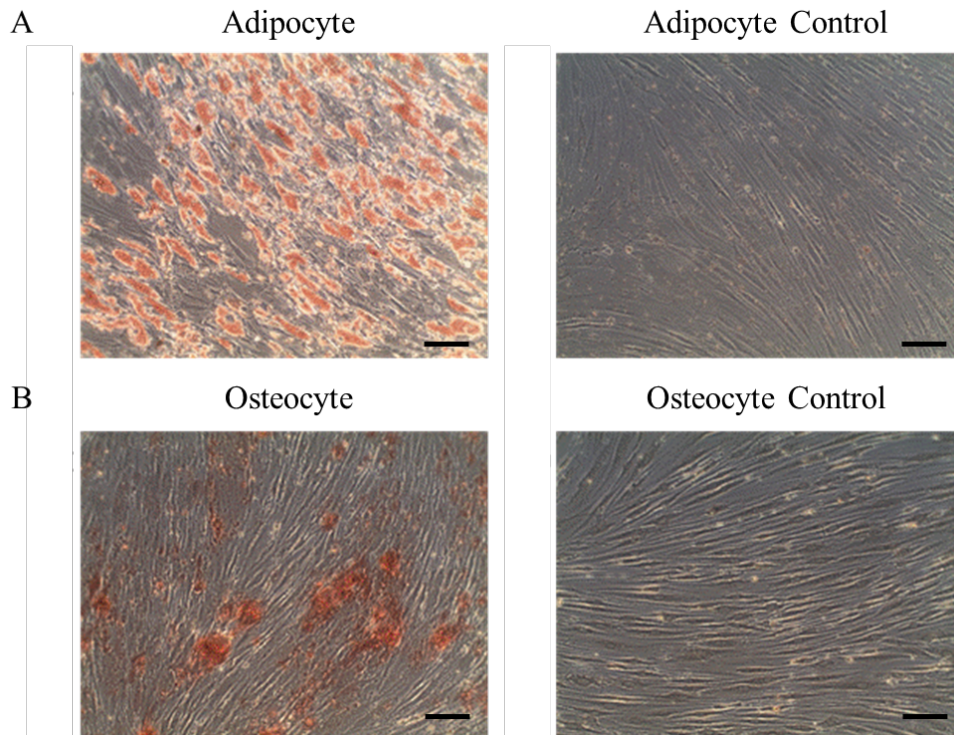


Figure 3.4 MAPC cells differentiate into adipocytes and osteocytes. MAPC cells were seeded into 6 well plates and when confluent, the appropriate differentiation media was added. Media was changed every 2-3 days and cells were stained on day 10 using Oil Red O to stain cells in adipocyte differentiation media and adipocyte control media (A). Alizarin Red S was used to stain cells in osteocyte differentiation media and osteocyte controls media (B). Adipocytes and osteocytes stained red, proving that MAPC cells can differentiate into adipocytes and osteocytes. Original magnification X10, phase-contrast, light microscopy. Scale bars indicate 100nm.

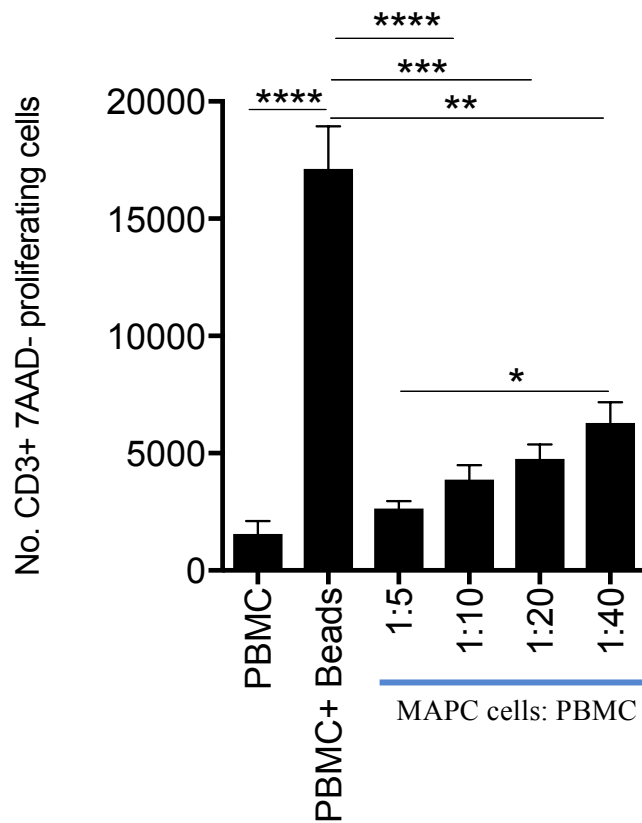


Figure 3.5 MAPC cells suppress T cell proliferation in a dose dependent manner.

MAPC cells were seeded into 96 well round bottom plates at a range of densities and incubated overnight. PBMC (5×10^4) were added to each well with CD3/CD28 activation beads at a ratio of 1:5. PBMC were harvested on day 4 and stained for 7AAD and CD3. MAPC cells were shown to suppress the proliferation of CD3⁺ cells in a dose dependent manner, with the proliferation of T cells increasing as the ratio of MAPC cells: PBMC increased. Counting beads were used to quantify results. This assay was done in duplicate with 4 MAPC cell donors and 2 PBMC donors and statistics were determined using Kruskal-Wallis analysis with the original FDR method of Benjamini and Hochberg to correct for multiple comparisons where $* \leq 0.05$, $** \leq 0.01$, $*** \leq 0.001$; and $**** \leq 0.001$ n = 8)

MAPC cells increased, showing that MAPC cells suppress T cell proliferation in a dose dependent manner (Fig. 3.5).

3.6 Human MAPC cells administered on day 7 but not day 0 significantly increase survival and reduce pathology in aGvHD mice.

Both MSC and MAPC cells have previously been shown to increase survival in animal models of GvHD (Highfill *et al.*, 2009; Kovacsovics-Bankowski *et al.*, 2009; Tobin *et al.*, 2013; Auletta *et al.*, 2015). In the humanised aGvHD model it has been shown by our group that MSC are effective at treating aGvHD when given on day 7 but not on day 0 (Tobin *et al.*, 2013). Therefore, I sought to compare the efficacy of MAPC cells administered along with PBMC on day 0 of the aGvHD model, to MAPC cells administered on day 7, in order to determine the optimal timing for MAPC cells administration. PBMC were isolated from buffy packs and administered to irradiated (2.4 Gy) NSG mice via tail vein injection ($8 \times 10^5/g$) as described in section 2.8.1. Control groups were established by administering sterile PBS to irradiated NSG mice, and by administering MAPC cells on day 7 to PBS mice. MAPC cells ($6.4 \times 10^5/g$) were administered either alongside PBMC on day 0 or on day 7 to both PBMC and PBS mice. All mice were monitored daily and weight loss was measured every 2 days until day 9 and then every day for the duration of the experiment. Each mouse was regularly assigned an aGvHD score based on the presentation of aGvHD symptoms such as weight loss, appearance and reduced activity. Animals which presented with a weight loss of more than 15% or an aGvHD score of 5 were sacrificed.

As expected, the administration of PBS to irradiated NSG mice had no effect on survival and did not result in an increased aGvHD score ($n = 6$). NSG mice which received PBMC only developed aGvHD symptoms including weight loss, reduced activity and a hunched posture from day 11 and had an overall aGvHD score of 4.255 ± 0.4845 ($n = 6$). MAPC cells administered on day 0 did not alleviate the symptoms of aGvHD with this group having a mean aGvHD score of 4.417 ± 0.5414 ($n = 6$). Unsurprisingly, animals that received MAPC cells on day 7 were slower to show signs of aGvHD than those that received PBMC

only, with a mean aGvHD score of 2.225 ± 0.2524 . From day 16 onwards the aGvHD score of mice that received MAPC cells on day 0 was significantly higher than the scores of those given MAPC cells on day 7 (Fig 3.6A).

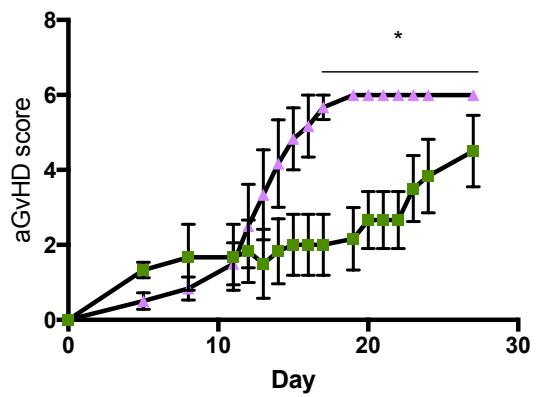
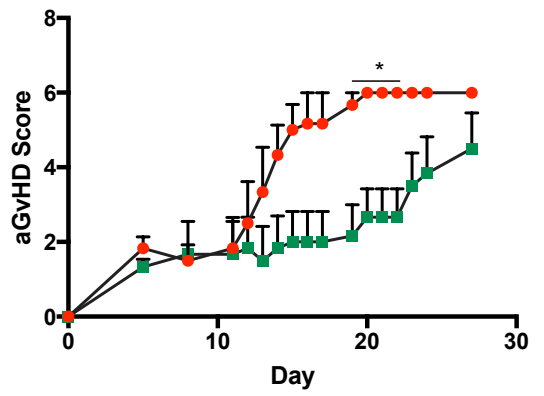
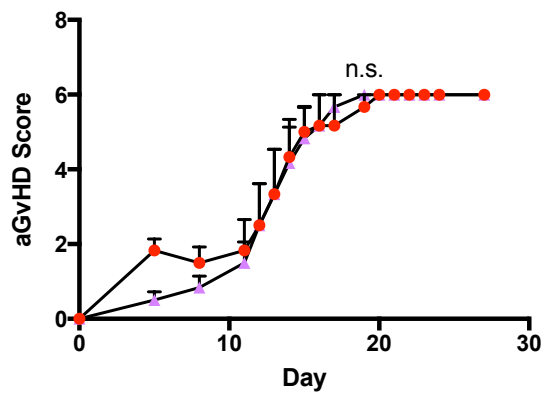
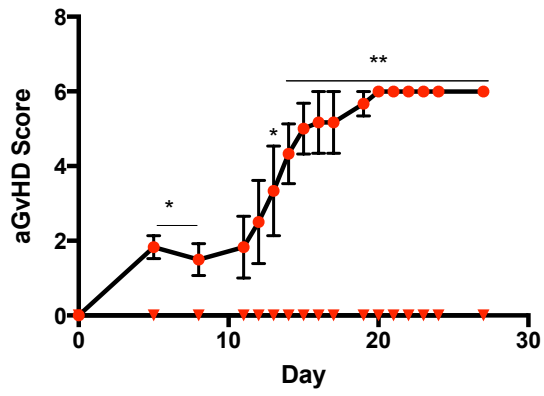
Similarly, the survival of aGvHD mice reflected that of the aGvHD score, with MAPC cells administered on day 7 but not day 0 significantly prolonging survival. Mice that received PBMC only were humanely euthanised between days 11 and 16 and had a median survival time of 13.5 days ($n = 6$). MAPC cells administered on day 0 did not significantly improve the survival of aGvHD mice, with the median survival time of this group being 15 days ($n = 6$), while MAPC cells administered on day 7 significantly prolonged the survival of aGvHD mice. Mice receiving MAPC cells on day 7 had a median survival time of 26 days, with 30% of the group surviving until the end of the study ($n = 6$) (Fig. 3.6B). Therefore, the optimal time to give MAPC cells to the aGvHD model is day 7, which aligns with previous work from our lab using MSC (Tobin *et al.*, 2013).

3.7 Human MAPC cells administered on day 7 decrease the pathology in target organs of aGvHD.

aGvHD is a systemic disease with detrimental effects in a number of organs including the lungs, liver and small intestine (Sung & Chao, 2013). Since MAPC cells significantly improved survival in the aGvHD model, it was hypothesised that tissue damage at these sites would be reduced following MAPC cells therapy. Thus, lung, liver, small intestine and colon were harvested on day 12 of the model and placed in 10% formalin for 24 hours, followed by immersion in 70% ethanol for 24-72 hours before being processed as described in section 2.12.1. Tissue was sectioned and collected on glass slides before being stained with H&E as described in section 2.12.2. Histological scores were blindly assigned to tissue samples following a scoring system previously used by Tobin *et al.* (2013) (Table 2.15).

The small intestine of mice that received PBMC showed increased blunting of the villi and ulceration compared to the PBS group. Thus, the pathological score increased from

A



B

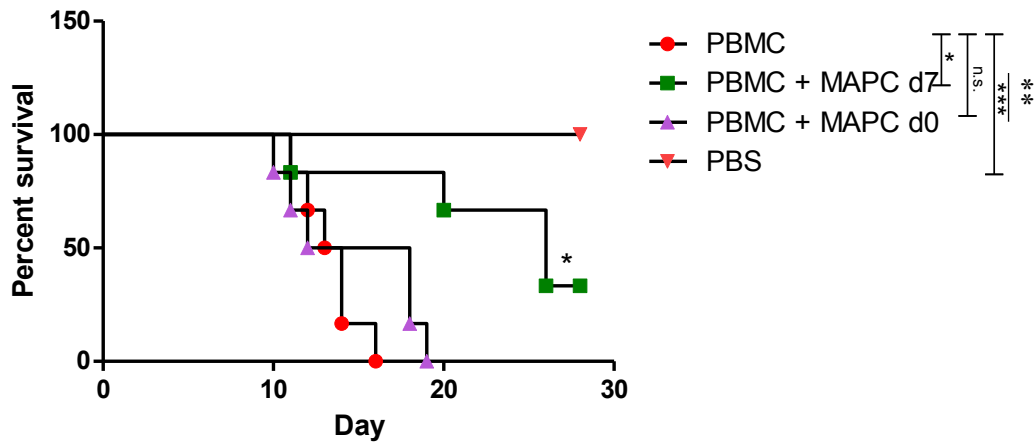
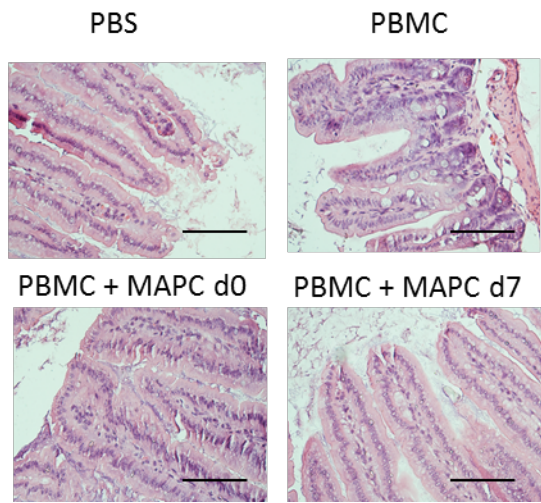


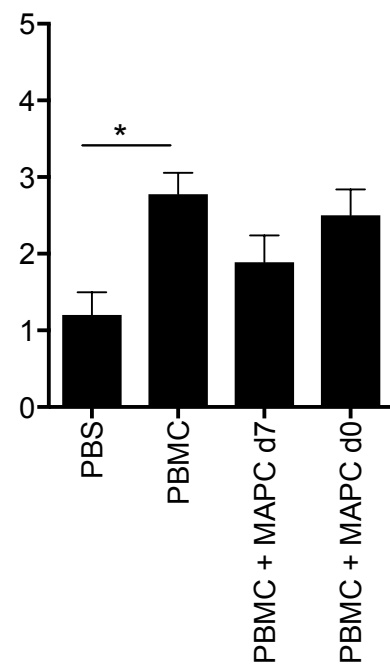
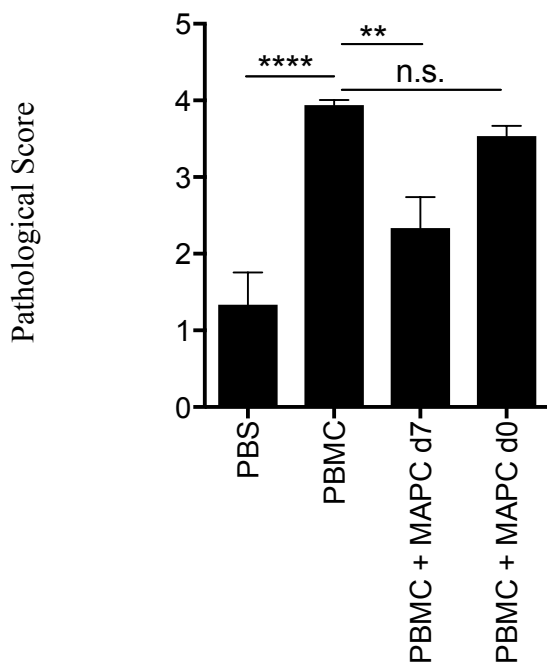
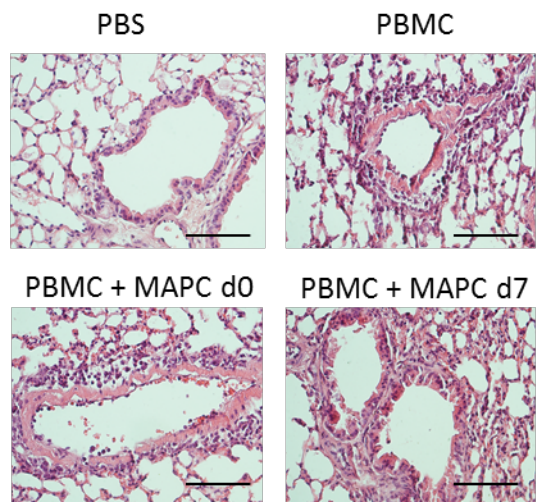
Figure 3.6 MAPC cells administered on day 7 but not day 0 reduce the pathological score and prolong survival in aGvHD. 8×10^5 human PBMC per gram were administered to irradiated NSG mice on day 0. 6.4×10^4 human MAPC cells per gram were administered along with PBMC on day 0 or 7 days later. Mice were monitored on a daily basis for symptoms of aGvHD and aGvHD scores were assigned every second day until day 9 and then every day until the end of experiment (A). Mice with a pathological score of 5 or higher were humanely euthanised by cervical dislocation (B). Statistical analysis of aGvHD scores between groups was carried out by completing a Mann-Whitney comparison of scores at each time point. Statistical analysis of the survival curve was carried out using a Mantel Cox test where $* \leq 0.05$ $** \leq 0.01$ and $*** \leq 0.001$. Experiments were carried out using 2 PBMC donors and 2 MAPC cell donors, $n = 6/\text{group}$.

1.333 ± 0.4216 in the PBS group to 3.933 ± 0.06667 in the PBMC group (n = 6). In animals where MAPC cells were administered on day 7, aGvHD associated damage was alleviated, and thus the score was significantly reduced to 2.333 ± 0.4082 (n = 6). MAPC cells administered on day 0 also slightly reduced the pathological score in the small intestine, however this was to a lesser extent than MAPC cells administered on day 7 (n = 6) (Fig. 3.7A). In the lung, scores were given based on mononuclear cell infiltration around vessels and alveolar spaces. As expected, infiltration was increased in the PBMC group compared to the PBS group, with the pathological score increasing from 1.200±0.2960 to 2.778 ± 0.2778 (n = 6). MAPC cells administered on day 0 had little to no effect in the lung, while MAPC cells administered on day 7 reduced infiltration and slightly decreased the pathological score to 1.889 ± 0.3514 (Fig. 3.7B). Similarly, in the liver, scores were given based on mononuclear cell infiltration around blood vessels. Pathological score was increased from 0.444 ± 0.2422 in the PBS group to 3.267 ± 0.1533 in the PBMC group (n = 6). This was reduced to 2.333 ± 0.1880 following MAPC cells therapy on day 7 (n = 6) and 1.333 ± 0.2887 by MAPC cells administered on day 0 (n = 6) (Fig. 3.7C). In the colon, PBMC resulted in ulceration in the lamina propria, thus the score increased from 1.667 ± 0.2108 in the PBS group to 3.333 ± 0.2108 in the PBMC group (n = 6). MAPC cells administered on day 0 had no effect on the pathological score in the colon, while MAPC cells administered on day 7 reduced the score to 2.444 ± 0.4120 (n = 6) (Fig. 3.7D). Thus, as expected based on the survival data, MAPC cells administered on day 7 reduced damage in aGvHD target organs to a greater extent than MAPC cells administered on day 0.

(A) **Small Intestine**



(B) **Lung**



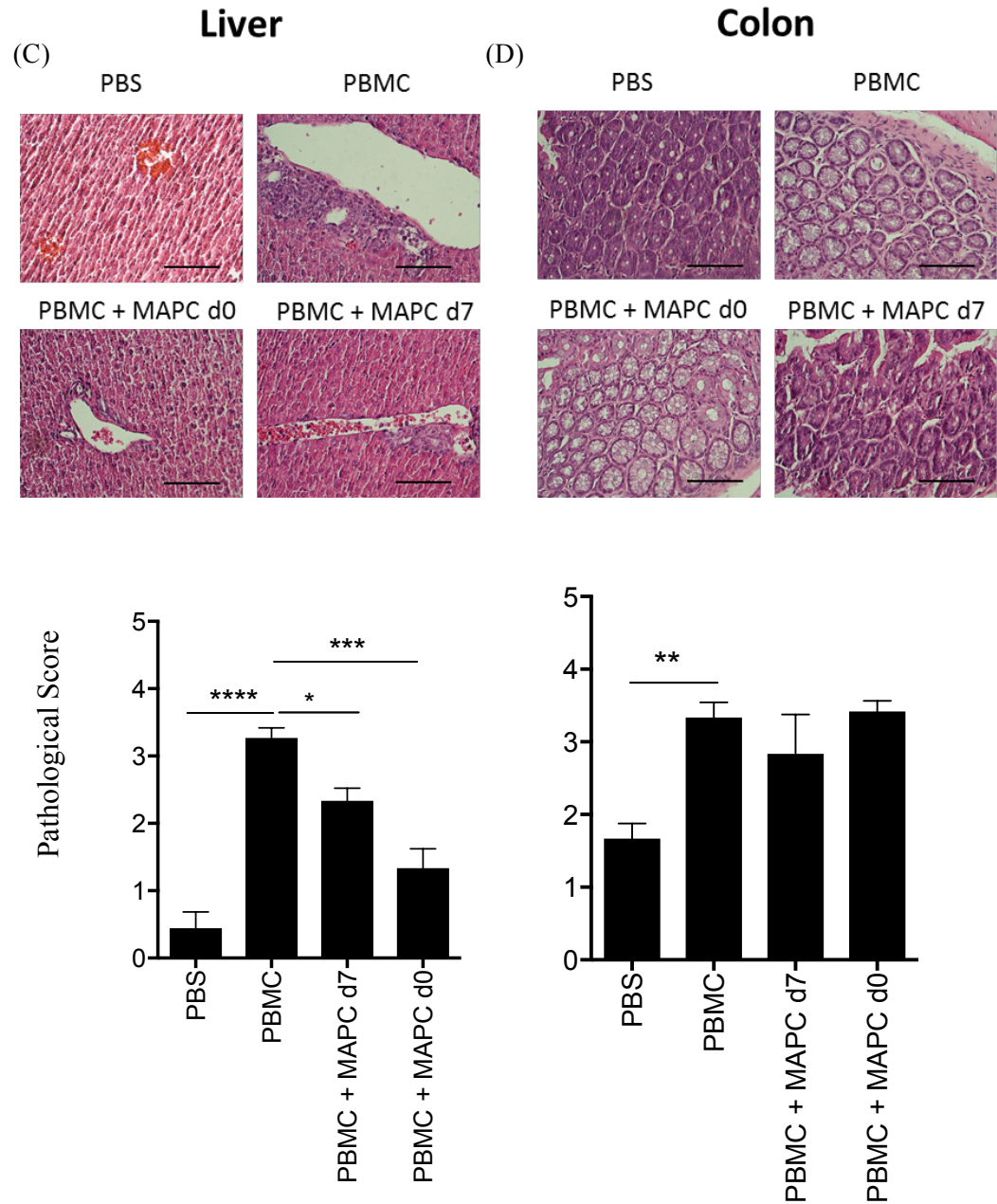


Figure 3.7 MAPC cells administered on day 7 but not day 0 reduce the pathological score aGvHD target tissues. The aGvHD model was set up as described in figure legend 3.6 and small intestine (A), lung (B), liver (C) and colon (D) harvested on day 12. Tissue was processed and stained using H&E as described in section 2.12 and tissue sections were blindly assigned pathological scores based on the criteria outlined in table 2.15. Statistical analysis of pathological scores was carried out using Kruskal-Wallis analysis with the original FDR method of Benjamini and Hochberg to correct for multiple comparisons where $* \leq 0.05$, $** \leq 0.01$, $*** \leq 0.001$; and $**** \leq 0.001$ Experiments were carried out using 2 PBMC donors and 2 MAPC cell donors ($n = 6/\text{group}$). Pictures were taken at 40X objective, scale bars indicate 50 μm .

3.8 The number of MAPC cells detected in target organs following IV injection is higher in mice that have received PBMC than healthy controls.

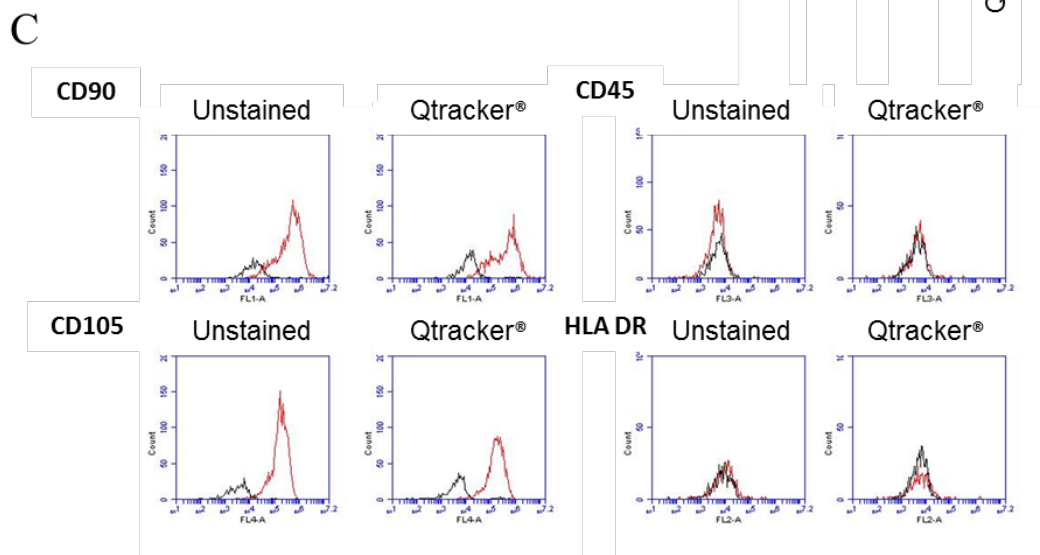
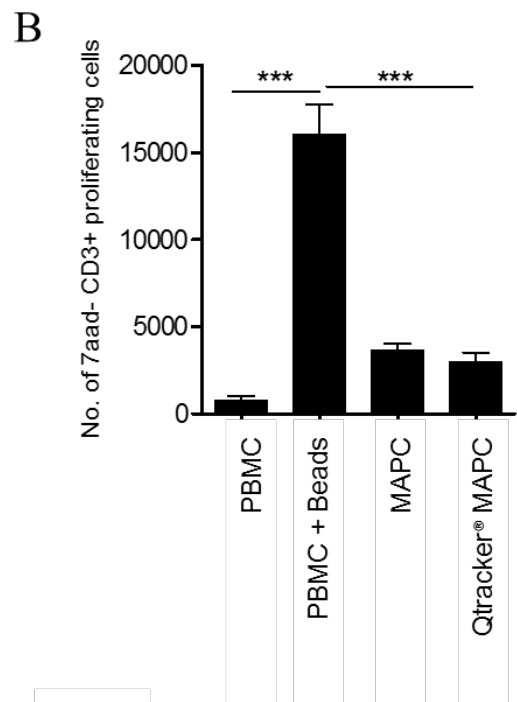
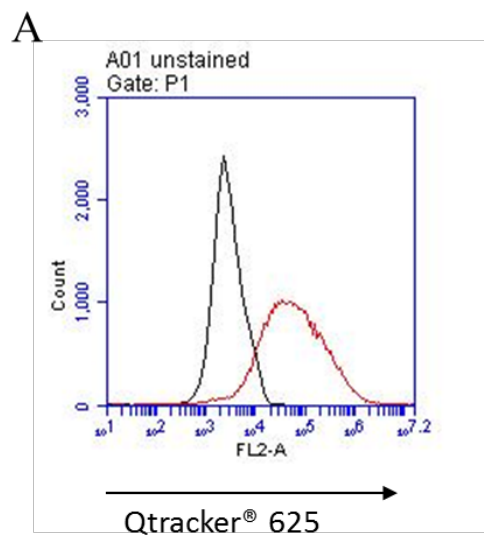
As shown in sections 3.6 and 3.7, systemically infused MAPC cells on day 7 are effective at prolonging survival of aGvHD mice. One of the major obstacles surrounding the use of systemically infused cellular therapies is the entrapment of cells in the lungs, decreasing the therapeutic outcome of MSC or MAPC cells (Eggenhofer *et al.*, 2014). MAPC cells are only effective at treating GvHD when injected locally to the spleen, suggesting that MAPC cells mediate their effects from contact with T cells at allo-priming sites (Highfill *et al.*, 2009). It has previously been shown that some MSC migrate to the spleen in a murine model of GvHD (Auletta *et al.*, 2015), however I wondered whether the homing of MSC to the spleen in this instance was passive, or whether MSC were actively migrating towards stimuli such as inflammatory and chemotactic signals from T cells. Therefore, I sought to compare the biodistribution of MAPC cells in PBS and PBMC mice to determine whether MAPC cells would respond to the inflammatory environment *in vivo*, and migrate to target organs accordingly.

In order to visualise MAPC cells *in vivo*, MAPC cells were fluorescently labelled by incubating cells with the Qtracker[®] 625 labelling kit for 1 hour as described in section 2.11.1 (Fig. 3.8A). Validation assays confirmed that Qtracker[®] staining had no effect on the *in vitro* immunosuppressive capacity (Fig. 3.8B) or surface phenotype (Fig. 3.8C) of MAPC cells. The aGvHD model was set up as described in section 3.6 and 1×10^6 Qtracker[®] labelled MAPC cells were administered on day 7 to PBMC or PBS mice. Lung, liver and spleens were harvested either 4 or 24 hours later, and snap frozen in black OCT in cryomolds and stored at -80°C . Whole mice were harvested 48 hours after MAPC cells administration. Samples were then sectioned and brightfield and fluorescent images taken using the CryoViz[™] as described in section 2.11.3. MAPC cells could be visualised in fluorescent images in red (Fig. 3.8D). Sections were then processed into 3D images using CryoViz[™] pre-processor software, and fluorescent MAPC cells were quantified using CryoViz[™] cell detection software. Overlays of

3D images and detected cells were generated using the Amira software package and for presentation purposes detected cells were displayed as yellow beads.

At 4 hours post MAPC cell administration, approximately 150,000 – 200,000 cells were detected in the lungs, with a slightly higher number of cells detected in the lungs of PBMC mice than PBS mice. However, at 24 hours post administration the number of MAPC cells detected in the lungs was reduced to 38660 ± 10290 ($n = 4$) in the PBS group and 17470 ± 2390 ($n = 4$) in the PBMC group (Fig. 3.9A). This data suggests that the majority of MAPC cells are either migrating from the lungs to other sites between 4 and 24 hours, or are being cleared at this time point. Furthermore, the difference seen in the PBS and PBMC group at 24 hours suggests that MAPC cells in mice that received PBMC are migrating from the lungs in higher numbers than MAPC cells in healthy mice, or are being cleared faster due to the presence of PBMC.

In the liver, the number of cells detected at 4 hours was 2479 ± 972.3 in the PBS group compared to 16430 ± 3435 in the PBMC group ($n = 4$). Interestingly, in the PBS group this number increased to 5676 ± 2159 at 24 hours, while in the PBMC group it decreased to 5428 ± 1473 ($n = 4$) (Fig. 3.9B). In the spleen at 4 hours, just 9.111 ± 2.884 cells were detected in PBS group compared to 46.222 ± 14.66 in the PBMC group ($n = 9$), and these numbers increased to 32.2 ± 12.19 and 83.20 ± 7.908 at 24 hours respectively ($n = 9$) (Fig. 3.9C). This suggests that MAPC cells are mobilised to the spleen faster in PBMC mice than PBS mice, however in the lung and liver MAPC cells may be being cleared quicker in the presence of PBMC. To check if MAPC cells were being cleared faster in PBMC mice than PBS mice, the total number of MAPC cells in a whole mouse was measured 48 hours after administration. There was no striking difference in biodistribution of MAPC cells in whole mice when comparing PBS mice to PBMC mice, however the total number of cells detected was higher in the PBMC mouse than the PBS mouse (Fig. 3.10). This suggests that MAPC cells are not subject to accelerated clearance in PBMC mice than PBS mice, and so the lower number of cells detected in the lungs of PBMC mice may be due to migration of MAPC cells to other sites.



D

Brightfield



Fluorescent

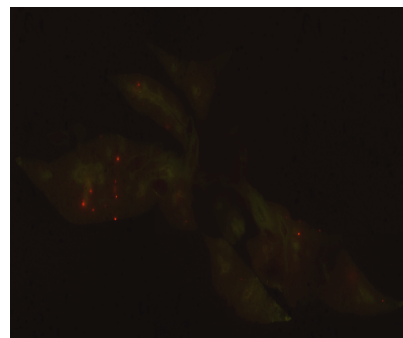
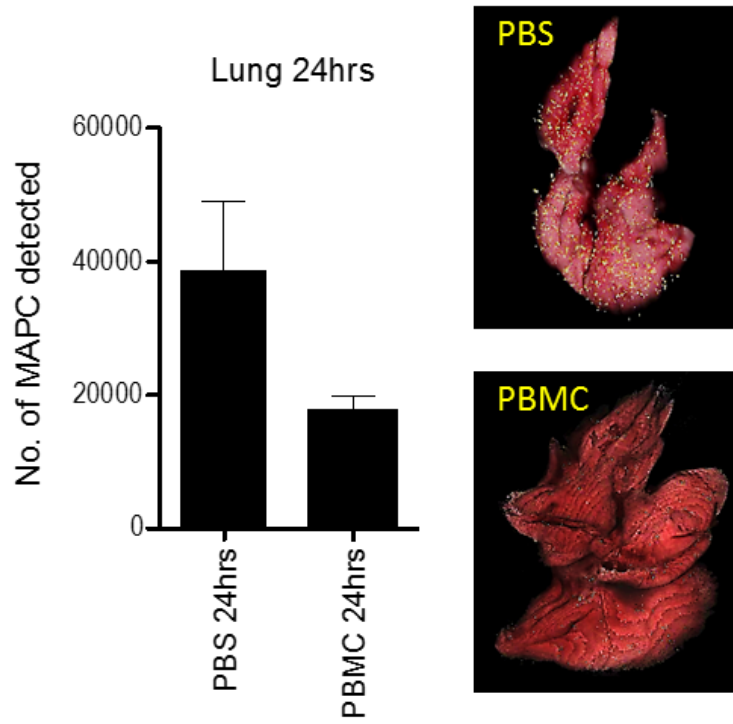
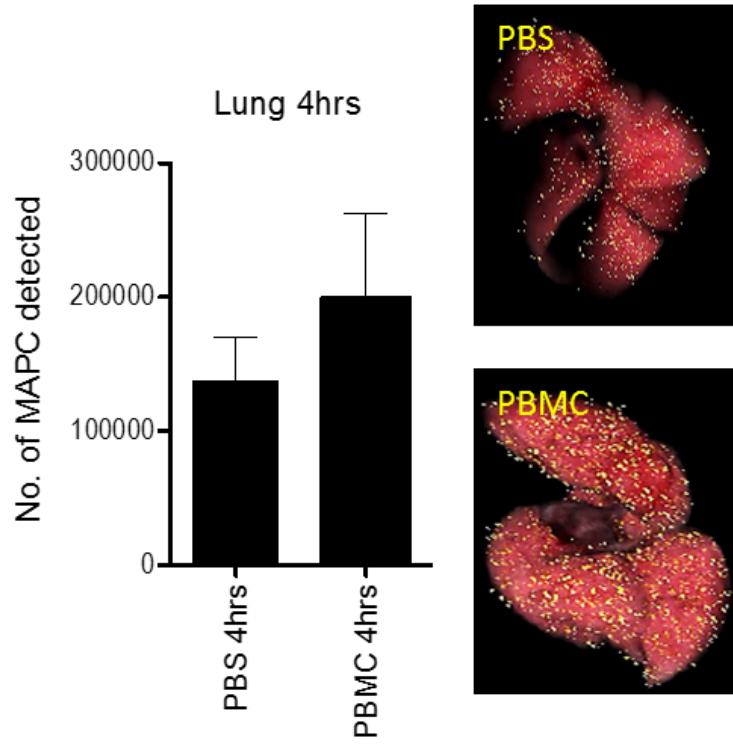
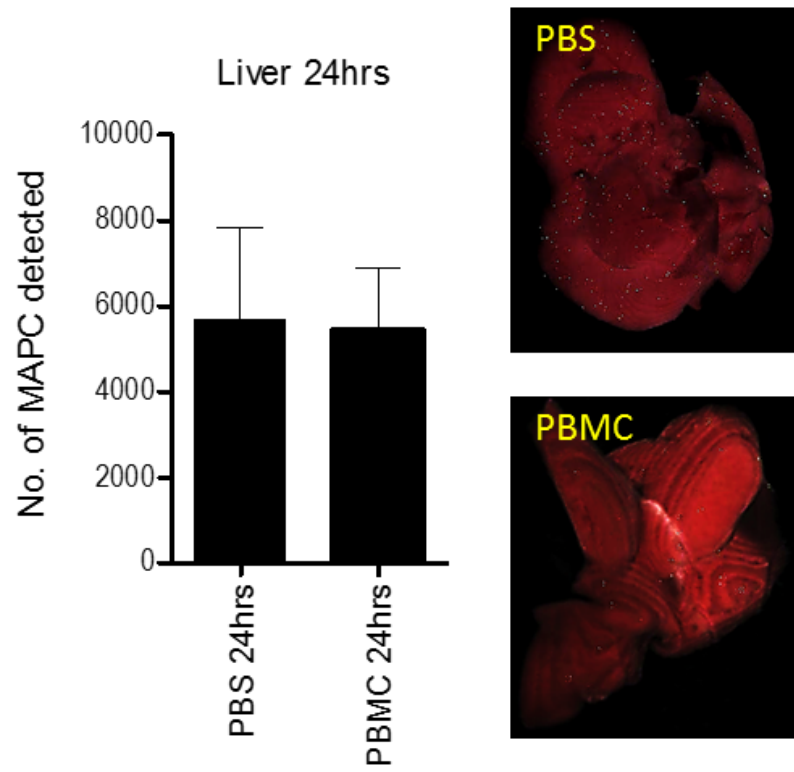
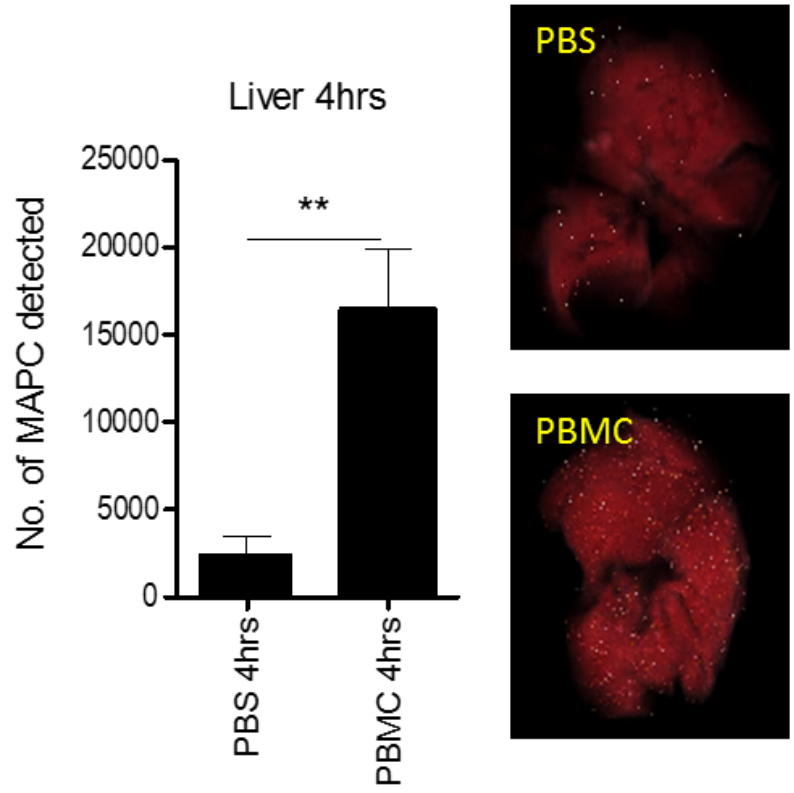


Figure 3.8 MAPC cells stained with Qtracker[®] 625 retain their immunosuppressive capacities and surface phenotype. MAPC cells washed and incubated with Qtracker[®] 625 labelling kit at a concentration of 10×10^6 cells/ml for 1 hour at 37°C with gentle rocking. Cells were washed and checked for fluorescence by flow cytometry prior to IV administration. Black overlays show unstained cells. Red overlays show Qtracker[®] stained cells (A). The immunosuppressive capacity of MAPC cells and Qtracker[®] stained MAPC cells was compared in a T cell proliferation assay as described in figure legend 3.7 (B). The surface phenotype of unstained MAPC cells and Qtracker[®] stained MAPC cells was compared by looking at expression of CD90, CD105, CD45 and HLA-DR. Black overlays indicated isotype controls and red overlays indicate antibody stained cells (C). Brightfield and fluorescent images of lung tissue showing Qtracker[®] stained MAPC cells in lung tissue (D). Statistical analysis of proliferation assay was carried out using Kruskal-Wallis analysis with the original FDR method of Benjamini and Hochberg to correct for multiple comparisons where $* \leq 0.05$, $** \leq 0.01$, $*** \leq 0.001$; and $**** \leq 0.001$

A



B



C

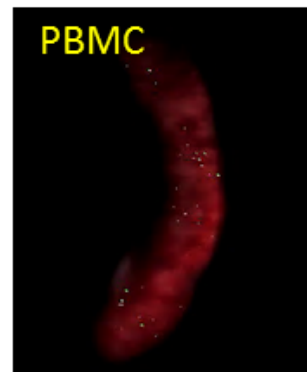
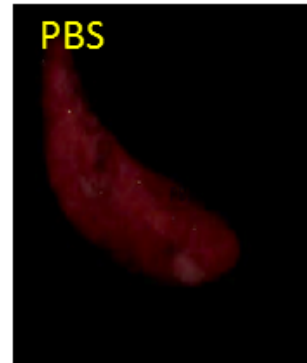
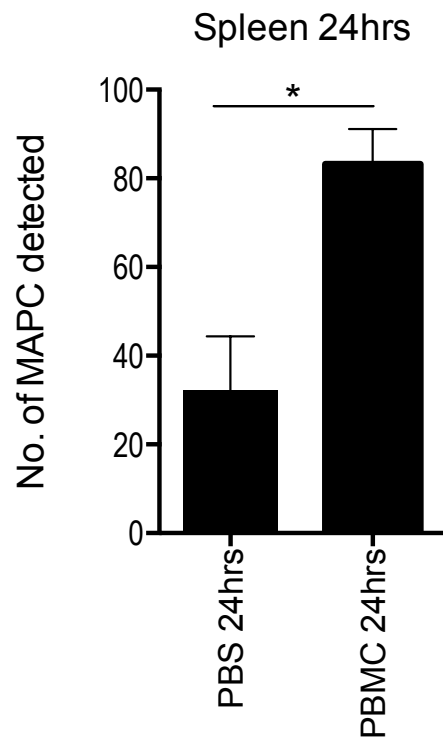
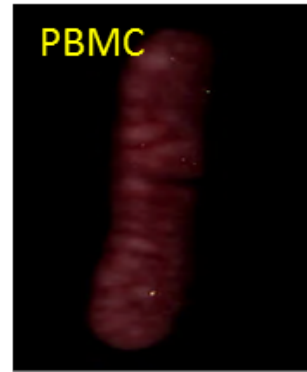
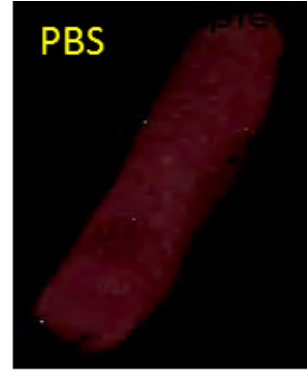
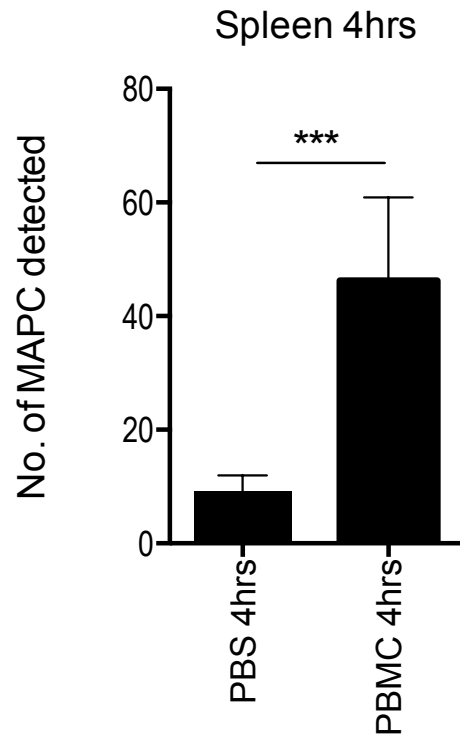


Figure 3.9 Biodistribution of MAPC cells differs in healthy and aGvHD mice. MAPC cells were stained with Qtracker[®] 625 as described in figure legend 3.8. MAPC cells were administered IV to PBS or PBMC mice on day 7 of the aGvHD model. Lung (A), liver (B) and spleen (C) were harvested at 4 and 24 hours post MAPC cell administration and snap frozen in black OCT. Organs were sectioned and imaged using the CryoViz[™]. Images were processed and the number of MAPC cells detected were quantified using CryoViz[™] software packages. The number of MAPC cells detected in the lung and liver reduced over time, while the number of MAPC cells in the spleen increased over time. The number of MAPC cells detected in the spleen was increased in PBMC mice compared to healthy mice. Statistical analysis of pathological scores was carried out using Mann Whitney tests where * ≤ 0.05 and ** ≤ 0.01 and *** ≤ 0.001 . This data is representative of 2 MAPC cell donors and 2 PBMC donors.

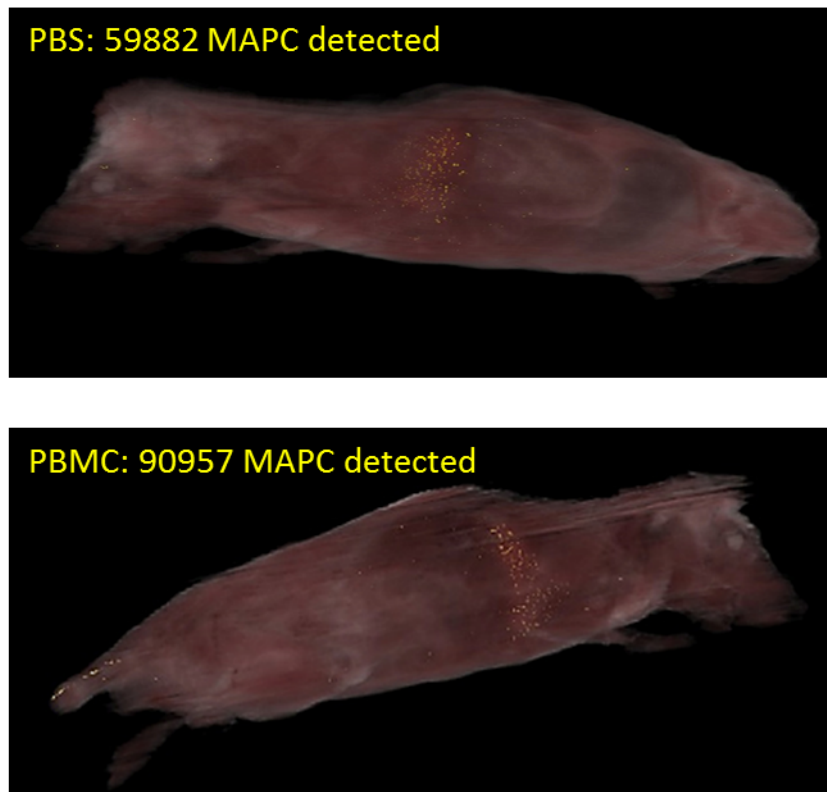


Figure 3.10 Biodistribution of MAPC cells differs in healthy and aGvHD mice. MAPC cells were stained with Qtracker[®] 625 as described in figure legend 3.8. MAPC cells were administered IV to PBS or PBMC mice on day 7 of the aGvHD model. Whole mice were humanely euthanised at 48 hours post MAPC cell administration and snap frozen in black OCT. Mice were sectioned and imaged using the CryoViz[™]. Images were processed and the number of MAPC cells detected were quantified using CryoViz[™] software packages. In both instances, the majority of MAPC cells detected could be visualised in the lung. The number of MAPC cells detected was higher in the PBMC mouse than the PBS mouse (n = 1).

3.9 IFN- γ stimulation improves the immunosuppressive capacity of MAPC cells *in vitro*

It is well known that MSC and MAPC cells require licensing by pro-inflammatory cytokines in order to produce anti-inflammatory mediators such as IDO and PGE2 (Ryan *et al.*, 2005; Chinnadurai *et al.*, 2014; Reading *et al.*, 2015; Sivanathan *et al.*, 2014). Furthermore, in the case of MSC it has been shown by our group that pre-stimulation of cells with IFN- γ prior to *in vivo* administration improves their efficacy (Tobin *et al.*, 2013). Thus, I sought to examine the effects of IFN- γ treatment on the immunosuppressive effects of MAPC cells. MAPC cells were seeded into 96 well round bottom plates at a density of 0.625×10^3 /well with or without 50 ng/ml IFN- γ . 24 hours later, MAPC cell medium was removed and cells were washed with PBS. 5×10^4 CFSE labelled PBMC were then added to each well with 1×10^4 anti CD3/CD28 beads as described in section 2.6.5. 4 days later PBMC were collected and stained with CD3 antibody and 7AAD to examine the proliferation of live T cells by flow cytometry. The number of proliferating T cells was enumerated using counting beads. As expected, culture of PBMC with anti CD3/CD28 beads significantly increased the number of proliferating T cells from 320.1 ± 74.87 to 26720 ± 6408 ($n = 11$). The number of proliferating T cells was reduced to 8728 ± 1271 in wells where MAPC cells were included ($n = 11$), however MAPC cells stimulated with IFN- γ prior to the addition of PBMC were more potent with the number of proliferating T cells in these wells being 1501 ± 278.6 ($n = 11$) (Fig. 3.11). Thus, as expected MAPC cells stimulated with IFN- γ (γ MAPC cells) were more potent at suppressing T cell proliferation than unstimulated MAPC cells.

3.10 IFN- γ stimulated MAPC cells administered on day 0 prolong survival in aGvHD.

As shown in section 3.9, the immunosuppressive capacity of MAPC cells is improved following pre-treatment with IFN- γ . Similarly, previous work in our lab showed that stimulation of MSC with IFN- γ improves the therapeutic efficacy of MSC in the humanised model of aGvHD (Tobin *et al.*, 2013). Here I investigated the effects of pre-stimulation on

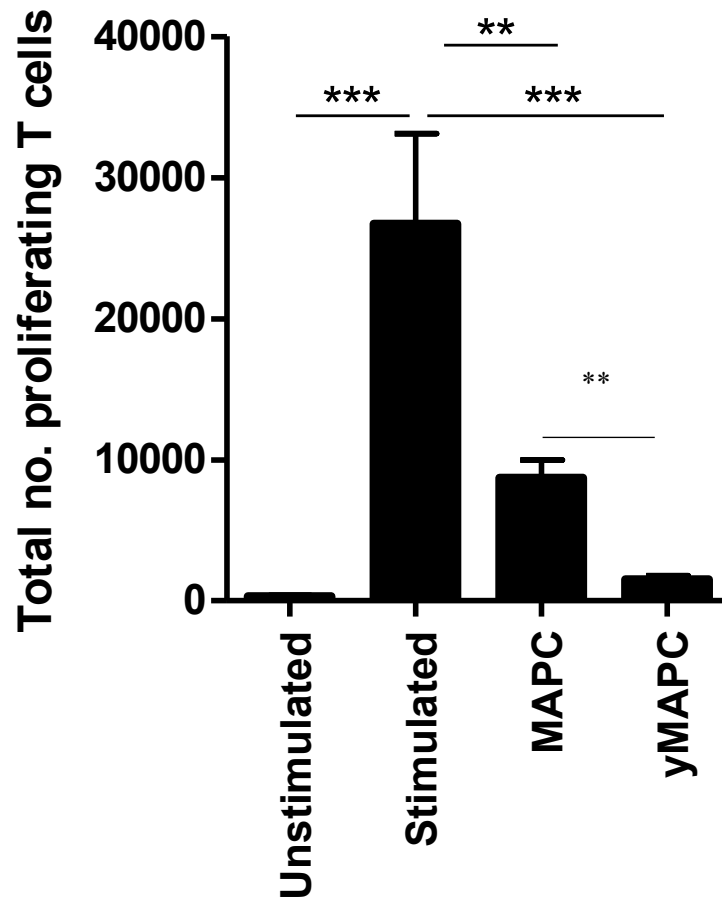


Figure 3.11 IFN- γ stimulation improves the potency of MAPC cells in a T cell proliferation assay. MAPC cells were seeded into 96 well round bottom plates at a density of 0.625×10^3 and incubated for 24 hours with or without 50ng/ml IFN- γ . PBMC (5×10^4) were added to each well with CD3/CD28 activation beads at a ratio of 1:5. PBMC were harvested on day 4 and stained for 7AAD and CD3. Counting beads were used to quantify results. MAPC cells stimulated with IFN- γ (γ MAPC cells) prior to the assay were superior at suppressing T cell proliferation than unstimulated MAPC cells. This assay was done in triplicate with 4 MAPC cell donors and 2 PBMC donors. Data was determined as normal using the d'Agostino and Pearson omnibus test and experimental groups were compared using One-way ANOVA with post-hoc Tukey testing where ** ≤ 0.01 and *** ≤ 0.001 ; n = 11.

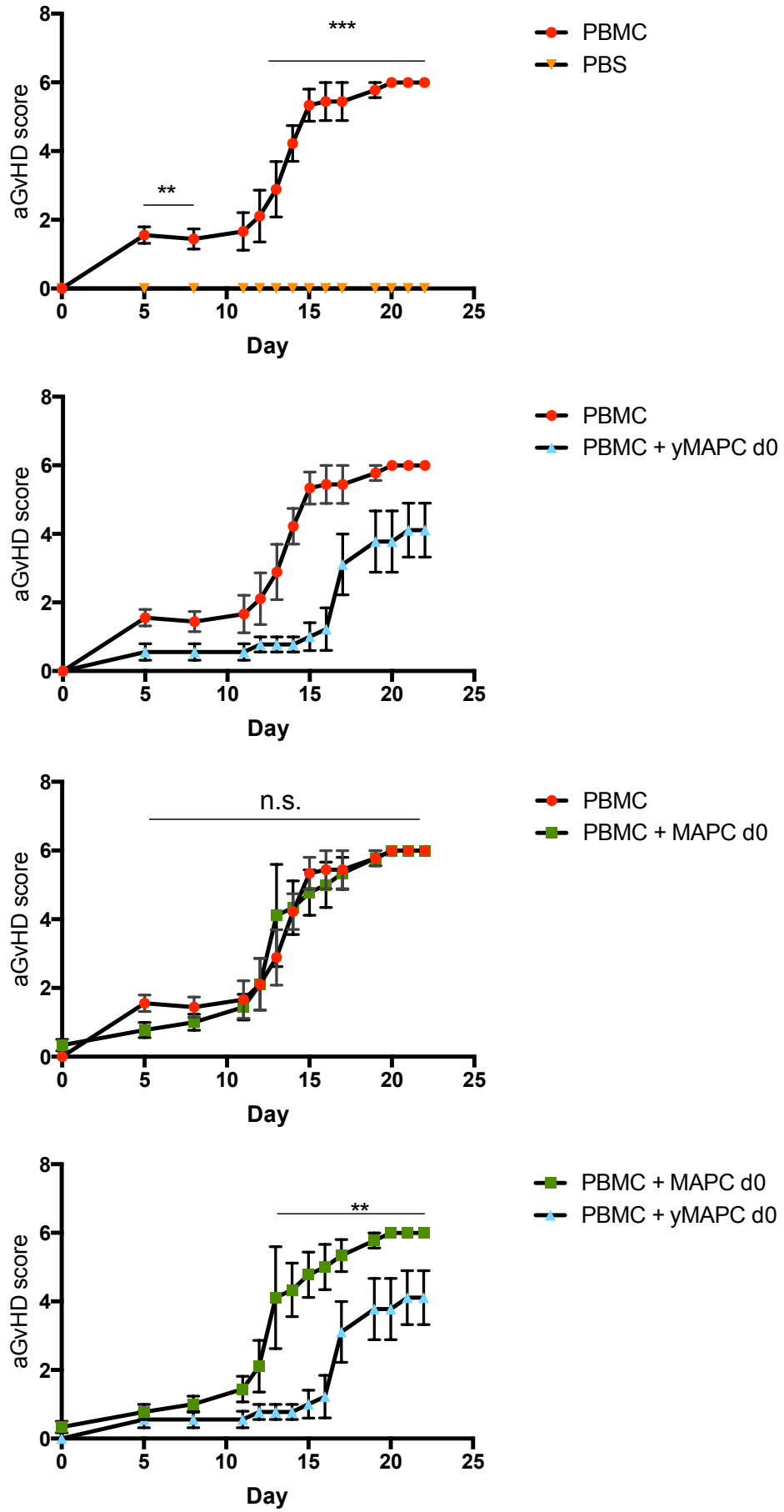
the efficacy of MAPC cells as a treatment for the humanised aGvHD model. It was hypothesised that the efficacy of MAPC cells administered on day 0 would be improved when stimulated with IFN- γ prior to administration. MAPC cells were stimulated with 50 ng/ml IFN- γ for 24 hours and then administered in conjunction with PBMC on day 0 following the same protocol as described previously in this chapter. Unstimulated MAPC cells were used as a control. As expected, mice that received PBMC only showed signs of aGvHD from day 11 and had a mean aGvHD score of 4.22 ± 0.511 (n = 9). MAPC cells administered on day 0 did not alleviate the symptoms of aGvHD with this group having a mean aGvHD score of 4.176 ± 0.5183 (n = 9). Mice that received γ MAPC cells had a lower aGvHD score on day 14 than those that received PBMC only, with a mean aGvHD score of 2.307 ± 0.442 (Fig. 3.12A).

Similarly, the survival of aGvHD mice reflected that of the aGvHD score, with γ MAPC cells but not unstimulated MAPC cells significantly prolonging survival. Mice which received PBMC only were sacrificed by day 16 with a median survival time of 14 days (n = 9). While unstimulated MAPC cells administered on day 0 failed to alleviate aGvHD, with 90% of animals sacrificed by day 14, γ MAPC cells significantly prolonged survival of mice compared to those which did not receive a therapy, with a median survival time of 18 days (n = 9) (Fig. 3.12B). Thus, as expected based on previous studies in our group on MSC (Tobin *et al.*, 2013), IFN- γ stimulation improves the immunosuppressive capacity of MAPC cells administered to aGvHD on day 0.

3.11 γ MAPC cells reduce the pathology of target organs in aGvHD.

Since γ MAPC cells administered on day 0 significantly improved survival in the aGvHD model, it was hypothesised that they would protect tissue from damage associated with aGvHD in a similar manner to MAPC cells administered on day 7 as seen in section 3.9. Thus, lung, liver, small intestine and colon was harvested on day 12 of the model and processed for imaging and scoring as described previously in this chapter.

A



B

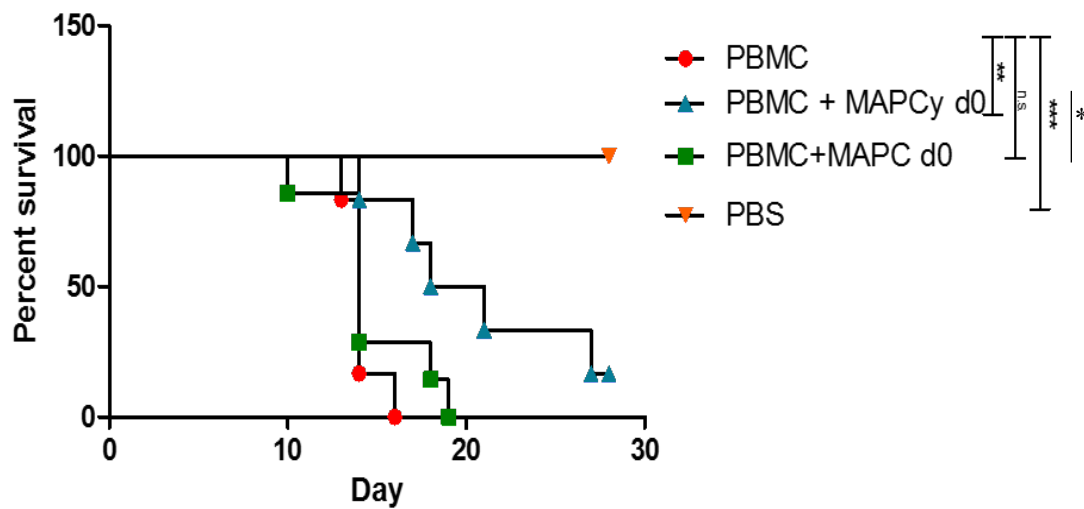
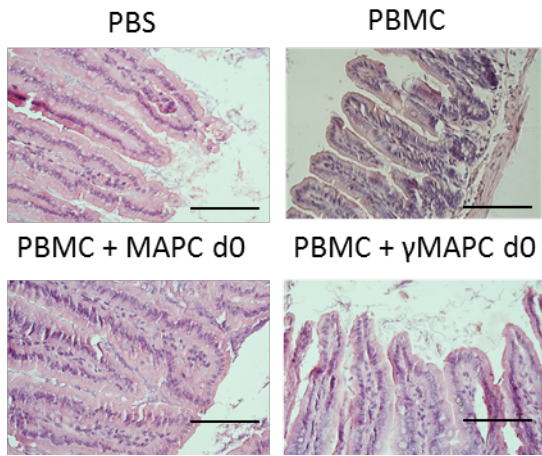


Figure 3.12 γ MAPC cells administered on day 0 reduce the pathological score and prolong survival in aGvHD. 8×10^5 human PBMC per gram were administered to irradiated NSG mice on day 0. 6.4×10^4 γ MAPC cells or unstimulated MAPC cells per gram were administered along with PBMC on day 0. Mice were monitored on a daily basis for symptoms of aGvHD and scores were assigned every second day until day 9 and then every day until the end of experiment (A). Mice with an aGvHD score of 5 or higher were humanely euthanised by cervical dislocation and survival was graphed (B). γ MAPC cells significantly prolonged survival in the aGvHD model, while unstimulated MAPC cells had no effect. Statistical analysis of aGvHD scores were carried out by doing Mann-Whitney tests at each time point. Lines indicate the time points at which the indicated significance was achieved. Statistical analysis of the survival curve was carried out using a Mantel Cox test where $* \leq 0.05$, $** \leq 0.01$, and $*** \leq 0.001$. Experiments were carried out using 3 PBMC donors and 3 MAPC cell donors, $n = 9/\text{group}$.

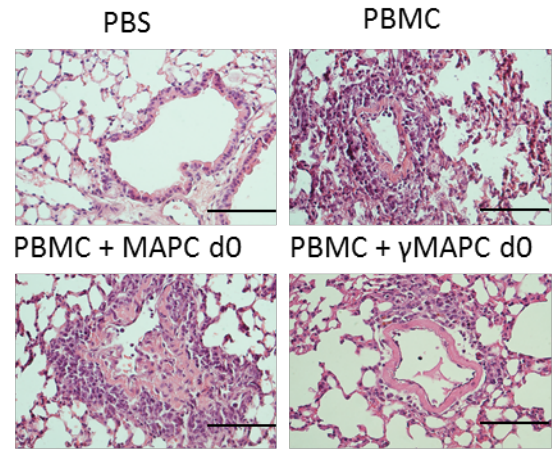
(A)

Small Intestine

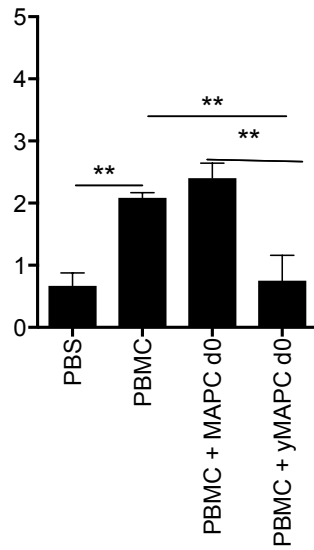


(B)

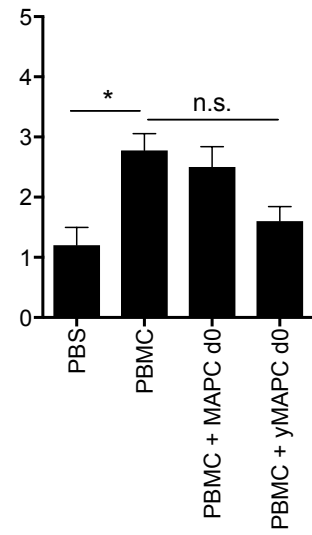
Lung



Pathological score



Pathological score



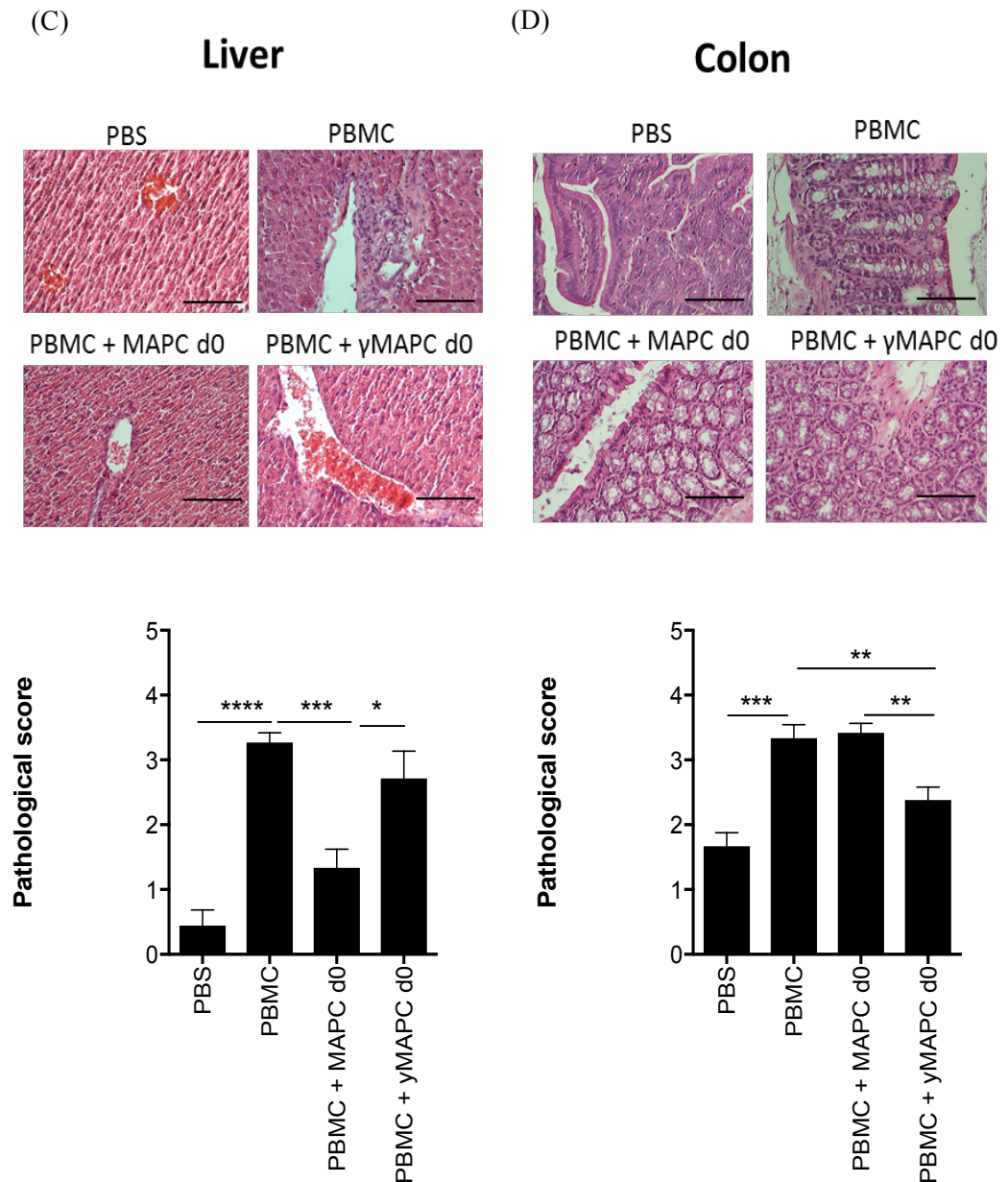


Figure 3.13 γ MAPC cells reduce the pathological score aGvHD target tissues. The aGvHD model was set up as described in figure legend 3.12 and mice were humanely euthanised and small intestine, lung, liver and colon harvested on day 12. Tissue was processed and stained with H&E to examine pathology. γ MAPC cells but not MAPC cells reduced the pathological score in the small intestine (A), lung (B) and colon (D) while MAPC cells but not γ MAPC cells reduced the pathological score in the liver (C). Statistical analysis of pathological scores was carried out using Kruskal-Wallis analysis with the original FDR method of Benjamini and Hochberg to correct for multiple comparisons where $* \leq 0.05$, $** \leq 0.01$, $*** \leq 0.001$; and $**** \leq 0.001$. Experiments were carried out using 2 PBMC donors and 2 MAPC cell donors (n=6). Pictures were taken at 40X objective, scale bars indicate 50 μ m.

As expected, the small intestine of PBMC mice showed increased blunting of the villi and ulceration compared to the PBS group. Thus, the pathological score increased from 0.6667 ± 0.2108 in the PBS group to 2.083 ± 0.0833 in the PBMC group ($n = 9$). Unstimulated MAPC cells administered on day 0 had no effect on this score, however γ MAPC cells alleviated the damage associated with aGvHD and so, significantly reduced the score to 0.75 ± 0.4119 ($n = 9$) (Fig. 3.13A). In the lung, mononuclear cell infiltration was increased in the PBMC group compared to the PBS group as before, with the pathological score increasing from 1.200 ± 0.2960 to 2.8 ± 0.2000 ($n = 9$). As expected, unstimulated MAPC cells administered on day 0 had no effect in the lung, while γ MAPC cells administered on day 0 reduced cellular infiltration and the pathological score to 1.6 ± 0.2449 ($n = 9$) (Fig. 3.13B). Pathological score in the liver was increased from 0.444 ± 0.2422 in the PBS group to 3.333 ± 0.1667 in the PBMC group ($n = 9$). This was reduced to 1.455 ± 0.2473 by MAPC cells administered on day 0 ($n = 9$), although a small reduction in pathology was observed, γ MAPC cells had no significant effect in this instance (Fig. 3.13C). In the colon, PBMC resulted in ulceration in the lamina propria, thus the score increased from 1.667 ± 0.1421 in the PBS group to 3.417 ± 0.2289 in the PBMC group ($n = 9$). Unstimulated MAPC cells had no effect on the pathological score in the colon, while γ MAPC cells reduced the score to 2.381 ± 0.2009 ($n = 9$) (Fig. 3.13D).

3.12 The number of MAPC cells detected in aGvHD target organs is increased when cells were pre-stimulated with IFN- γ .

Due to the enhanced survival of aGvHD mice following treatment with γ MAPC cells, I sought to investigate the biodistribution of γ MAPC cells in comparison to unstimulated MAPC cells. IFN- γ stimulation of MSC increases expression of adhesion molecules such as ICAM1, and chemokines such as CXCL9 and CXCL12 (K. English, unpublished data). Therefore, I hypothesised that γ MAPC cells may be better equipped to escape entrapment in the lungs and migrate to sites of injury than unstimulated MAPC cells. MAPC cells were cultured with or without 50 ng/ml IFN- γ for 24 hours and then stained with the Qtracker[®] 625 labelling kit

before being administered to the aGvHD model on day 0 along with PBMC. 24 hours after PBMC and MAPC cells administration, the lung, liver and spleen were harvested and snap frozen in black OCT as described in section 2.11.2. Samples were sectioned and imaged using the CryoViz™ and subsequently processed using CryoViz™ pre-processing and cell quantification software.

There was no significant difference in the number of MAPC cells or γ MAPC cells detected in the lungs of aGvHD mice, with the number of unstimulated MAPC cells detected being 76900 ± 19810 and the number of γ MAPC cells detected being 95630 ± 27000 ($n = 10$). In the spleen however, the number of MAPC cells was significantly increased following stimulation with IFN- γ , with 58.75 ± 7.810 MAPC cells detected compared to 245.3 ± 39.19 γ MAPC cells ($n = 8$). Similarly, the number of MAPC cells detected in the liver increased from 6479 ± 885.5 to 12930 ± 1250 following IFN- γ stimulation ($n = 5$) (Fig. 3.14). Therefore, this data suggests that IFN- γ stimulation of MAPC cells improves migration of MAPC cells towards aGvHD target organs, which may be the reason for the increased efficacy of γ MAPC cells demonstrated in Figs. 3.12 and 3.13.

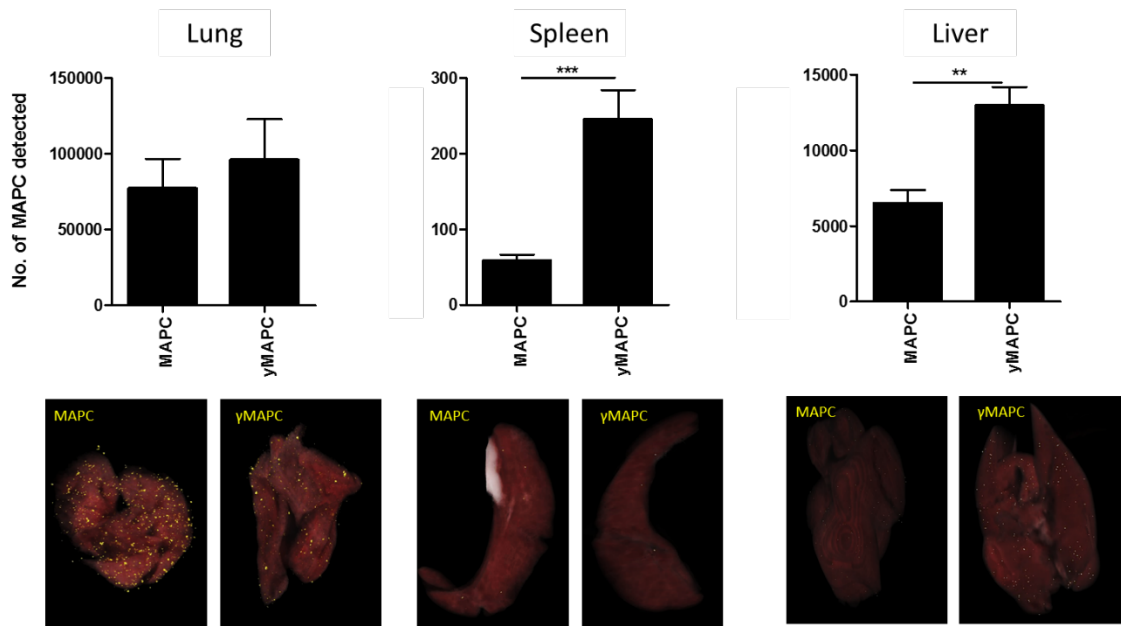


Figure 3.14 IFN- γ stimulation of MAPC cells increases their biodistribution to aGvHD target tissues. MAPC cells and γ MAPC cells were labelled with Qtracker[®] 625 and administered to the aGvHD model on day 0 as described in figure legend 3.8. Lung, spleen and liver were harvested and snap frozen 24 hours after MAPC cell administration. Tissue was imaged and processed using CryoViz[™] technology. Statistical analysis was carried out using Mann-Whitney analysis where * ≤ 0.05 , ** ≤ 0.01 and *** ≤ 0.001 . Experiments were carried out using 2 PBMC donors and 2 MAPC cell donors.

3.13 PPAR δ agonism inhibits the efficacy of MAPC cells administered on day 7 to the aGvHD model.

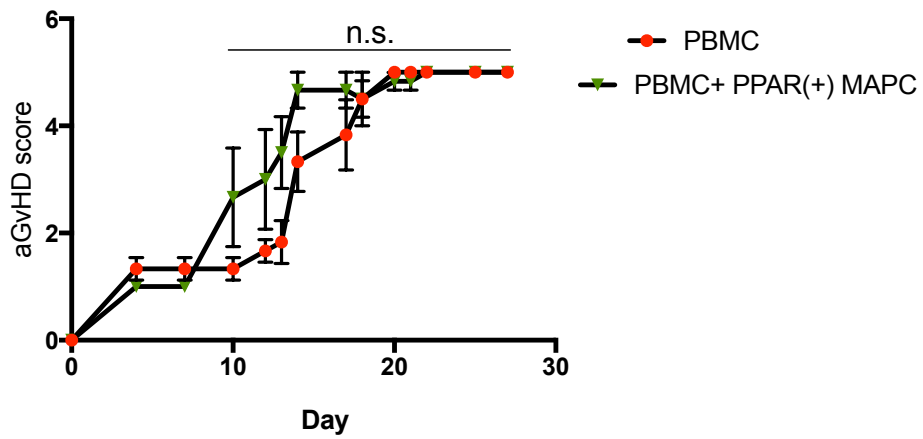
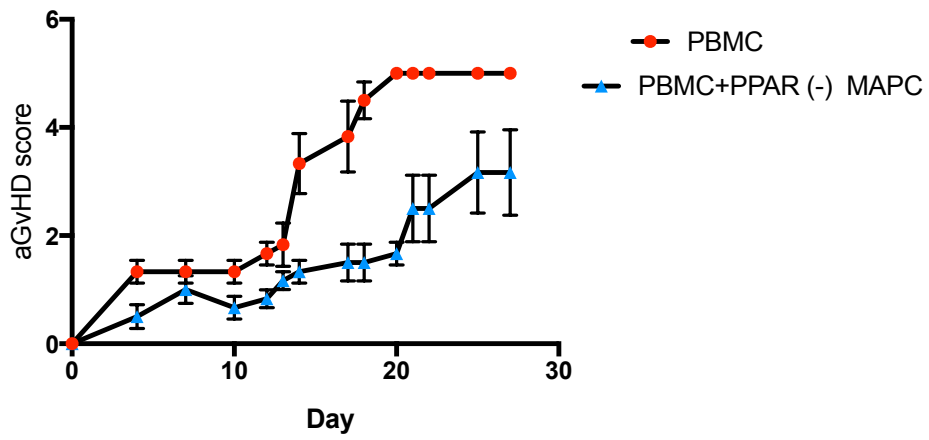
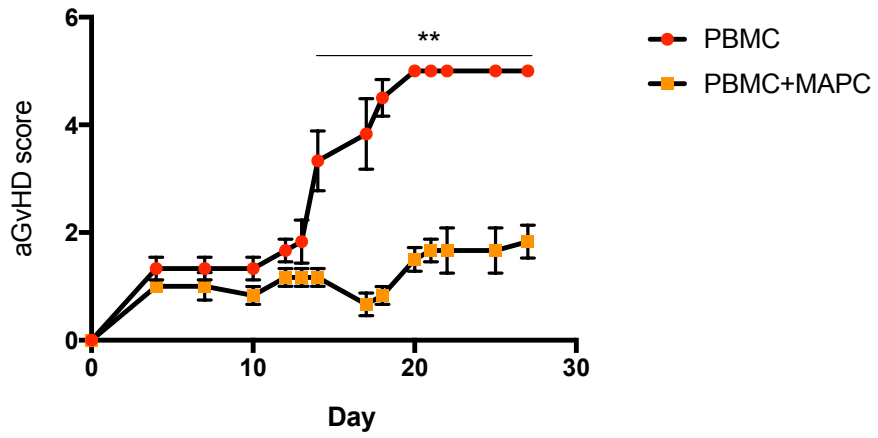
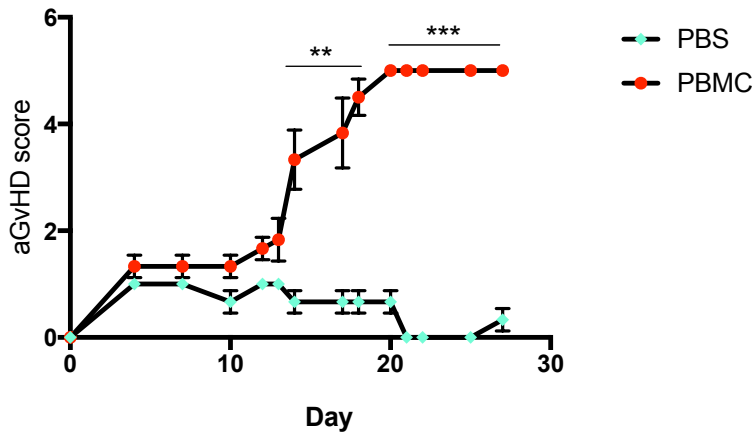
A recent study by Luz-Crawford *et al.* (2016) showed that PPAR $\delta^{-/-}$ murine MSC exhibited enhanced therapeutic efficacy in a collagen induced arthritis model. PPAR $\delta^{-/-}$ MSC showed increased expression of ICAM1, VCAM1 and iNOS in response to stimulation with pro-inflammatory cytokines. Therefore, I hypothesised that agonising PPAR δ would reduce the therapeutic efficacy of MAPC cells while antagonism of PPAR δ would increase the therapeutic efficacy of MAPC cells in the humanised aGvHD model. In order to test this theory, MAPC cells were cultured with or without a PPAR δ agonist or antagonist for 24 hours as described in section 2.7.2 prior to administration to the humanised aGvHD model on day 7. A concentration of 1 μ M of the agonist and antagonist was used based on previous publications using murine MSC and human macrophages (Luz-Crawford *et al.*, 2016b; Adhikary *et al.*, 2015).

As expected, mice that received PBMC only showed signs of aGvHD from day 11 and had a mean aGvHD score of 3.397 ± 0.4562 (n = 11). MAPC cells alleviated the symptoms of aGvHD with this group having a mean aGvHD score of 1.244 ± 0.1061 (n = 11). Interestingly, mice that received MAPC cells treated with the PPAR δ agonist (PPAR(+)) MAPC cells) had a mean aGvHD score of 3.821 ± 0.4093 (n = 11) while the group that received MAPC cells treated with the PPAR δ antagonist (PPAR(-)) MAPC cells) had a mean pathological score of 1.654 ± 0.2507 (n = 11) (Fig. 3.15A).

In the PBMC only group mice were humanely euthanised between days 7 and 20, with median survival being day 12 (n = 11). As expected, MAPC cell therapy significantly prolonged survival to a median of 25.5 days (n = 11). Only one mouse treated with PPAR(+) MAPC cells survived for the duration of the model with this group having a median survival time of 14 days. Mice treated with PPAR(-) MAPC cells showed similar survival rates to

those treated with normal MAPC with this group having a median survival of 25 days (n = 6) (Fig. 3.15B).

Since treatment with the PPAR agonist impaired the efficacy of MAPC cells in prolonging survival of aGvHD mice, I hypothesised that PPAR(+) MAPC cells would be unable to protect aGvHD target tissue from damage as previously seen with MAPC cells in section 3.7. Lung, liver, small intestine and colon were harvested and processed for imaging and pathological analysis as previously described in this chapter. In the small intestine, PBMC administration increased the pathological score from 0.1667 ± 0.1667 to 3.667 ± 0.2108 (n = 6). Administration of MAPC cells significantly reduced the score to 2.167 ± 0.1667 (n = 6) while the pathological score remained at 4.00 ± 0.3651 when PPAR(+) MAPC cells were administered (n = 6) (Fig. 3.16A). In the lung PBMC increased the score from 0.500 ± 0.2236 to 4.667 ± 0.2103 (n = 6). MAPC cells reduced this to 3.333 ± 0.4216 (n = 6), while PPAR(+) MAPC cells also reduced the score to 4.00 ± 0.3651 , however this change was not significant (n = 6) (Fig. 3.16B). In the liver, administration of PBMC increased the score from 0.1667 ± 0.1667 to 3.5 ± 0.4282 (n = 6). This was slightly reduced by MAPC cells to 2.667 ± 0.4216 (n = 6) while PPAR(+) MAPC cells had no effect (Fig. 3.16C). Similarly, in the colon PBMC increased the pathological score from 0.500 ± 0.2236 to 4.333 ± 0.2108 (n = 6). This was reduced to 2.333 ± 0.2108 by MAPC cells (n = 6) while PPAR(+) MAPC cells had no effect (Fig. 3.16D). Therefore, PPAR δ agonism inhibits the therapeutic efficacy of MAPC cells in GvHD, which corroborates well with the study by Luz-Crawford *et al.* (2016).



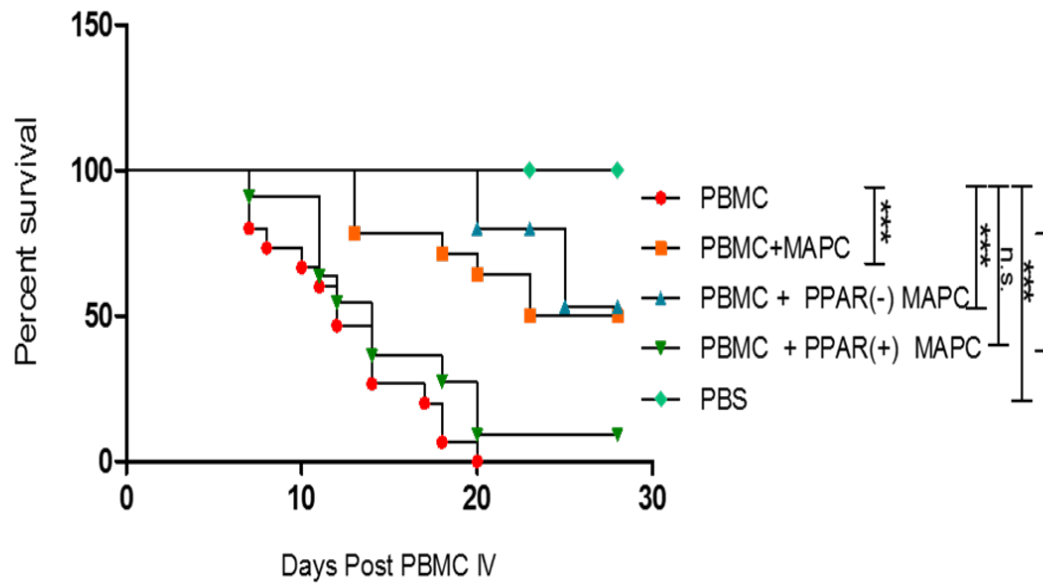
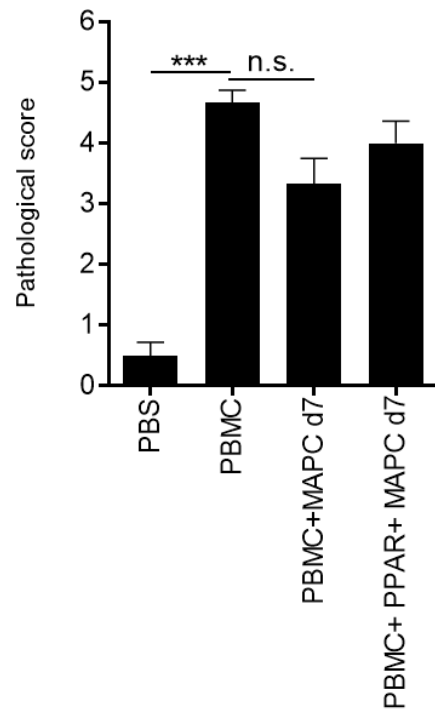
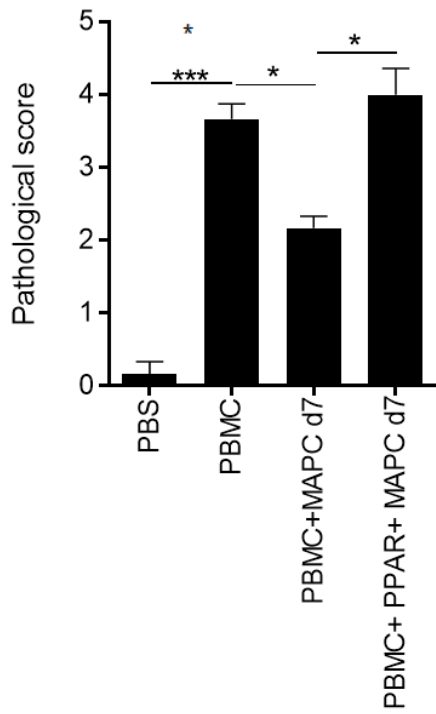
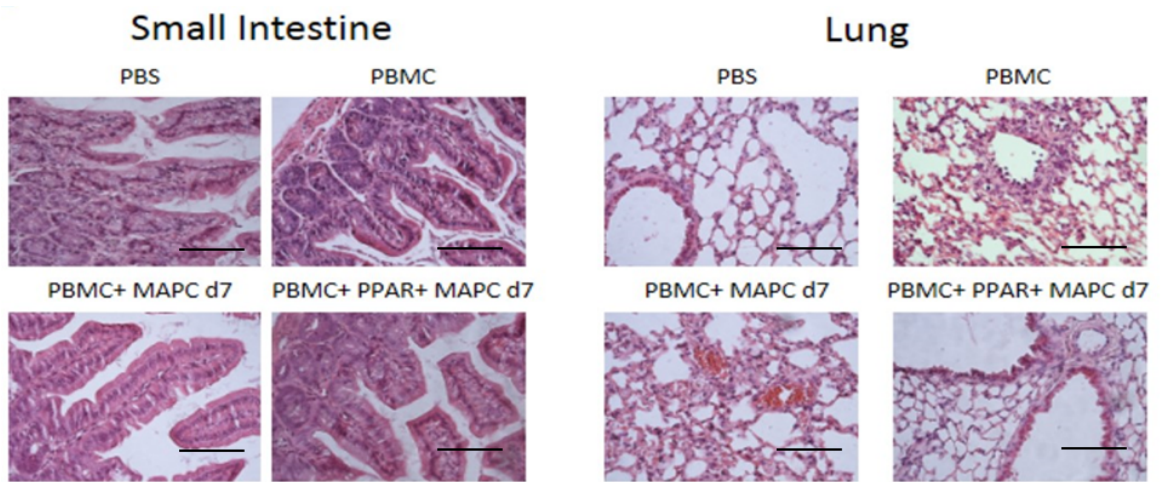


Figure 3.15 PPAR(+) MAPC cells show reduced therapeutic efficacy in the humanised model of aGvHD. 8×10^5 human PBMC per gram were administered to irradiated NSG mice on day 0. 6.4×10^4 MAPC cells, PPAR δ agonist treated MAPC cells (PPAR (+) MAPC cells), or PPAR δ antagonist treated MAPC cells (PPAR(-) MAPC cells) per gram were administered to the aGvHD model on day 7. Mice were monitored on a daily basis for symptoms of aGvHD and scores were assigned every second day until day 9 and then every day until the end of experiment (A). Mice with an aGvHD score of 5 or higher were humanely euthanised by cervical dislocation (B). MAPC cells and PPAR(-) MAPC cells significantly prolonged survival in the aGvHD model, while PPAR(+) MAPC cells had no effect. Statistical analysis of aGvHD scores were carried out by doing Mann-Whitney tests at each time point. Lines indicate the time points at which the indicated significance was achieved. Statistical analysis of the survival curve was carried out using a Mantel Cox test where $** \leq 0.01$ and $*** \leq 0.001$. Experiments were carried out using 4 PBMC donors and 2 MAPC cell donors.



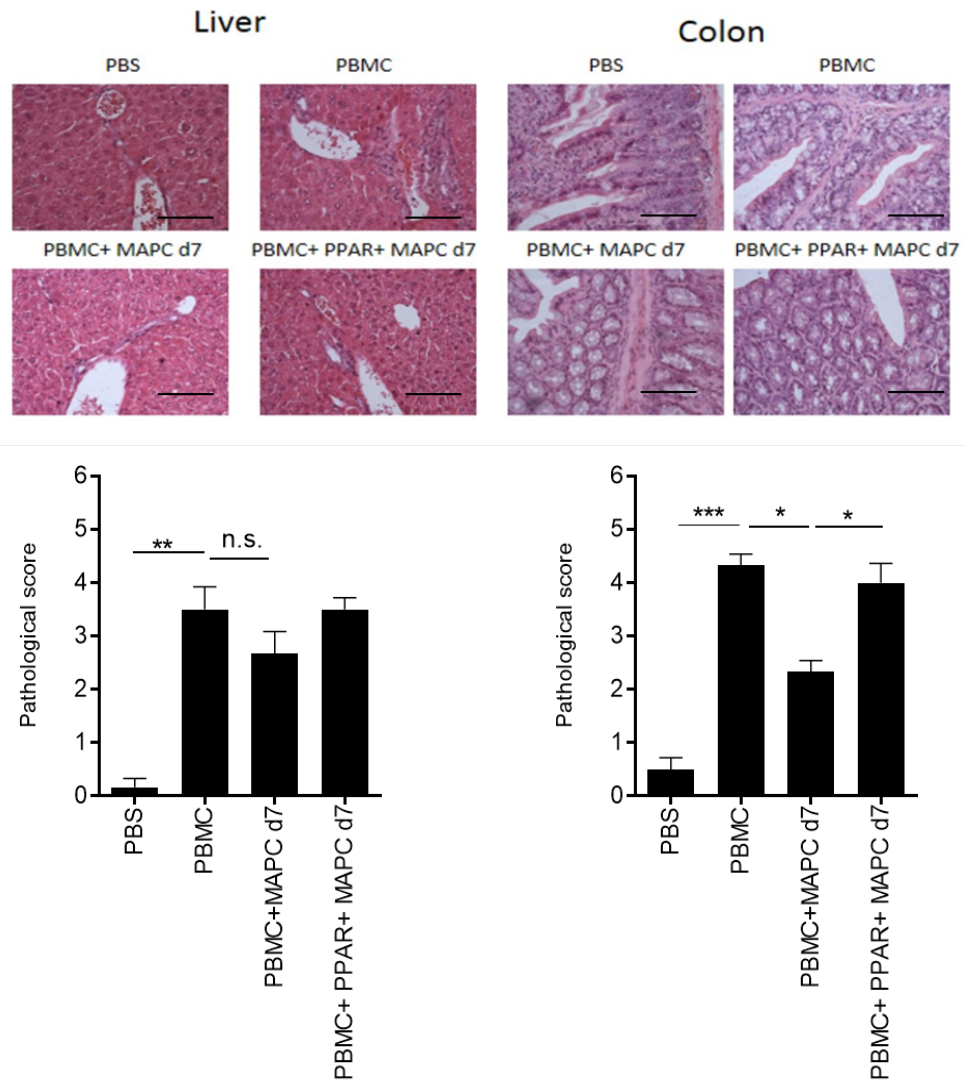


Figure 3.16 PPAR(+) MAPC cells have no effect on pathological scores in aGvHD target tissues. The aGvHD model was set up as described in figure legend 3.15. Mice which received MAPC cells and PPAR(+) MAPC cells were humanely euthanised and small intestine, lung, liver and colon harvested on day 12. Tissue was processed and imaged as described in section 3.9. MAPC cells reduced the pathological score in each of the aGvHD target tissues, while PPAR(+) MAPC cells had no effect. Statistical analysis of pathological scores was carried out using Kruskal-Wallis analysis with the original FDR method of Benjamini and Hochberg to correct for multiple comparisons where $* \leq 0.05$, $** \leq 0.01$, $*** \leq 0.001$; and $**** \leq 0.001$ where $* \leq 0.05$ and $*** \leq 0.001$. Experiments were carried out using 2 PBMC donors and 2 MAPC cell donors (n=6).

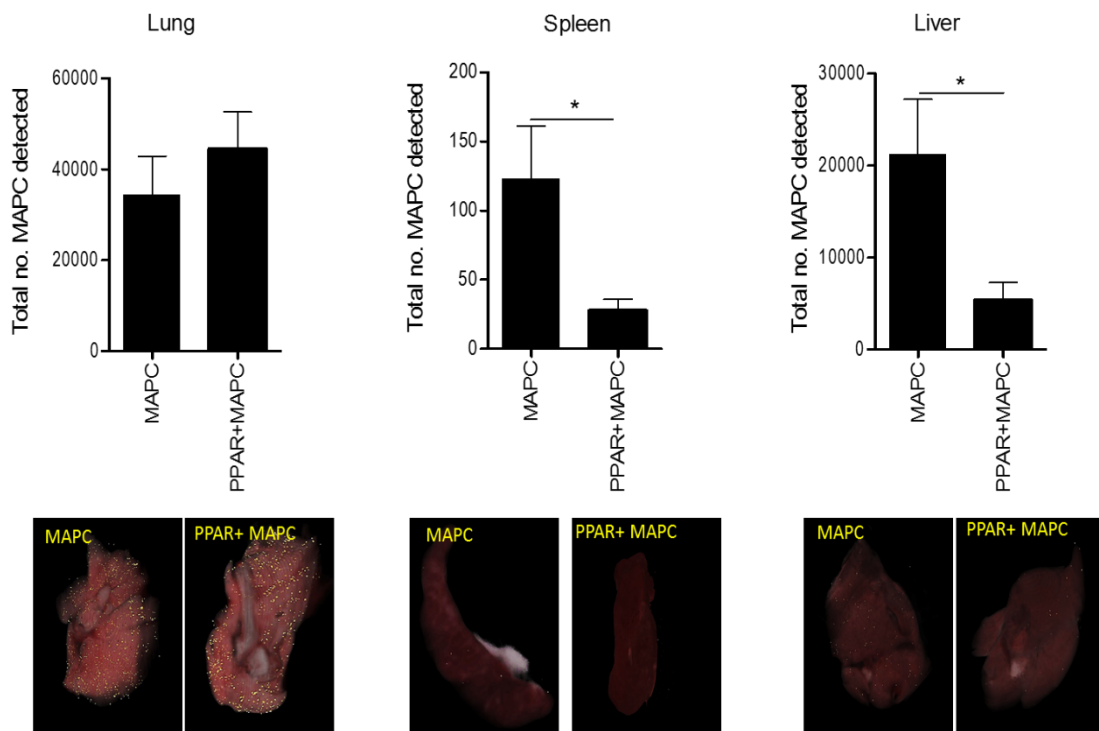


Figure 3.17 Agonism of PPAR δ reduces the biodistribution of MAPC cells to aGvHD target organs. MAPC cells and PPAR(+) MAPC cells were labelled with Qtracker[®] 625 and administered to the aGvHD model on day 7. Mice were humanely euthanised and lung, spleen and liver harvested 24 hours after MAPC cells administration. Tissue was processed and imaged as described in section 3.10. The number of MAPC cells detected in the liver and spleen was reduced when MAPC cells were treated with PPAR δ agonist prior to administration. Statistical analysis was carried out using Mann Whitney test where * ≤ 0.05 . Experiments were carried out using 2 PBMC donors and 2 MAPC cell donors (n = 6/group).

3.15 PPAR δ agonism reduces the biodistribution of day 7 MAPC cells in aGvHD.

Since treatment with the PPAR δ agonist hindered the therapeutic efficacy of MAPC cells, and PPAR δ knock out MSC showed increased expression of adhesion molecules such as ICAM1 and VCAM1 in response to pro-inflammatory cytokines, I hypothesised that PPAR(+)
MAPC cells would show decreased biodistribution compared to normal MAPC cells. MAPC cells and PPAR(+)
MAPC cells were labelled with the Qtracker[®] labelling kit as previously described and administered to aGvHD mice on day 7. 24 hours later lung, liver and spleen were harvested and snap frozen in black OCT before being imaged using the CryoViz[™]. In the lung, the number of MAPC cells detected at 24 hours was 34430 \pm 8385 and this slightly increased to 44410 \pm 8137 when MAPC cells were treated with the PPAR agonist (n = 6). In the distal organs however, PPAR agonism significantly reduced the number of MAPC cells detected, with the number of cells detected in the spleen being reduced from 123.3 \pm 37.74 to 27.57 \pm 8.138 (n = 7) and the number of cells in the liver being reduced from 21180 \pm 5998 to 5332 \pm 1934 (n = 6) (Fig. 3.17). Therefore, the reduced efficacy of PPAR(+)
MAPC cells in the GvHD model correlates with a reduction in the number of cells reaching GvHD target organs.

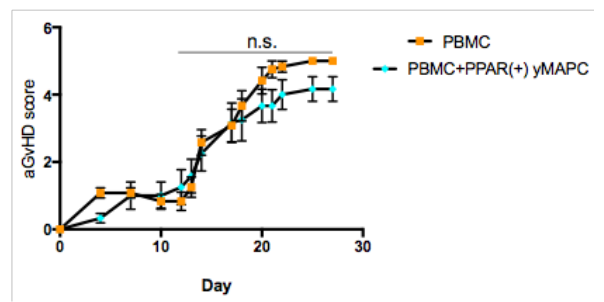
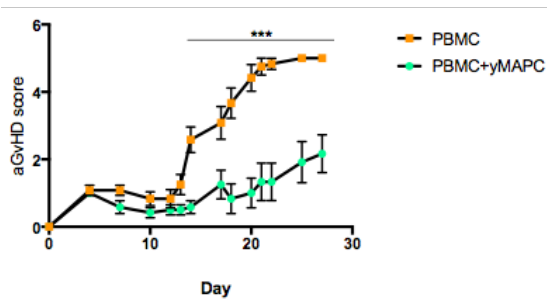
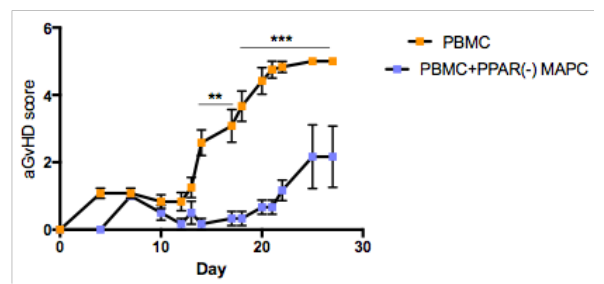
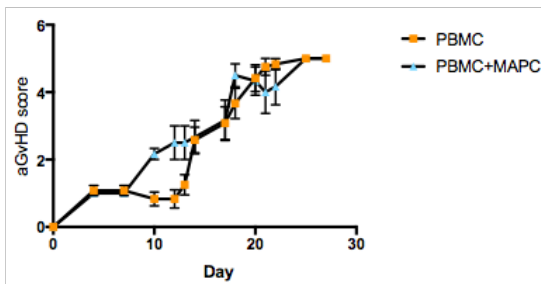
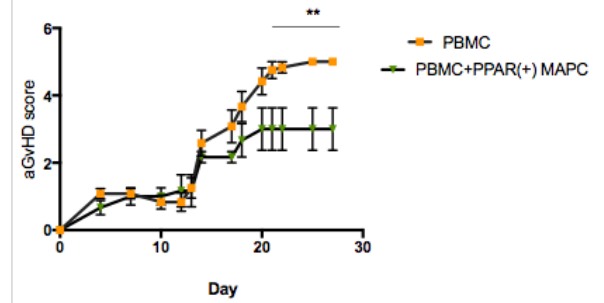
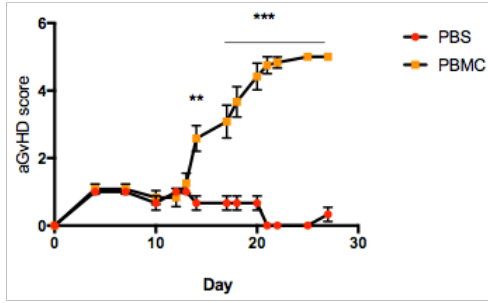
3.15 PPAR δ agonism inhibits the efficacy of IFN- γ stimulated MAPC cells administered on day 0 to the aGvHD model.

Following on from sections 3.13 and 3.14 where PPAR δ agonism affected the efficacy of MAPC cells administered to the aGvHD model on day 7, I sought to examine the effects of PPAR δ agonism and antagonism on MAPC cells administered on day 0 to the aGvHD model. It was hypothesised that PPAR δ agonism would hinder the efficacy of γ MAPC cells, and that PPAR δ antagonism would improve the efficacy of MAPC cells administered on day 0. MAPC cells were treated with 1 μ M GW0742 or GSK3787 for 48 hours before administration to the aGvHD model. IFN- γ was added at a concentration of 50 ng/ml to some cultures for the last 24 hours prior to harvest to generate γ MAPC cells. Cells were counted and washed 3 times before being administered alongside PBMC at a concentration of 6.4x10⁴ cells/gram.

Mice were monitored regularly for signs of aGvHD and assigned an aGvHD score based on symptoms as described in section 2.8.1. The mean aGvHD score of mice in the PBS group over the 28 days was 0.5897 ± 0.1078 and this increased to 2.955 ± 0.4859 in the PBMC group ($n = 12$). This score was unchanged by administration of MAPC cells, with this group having a median score of 3.231 ± 0.3842 ($n = 12$). As expected γ MAPC cells reduced the pathological score to 1.032 ± 0.1538 ($n = 12$). PPAR δ agonism of MAPC cells (in the absence of IFN- γ licensing) had little effect on their therapeutic efficacy, with groups receiving this treatment having a median score of 2.667 ± 0.2605 ($n = 6$), while antagonism of PPAR δ increased the efficacy of MAPC cells, with groups receiving this treatment having a reduced median score of 0.7564 ± 0.1958 ($n = 6$). Interestingly, agonism of PPAR δ hindered the efficacy of γ MAPC cells with this group having a score of 2.577 ± 0.3850 ($n = 12$) (Fig. 3.18A).

Survival of each group correlated with the aGvHD scores as expected. The PBS group showed 100% survival out to day 28 of the model, while the PBMC group had a median survival of 17.5 ($n = 12$). Unstimulated MAPC cells had no effect on the survival of aGvHD mice, with this group also having a median survival time of day 17.5 ($n = 12$). PPAR(+) MAPC cells increased the median survival time to day 25.5 ($n = 6$), however this increase in survival was not significant. PPAR(-) MAPC cells on the other hand significantly prolonged survival of aGvHD mice, with this groups having a median survival time of 28 days ($n = 6$). γ MAPC cells also improved survival of aGvHD mice as expected, with 10 out of 12 mice (83%) in this group being alive at the end of this experiment and this group also having a median survival time of 28 days. PPAR δ agonised γ MAPC cells (PPAR(+) γ MAPC cells) had no therapeutic effect, with this group having a median survival of 16 days ($n = 12$) (Fig. 3.18B).

A



B

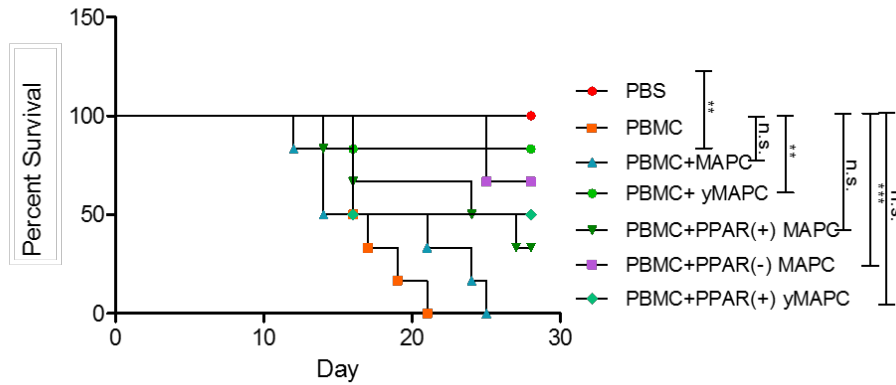


Figure 3.18 PPAR(+) γ MAPC cells show reduced therapeutic efficacy in the humanised model of aGvHD. 8×10^5 human PBMC per gram were administered to irradiated NSG mice on day 0. 6.4×10^4 MAPC cells, γ MAPC cells, PPAR δ agonist treated MAPC cells (PPAR(+) MAPC cells), PPAR δ agonist treated γ MAPC cells (PPAR(+) γ MAPC cells) or PPAR δ antagonist treated MAPC cells (PPAR(-) MAPC cells) per gram were administered to the GvHD model on day 0. Mice were monitored on a daily basis for symptoms of aGvHD and scores were assigned every second day until day 9 and then every day until the end of experiment (A). Mice with an aGvHD score of >5 were humanely euthanised and survival graphed at the study end-point (B). γ MAPC cells and PPAR(-) MAPC cells significantly prolonged survival in the aGvHD model, while MAPC cells, PPAR(+) MAPC cells and PPAR(+) γ MAPC cells had no significant effect. Statistical analysis of aGvHD scores were carried out by doing Mann-Whitney tests at each time point. Lines indicate the time points at which the indicated significance was achieved. Statistical analysis of the survival curve was carried out using a Mantel Cox test where $** \leq 0.001$ and $*** \leq 0.0001$. Experiments were carried out using 4 PBMC donors and 2 MAPC cell donors, $n = 6-12$ /group.

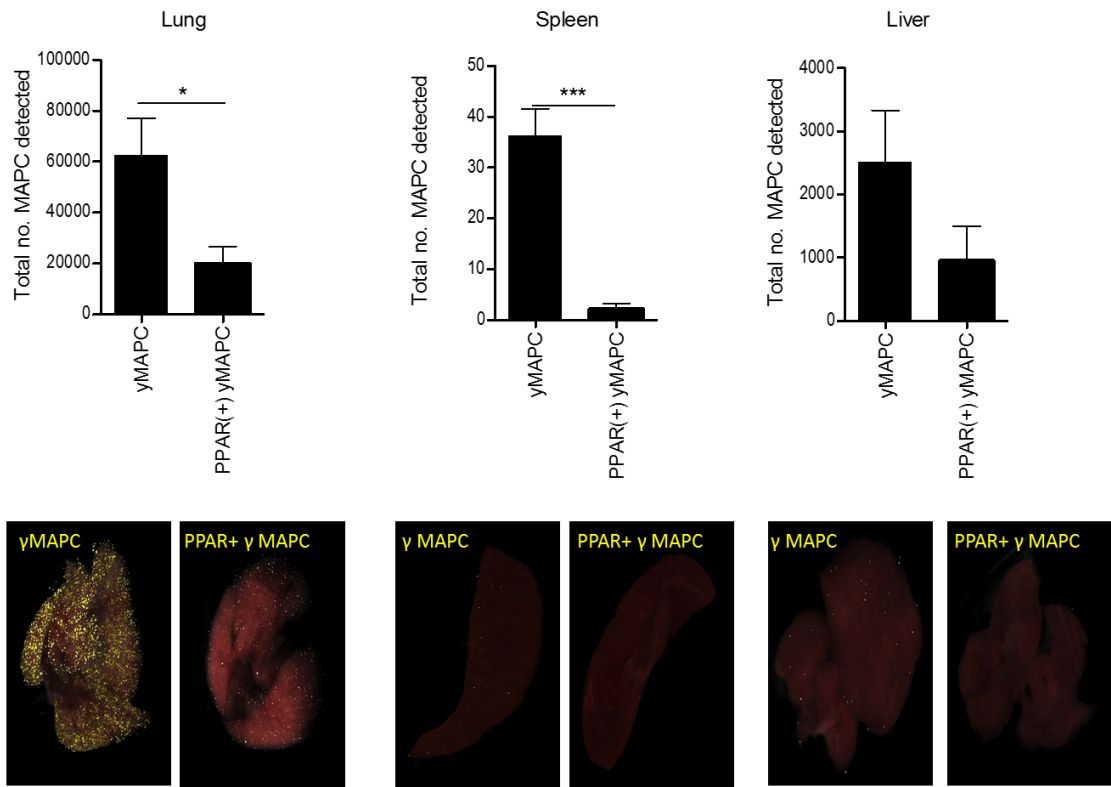


Figure 3.19 Agonism of PPAR δ reduces the biodistribution of γ MAPC cells to aGvHD target organs. γ MAPC cells and PPAR(+)- γ MAPC cells were labelled with Qtracker[®] 625 and administered to the aGvHD model on day 0. Mice were humanely euthanised and lung, liver and spleen harvested 24 hours after MAPC cell administration. Tissue was processed and imaged as described in section 3.10. The number of γ MAPC cells detected in the lung, spleen and liver was reduced when MAPC cells were treated with PPAR δ agonist prior to administration. Statistical analysis was carried out using Mann-Whitney tests where * ≤ 0.05 and *** ≤ 0.001 . Experiments were carried out using 2 PBMC donors and 2 MAPC cell donors.

3.17 PPAR δ agonism reduces the biodistribution of γ MAPC cells administered on day 0 to aGvHD.

Since treatment with the PPAR δ agonist hindered the biodistribution of MAPC cells administered to the aGvHD model on day 7, and reduced the therapeutic efficacy of γ MAPC cells administered to the aGvHD model on day 0, I hypothesised that PPAR(+) γ MAPC cells would show decreased biodistribution to GvHD target organs compared to γ MAPC cells. γ MAPC cells and PPAR(+) γ MAPC cells were labelled with the Qtracker[®] labelling kit as previously described and administered to aGvHD mice on day 0. 24 hours later lung, liver and spleen were harvested and snap frozen in black OCT before being imaged using the CryoViz[™].

In the lung, the number of γ MAPC cells detected at 24 hours was 62590 \pm 14420 and this was significantly reduced to 19940 \pm 6785 when γ MAPC cells were treated with the PPAR δ agonist (n = 8). Similarly, PPAR δ agonism significantly reduced the number of γ MAPC cells detected in the spleen and liver, with the number of cells detected in the spleen being reduced from 36.33 \pm 5.232 to 2.143 \pm 1.033 (n = 7, p<0.001) and the number of cells in the liver being reduced from 2512 \pm 821.3 to 948.8 \pm 548 (n = 6) (Fig. 3.19). Therefore, the reduced efficacy of PPAR(+) γ MAPC cells in the GvHD model correlates with a reduction in the number of cells detected in GvHD target organs.

3.18 PPAR δ agonism inhibits IFN- γ induced STAT1 signalling.

Notably, PPAR δ knock out murine MSC exhibit an enhanced response to pro-inflammatory cytokines *in vitro* with increased expression of ICAM, VCAM and iNOS compared to their wild type counterparts. Similarly, PPAR δ ^{-/-} MSC displayed increased NF- κ B activity in response to IFN- γ and TNF- α stimulation (Luz-Crawford *et al.*, 2016b). This study, taken together with our *in vivo* data suggests that PPAR δ may suppress IFN- γ signalling in MSC and MAPC cells. Since the immunosuppressive properties of MSC are dependent on the presence of IFN- γ in the microenvironment (Chinnadurai *et al.*, 2014; Liu *et al.*, 2012), I hypothesised that PPAR δ agonism would block IFN- γ signalling in MAPC cells which would explain the

reduced efficacy of PPAR(+) MAPC cells (Fig. 3.15 day 7) and PPAR(+) γ MAPC cells (Fig. 3.18 day 0) in the aGvHD model. IFN- γ induces phosphorylation of STAT1 which leads to its translocation to the nucleus where it induces expression of target genes. Exposure of both human and mouse MSC to IFN- γ results in STAT1 induction and phosphorylation. In murine MSC, STAT1 knockdown inhibits mRNA levels of PDL-1, NOS2 and IL18bp, and reduces the immunosuppressive capacity of murine MSC in a T cell proliferation assay, while in human MSC STAT1 knock down reduces IDO production (Vigo *et al.*, 2016; Mounayar *et al.*, 2015). Therefore, since PPAR δ agonism abrogated the immunosuppressive capacities of MAPC cells, I hypothesised that PPAR(+) MAPC cells might display reduced STAT1 signalling compared to normal MAPC cells.

MAPC cells were cultured in 6 well plates at a concentration of 2,000 cells/cm overnight before being treated with 1 μ M PPAR δ agonist or PPAR δ antagonist as described in section 2.7.2. 24 hours later, some wells were treated with 50 ng/ml IFN- γ for 24 hours, and cells were harvested and protein collected for western blotting as described in section 2.9. Protein was run on a 10% gel and transferred to a PVDF membrane before being examined for the presence of STAT1 and pSTAT1. Actin was used as a loading control, and densitometry was used to measure the ratio of STAT1 and pSTAT1 expression compared to Actin. As expected, IFN- γ stimulation increased protein levels of both STAT1 and pSTAT1 compared to unstimulated cells. Neither PPAR(+), PPAR(-) MAPC cells or PPAR(-) γ MAPC cells displayed an increase in STAT1 or pSTAT levels, however PPAR(+) γ MAPC cells showed a slight reduction in STAT1 and pSTAT1 levels compared to γ MAPC cells (Fig. 3.20). Therefore, PPAR δ agonism may be suppressing the efficacy of MAPC cells in the aGvHD model due to a decrease in STAT1 signalling in response to IFN- γ *in vivo*.

3.19 PPAR δ agonism does not affect IFN- γ driven expression of IDO, PDL1 or ICAM1 by MAPC cells *in vitro*.

Following on from the previous section, I hypothesised that STAT1 target proteins may be reduced in γ MAPC cells by PPAR δ agonism. IDO is a STAT1 target gene in MSC

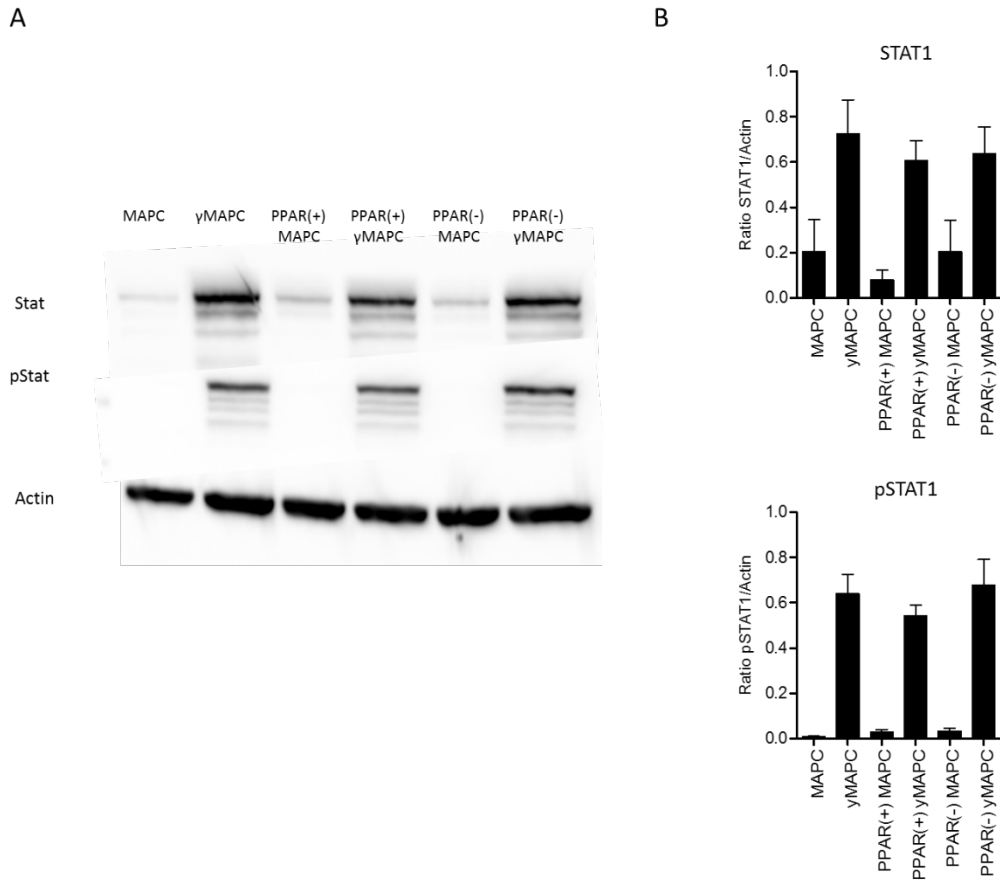


Figure 3.20 PPAR δ agonism slightly reduces IFN- γ induction of STAT1 and pSTAT1 in MAPC cells. MAPC cells, PPAR(+) MAPC cells and PPAR(-) MAPC cells were stimulated with IFN- γ for 24 hours before being collected and examined for protein levels of STAT1 and pSTAT1 by western blot. Actin was used as a loading control, and the ratio of proteins of interest to actin was measured using densitometry. Representative image (A) and densitometry (B) of STAT1 and pSTAT1 levels show that PPAR δ agonism of MAPC cells reduces the induction of STAT1 in response to IFN- γ . This data is representative of 4 independent experiments using 4 MAPC cell donors (n=4).

(Mounayar *et al.*, 2015; Vigo *et al.*, 2016) and is well known to be a key player in MSC mediated immunosuppression of T cells (Meisel *et al.*, 2004). Therefore, it was hypothesised that PPAR δ agonism may be suppressing IFN- γ induced IDO production by MAPC cells, which would explain why PPAR(+) MAPC cells (administered on day 7) and PPAR(+) γ MAPC (administered on day 0) cells are ineffective at treating GvHD. MAPC cells were cultured in 6 well plates and treated with the PPAR δ agonist or PPAR δ antagonist for 24 hours before being stimulated with 50 ng/ml IFN- γ as previously described in this chapter. Brefeldin A was added to cultures for the last 4 hours of the stimulation to prevent secretion of IDO from MAPC cells. Cells were harvested and surface stained with CD105 antibody before being stained intracellularly for IDO as described in section 2.10.1. Expression of IDO by CD105⁺ cells was then measured using flow cytometry. As expected, IFN- γ stimulation increased the percentage of MAPC cells producing IDO from 43.13% \pm 7.733 to 67.30 \pm 8.402 (n = 4). However, neither agonism or antagonism of PPAR δ in MAPC cells or γ MAPC cells had any effect on the frequency of cells producing IDO (Fig. 3.21).

Despite PPAR δ agonism having no effect on IDO, I next considered other IFN- γ target proteins which may be required for the efficacy and biodistribution of MAPC cells in the aGvHD model. According to Chinnadurai *et al.* (2014), IFN- γ stimulated human MSC require PDL1 to block T cell function *in vitro*, while STAT1 knock down MSC show reduced expression of PDL1 mRNA in response to IFN- γ stimulation (Vigo *et al.*, 2016). Similarly, ICAM1 expression is also induced by exposure to IFN- γ , and has been previously shown to be involved in immunosuppression by murine MSC (Ren *et al.*, 2010). Furthermore, PPAR δ knock out murine MSC express higher levels of ICAM1 in response to stimulation with pro-inflammatory cytokines than their wild type counterparts (Luz-Crawford *et al.*, 2016b). Thus, I sought to examine the effect of PPAR agonism and antagonism on both proteins.

MAPC cells were cultured with or without the PPAR δ agonist or antagonist for 24 hours as previously described before being stimulated with IFN- γ for either 4 or 24 hours. CD105⁺ MAPC cells were examined for the expression of ICAM1 and PDL1 by flow cytometry. As expected, IFN- γ stimulation increased expression of PDL1 by MAPC cells after 24 hours of

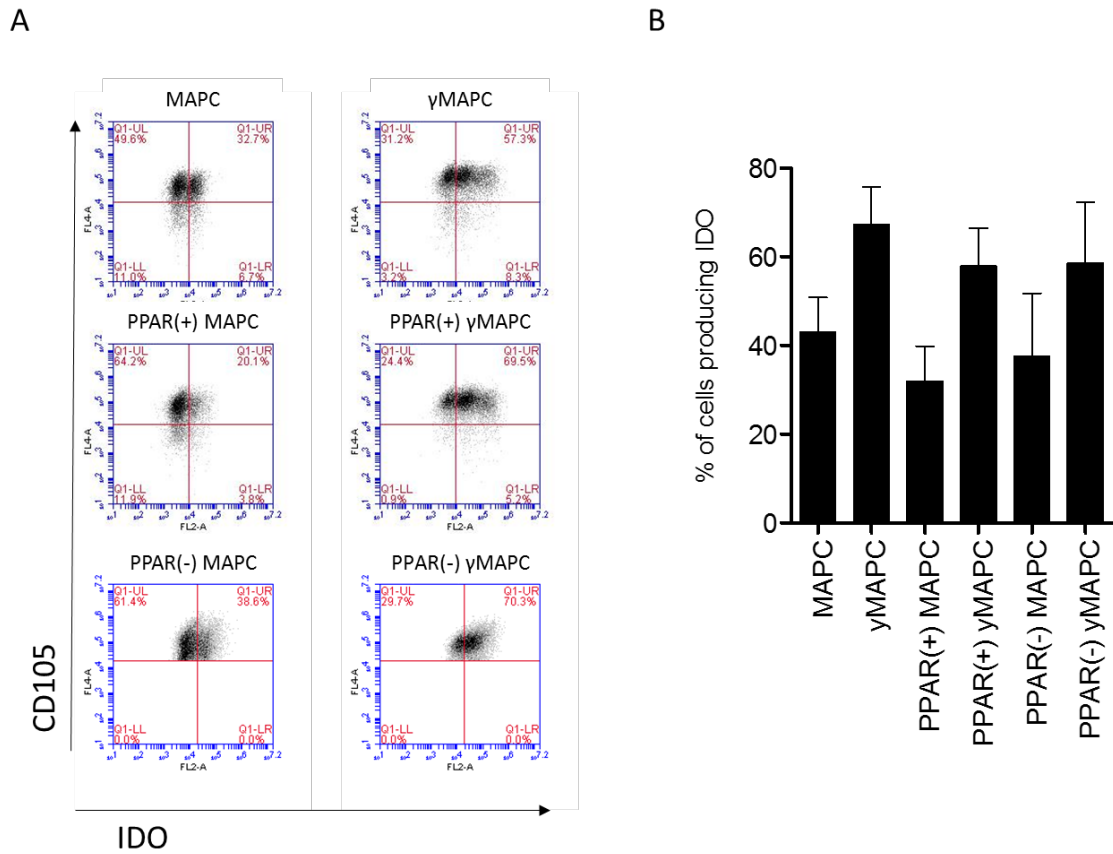


Figure 3.21 PPAR δ agonism or antagonism has no effect on IFN- γ induction of IDO in MAPC cells. MAPC cells, PPAR(+) MAPC cells and PPAR(-) MAPC cells were stimulated with IFN- γ for 24 hours with the addition of Brefeldin A for the last 4 hours of stimulation. Cells were surface stained for CD105 and stained intracellularly for IDO. CD105⁺ cells were pre-gated and examined for positive expression of IDO. Representative FACs plots (A) and bar graph (B) show that PPAR δ agonism or antagonism had no effect on IDO production by MAPC cells. This data is representative of 2 independent experiments using 2 MAPC cell donors (n = 4).

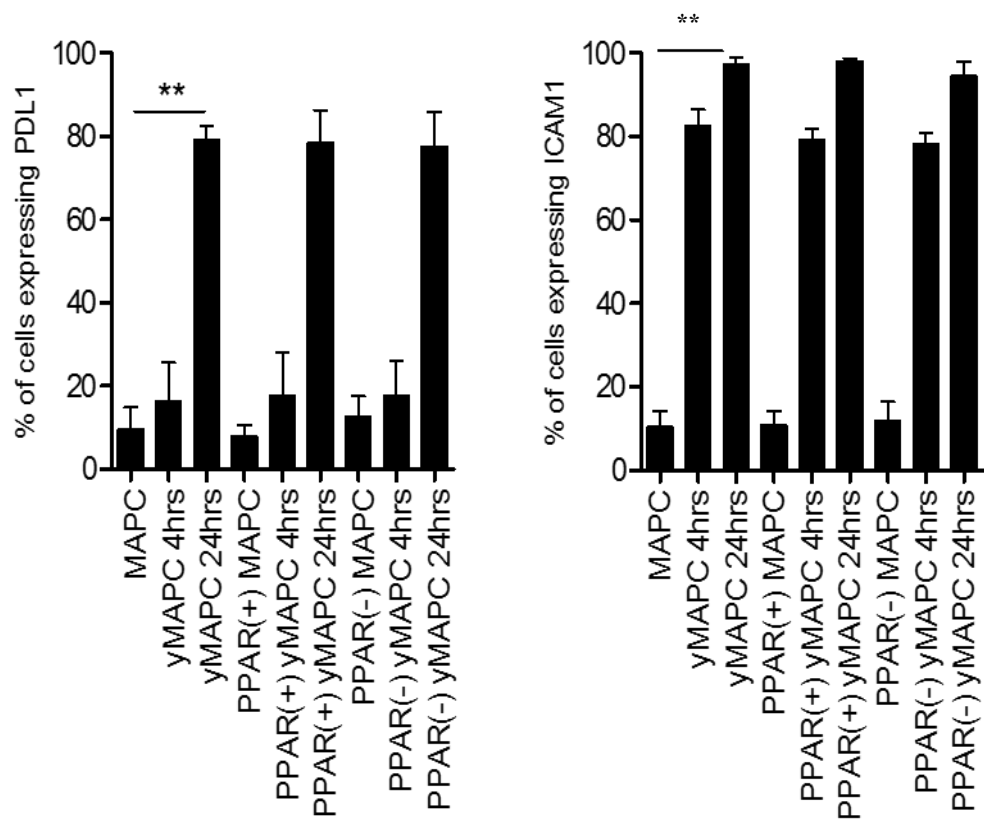


Figure 3.22 PPAR δ agonism or antagonism has no effect on IFN- γ induction PDL1 or ICAM1 in MAPC cells. MAPC cells, PPAR(+) MAPC cells and PPAR(-) MAPC cells were stimulated with IFN- γ for 4 or 24 hours. Cells were trypsinised and prepared for flow cytometry as described in section 2.10.1. Cells were surface stained for CD105 and PDL1 or ICAM1. Neither PPAR δ agonism or PPAR δ antagonism had an effect on the expression of PDL1 (A) or ICAM1 (B) by MAPC cells. This data is representative of 2 MAPC cell donors. Statistical analysis was carried out by using Kruskal-Wallis analysis with the original FDR method of Benjamini and Hochberg to correct for multiple comparisons where ** ≤ 0.01 .

stimulation (Fig. 3.22A), while ICAM1 was induced after both 4 and 24 hours (Fig. 3.22B). Neither PPAR δ agonism or antagonism had an effect of IFN- γ induction of PDL1 or ICAM1. Therefore, despite PPAR δ agonism having a slightly suppressive effect on STAT1 signalling, the STAT1 target proteins measured in this study were unaffected by PPAR δ agonism.

3.20 PPAR δ modulates expression of COX-2 by MAPC cells.

Along with IDO, PGE2 is the most widely reported mediator of MSC and MAPC cells immunosuppression, and has been reported to be required for MAPC cells and MSC efficacy in GvHD (Auletta *et al.*, 2015; Highfill *et al.*, 2009). PGE2 is converted from arachidonic acid by the enzyme COX-2 and both factors are constitutively expressed by both murine and human MSC, however their expression is further increased by exposure of MSC to IFN- γ or TNF- α (English *et al.*, 2007b; Aggarwal & Pittenger, 2005). Since COX-2 is an NF- κ B regulated protein, and Luz-Crawford *et al.*, (2016) reported increased NF- κ B activity following PPAR δ knock down, it was hypothesised that PPAR δ agonism and antagonism may alter COX-2 expression by MAPC cells. MAPC cells were treated with PPAR δ agonist and PPAR δ antagonist before being stimulated with IFN- γ as previously described. Cells were harvested and prepared for intracellular flow cytometry for the detection of COX-2. The mean fluorescence intensity (MFI) of COX-2 by unstimulated MAPC cells was 16270 \pm 595.6 and this increased to 22270 \pm 1564 after IFN- γ stimulation (n = 3).

PPAR(+) MAPC cells and PPAR(-) MAPC cells showed similar levels of COX-2 expression to unstimulated MAPC cells. However, PPAR δ agonism decreased the MFI of IFN- γ stimulated cells to 16500 \pm 1427 (n = 3) while PPAR δ antagonism increased the MFI of IFN- γ stimulated cells to 36330 \pm 3921 (n = 3) (Fig. 3.23). Overall, this data suggests for the first time that the reduced efficacy of PPAR(+) MAPC cells and γ MAPC cells in the GvHD model may be due to the inhibition of COX-2 expression, and subsequent PGE2 production.

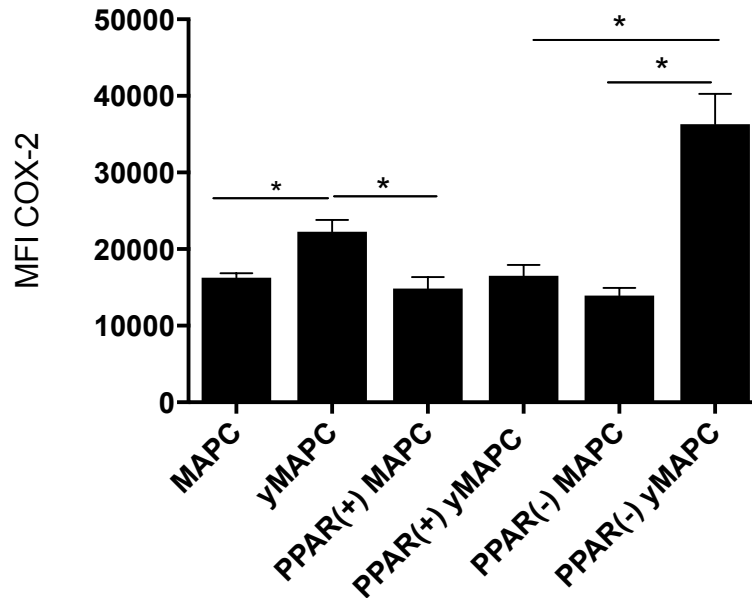


Figure 3.23 PPAR δ agonism and antagonism modulates IFN- γ induction of COX-2.

MAPC cells, PPAR(+) MAPC cells and PPAR(-) MAPC cells were stimulated with IFN- γ for 24 hours. Cells were trypsinised and prepared for flow cytometry as described in section 2.10.1. Cells were surface stained for CD105 and stained intracellularly for COX-2. The MFI of COX-2 was measured. IFN- γ stimulation increased COX-2 expression by MAPC cells and this effect was inhibited by PPAR δ agonism. Expression of COX-2 by γ MAPC cells was further increased when PPAR δ was antagonised. This data is representative of 3 MAPC cell donors. Statistical analysis was carried out using Kruskal-Wallis analysis with the original FDR method of Benjamini and Hochberg to correct for multiple comparisons where $*\leq 0.05$.

3.21 Summary

The aim of this chapter was to examine the biodistribution and mechanisms of action of MAPC cells in a humanised model of aGvHD. Our group and others have previously shown that manipulation of MSC prior to administration to animal models can improve their therapeutic efficacy (Tobin *et al.*, 2013; Luz-Crawford *et al.*, 2016b), and I sought to elucidate whether the improved functionality of MSC in these instances may be due to enhanced biodistribution *in vivo*. Prior to commencing *in vivo* experiments, *in vitro* validation assays were carried out to ensure that MAPC cells used for this study met the criteria of the ISCT and were functional. Once the quality of MAPC cells was confirmed, the cells were introduced to the humanised aGvHD model.

It is well documented in the literature that MSC and MAPC cells accumulate in the lungs following intravenous administration, however their localisation to the spleen is required for optimal immunosuppression (Highfill *et al.*, 2009). It was first shown that MAPC cells have the capacity to migrate towards the spleen in the humanised aGvHD model, as higher numbers of MAPC cells were detected in the spleen of aGvHD mice than healthy mice, indicating that localisation of MAPC cells to T cell priming sites is not a passive process. Secondly, I sought to examine the effects of IFN- γ activation of MAPC cells on their biodistribution *in vivo*. Our group have previously shown that IFN- γ licensing of MSC improves their efficacy in aGvHD (Tobin *et al.*, 2013), and that data was reproduced herein with MAPC cells. The increased therapeutic efficacy of γ MAPC cells in the humanised aGvHD model correlated with an increase in the number of MAPC cells detected in aGvHD target organs following licensing with IFN- γ . Thirdly, effects of PPAR δ agonism and antagonism on the therapeutic efficacy of MAPC cells was examined. It's previously been shown that inhibition of PPAR δ increases the therapeutic efficacy of murine MSC, and that data was reproduced here in our clinically relevant humanised mouse model of acute GvHD. Furthermore, PPAR δ agonism hindered the immunosuppressive capacity and biodistribution of MAPC cells and γ MAPC cells in aGvHD. The effects of PPAR δ agonism on MAPC cells was

then examined *in vitro*, and surprisingly, it was shown that PPAR δ agonism slightly reduces IFN- γ induction of STAT1 and pSTAT1 and impairs IFN- γ induction of COX-2.

Chapter 4
MAPC cells suppress IL-7 driven stimulation of
T cells *in vivo*.

4.1 Introduction

In the setting of transplantation, an individual is deliberately immunosuppressed in order to avoid allograft rejection by the immune system. Induction therapy is administered prior to or at the same time as transplantation to deplete the immune compartment, subsequently reducing the likelihood of acute rejection. In the lymphopenic environment following induction therapy, the effector memory T cells which remain undergo rapid homeostatic proliferation (HP), driven by the abundant availability of self MHC/peptide complexes and gamma chain cytokines such as IL-7 and IL-15 (Neujahr *et al.*, 2006; Traitanon *et al.*, 2014). IL-7 signaling blockade has been shown to prevent GvHD and promote islet and skin allograft survival in experimental models (Chung, Dudl & Min, 2007; Mai *et al.*, 2014), however, currently there are no approved therapies to target IL-7 driven HP in transplant recipients. Work carried out by our collaborators at Kings College London and the cell therapy company Athersys Inc. has shown that MAPC cells suppress IL-7 driven proliferation and pro-inflammatory cytokine production by CD4⁺ T cells *in vitro* in a PGE2 dependent manner (Reading *et al.*, 2015, 2013). Thus, the aim of this chapter was to build upon the *in vitro* work completed by Reading *et al.* (2015) by examining whether the inhibitory effect of MAPC cells on IL-7 stimulated T cells could be replicated *in vivo*. Furthermore, since Highfill *et al.* (2010) had reported that MAPC cells must be administered locally to sites of allo-priming in order to be therapeutic in a murine model of aGvHD, I sought to compare the efficacy of MAPC cells delivered by two different routes at suppressing homeostatic proliferation of T cells *in vivo*.

4.2 Optimisation of IL-7 driven homeostatic proliferation *in vivo* model.

In order to measure the effects of MAPC cells on IL-7 induced proliferation of T cells *in vivo*, an *in vivo* model of HP was developed and optimised based on the system outlined in Boyman *et al.* (2008). Spleens were collected from CD45.2⁺ mice and splenocytes were prepared as described in section 2.8.2. CD4⁺ cells were isolated using a murine CD4⁺ T cell isolation kit with 90% purity (Fig. 4.1A) and were subsequently stained with eFluor proliferation dye (Fig.

4.1B). Cells were CD45.1⁻ and CD45.2⁺ (Fig. 4.1C and 4.1D respectively). Cells were then administered IV to CD45.1 mice on day -2. T cells were driven to proliferate using IP administration of IL-7/anti-IL-7 mAb (M25) on days 0, 2 and 4 as outlined in section 2.8.2. In order to determine the optimal concentration of IL-7/M25 to use, either 1 µg IL-7 conjugated to 5 µg M25 or 2 µg IL-7 conjugated to 10 µg M25 was tested.

Spleens and lymph nodes were harvested on day 5 to examine the proliferation of CD4⁺ T cells. Two approaches were used to determine the most appropriate method to measure proliferation. Proliferation of adoptively transferred cells was investigated using dilution of eFluor proliferation dye, while proliferating endogenous cells were measured using Ki67 as a marker of proliferation. The number of CD45.1⁺ CD4⁺ Ki67⁺ cells was significantly increased in the lymph nodes following administration of 1 µg IL-7 conjugated to 5 µg M25 (n = 3). This significance was enhanced following administration of 2 µg IL-7 conjugated to 10 µg M25 (n = 3) (Fig. 4.2A). The number of CD45.1⁺ CD4⁺ Ki67⁺ cells was significantly increased in the spleen following administration of 2 µg IL-7 conjugated to 10 µg M25 (n = 3) (Fig. 4.2A). The number of proliferating adoptively transferred cells measured using eFluor proliferation dye was not significantly increased in either the spleen or the lymph nodes by the IL-7/M25 at both concentrations used (Fig. 4.2B). The number of CD45.2⁺ cells detected was very low and as a result of this, data was not robust. As the CD45.1⁺ endogenous cells were responding to IL-7, it was decided that future experiments would be carried out using the higher dose of IL-7/M25, examining Ki67 expression in endogenous cells.

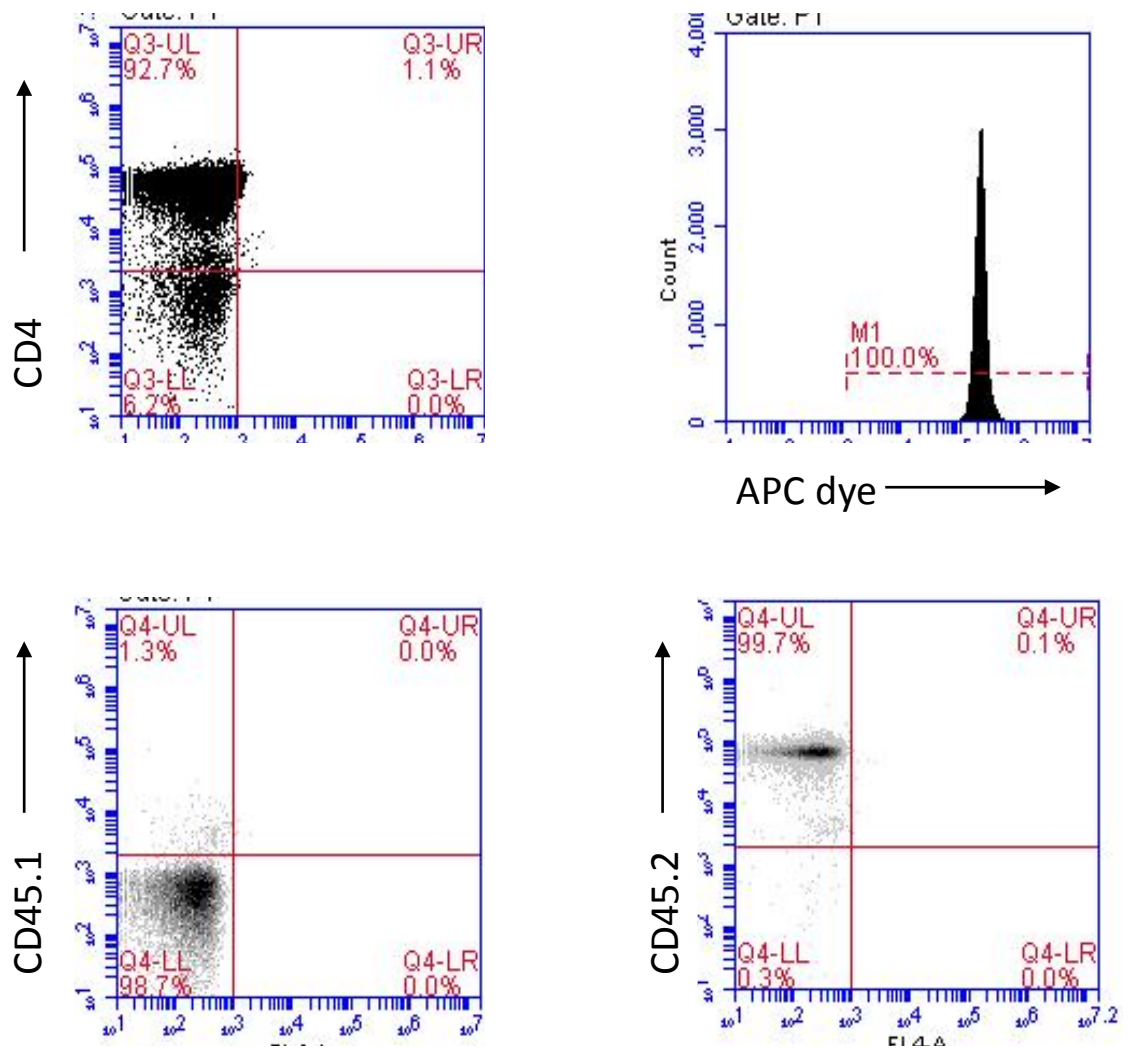


Figure 4.1 Isolation and staining of CD45.2⁺ CD4⁺ splenocytes with eFluor proliferation dye. Splens were harvested from CD45.2 mice and CD4⁺ T cells were isolated using a negative selection kit. 90% of the collected cells were positive for CD4⁺ expression (A). CD4⁺ cells were subsequently stained with an APC eFluor proliferation dye (B). Cells were verified to be suitable for adoptive transfer by staining for negative expression of CD45.1 (C) and positive expression of CD45.2 (D).

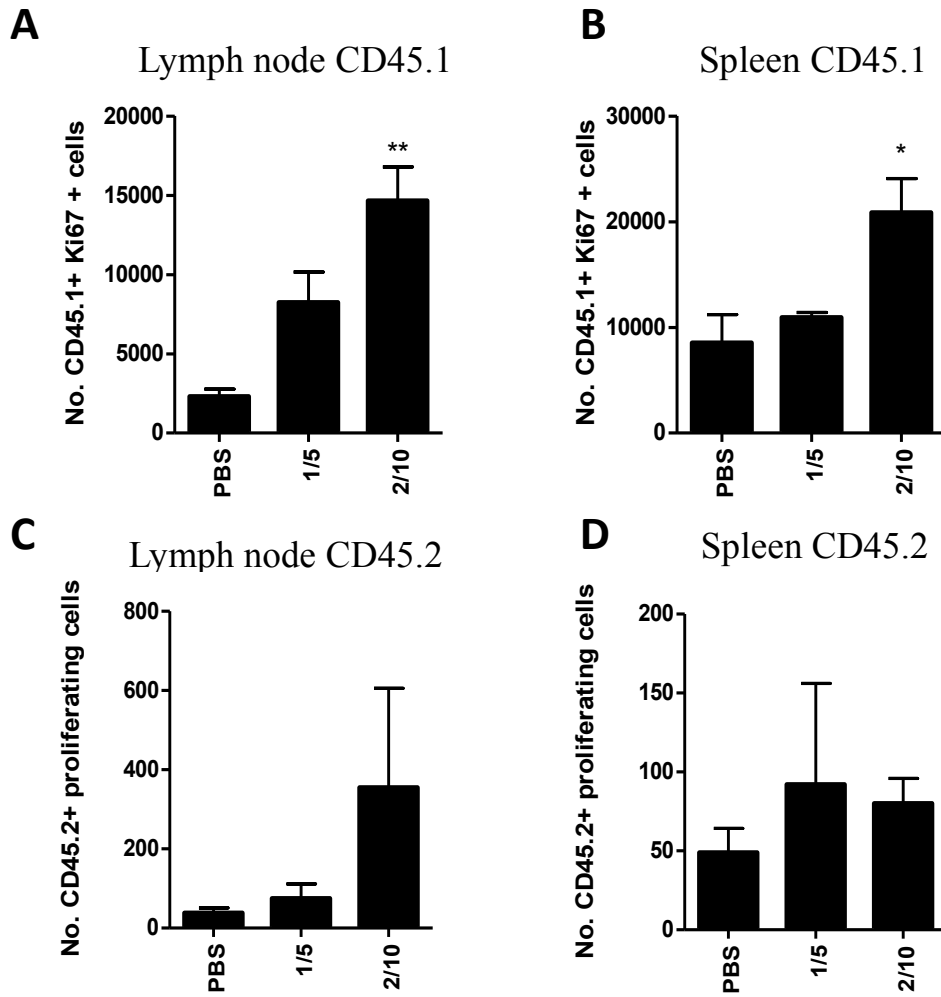
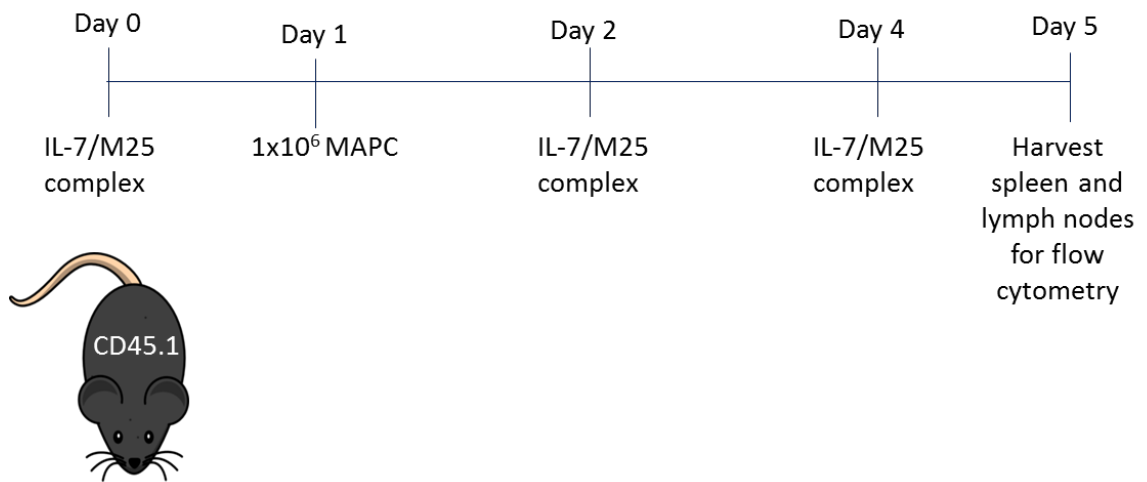


Figure 4.2 Optimisation of IL-7 driven homeostatic proliferation *in vivo* model. CD45.2⁺ CD4⁺ cells stained with eFluor proliferation dye were administered to CD45.1 mice on day -2. On days 0, 2 and 4, IL-7 conjugated to M25 was administered at two different concentrations, 1 μ g IL-7 with 5 μ g M25, or 2 μ g IL-7 with 10 μ g M25. Proliferation of endogenous CD45.1⁺ CD4⁺ cells was measured in the lymph nodes and spleen using Ki67 as a marker of proliferation (A and B respectively). Proliferation of CD45.2⁺ CD4⁺ cells was measured in the lymph nodes and spleen by quantifying the number of cells which had diluted eFluor proliferation dye compared to unproliferated cells (C and D respectively). The number of CD45.1⁺ CD4⁺ cells expressing Ki67 in the lymph nodes was increased by both concentrations of IL-7/M25 (A), while only the higher concentration of IL-7/M25 significantly increased proliferation in the spleen (B). Neither concentrations of IL-7/M25 had a significant effect on proliferation of CD45.2⁺ CD4⁺ cells in the lymph nodes or the spleen (C and D respectively). Normality was confirmed using the Shapiro-Wilk normality test. Statistical analysis was carried out using ANOVA analysis where * ≤ 0.05 and ** ≤ 0.01 .



Groups:

A: PBS

B: PBS + MAPC

C: IL-7

D: IL-7 + MAPC

Figure 4.3 Timeline of *in vivo* IL-7 driven homeostatic proliferation model. CD45.1 mice were injected IP with either PBS or $2\mu\text{g}/10\mu\text{g}$ IL-7/M25 on days 0, 2 and 4. On day 1 1×10^6 MAPC cells IV were administered to treatment groups. On day 5 spleens and lymph nodes were harvested and prepared for flow cytometry as described in section 2.10.

4.3 MAPC cells administered IV reduce proliferation and production of IFN- γ by T cells in response to IL-7 in the spleen but not the lymph nodes.

Following the optimization of the IL-7 driven homeostatic proliferation model, MAPC cells were introduced to the system. It has previously been shown *in vitro* that MAPC cells suppress the proliferation and production of pro-inflammatory cytokines by T cells in response to IL-7 (Reading *et al.*, 2013), however this has not yet been shown *in vivo*. It was hypothesized that the activity of MAPC cells *in vivo* would mirror that of their activity *in vitro*, and therefore suppress the activity of T cells in response to IL-7. Three doses of IL-7/M25 were administered to CD45.1 mice on days 0, 2 and 4 as shown schematically in figure 4.3. 1×10^6 MAPC cells were administered IV (MAPC cells IV) on day 1. Spleens and lymph nodes were harvested on day 5 and processed for intracellular flow cytometry to examine expression of Ki67 and production of IFN- γ as described in section 2.10. PBS administered mice were used as a negative control, and mice that received PBS and MAPC cells IV were used as an internal control to ensure that MAPC cells alone weren't affecting the proliferation or cytokine production of T cells *in vivo*. As expected, IL-7 significantly enhanced the number of Ki67⁺, IFN- γ ⁺, and TNF- α ⁺ T cells in both the CD4 and CD8 compartments in the spleen. IV administration of MAPC cells (MAPC cells IV) on day 1 reduced the number of Ki67⁺, IFN- γ ⁺ and TNF- α ⁺ T cells in the spleen in both the CD4 (n = 6) (Fig. 4.4) and CD8 compartments (n = 6-8) (Fig. 4.5).

In the lymph nodes, IL-7 similarly increased the number of Ki67 and IFN- γ expressing CD4⁺ and CD8⁺ T cells, however this was not as significant as seen in the spleen. MAPC cells IV did not have a suppressive effect on either Ki67 expression or IFN- γ production by T cells in the lymph nodes (Fig. 4.6). This data suggests that MAPC cells can suppress IL-7 stimulation of T cells *in vivo*, however this suppression is not systemic, but is site specific.

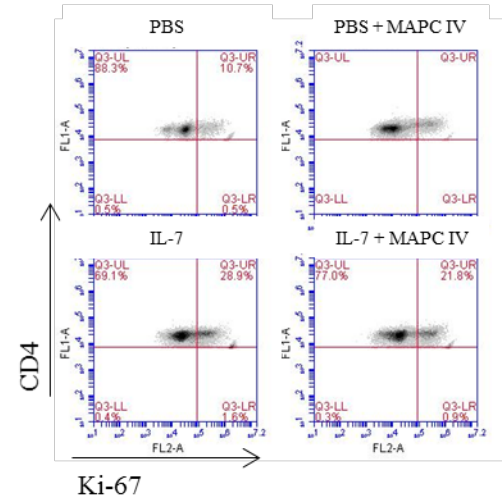
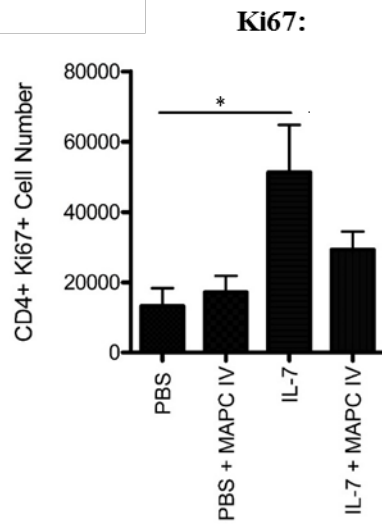
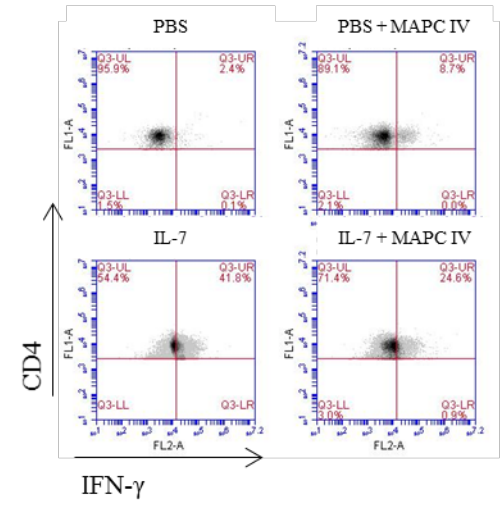
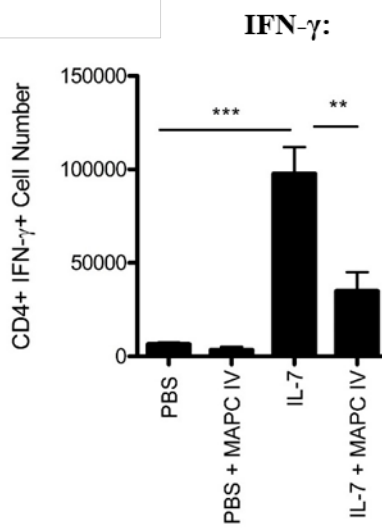
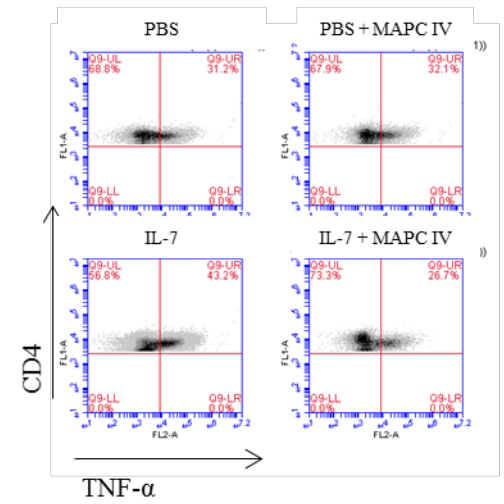
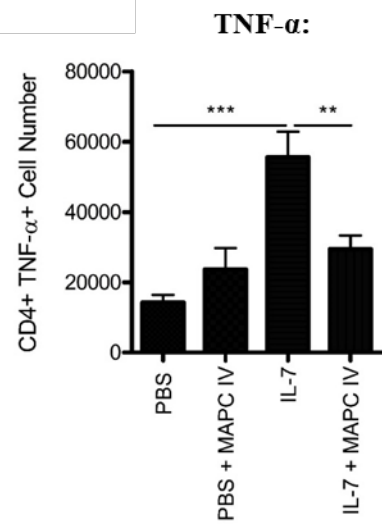
A**B****C**

Figure 4.4 MAPC cells suppress IL-7 driven proliferation of CD4⁺ T cells and production of IFN- γ and TNF- α in the spleen. 2/10 μ g of IL-7/M25 was administered IP to CD45.1mice on days 0, 2 and 4. On day 1, 1 \times 10⁶ MAPC cells were administered IV. On day 5, spleens were harvested and prepared for intracellular flow cytometry as described in section 2.10. IL-7 significantly increased the number of CD4⁺ T cells expressing Ki67 and MAPC cells reduced this (A). Similarly, MAPC cells significantly suppressed IL-7 driven production of IFN- γ and TNF- α (B and C respectively). Normality was confirmed using the Shapiro-Wilk normality test. Statistical analysis was carried out using ANOVA analysis where * \leq 0.05, ** \leq 0.01 and *** \leq 0.001. Data is representative of 2 independent experiments using 2 MAPC cell donors, n = 6/group.

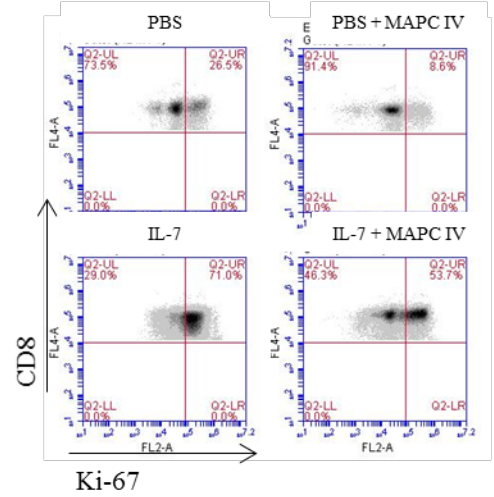
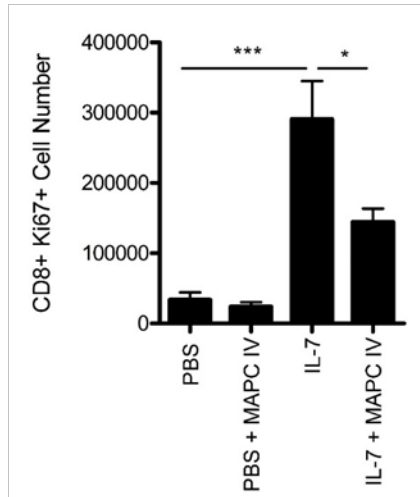
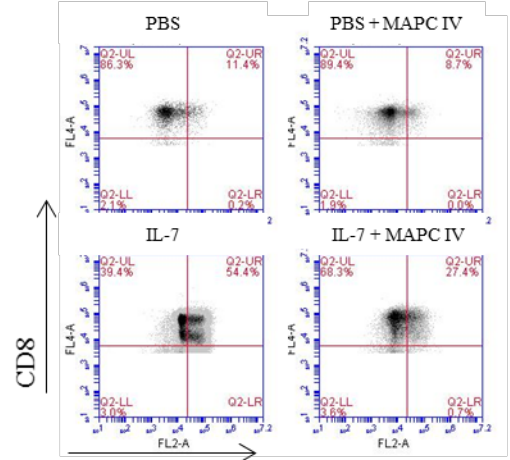
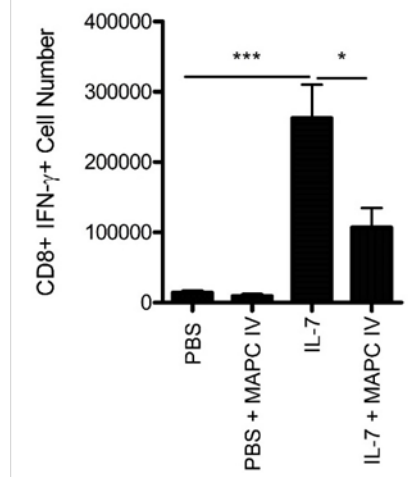
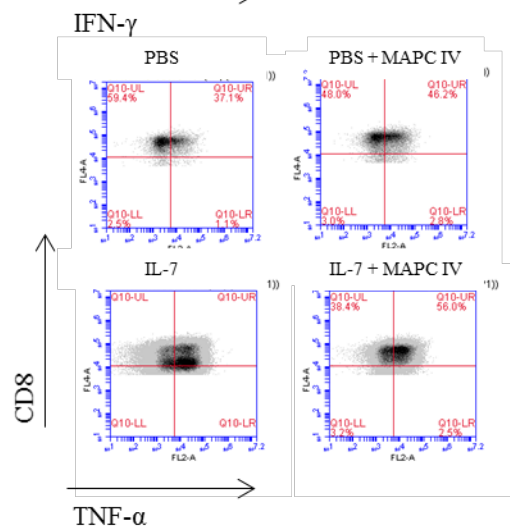
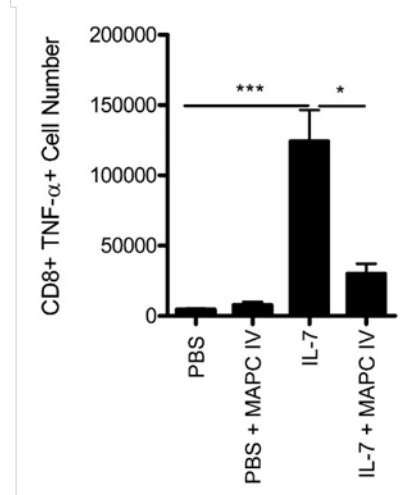
A**B****C**

Figure 4.5 MAPC cells suppress IL-7 driven proliferation of CD8⁺ T cells and production of IFN- γ and TNF- α in the spleen. The IL-7 model was set up as described in figure legend 4.4. IL-7 significantly increased the number of CD8⁺ T cells expressing Ki67, and MAPC cells significantly reduced this (A). Similarly, MAPC cells significantly suppressed IL-7 driven production of IFN- γ and TNF- α by CD8⁺ T cells (B and C respectively). Normality was confirmed using the Shapiro-Wilk normality test. Statistical analysis was carried out using ANOVA analysis where * ≤ 0.05 and *** ≤ 0.001 . Data is representative of 2 independent experiments using 2 MAPC cell donors, n = 6/group.

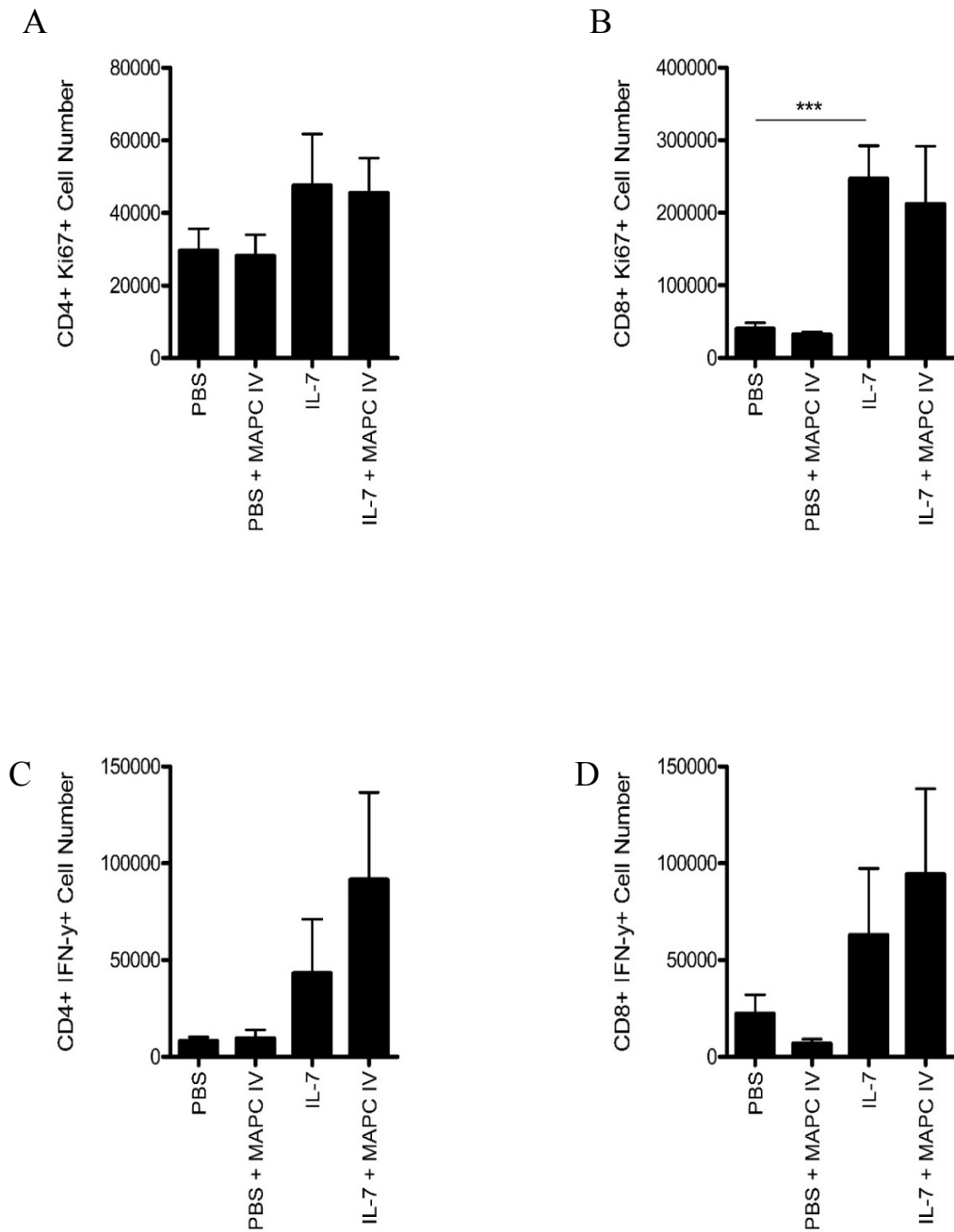


Figure 4.6 MAPC cells do not suppress IL-7 driven proliferation or production of IFN- γ by T cells in the lymph nodes. The IL-7 model was set up as described in figure legend 4.4. On day 5, lymph nodes were harvested from CD45.1 mice and prepared for intracellular flow cytometry as described in section 2.10. IL-7 increased the number of CD4⁺ and CD8⁺ T cells expressing Ki67 (A and B respectively) and IFN- γ (C and D respectively). MAPC cells didn't reduce the number of Ki67⁺ or IFN- γ ⁺ cells in either the CD4⁺ or CD8⁺ compartments in the lymph nodes. Statistical analysis was carried out using Kruskal-Wallis analysis with the original FDR method of Benjamini and Hochberg to correct for multiple comparisons where *** ≤ 0.001 . Data is representative of 2 independent experiments using 2 MAPC cell donors, n = 6/group.

4.4 MAPC cells administered IP reduce proliferation and production of IFN- γ by T cells in response to IL-7 in the spleen and lymph nodes.

According to Highfill *et al.* (2010), MAPC cells are only therapeutic in GvHD when injected intrasplenically as opposed to systemically. Following on from the previous result, I sought to determine if an alternative method of MAPC cells administration would affect the efficacy of MAPC cells on T cell HP. The experiment described in section 4.3 was repeated with the addition of an IP administered MAPC cells (MAPC cells IP) group. A PBS + MAPC cells IP group was used as an internal control to ensure MAPC cells IP were not affecting T cell proliferation or IFN- γ production. As expected, IL-7 increased the number Ki67⁺ and IFN- γ ⁺ T cells in both the spleen and lymph nodes (Figs. 4.7 and 4.8 respectively). While both MAPC cells IP and MAPC cells IV suppressed the effects of IL-7 on Ki67 expression and IFN- γ production in CD4⁺ and CD8⁺ T cells in the spleen (n = 6) (Fig. 4.7), only MAPC cells IP suppressed CD8⁺ T cell proliferation and IFN- γ production by CD4⁺ and CD8⁺ T cells in the lymph nodes. Neither MAPC cells IV or MAPC cells IP suppressed the proliferation of CD4⁺ T cells in the lymph nodes (Fig. 4.8). Therefore, while both MAPC cells IV and MAPC cells IP reduce IL-7 driven HP of T cells in the spleen, only MAPC cells IP are effective at suppressing T cell stimulation in the lymph nodes.

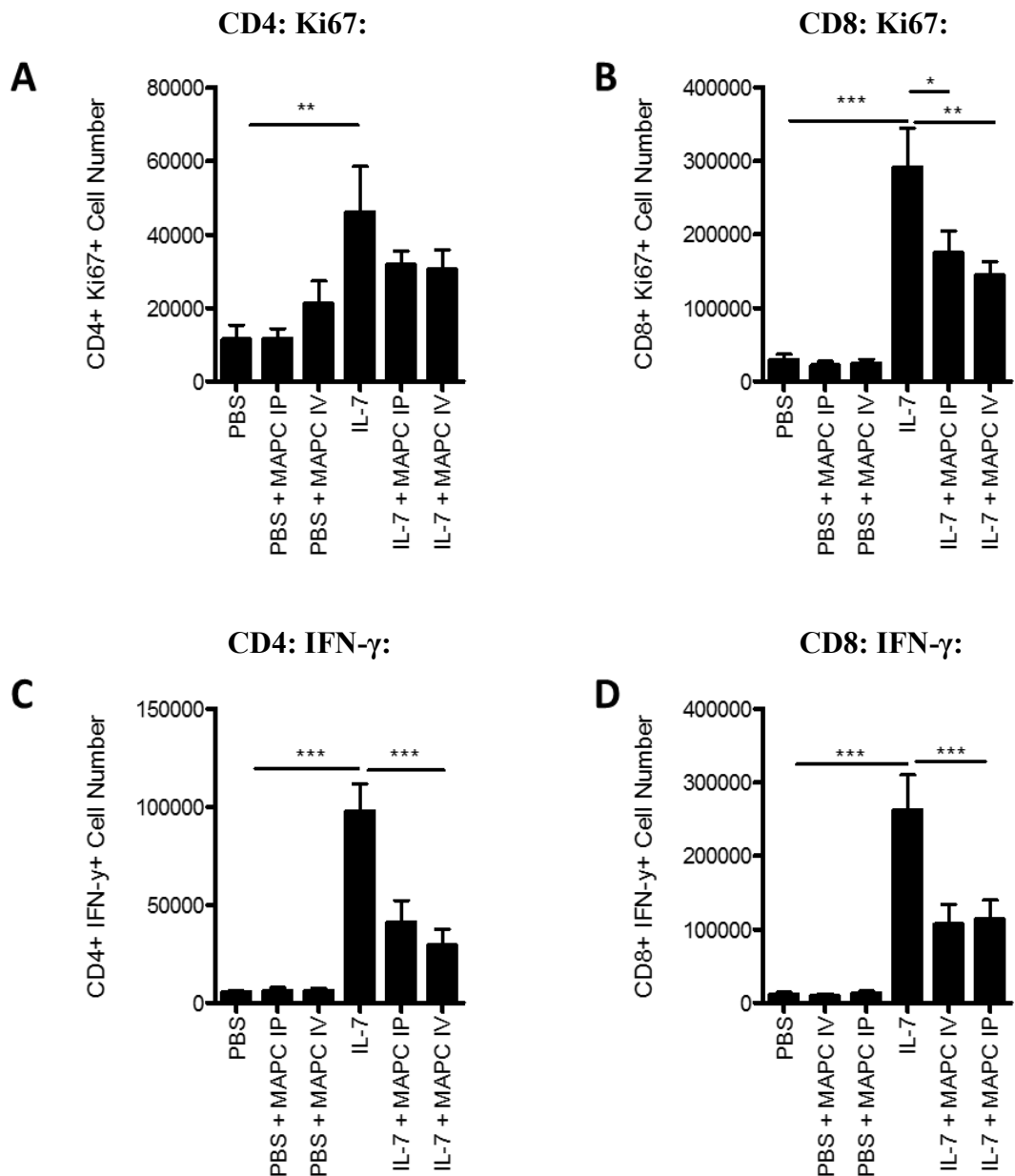


Figure 4.7 MAPC cells IP suppress IL-7 driven proliferation and production of IFN- γ by T cells in the spleen. IL-7/M25 was administered IP to CD45.1 mice on days 0, 2 and 4. On day 1, 1×10^6 MAPC cells were administered IV or IP. On day 5, spleens were harvested and prepared for intracellular flow cytometry as described in section 2.10. IL-7 significantly increased the number of CD4⁺ and CD8⁺ T cells expressing Ki67 (A and B respectively) and IFN- γ (C and D respectively). Both MAPC cells IP and MAPC cells IV suppressed the proliferation and production of IFN- γ with similar efficacy. Normality was confirmed using the Shapiro-Wilk normality test. Statistical analysis was carried out using ANOVA analysis where * ≤ 0.05 , ** ≤ 0.01 and *** ≤ 0.001 . Data is representative of 2 independent experiments using 2 MAPC cell donors, n = 6/group.

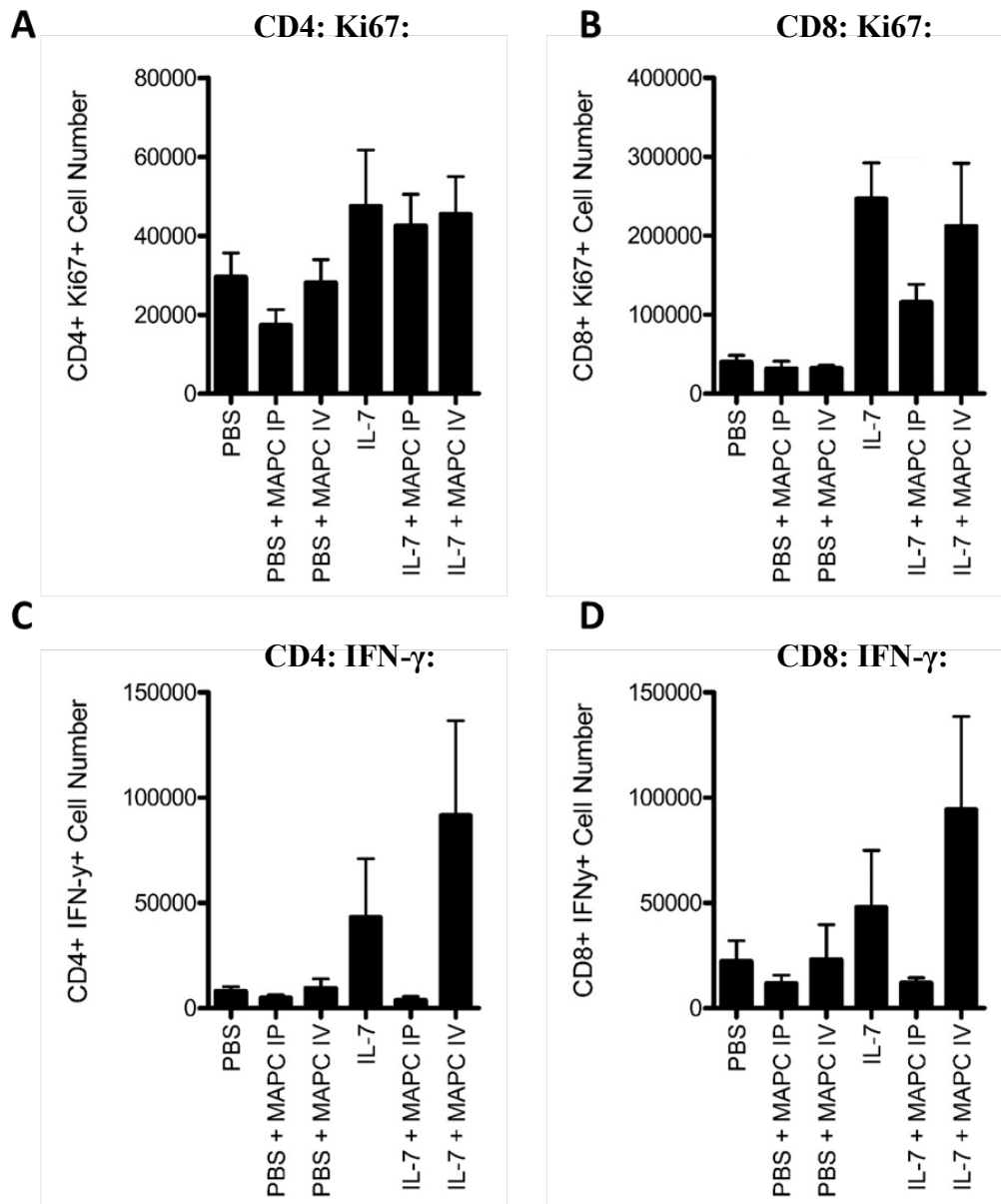


Figure 4.8 MAPC cells IP suppress IL-7 driven proliferation and production of IFN- γ by T cells in the lymph nodes. The IL-7 model was set up as described in figure legend 4.7. On day 5, lymph nodes were harvested and prepared for intracellular flow cytometry as described in section 2.10. IL-7 didn't significantly increase the number of CD4⁺ Ki67⁺ cells in the lymph nodes, and MAPC cells didn't change this any further (A). The number of CD8⁺ T cells expressing Ki67 was increased with IL-7 administration. MAPC cells IP suppressed this proliferation while MAPC cells IV did not (B). Similarly, IL-7 increased the production of IFN- γ in both the CD4⁺ and CD8⁺ compartments (C and D respectively) and this was suppressed by MAPC cells IP but not MAPC cells IV. Data is representative of 2 independent experiments using 2 MAPC cell donors, n = 6/group.

4.5 IL-7 and MAPC cells alter the frequency and number of the immune cell compartments in the spleen.

Following on from the T cell proliferation and cytokine data described in previous sections, it was decided that a more extensive immunophenotyping study would be carried out in a collaborative effort with researchers James Reading, Tim Tree and the 3i team in Kings College London. Since both MSC and MAPC cells can mediate their effects on T cells through alternative cell types, the effects of MAPC cells on other components of the immune system was of interest (Cahill *et al.*, 2015; Eggenhofer *et al.*, 2013). The experiment described in section 4.3 was repeated and spleens were harvested and shipped (at 4°C) to Kings College London where James Reading and the 3i team prepared the samples for flow cytometry using the T cell, B cell, and myeloid panels outlined in tables 2.12-2.14 and acquired the samples. The data was generated using an automated gating pipeline in the DIVA software pack. This data was then sent back to me for statistical analysis. Gating was based on the gating dendrograms in Fig. 4.9. The results stated in sections 4.10 – 4.18 were obtained from this experiment, and thus were completed in collaboration with James Reading, Tim Tree and the 3i team.

The purpose of the study was to examine the effects of MAPC cells on the wider immune system outside the T cell panels that had been looked at in MU. Three 12 colour panels were used to characterize the effects of IL-7 and MAPC cells on the T cell, B cell and myeloid populations in the spleen. All of these panels were based on the gating of CD45⁺, live, single cells. After gating on these cells, myeloid cells were characterized as CD3⁻ CD19⁻ and CD161⁻. The number of myeloid cells in the spleen increased from 11300±697.9 in the PBS group to 15700±746.1 in the IL-7 group (n = 6). MAPC cells IV significantly reduced the number of myeloid cells to 10470±764.7 (n = 6), while MAPC cells IP didn't have a significant effect on the number of myeloid cells (Fig. 4.10A). The percentage of each of these populations follows the same trend as the number data (Fig. 4.10B).

T cells were characterized as CD161⁻, TCRβ⁺ and TCRδ⁺. The number of T cells in the spleen was increased from 80770±3702 to 110500±7445 when IL-7 was administered (n = 6).

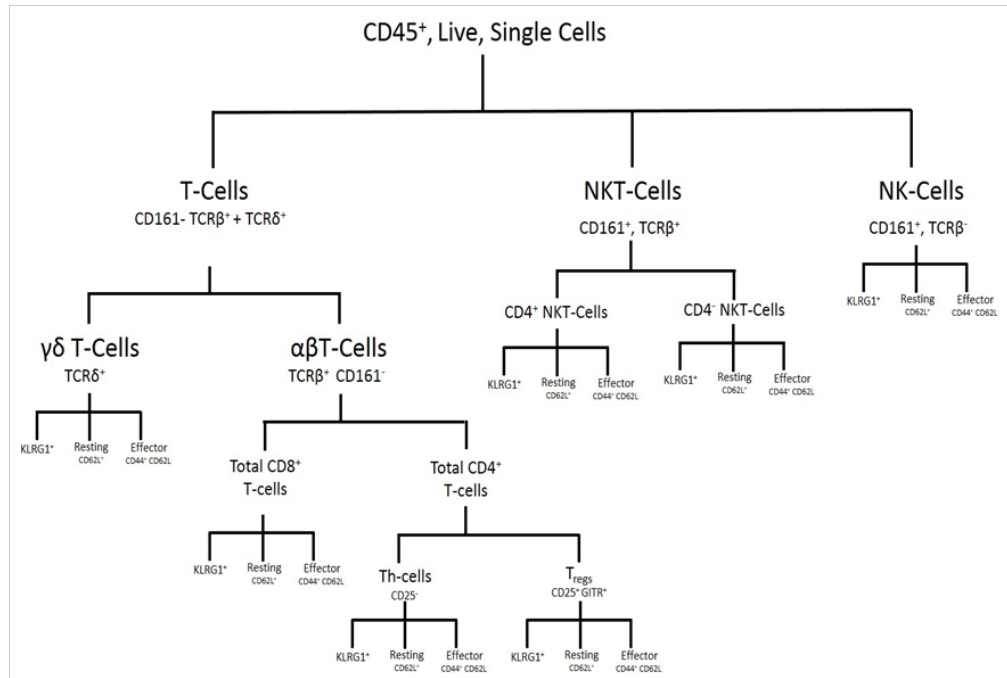
Neither MAPC cells IV or MAPC cells IP significantly reduced the number of T cells (Fig. 4.10C). The percentage data for this data-set follows the same trend as the cell number data (Fig. 4.10D).

B cells were characterized as CD19⁺ cells. The number of B cells in the spleen was unchanged between the PBS and the IL-7 groups. However, the number of B cells in the spleens of the IL-7 group increased from 79470±9112 to 132000±10670 with MAPC cells IV and 124800±11930 with MAPC cells IP (n = 6). The percentage of CD45, live, single cells in the spleen which were B cells decreased from 58.35%±1.184 to 45.75%±2.089 when IL-7 was administered (n = 6). This is presumably due to the growth of the T cell pool following IL-7 administration, thus does not represent an actual effect of IL-7 on B cells. This percentage was enhanced to 50.89±1.512 with MAPC cells IV and 54.75% ±2.541 with MAPC cells IP (n = 6) (Figs. 4.10E and 4.10F). Taken together, these results show that IL-7 and MAPC cells alter the immune compartments in the spleen when looking at both number and percentage data.

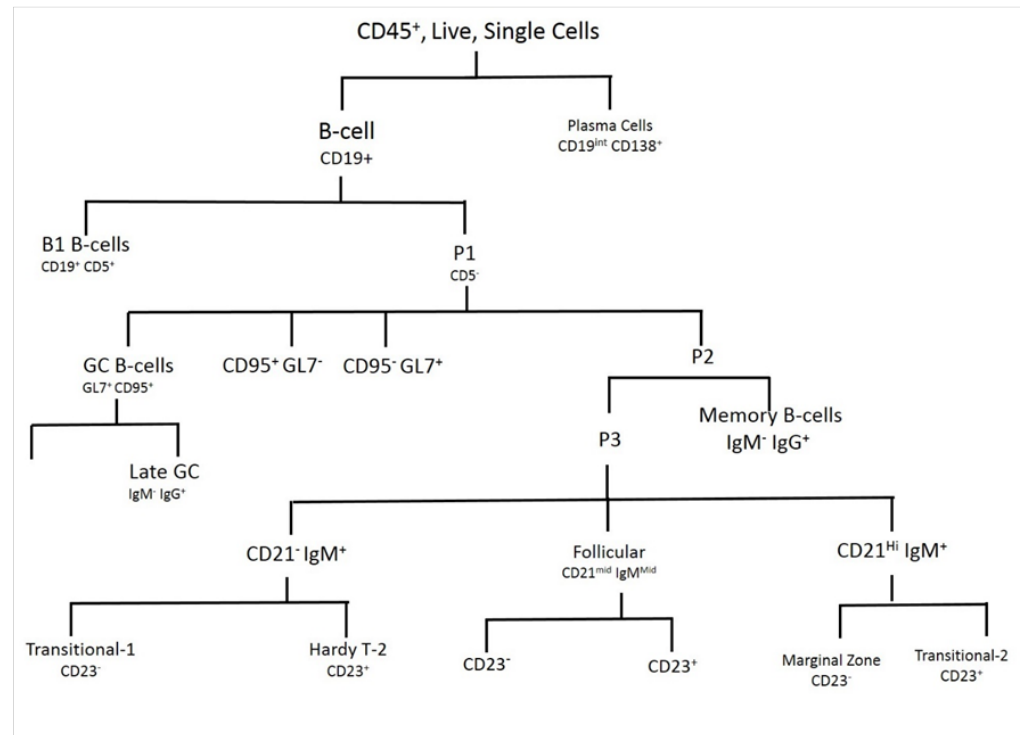
4.6 MAPC cells suppress the number and frequency of monocytes, eosinophils and granulocytes in the spleen.

While the effects of IL-7 on the HP of T cells has been widely documented (Monti & Piemonti, 2013), the effects of IL-7 on myeloid cells in the context of homeostatic proliferation has not been well studied. Due to the role of APC as providers of self MHC/peptide complexes, I sought to understand the effects of both IL-7 and MAPC cells on the myeloid populations. Since MSC are known to modulate innate immune cells (Le Blanc & Davies, 2015), It was hypothesised that MAPC cells may reduce the number of APC *in vivo*, limiting the abundance of homeostatic stimuli available to T cells in the model.

A



B



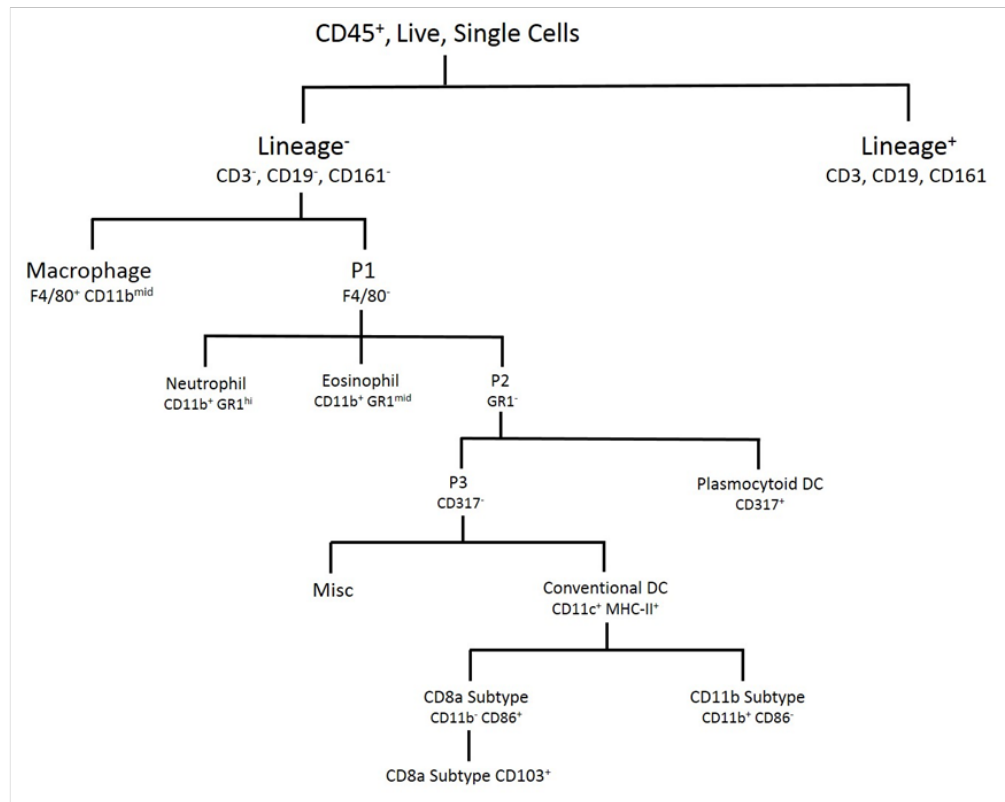
C

Figure 4.9 Gating dendrograms used for the 3i study. The above gating dendrograms were designed and provided by the 3i team in Kings College London to allow for the characterisation of T cells (A), B cells (B) and myeloid cells (C) in the immunophenotyping study.

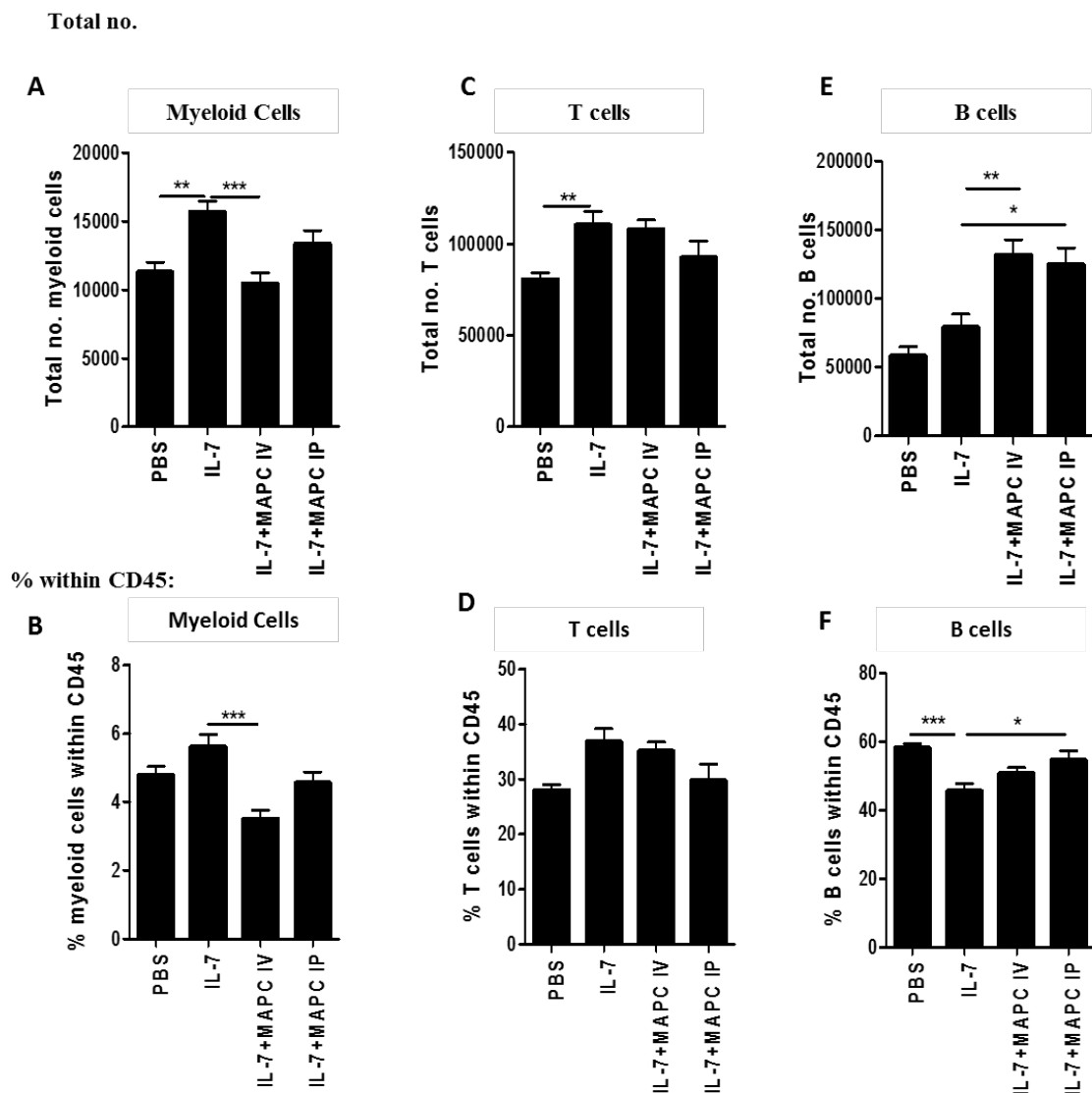


Figure 4.10 IL-7 and MAPC cells altered the immune compartments in the spleen. The IL-7 model was set up as described in figure legend 4.7. On day 5, spleens were harvested and sent to the 3i team for processing and flow cytometric analysis. IL-7 increased the number (A) and frequency (B) of myeloid cells in the spleen, and this effect was reduced by MAPC cells IV. IL-7 also increased the number (C) and frequency (D) of T cells in the spleen. This was slightly reduced by MAPC cells IP, though this was not significant. IL-7 treatment had no effect on the number of B cells in the spleen (E) but significantly reduced the frequency (F). Both MAPC cells IV and MAPC cells IP increased the number (E) and frequency (F) of B cells in the spleen. Normality of number data was confirmed using the Shapiro-Wilk normality test. Statistical analysis of number data was carried out using ANOVA analysis, and analysis of frequency data was carried out using Kruskal-Wallis analysis where * ≤ 0.05 , ** ≤ 0.01 and *** ≤ 0.001 . n = 6/group.

The number and frequencies of monocytes and granulocytes remained unchanged with the administration of IL-7. However, in both of these cases, MAPC cells IP reduced the number and frequency of these populations (Fig. 4.11A and B and 4.11 C and D respectively). The number of eosinophils in the spleen was significantly enhanced from 830 ± 66.02 to 2246 ± 211.7 when IL-7 was administered ($n = 6$). MAPC cells restored the number of eosinophils to normal levels, with MAPC cells IV significantly reducing this number to 1076 ± 181.5 ($n = 6$) and MAPC cells IP significantly reducing the number to 1247 ± 264 . The percentage data for eosinophils followed the same trend (Fig. 4.11E and F). This was repeated in MU with a 4 colour panel and the same trend was seen as shown in figure 4.12. Overall this data shows that MAPC cells reduce the numbers of myeloid cells in the spleen, which may contribute to the inhibitory effect of MAPC cells on T cell HP.

4.7 IL-7 reduces the number and frequency of macrophages in the spleen, and MAPC cells suppress their expression of MHC class II.

Like the other myeloid cell populations, the effects of IL-7 on macrophages is mostly unknown, however interactions between MSC and macrophages have been an area of extensive research of late with a number of studies showing that MSC promote the activity of anti-inflammatory macrophages, while simultaneously suppressing pro-inflammatory macrophages (Carty, Mahon & English, 2017). Here, a significant reduction in the number and percentage of macrophages in the spleen when IL-7 was administered was observed, with numbers reducing from 1394 ± 113.3 in the PBS group to 813.0 ± 48.81 in the IL-7 group ($n = 6$). The administration of MAPC cells IV or MAPC cells IP did not change the effects of IL-7 on the frequency or number of macrophages in the spleen (Fig. 4.13A and B respectively). However, it was hypothesized that MAPC cells may reduce the expression of MHCII on the macrophage surface. MAPC cells significantly reduced the MFI of MHCII on the surface of macrophages from 5272 ± 313.2 in the IL-7 group, to 3401 ± 192.5 when MAPC cells IP were administered ($n = 6$) (Fig. 4.13C).

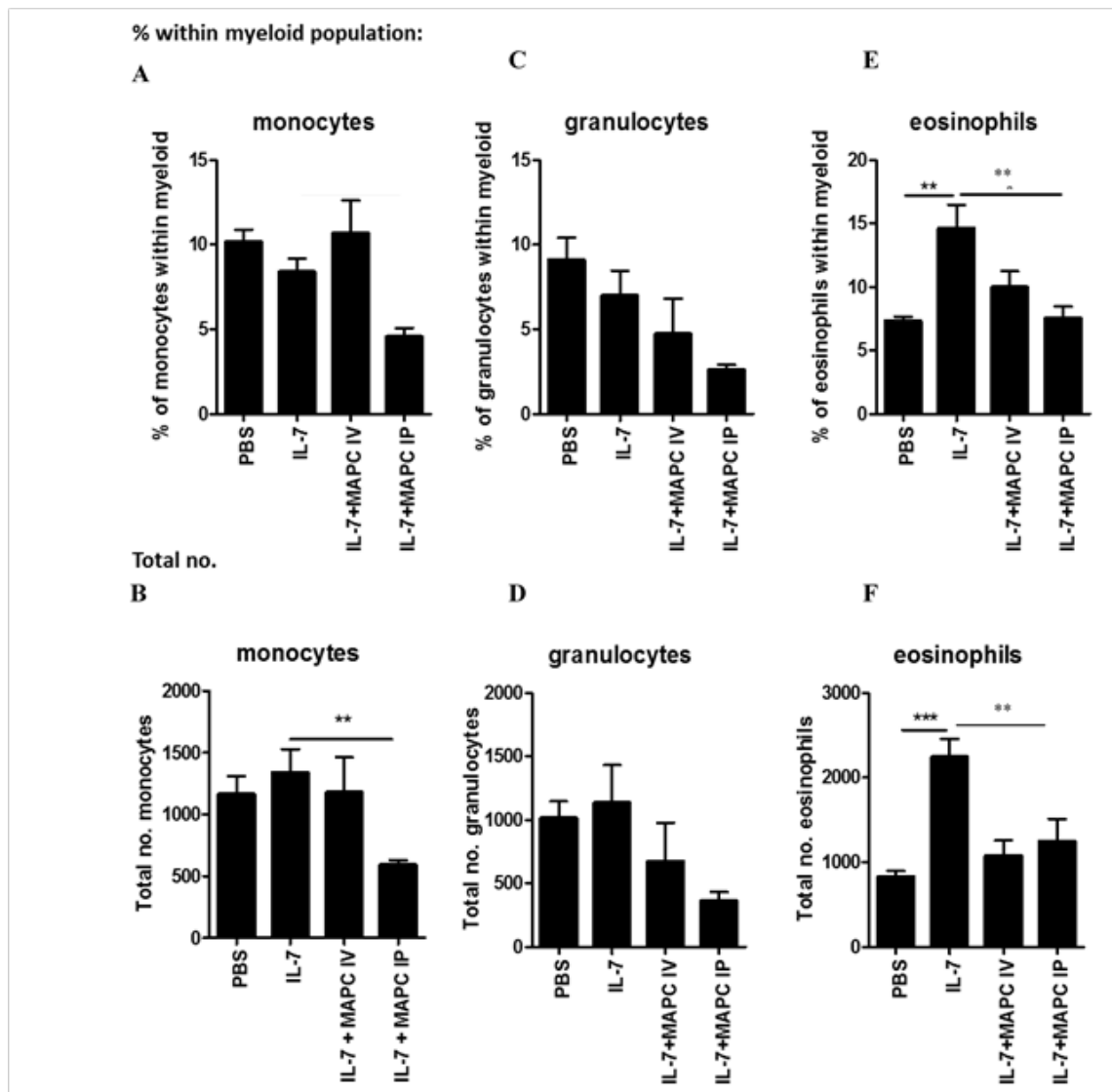


Figure 4.11 MAPC cells suppress the number and frequency of monocytes, granulocytes and eosinophils in the spleen. Neither IL-7 or MAPC cells IV had an effect on the frequency (A) or number (B) of monocytes in the spleen, however MAPC cells IP significantly suppressed monocytes in both instances. Similarly, neither IL-7 or MAPC cells IV had an effect on the level of granulocytes in the spleen, however MAPC cells IP reduced both the number (C) and frequency (D). IL-7 significantly increased the frequency (E) and number (F) of eosinophils in the spleen, and this was significantly suppressed by both MAPC cells IV and MAPC cells IP. Normality of number data was confirmed using the Shapiro-Wilk normality test. Statistical analysis of number data was carried out using ANOVA analysis, and analysis of frequency data was carried out using Kruskal-Wallis analysis. analysis where $** \leq 0.01$ and $*** \leq 0.001$. $n = 6/\text{group}$.

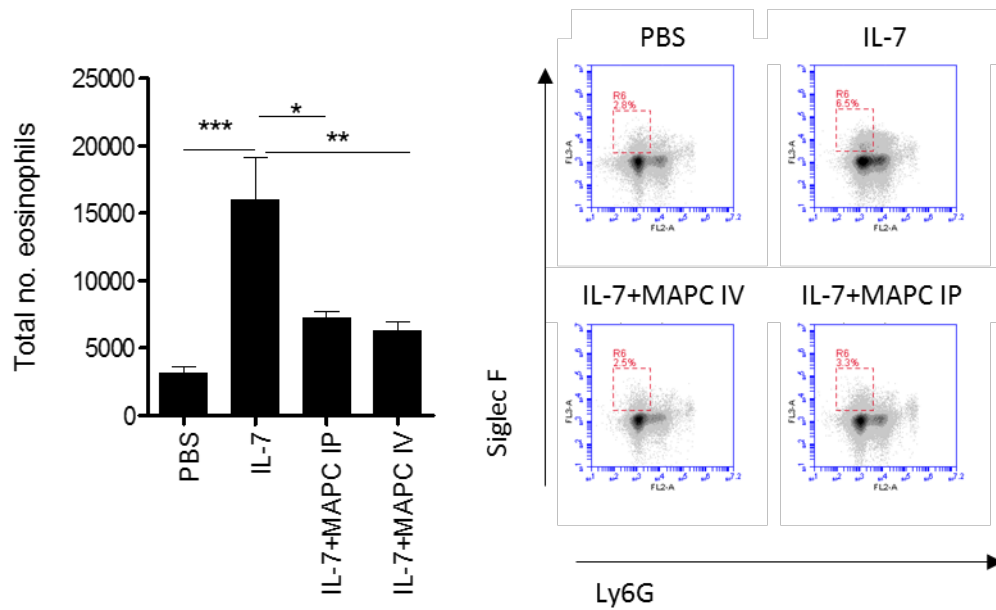


Figure 4.12 MAPC cells suppress the number and frequency of eosinophils in the spleen. The effects of IL-7 and MAPC cells on splenic eosinophils was re-examined in MU using a 4 colour panel. Eosinophils were identified as MHC II⁺, F4/80⁻, Ly6G⁻, Siglec F⁺. The data followed the same trend as the data generated by the 3i team with IL-7 significantly increasing the number of eosinophils in the spleen, and MAPC cells IP and MAPC cells IV significantly suppressed this. Normality was confirmed using the Shapiro-Wilk normality test, and statistical analysis was carried out using ANOVA analysis where * ≤ 0.05 , ** ≤ 0.01 and *** ≤ 0.001 . n = 5/group.

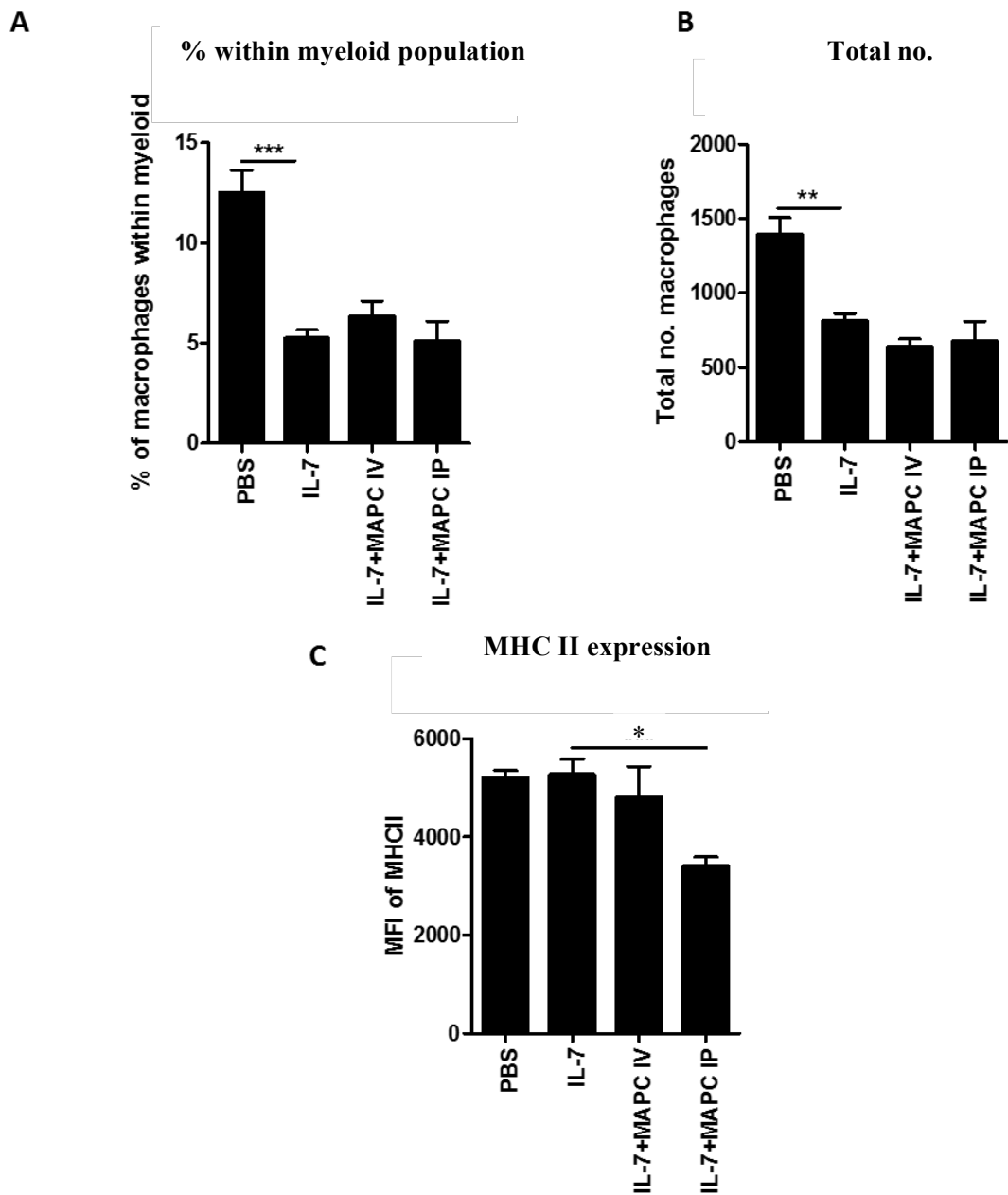


Figure 4.13 IL-7 suppresses the number and frequency of macrophage in the spleen, while MAPC cells IP suppress MHC II expression by macrophages IL-7 significantly reduced the number (A) and frequency (B) of macrophages in the spleen. MAPC cells IV further reduced the number of macrophages in the spleen (B). Interestingly, MAPC cells IP but not MAPC cells IV significantly reduced the intensity of MHC II expression on the macrophage surface (C). Normality of number data was confirmed using the Shapiro-Wilk normality test. Statistical analysis of number data was carried out using ANOVA analysis, and analysis of frequency data was carried out using Kruskal-Wallis analysis. where * ≤ 0.05 , ** ≤ 0.01 and *** ≤ 0.001 . n = 6/group.

4.8 IL-7 and MAPC cells have no effects on the number or frequency of DC in the spleen but the populations within the dendritic cell compartment are altered.

As with the other myeloid populations, there is little known about the effects of IL-7 on splenic DC. On the other hand, it's well documented that MSC suppress the maturation and antigen presenting capacities of DC (Cahill *et al.*, 2015; English *et al.*, 2007a). Therefore, it was hypothesized that MAPC cells would suppress the antigen presenting capacities of DC, and that this may play a role in the suppression of T cell proliferation by MAPC cells. In this study, DC were identified as CD3⁻, CD19⁻, CD161⁻, F4/80⁻, GR1⁻. IL-7 had no significant effect on either the percentage or number of DC in the spleen, and this was also unchanged by MAPC cells (Fig. 4.14A and B). Within the DC compartments, plasmacytoid DC (pDC) were identified as DC expressing CD317, while conventional DC (cDC) were identified as DC which were CD317⁻, CD11c⁺, MHCII⁺. cDC are generally regarded to be superior APCs than pDC. As expected, MAPC cells reduced the frequency and number of cDC, while they enhanced the frequency of pDC (Fig. 4.14C-4.14F; n = 6). This effect was seen only when MAPC cells were administered IP but not with MAPC cells IV, and was only significant when analysed using a t test rather than ANOVA.

Splenic cDC are further separated into CD8⁺, CD11b⁻ and CD8⁻, CD11b⁺ populations. These subsets have differences in their cross presentation and cytokine producing capacities, with the CD8⁺ population having stronger cross presentation capacities than CD8⁻ (Hildner *et al.*, 2008). Furthermore, the CD8⁺ population are thought to have a role in the maintenance of T cell tolerance to self-antigen (Hey & O'Neill, 2012). IL-7 enhanced the frequency and number of CD11b⁺ CD8⁻ DC and MAPC cells returned these to normal levels (Fig. 4.15A and B), while IL-7 decreased the number and frequency of CD8⁺ CD11b⁻ DC. MAPC cells IP again returned these to normal levels (Fig. 4.15C and D). Overall this data suggests that MAPC cells IP may suppress the antigen presenting capacities of DC which may contribute to the suppression of T cell stimulation by MAPC cells.

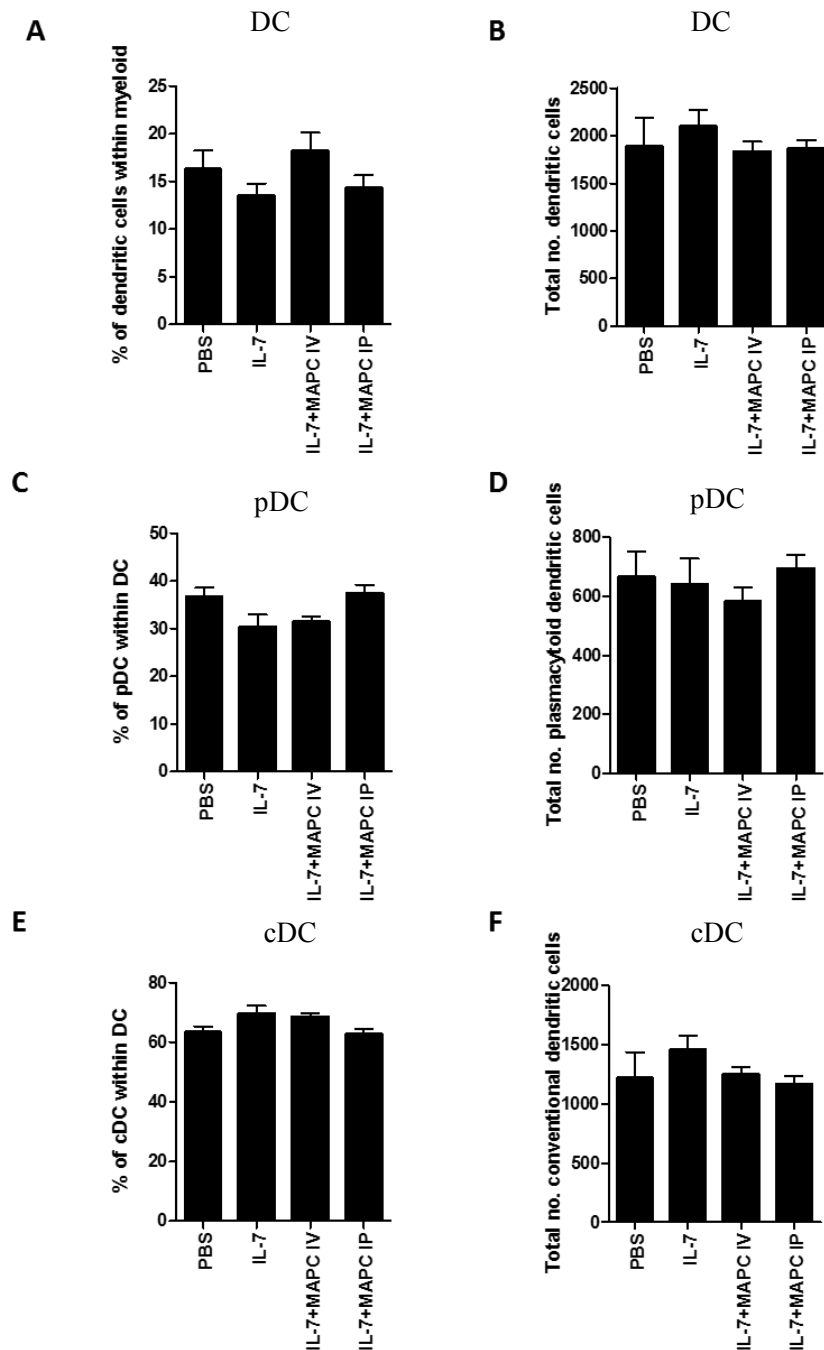


Figure 4.14 IL-7 reduces the frequency of pDC and increases the frequency of cDC. MAPC cells IP restore these populations to normal levels. IL-7 and MAPC cells had no effect on the number or frequency of the whole DC population (A and B respectively). Within the DC population IL-7 reduced the number (C) and frequency (D) of pDC and MAPC cells IP restored this to normal levels. IL-7 increased the number and frequency of cDC in the spleen (E and F respectively) and MAPC cells IP again restored this to normal levels. Normality of number data was confirmed using the Shapiro-Wilk normality test. Statistical analysis of number data was carried out using ANOVA analysis, and analysis of frequency data was carried out using Kruskal-Wallis analysis, n = 6/group.

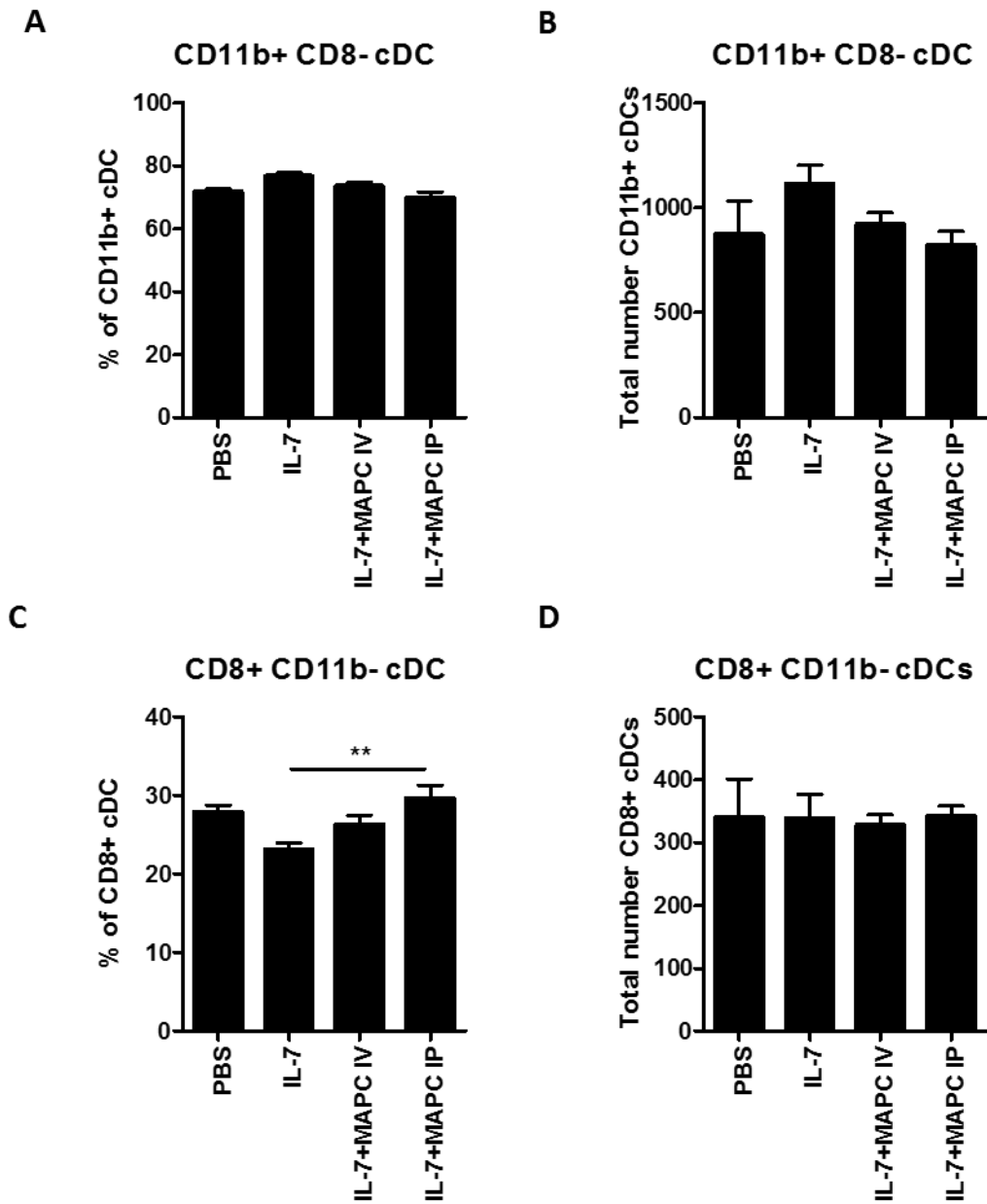


Figure 4.15 IL-7 alters the frequency of cDC subsets, and MAPC cells IP restore this to normal levels. IL-7 increased the frequency and number of CD11b⁺ CD8⁻ cDC (A and B respectively). Within the DC population, IL-7 increased the frequency (A) and number (B) of CD11b⁺, CD8⁻ cDC and MAPC cells IP restored this to normal levels. IL-7 decreased the frequency of CD8⁺ CD11b⁻ cDC in the spleen and MAPC cells IP again restored this to normal levels (C), Neither IL-7 or MAPC cells had any effect on the total number of CD8⁺ CD11b⁻ cDC in the spleen. Statistical analysis was carried out using Kruskal wallis analysis where ** ≤ 0.01 . n = 6/group.

4.9 MAPC cells IP enhance the frequency and alter the phenotype of CD4⁺ CD25⁺ GITR⁺ cells in the spleen.

In the context of allograft rejection, it is thought that the outcome of the immune reaction may depend on the ratio of allo-reactive T cells to Treg. Nguyen et al (2014) have shown that the suppressive capacity of Treg in transplant recipients prior to transplantation correlates with the success of immediate graft function. Furthermore, Treg derived IL-10 also dampens inflammation by inhibiting APC activity and inducing the conversion of T cells to T regulatory type 1 cells (Wood, Bushell & Hester, 2012). MSC and MAPC cells have been shown to expand Treg populations in murine models of inflammation (Eggenhofer *et al.*, 2013; Cahill *et al.*, 2015), thus, the effects of MAPC cells on Treg was investigated in this model. The panels used by the 3i team in Kings College London did not include intracellular staining, therefore the traditional marker of Treg, FoxP3, was not used in this instance. Here, Treg were identified as TCRβ⁺, CD161⁻, CD4⁺, CD25⁺, glucocorticoid-induced TNFR family related gene (GITR)⁺.

Within the CD4⁺ T cell compartment the frequency of Treg was significantly enhanced from 16.05%±0.9943 in the IL-7 group to 21.58%±0.9526 following the addition of MAPC cells IP (n = 6) (Fig. 4.16A). Within the Treg compartment, effector Treg were characterised as CD44⁺, CD62L⁻ while resting Treg were characterised as CD62L⁺. The percentage of effector Treg in the spleen was significantly increased by MAPC cells IP (Fig. 4.16B), while the percentage of resting Treg was significantly reduced by MAPC cells IP (Fig. 4.16C). MAPC cells IV did not change the frequency or activation state of Treg in the spleen. Furthermore, the panel also included killer-cell lectin like receptor G1 (KLRG1) which is a marker of Treg that have undergone extensive proliferation, and this population is prone to apoptosis (Cheng *et al.*, 2012). In the spleen, under normal conditions 5.058%±0.4802 of Treg expressed KLRG1. Administration of IL-7 significantly increased expression of KLRG1 to 9.714%±1.118 (n = 6). MAPC cells IV did not effect this IL-7 driven increase in KLRG1 expression, however MAPC cells IP significantly increased KLRG1 expression to

12.93%±0.6699 (n = 6) (Fig. 4.16D). This may indicate that MAPC cells IP promote the proliferation of Treg in the spleen, or may protect KLRG1⁺ Treg from undergoing apoptosis.

This experiment was then repeated in MU using co-expression of CD25 and FoxP3 as markers of Treg. Using this panel, it was discovered that IL-7 increased the frequency of Treg within the CD4 population from 2.520%±0.3779 to 5.576%±0.6714 (n = 5). Administration of both MAPC cells IV and MAPC cells IP slightly decreased the frequency of CD25⁺ FoxP3⁺ cells in mice treated with IL-7, though this was not significant (Fig. 4.17). Since FoxP3 is a reliable marker of thymus derived or natural Treg, it was concluded here that MAPC cells are not expanding natural Treg in this model. GITR however can be expressed by induced peripheral Treg, or suppressive T cells (Ronchetti *et al.*, 2015). Thus, MAPC cells may be promoting the differentiation of peripheral T cells into suppressive FoxP3⁻ populations.

4.10 MAPC cells enhance the number of B2 cells and alter the subsets within this population

IL-7 is required for the development of pre-B cells and immature B cells, however the effects of IL-7 on mature B cells is not as well characterized (Fry & Mackall, 2009; Mackall, Fry & Gress, 2011). Similarly, the effects of MAPC cells on B cells has not yet been investigated. Studies addressing the effects of MSC on B cells have led to diverse findings with some reports showing that MSC enhance B cell proliferation and survival, and other studies reporting the contrary (Healy *et al.*, 2015; Rosado *et al.*, 2015).

In this study, B cells were characterized as CD45⁺ CD19⁺. The majority of B cells are B2 cells which are characterized as CD19⁺ CD5⁻. IL-7 had no effect on the total number of B2 cells in the spleen, however MAPC cells IV and MAPC cells IP significantly increased this number from 77510±8994 to 126900±10130 and 121700±11580 respectively (Fig. 4.18A; n = 6). Follicular B cells make up the vast majority of splenic B2 cells. Here follicular B cells were identified as CD19⁺, CD5⁻, GL7⁻, CD95⁻, CD21^{MID}, immunoglobulin (Ig)M^{MID}.

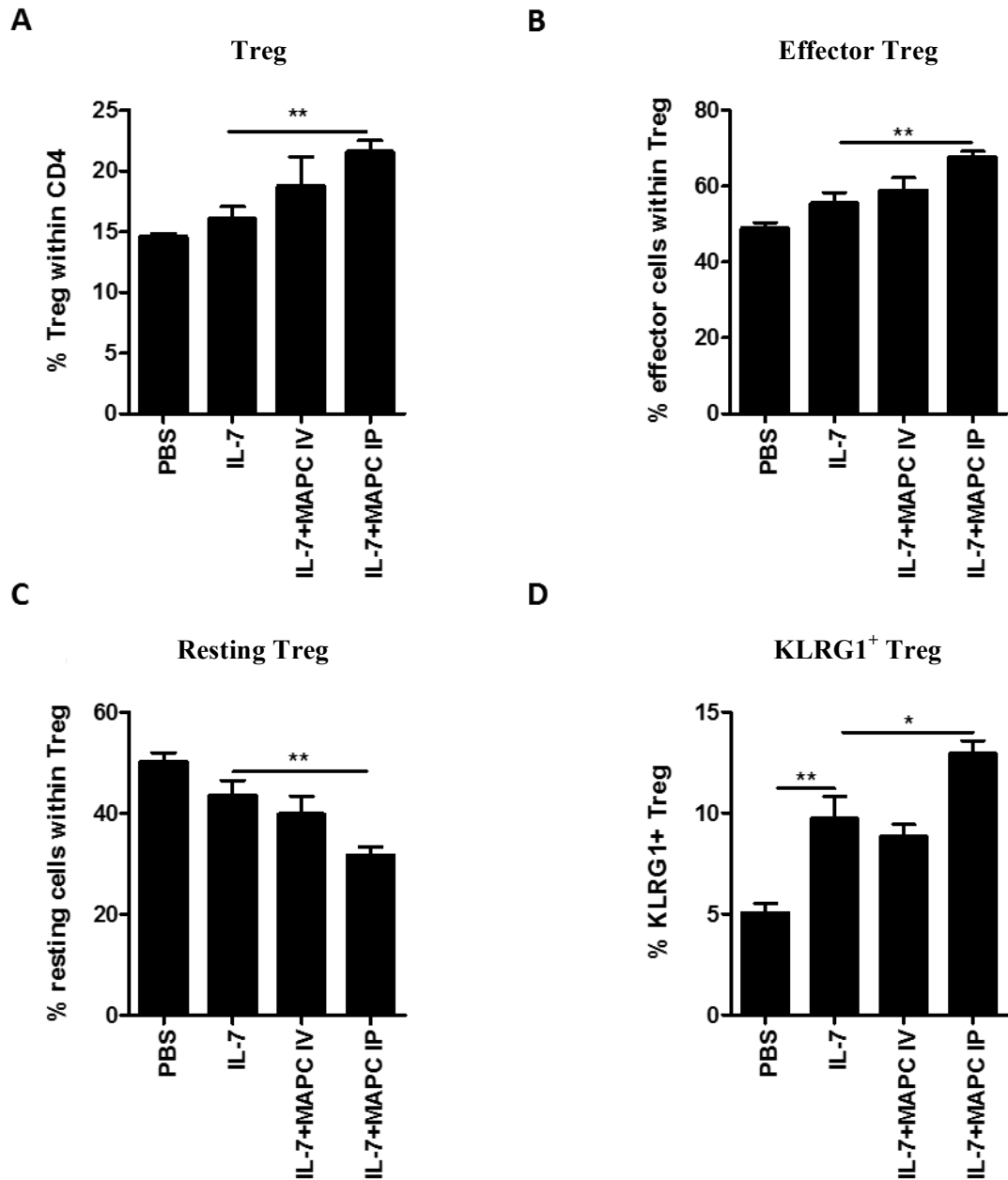


Figure 4.16 MAPC cells IP enhanced the frequency of GITR⁺ Treg within the CD4⁺ population. MAPC cells IP but not MAPC cells IV increased the frequency GITR⁺ Treg within the CD4 population in IL-7 treated mice (A). Within the GITR⁺ population, MAPC cells IP increased the frequency of effector cells (B) and decreased the frequency of resting cells (C). IL-7 increased the frequency of KLRG1⁺ Treg and this was further enhanced by MAPC cells IP, but not MAPC cells IV. Statistical analysis was carried out using Kruskal-Wallis analysis where * ≤ 0.05 and ** ≤ 0.01 . n = 6/group.

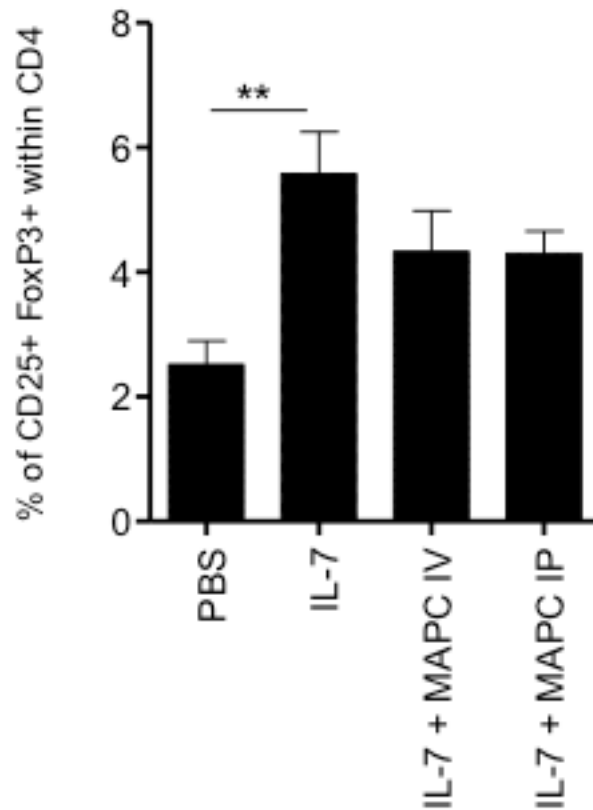


Figure 4.17 MAPC cells did not significantly change the frequency of CD4⁺ CD25⁺ FoxP3⁺ cells. IL-7 increased the frequency of CD25⁺ FoxP3⁺ cells within the CD4 population, however both MAPC cells IP and MAPC cells IV slightly reduced this increase, though this effect was not significant. Statistical analysis was carried out using Kruskal-Wallis analysis where ** ≤ 0.01 , n = 5/group.

The frequency of follicular B cells was slightly decreased by IL-7 treatment from 79.42%±0.7286 to 75.07%±1.256 (n = 6). This was unchanged by MAPC cells IV, however MAPC cells IP further reduced the frequency of follicular B cells to 61.91%±2.195 (Fig. 4.18B). The frequency of marginal zone B cells, characterized as CD19⁺, CD5⁻, GL7⁻, CD95⁻, CD21^{HI}, IgM⁺, CD23⁻ was significantly reduced from 7.403%±0.7354 to 4.285%±0.3638 with IL-7 treatment (n = 6). Administration of neither MAPC cells IV or MAPC cells IP affected the frequency of marginal zone B cells (Fig. 4.18C). Germinal centre B cells were identified by expression of GL7 and CD95. While IL-7 treatment didn't change the frequency of germinal centre B cells, administration of MAPC cells IV, but not MAPC cells IP significantly increased their frequency from 0.1355%±0.01148 to 0.7300%±0.1384 (n = 6) (Fig. 4.18D). Transitional-1 B cells were identified as CD19⁺, CD5⁻, GL7⁻, CD95⁻, CD21⁻, IgM⁺, CD23⁻. IL-7 increased the frequency of splenic transitional-1 B cells from 4.253%±0.4078 to 9.799%±1.203 (n = 6). MAPC cells IV didn't affect this increase, however MAPC cells IP significantly increased the frequency of transitional-1 B cells to 24.26%±2.419 (n = 6) (Fig. 4.18E). Transitional-2 B cells differ from transitional-1 B cells in expression of CD23 only. While the frequency of splenic transitional 2 B cells was increased from 3.698%±0.3147 to 5.623%±0.3147 with IL-7 treatment, neither MAPC cells IV or MAPC cells IP significantly affected this increase (Fig. 4.18F).

4.11 MAPC cells IV enhance the number and frequency of B1a and plasma cells.

In mice, B1a cells are characterized as CD5⁺ B cells, and are generally found in the peritoneal and pleural cavities of adult mice. They are considered to be innate cells which produce an abundance of natural IgM, while within the spleen B1a cells are thought to be major producers of GM-CSF (Rauch *et al.*, 2012; Deng *et al.*, 2016). Following IL-7 administration there was a slight increase of B1a cells in the spleen with the frequency increasing from 1.861%±0.2638 in the PBS group to 2.578%±0.3487 in the IL-7 group (n = 6), and total number increasing from 1076 ± 0.181.3 in the PBS group to 1959±218.4 in the IL-7 group (n = 6). Administration of MAPC cells IV following IL-7 treatment significantly increased both the frequency and number of B1a cells in the spleen, with the B1a cell population increasing to 3.816%±0.2794

(n = 6) or 5096 ± 640.9 (n = 6). Interestingly, MAPC cells IP did not significantly increase the frequency or total number of B1a cells with the frequency remaining at $2.493\% \pm 0.3429$ (n = 6) and the total number slightly increasing 3144 ± 562.2 (n = 6) (Fig. 4.19A and B respectively). This experiment was repeated at MU using the same panel and a similar trend was observed (Fig. 4.20)

Plasma cells are a differentiated B cell with CD19^{INT} and CD138⁺. The exact effects of IL-7 on plasma cells are unknown, however in this case IL-7 administration increased the frequency of plasma cells in the spleen from $0.2222\% \pm 0.01468$ in the PBS group to $0.4940\% \pm 0.06831$ (n = 6). Similarly, the total number of plasma cells was increased from 134 ± 20.88 to 390.7 ± 72.99 (n = 6). Treatment with MAPC cells IV following IL-7 treatment further enhanced the frequency of plasma cells to $0.8405\% \pm 0.05175$ (n = 6) and total number to 1078 ± 131.3 (n = 6). MAPC cells IP had no further effect on the frequency of plasma cells, with frequency being $0.4878\% \pm 0.07407$ (n = 5) and only slightly increased the number of plasma cells in the spleen to 578.8 ± 73.87 (n = 5) (Fig. 4.19C and D respectively).

4.12 MAPC cells IV and MAPC cells IP exhibit differential biodistribution patterns.

As shown in previous sections, the effects of MAPC cell therapy varies depending on the route of administration employed. Therefore, I sought to examine the biodistribution of MAPC cells in the IL-7 model following IP and IV administration. The majority of preclinical studies using MSC and MAPC cells administer the cells IV, and it is well known that IV administered MSC and MAPC cells accumulate in the lung, with only a small percentage migrating to distal organs (Eggenhofer *et al.*, 2014). However, the biodistribution of IP administered MAPC cells is less well characterized. IP administered murine MSC have been shown to form aggregates with immune cells in the peritoneal cavity (Sala *et al.*, 2015), but whether MAPC cells would migrate to the spleen and lymph nodes following IP administration is unknown. MAPC cells were labelled with the Qtracker[®] labelling kit as described in section 2.11.1 and Qtracker[®]

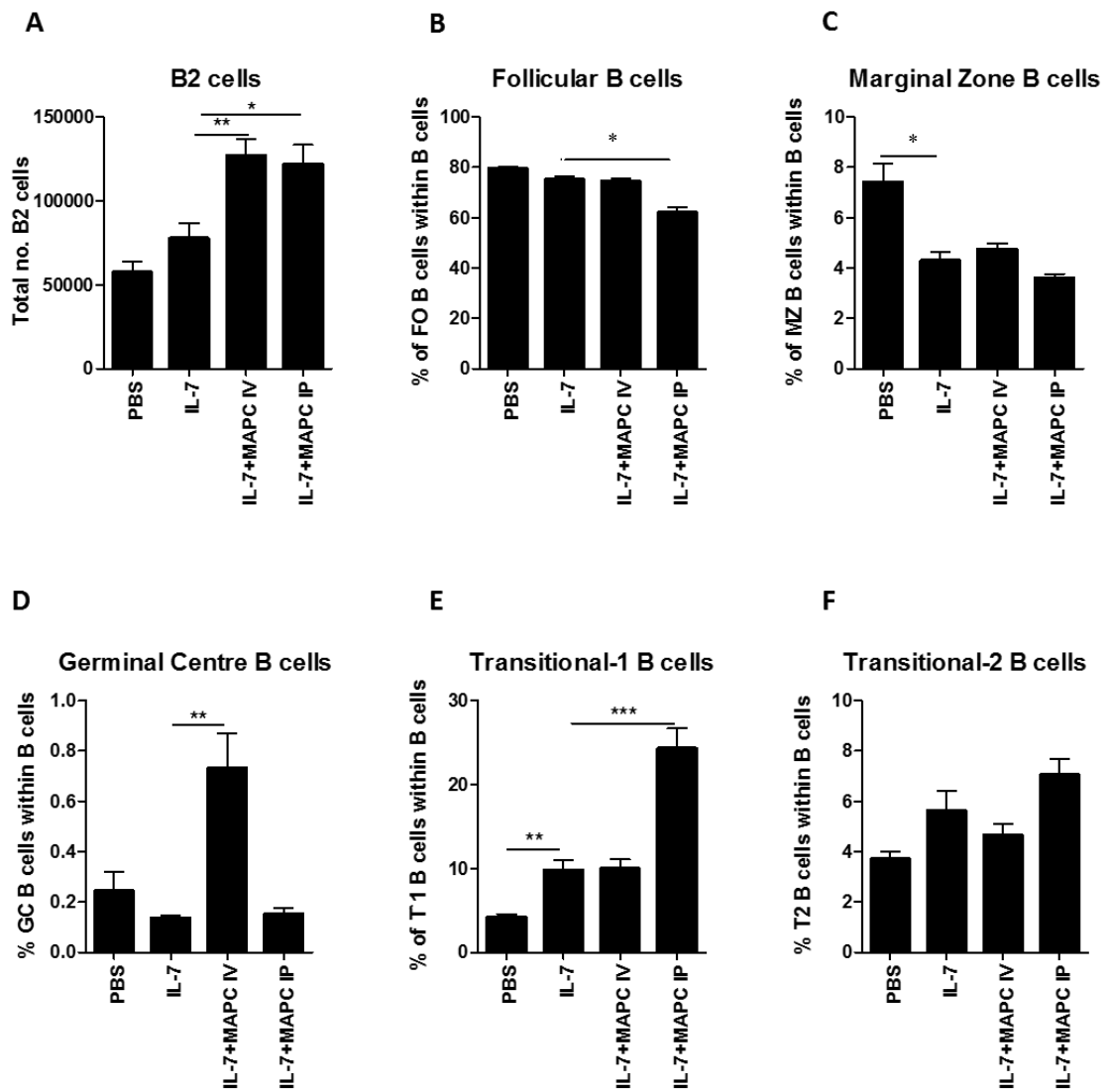


Figure 4.18 MAPC cells enhance the total number of B2 cells and alter the subsets within this population. Both MAPC cells IP and MAPC cells IV increased the total number of B2 cells in the spleen (A). Within the B2 cell population MAPC cells IP, but not MAPC cells IV reduced the frequency of follicular B cells (B). IL-7 decreased the frequency of marginal zone B cells and neither MAPC cells IV or MAPC cells IP had an effect on this (C). MAPC cells IV significantly increased the frequency of germinal centre B cells (D). IL-7 significantly increased the frequency of transitional-1 B cells and MAPC cells IP only significantly increased this further (E). The frequency of transitional-2 B cells was also increased by IL-7, and neither MAPC cells IV or MAPC cells IP significantly changed this. Normality of number data was confirmed using the Shapiro-Wilk normality test. Statistical analysis of number data was carried out using ANOVA analysis, and analysis of frequency data was carried out using Kruskal-Wallis analysis where $*\leq 0.05$, $**\leq 0.01$ and $***\leq 0.001$, $n = 6/\text{group}$.

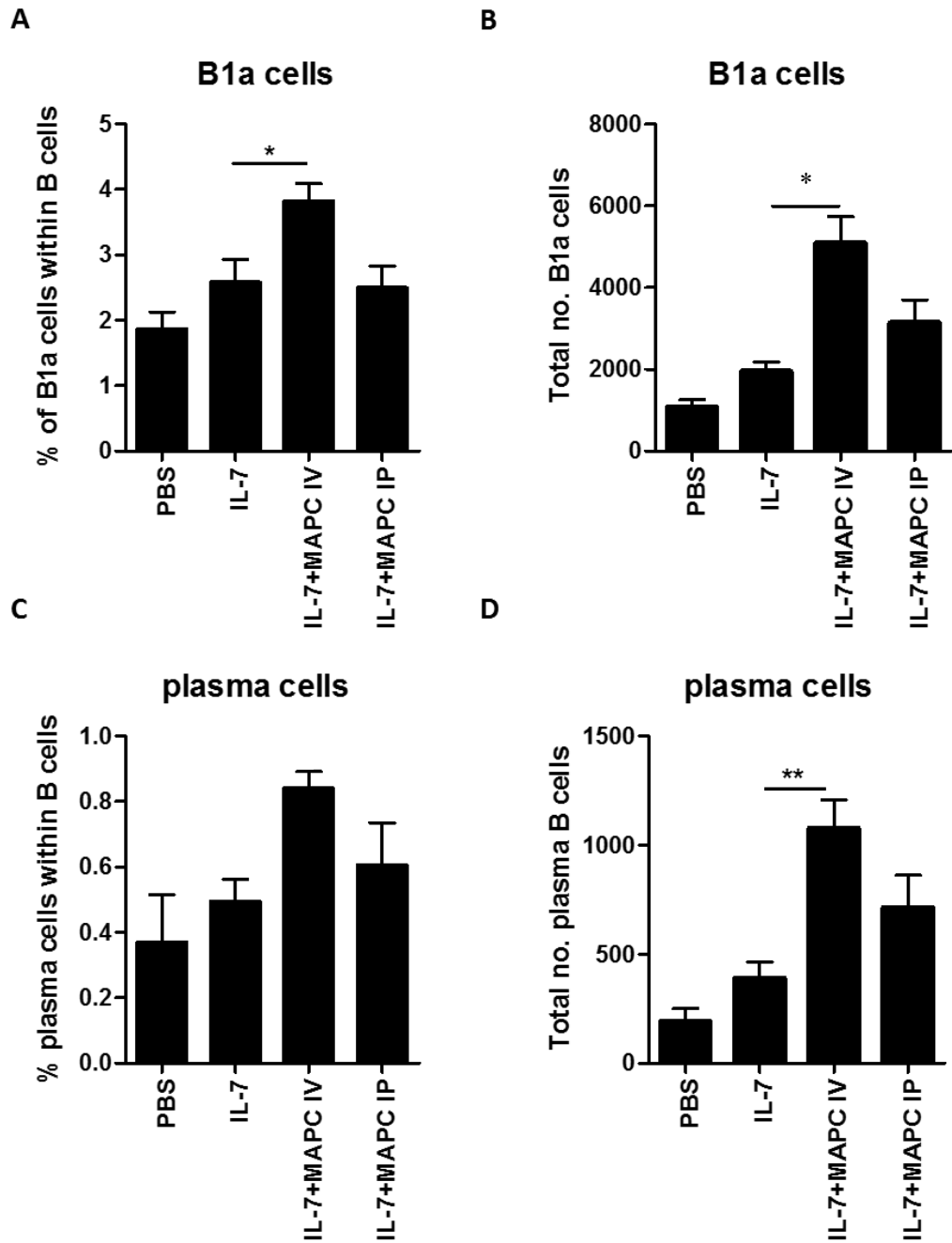


Figure 4.19 MAPC cells IV enhance the frequency and total number of B1a cells and plasma cells. IL-7 enhanced the frequency and number of B1a cells (A and B respectively) and MAPC cells IV, but not MAPC cells IP significantly increased this further. IL-7 had no effect on plasma cells in the spleen, however MAPC cells IV increased both the frequency and number (C and D respectively) while MAPC cells IP had no effect. Normality of number data was confirmed using the Shapiro-Wilk normality test. Statistical analysis of number data was carried out using ANOVA analysis, and analysis of frequency data was carried out using Kruskal-Wallis analysis where * ≤ 0.05 , ** ≤ 0.01 and *** ≤ 0.001 , $n = 6/\text{group}$.

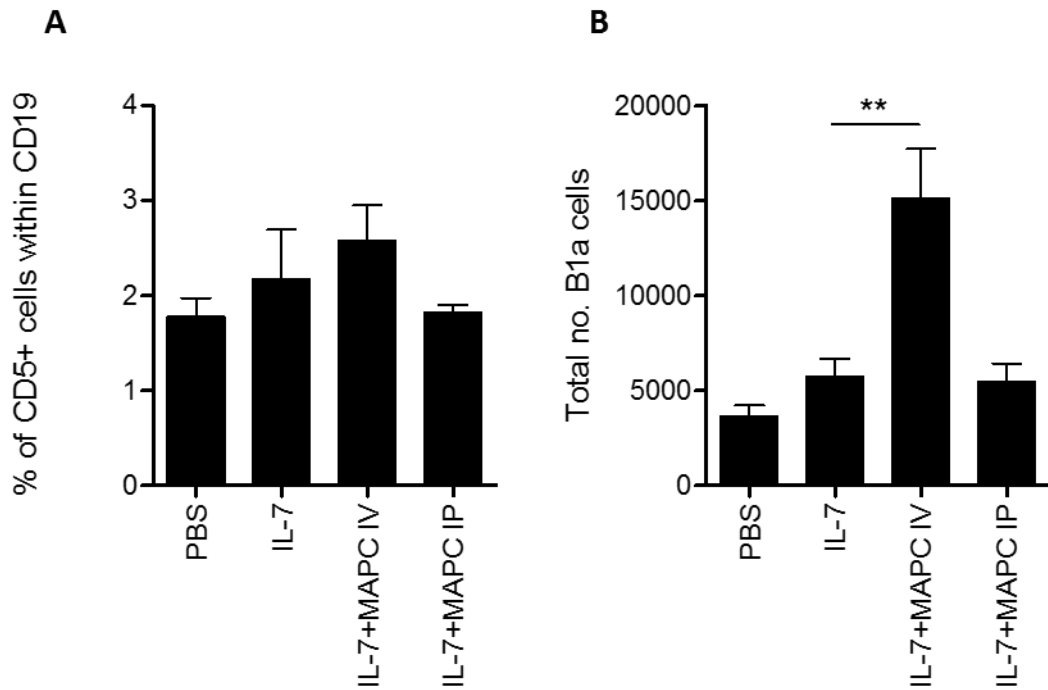


Figure 4.20 MAPC cells IV enhance the frequency and total number of B1a cells. The effects of IL-7 and MAPC cells on splenic B1a cells was re-examined in MU. B1a cells were identified as CD19⁺ CD5⁺. The frequency (A) and number (B) data followed the same trend as the data generated by the 3i team with MAPC cells IV significantly increasing the total number of B1a cells in the spleen. Normality of number data was confirmed using the Shapiro-Wilk normality test. Statistical analysis of number data was carried out using ANOVA analysis, and analysis of frequency data was carried out using Kruskal-Wallis analysis where ** ≤ 0.01 , n = 6/group.

labelled MAPC cells were confirmed to be functional in an *in vitro* T cell proliferation assay as shown in figure 3.8. Mice were humanely euthanized 72 hours later and whole mice as well as spleens and lymph nodes were prepared for cryo-imaging as described in section 2.11. Following IV administration to either the PBS or IL-7 mouse only 6000-7000 cells were detected in whole mice 72 hours later. The majority of these cells were detected in the lung and liver, and some were detected in the spleen. Over 100,000 MAPC cells were detected at 72 hours when administered IP, with 148,972 cells detected in the PBS mouse and 125,952 in the IL-7 mouse (Fig. 4.21). MAPC cells IP were detected in the peritoneal area surrounding abdominal organs, and appeared to be in clusters, which aligns well with the observations made by Sala *et al.* (2015) and Bazhanov *et al.* (2016). Next the distribution of MAPC cells to the lymphoid organs of IL-7 treated mice was examined. Neither MAPC cells administered IV or IP were detected in the lymph nodes (Fig. 4.22). Interestingly, while MAPC cells administered IV were detected within the spleen, MAPC cells IP were detected only in the omental tissue surrounding the spleen, and did not gain access to splenic tissue (Fig.4.22). Therefore, the differential effects of MAPC cells on the various immune compartments in the spleen may be due to the contrast in persistence of MAPC cells IV compared to MAPC cells IP, or it may be due to their distinct locations *in vivo*.

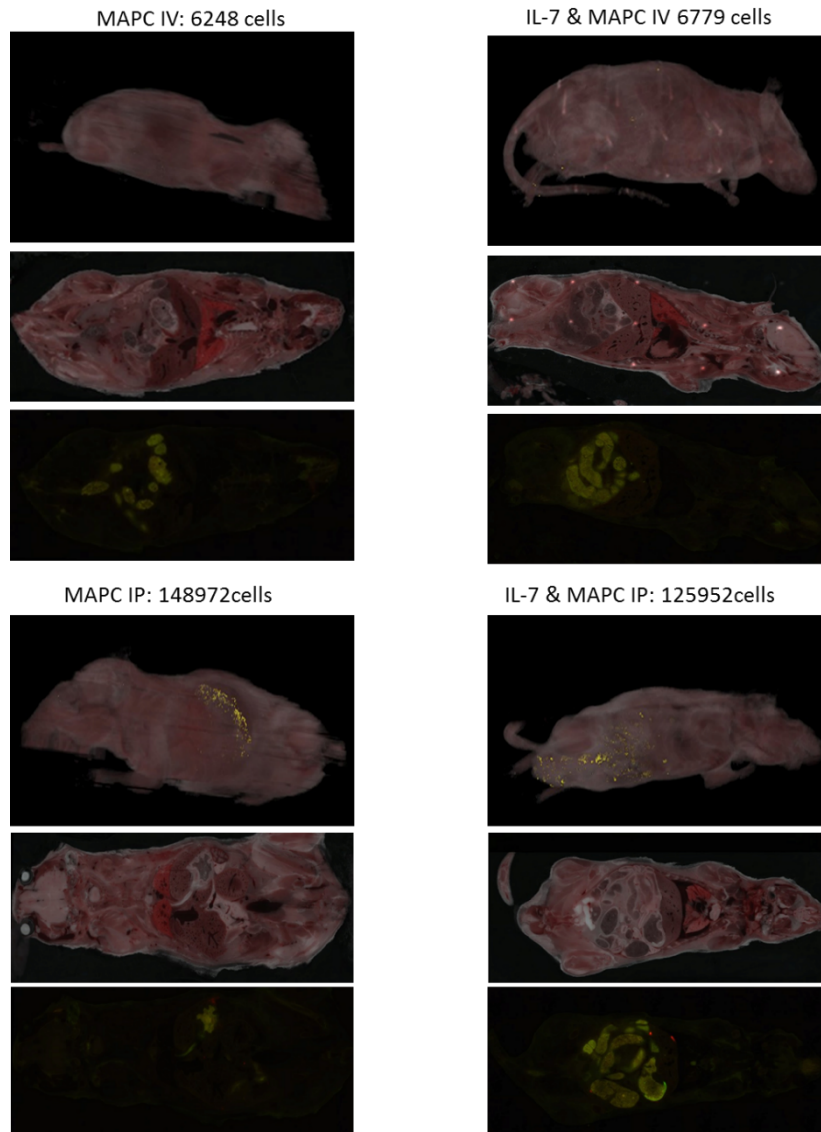


Figure 4.21 MAPC cells IP persist longer *in vivo* than MAPC cells IV. 1×10^6 Qtracker[®] 625 labelled MAPC cells were administered to PBS and IL-7 treated mice and whole mice were harvested 72 hours later as described in section 2.11. Of the 1×10^6 MAPC cells administered, only 6000-7000 cells were detected 72 hours later when administered IV to either the PBS or IL-7 mouse. The majority of these cells were detected in the lung and liver. Over 100,000 MAPC cells were detected at 72 hours when administered IP, with 148972 cells detected in the PBS mouse and 125952 in the IL-7 mouse. MAPC cells IP were detected in the peritoneal area surrounding abdominal organs. The top panels present 3D images of each mouse with detected MAPC cells shown in yellow. Brightfield (middle panels) and corresponding fluorescent sections (bottom panels) show the location of MAPC cells in 2D sections which can be seen as red.

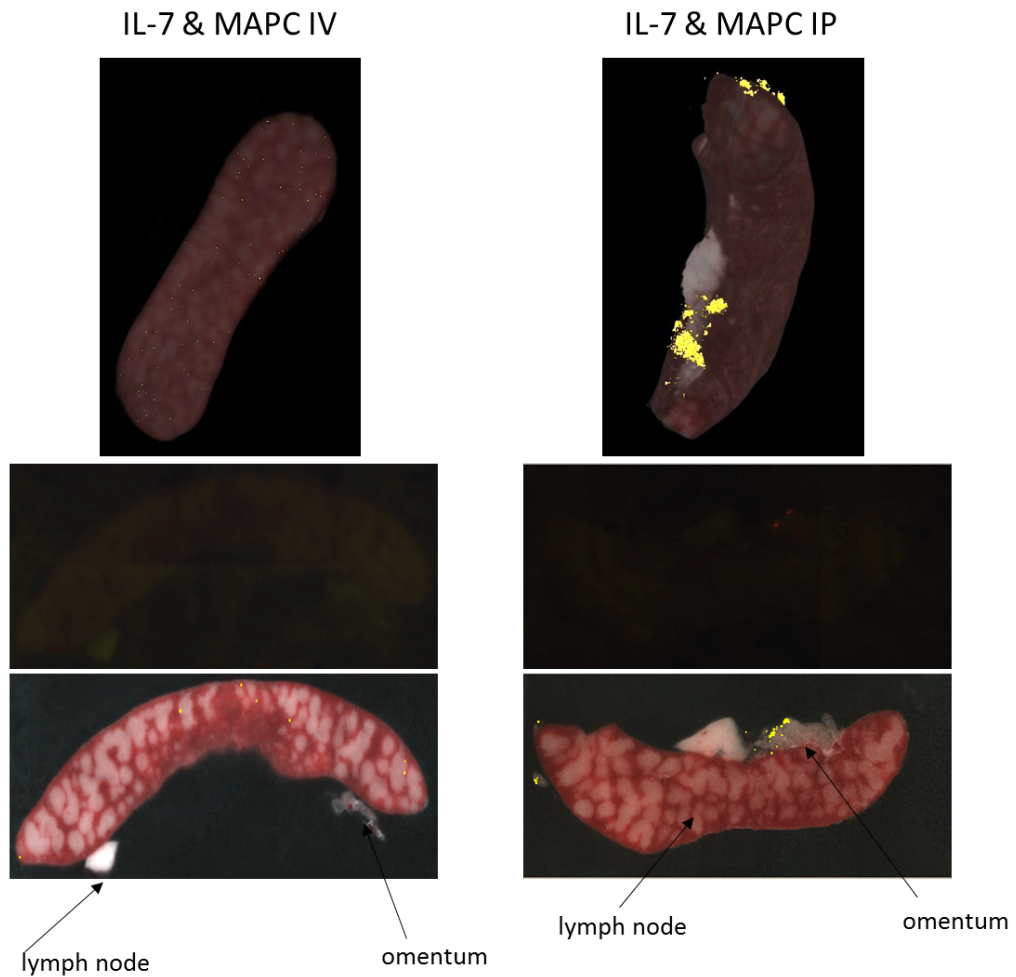


Figure 4.22 MAPC cells IV gain access to the spleen, while MAPC cells IP do not. Qtracker[®] labelled MAPC cells were administered to IL-7 treated mice and organs were harvested for imaging 72 hours later as described in section 2.11. MAPC cells administered IV were detected in the spleen, however MAPC cells administered IP did not gain access to the spleen, but were detected in the omental tissue surrounding the spleen. Neither MAPC cells IV or MAPC cells IP were detected in the lymph nodes (n = 4). The top panels present 3D images of representative spleens with detected MAPC cells shown in yellow. Fluorescent (middle panels) and corresponding brightfield sections (bottom panels) show the location of MAPC cells in 2D sections which can be seen as red fluorescence or overlaying yellow beads.

4.13 Summary

T cell depletive therapies are commonly used in the clinic to prevent or delay allograft rejection, however the consequential abundance of homeostatic stimuli such as IL-7 leads to the promotion of a pro-inflammatory T cell pool. While maintenance immunosuppression is used to inhibit the proliferation of T cells following induction therapy, none of the therapies currently on the market target the IL-7 axis, despite its known role in the homeostatic expansion of T cells during lymphopenia (Monti & Piemonti, 2013). We have previously shown that human MAPC cells suppress IL-7 driven proliferation and activation of T cells *in vitro* (Reading *et al.*, 2015), and so the aim of this chapter was to build on that data, by translating the findings to an *in vivo* setting.

Within this chapter, it was shown that MAPC cells suppress proliferation and IFN- γ production by both CD4⁺ and CD8⁺ T cells in response to IL-7. MAPC cells were administered both IV and IP to this model, with only MAPC cells IP demonstrating efficacy in the lymph nodes. A larger scale immunophenotyping study was then carried out with collaborators in Kings College London in order to examine the effects of IL-7 and MAPC cells on a wider range of immune cells in the spleen. The most interesting data acquired from this experiment showed that MAPC cells reduce IL-7 induced expansion of eosinophils, while MAPC cells IP promote transitional-1 B cells and MAPC cells IV promote B1a cells. Analysis of Treg using different panels suggests that MAPC cells IP may expand FoxP3⁻ GITR⁺ suppressive T cells, but not thymus derived FoxP3⁺ Treg, however this requires further analysis.

Taken together, this data shows that MAPC cells have differing effects *in vivo* depending on the route of administration. In an effort to elucidate the reason for these differences, human (xenogeneic) MAPC cells were fluorescently labelled and their biodistribution in control (PBS) or IL-7 induced HP mice was examined using CryoViz™ technology. Imaging experiments revealed that 72 hours after IV administration the vast majority of MAPC cells had disappeared, while roughly 10% of MAPC cells IP persisted in the peritoneal cavity. On closer inspection, it was shown that MAPC cells IP did not gain

access to the spleen or lymph nodes, however they were retained in the omental tissue surrounding these sites which aligns well with previously published studies by other groups (Bazhanov *et al.*, 2016; Sala *et al.*, 2015). On the contrary, some MAPC cells IV did gain access to the spleen, however they were not detected in the lymph nodes.

In conclusion this chapter has shown that MAPC cells suppress IL-7 stimulation of T cells *in vivo*, however their efficacy varies depending on the route of administration. Highfill *et al.* (2010) have previously reported that the poor efficacy of systemically delivered MAPC cells in GvHD may be due to the short half-life of their soluble factors, and so localized delivery may be more effective for this reason. This data supports their findings, and suggests that MAPC cells IP may be more effective than MAPC cells IV due to their enhanced persistence *in vivo*, along with their closer proximity to lymphoid organs.

Chapter 5
MAPC cells suppress pro-inflammatory T cells
following lymphodepletion

5.1 Introduction

Chapter 4 looked at the effects of MAPC cells on T cell activity following stimulation with IL-7. This was a meaningful first step to investigate the effects of MAPC cells on homeostatic expansion, however it is not a clinically relevant model of HP. In order to reduce the likelihood of acute rejection, induction therapy is administered prior to transplantation to deplete host T cells. One of the most commonly used drugs for this purpose is ATG which depletes target cells (predominantly T cells) by inducing complement or antibody dependent cytotoxicity, and apoptosis (Valdez-Ortiz *et al.*, 2015; Zwang & Turka, 2014). Some T cells escape depletion, and so HP occurs due to the increased homeostatic stimuli available to these cells due to the lack of competition (Wu *et al.*, 2004). Thus, a more appropriate model for examining the effects of MAPC cells on HP in the context of transplantation, is the addition of MAPC cells to a model of HP following lymphodepletion.

As described in chapter 4, the availability of IL-7 increases and T cells undergo accelerated HP in lymphopenic conditions (Moxham *et al.*, 2008; Wu *et al.*, 2004). Overall, it is thought that HP in lymphopenic conditions promotes the expansion of a pro-inflammatory T cell pool which is likely to cause allograft rejection and autoimmunity (Neujahr *et al.*, 2006; Moxham *et al.*, 2008; Wu *et al.*, 2004; Grimaldi *et al.*, 2016). There are no studies to date which have addressed the effects of MSC or MAPC cells on T cell HP following lymphodepletion, however both the *in vitro* studies by Reading *et al.* (2015) and the *in vivo* work outlined in Chapter 4 suggest that MAPC cells can suppress the stimulation of T cells in response to the increased availability of homeostatic stimuli. Similarly, published GvHD studies and the GvHD data obtained in Chapter 3 suggest that MAPC cells might alter the phenotype T cell pool during reconstitution in lymphopenic hosts (Highfill *et al.*, 2009). Thus, it was hypothesised that MAPC cells may delay or suppress graft rejection by preventing the skew of T cells towards pro-inflammatory populations following lymphodepletion.

In order to test this hypothesis, an *in vivo* model of HP following lymphodepletion was set up using ATG as a depletive agent. MAPC cells were administered and the effects of

MAPC cells on T cell proliferation, IFN- γ production, and Treg promotion were examined. Furthermore, the effects of administrative routes of MAPC cell delivery was examined, and finally the mode of action of MAPC cells in this model was clarified. It was hypothesised that MAPC cells would mediate their effects through the production of PGE2, as PGE2 production by MAPC cells has been attributed to their suppression of IL-7 driven T cell activation *in vitro*, and prevention of GvHD development *in vivo* (Reading *et al.*, 2015; Highfill *et al.*, 2009). Thus, a COX inhibitor was introduced to the *in vivo* model to determine whether PGE2 was required for the therapeutic effect of MAPC cells in this system. Overall, the aim of this chapter was to investigate the effects and mode of action of MAPC cells on T cell HP using a clinically relevant *in vivo* model.

5.2 100 mg of ATG administered IP depletes the number of CD4 and CD8 T cells in the spleen and lymph nodes.

ATG is prepared by immunizing rabbits with murine thymocytes, followed by the purification of IgG sera. Since ATG is a biological therapy, and differences in efficacy may exist depending on the manufacturer, it was important to show that ATG used in this study could effectively deplete T cells *in vitro* before moving on to *in vivo* experiments. Studies by Valdez-Ortiz *et al.* (2015) and Ruzek *et al.*, (2008) were used as guides to determine if equivalent levels of T cell depletion could be repeated using similar concentrations of ATG and time points.

Splenocytes were harvested from CD45.1 mice and 1×10^5 cells were seeded per well in cRPMI supplemented with or without ATG or normal rabbit serum as a control. Cells were harvested after 16, 24, and 48 hours and enumerated using flow cytometry and counting beads as described in section 2.10.2. 10 $\mu\text{g/ml}$ ATG did not deplete CD8⁺ T cells at any time point, while 50 $\mu\text{g/ml}$ ATG depleted CD8⁺ T cells at 24 hours only (n = 3). CD8⁺ T cells were depleted by 250 $\mu\text{g/ml}$ ATG after 16, 24 and 48 hours (n = 3). 250 $\mu\text{g/ml}$ was the only concentration of ATG that depleted CD4⁺ T cells, and this only had an effect after 48 hours (n = 3). This effect of ATG on T cells was not significant when analysed using Kruskal-Wallis

analysis, however this is probably due to the small number of replicates used for preliminary experiments. Due to the high cost of ATG, optimisation experiments were carried out with small n numbers (n=3) which hindered the ability to achieve significance. Control serum had no depletive effect on T cells, confirming that it is the depletive antibodies within ATG causing the reduction in T cell numbers (Fig. 5.1). This corroborates well with previously published data which demonstrates that ATG binds more efficiently to CD8⁺ T cells than CD4⁺ T cells resulting in more rapid depletion of the CD8⁺ T cell population (Ruzek *et al.*, 2009). Moreover, depletion levels are similar to those observed by Valdez-Ortiz *et al.* (2015) and Ruzek *et al.* (2008).

Next, an *in vivo* model of depletion required optimization. In order to develop a model of lymphopenia driven HP, the correct concentration and route of administration of ATG needed to be determined. The model developed by Ruzek *et al.* (2009) was used to determine the dosing pattern of administering ATG on days 0 and 3, followed by harvest of spleen and lymph nodes on day 7. Two doses of ATG were tested, with each mouse being given either 25 mg/kg or 50 mg/kg on each day. Therefore, each mouse received either a total dose of 50 mg/kg or 100 mg/kg. Administrative routes were also tested, with each dose being administered either IP or IV. Normal rat serum which didn't contain T cell depleting antibodies were used as a control.

In the lymph nodes, the number of CD4⁺ and CD8⁺ T cells was reduced by each concentration and route of administration of ATG (Fig. 5.2A and 5.2B respectively). However, in the spleen, 100 mg of ATG administered was the only treatment which reduced the number of both CD4⁺ and CD8⁺ T cells. CD4⁺ T cells were reduced from 75450 ± 15310 to 29550 ± 7165 with 100 mg ATG administered IP (Fig. 5.2C) while the number of CD8⁺ T cells was reduced from 85590 ± 17970 in the PBS control to 19970 ± 3785 with 100 mg/kg ATG (Fig. 5.2D) (n = 3). This level of reduction was not seen with 50 mg/kg ATG, or with 100 mg/kg ATG administered IV. Therefore, it was decided to progress with future experiments using 100 mg of ATG administered IP. There was no depletion of T cells observed when control serum was adminis-

tered, which confirms that it is the depletive antibodies within the serum causing the reduction in T cell numbers (Fig. 5.2).

5.3 T cells in the spleen are depleted at day 4, while in the lymph nodes they're depleted at day 7.

The result shown in section 5.2 suggested that depletion of T cells by ATG was more effective in the lymph nodes than the spleen. However, it was hypothesized that since the ATG was administered on days 0 and 3, that the cells in the spleen may be already undergoing HP before day 7, and thus, day 7 was not the best time point to look at depletion. The dosing pattern outlined in 5.2 was repeated with just the 100 mg/kg dose administered IP with a harvest on day 4, to compare depletion of T cells one day after ATG administration to three days after ATG administration.

In this section, statistical significance was not achieved using ANOVA analysis, despite clear differences between groups. Thus, statistics generated in this section were generated using the student's t test. While the number of CD4⁺ T cells in the lymph nodes was reduced on day 4, this reduction was not significant until day 7 (n = 4) (Fig. 5.3A). In the CD8⁺ compartment, depletion was robust at both days 4 and 7 (n = 4) (Fig. 5.3B). This aligns with our *in vitro* data, and previous studies showing that ATG is superior at depleting CD8⁺ T cells compared to CD4⁺ T cells (Ruzek *et al.*, 2009). As hypothesized, the CD4⁺ compartment was depleted in the spleen at day 4 while depletion on day 7 was not robust (Fig. 5.3C), likely a result associated with reconstitution of the CD4⁺ compartment, induced by HP. Similarly, depletion of CD8⁺ T cells in the spleen was more pronounced at day 4 than day 7 (n = 4) (Fig. 5.3D). Therefore, the effects of ATG are differential in the spleen and lymph nodes and this needs to be considered when analyzing future results.

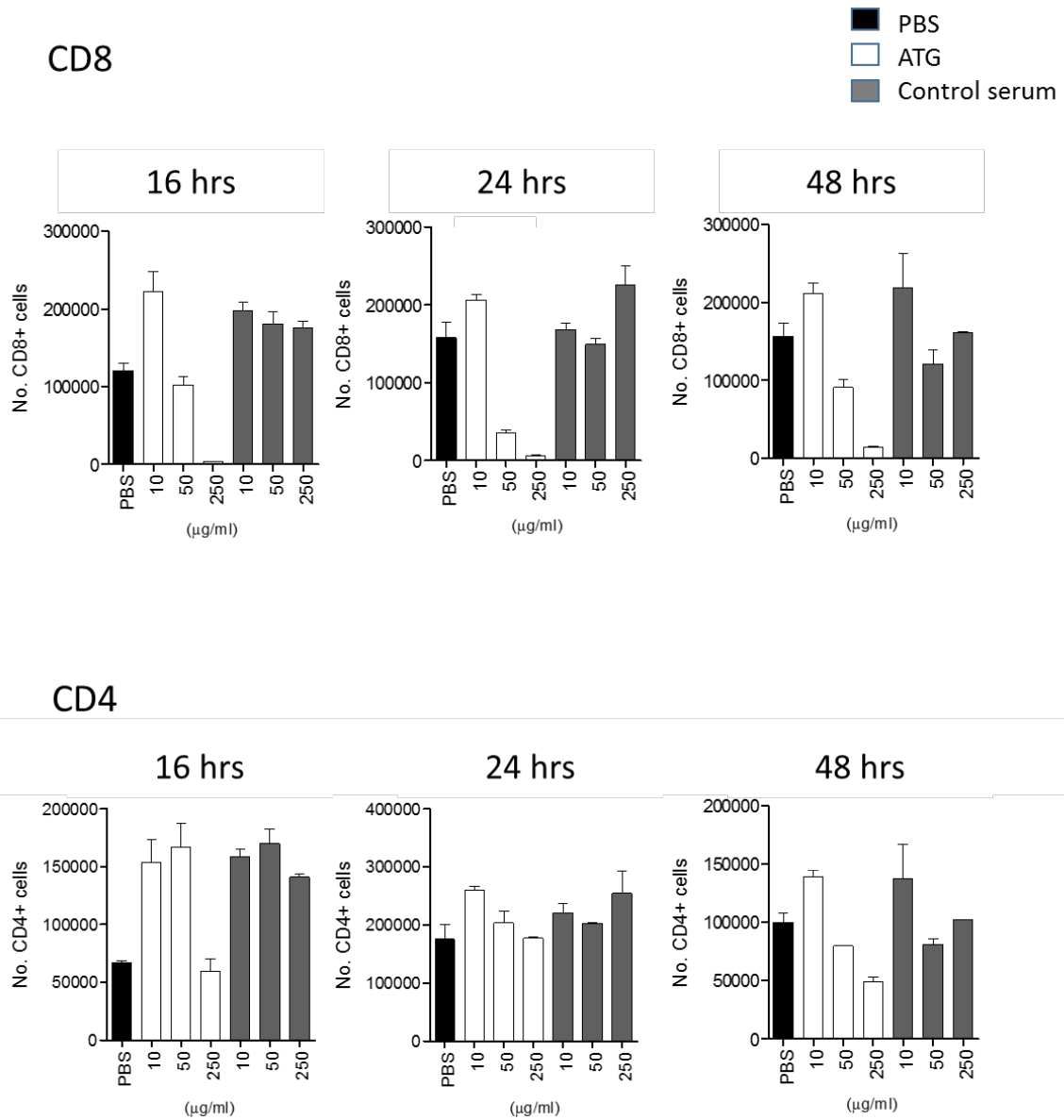


Figure 5.1 ATG depletes CD8⁺ T cells quicker than CD4⁺ T cells *in vitro*. Splenocytes were harvested from CD45.1 mice and 1×10^5 cells were seeded per well in cRPMI supplemented with or without ATG or normal rabbit serum as a control. Cells were harvested after 16, 24, and 48 hours and enumerated using flow cytometry and counting beads as described in section 2.10.1. 10µg/ml ATG doesn't deplete CD8⁺ or CD4⁺ T cells *in vitro*. 50µg ATG depletes CD8⁺ T cells after 24 hours but does not affect CD4⁺ T cell number. 250µg/ml depletes CD8⁺ T cells from 16 hours onwards, but doesn't deplete CD4⁺ T cells until 48 hours. Statistical analysis was carried out using Kruskal-Wallis analysis, n = 3.

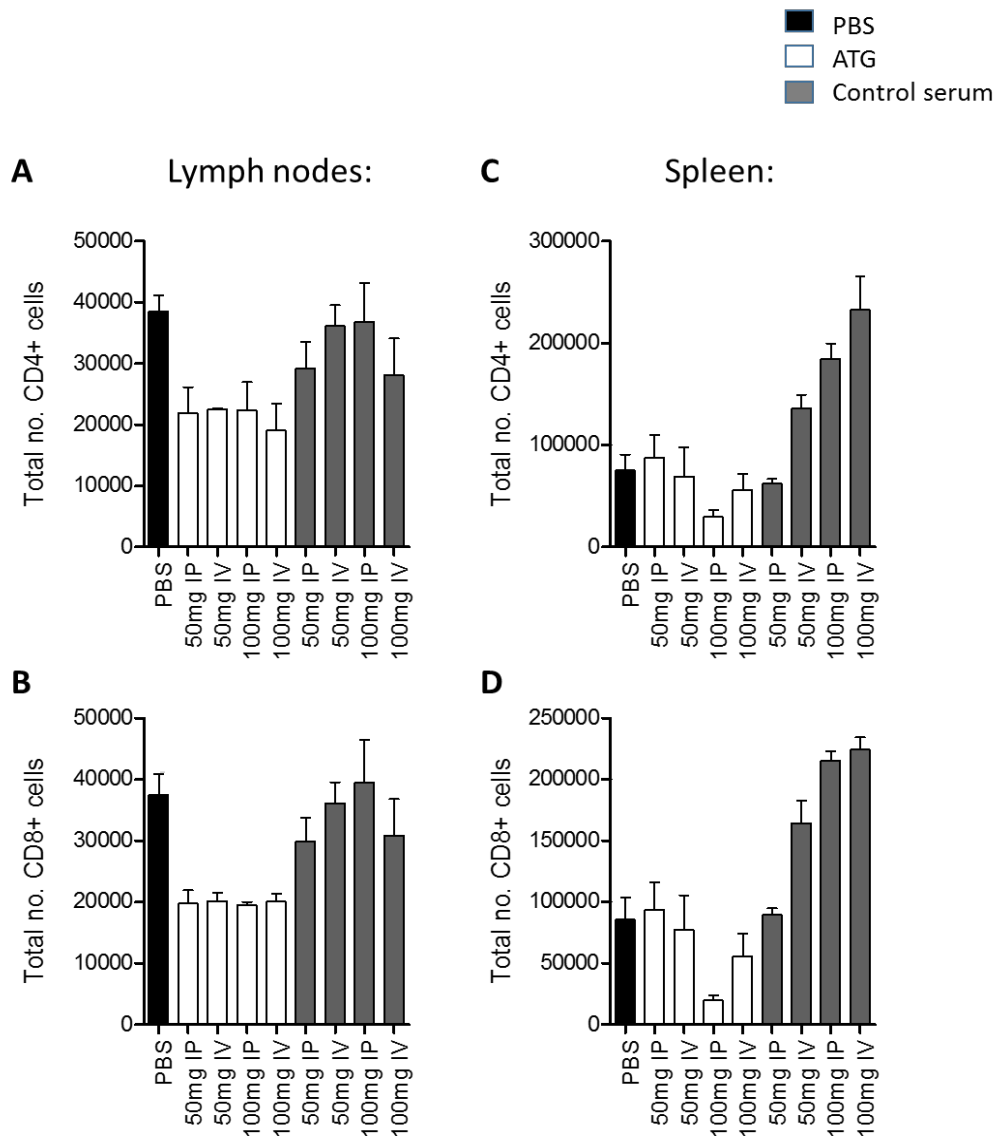


Figure 5.2 100 mg administered IP is the most effective dose and route of administration for ATG. CD45.1 mice were injected either IP or IV on days 0 and 3 with a total concentration of either 50 mg/kg or 100 mg/kg ATG followed by the harvest of spleens and lymph nodes on day 7. The total number of CD4⁺ and CD8⁺ T cells in each organ was enumerated by flow cytometry. Total number of CD4⁺ and CD8⁺ T cells is reduced in the lymph nodes on day 7 by 50 mg/kg and 100 mg/kg ATG administered IV and IP (A and B respectively). In the spleen only 100 mg/kg administered IP significantly reduced the number of CD4⁺ and CD8⁺ T cells on day 7 (C and D respectively). Normal rabbit serum was used as a control and had no depletive effect on T cells. Statistical analysis was carried out using Kruskal-Wallis analysis, n = 3.

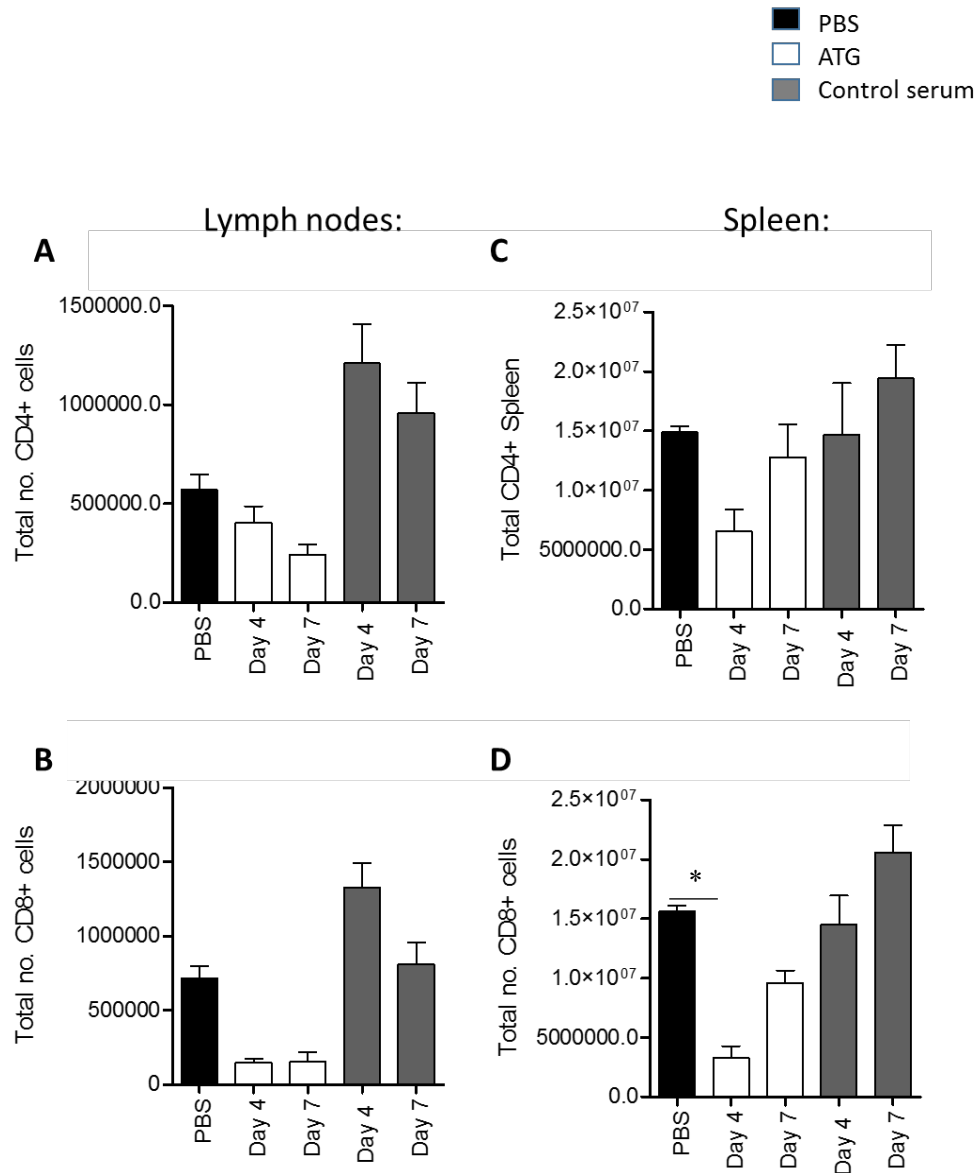


Figure 5.3 The rate of T cell depletion by ATG varies between CD4 and CD8 T cells in the spleen and lymph nodes. 100 mg/kg ATG or control serum was administered over 2 doses given on day 0 and day 3, followed by a harvest on days 4 and 7. Spleens and lymph nodes were processed and stained for flow cytometric analysis of CD4⁺ and CD8⁺ T cells. Total number of CD4⁺ T cells is significantly reduced in the lymph nodes by ATG on day 7 (A), while the number of CD8⁺ T cells is significantly reduced on both day 4 and day 7 (B). In the spleen, the total number of CD4⁺ T cells is significantly reduced at day 4 but this number is restored to normal levels by day 7 (C). The number of CD8⁺ T cells is significantly reduced at day both days 4 and 7 (D). Normal rabbit serum was used as a control and had no depletive effect on T cells. Statistical analysis was carried out using Kruskal-Wallis analysis with the original FDR method of Benjamini and Hochberg to correct for multiple comparisons where * ≤ 0.05 n = 3.

5.4 T cells in the spleen and lymph nodes are undergoing proliferation on day 7 of the lymphodepletion model.

In order to ensure that day 7 was an appropriate time point to measure the effects of MAPC cells on HP, the frequency of Ki67⁺ cells within the CD4 and CD8 compartments was determined in the spleen and lymph nodes following ATG administration. It was hypothesised that as the number of T cells in the spleen had increased by day 7 following ATG administration, that these cells may already be undergoing HP. Thus, the ATG model was set up as described in section and spleens and lymph nodes were harvested on day 7 for intracellular staining of Ki67.

In the lymph nodes on day 7 the frequency of Ki67⁺ cells within the CD8 compartment increased from 13.58%±2.650 to 42.53%±5.065 with ATG administration (n = 3), while in the CD4 compartment this increase was more pronounced with the frequency of Ki67⁺ cells increasing from 13.37%±2.172 to 81%±8.220 following lymphodepletion. Within the spleen, the frequency of CD8⁺ cells expressing Ki67 increased from 9.110%±0.6004 to 24.83%±2.868 following lymphodepletion (n = 3). Similarly, the frequency of Ki67⁺ CD4⁺ cells in the spleen increased from 12.98%±1.282 in the PBS group to 57.01%±8.710 in the ATG group (n = 3). Normal rabbit serum was used as a control, and did not increase Ki67 expression by T cells to the same levels as ATG (Fig. 5.4). Since proliferation was increased by T cells at day 7, it was decided that day 7 was an appropriate time point to measure the effects of MAPC cells on HP following lymphodepletion.

5.5 MAPC cells IP suppress T cell proliferation in the spleen but not in the lymph nodes

As shown in chapter 4, MAPC cells IP and MAPC cells IV suppress IL-7 driven proliferation of T cells *in vivo*. Following on from that result, it was hypothesized that MAPC cells would similarly suppress proliferation of T cells following ATG administration. Since depletion had occurred in most cases at day 4, 1x10⁶ MAPC cells were administered IV or IP at this point with the hypothesis that MAPC cell therapy would suppress proliferation of the T cell compartment.

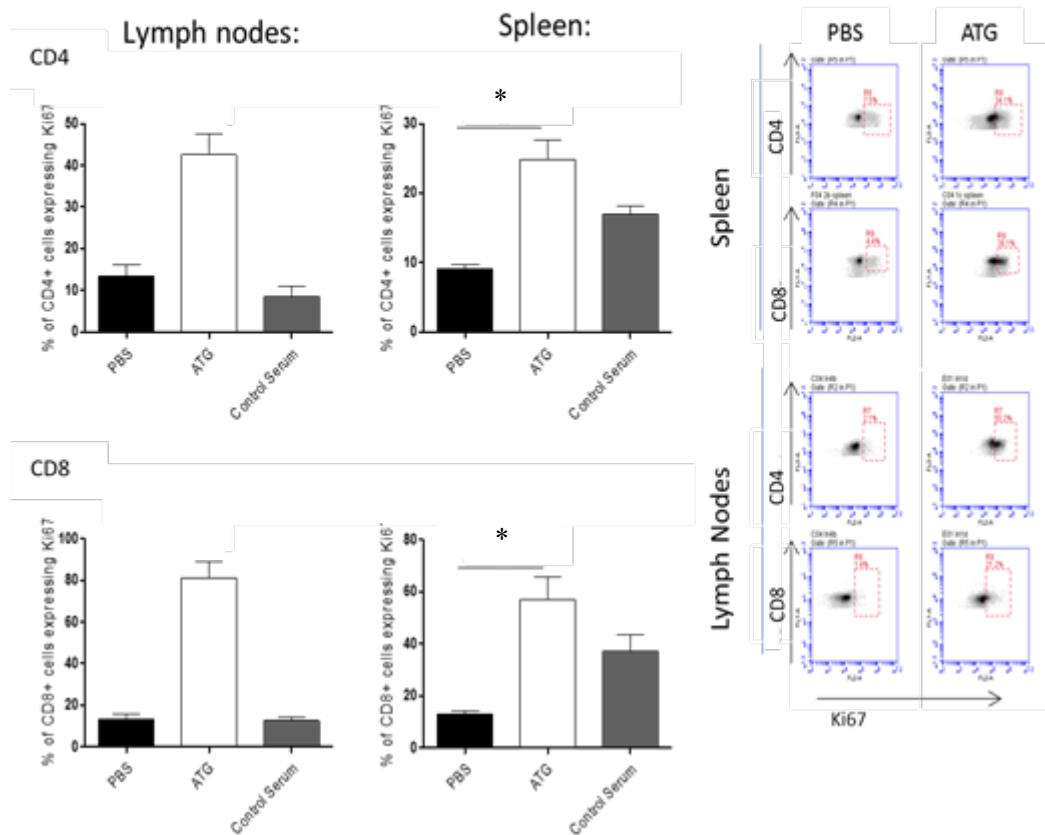


Figure 5.4 CD4⁺ and CD8⁺ T cells in the lymph nodes and spleen are proliferating on day 7 of the ATG model. 100 mg/kg ATG or control serum was administered over 2 doses given on day 0 and day 3, followed by a harvest on day 7. Spleens and lymph nodes were processed and stained for flow cytometric analysis of Ki67 expression by CD4⁺ and CD8⁺ T cells. The percentage of CD4⁺ and CD8⁺ T cells proliferating in the lymph nodes and spleen is significantly increased on day 7 following ATG administration. Normal rabbit serum was used as a control. Statistical analysis was carried out using Kruskal-Wallis analysis with the original FDR method of Benjamini and Hochberg to correct for multiple comparisons where where * ≤ 0.05 and *** ≤ 0.001 . n = 3

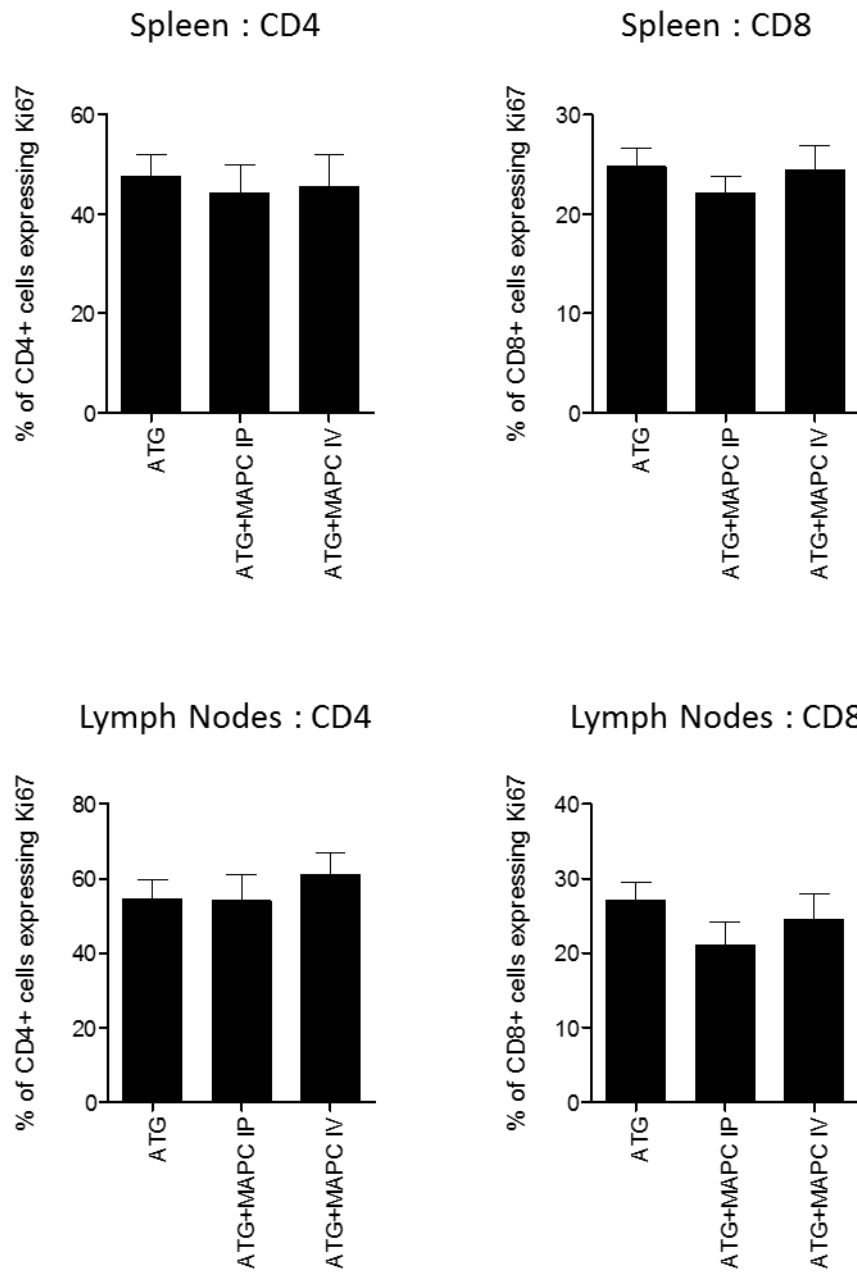


Figure 5.5 MAPC cells do not suppress proliferation of T cells following ATG administration. The ATG model was set up with administration of MAPC cells on day 4. Neither MAPC cells IP or MAPC cells IV had any significant effect on proliferation of CD4⁺ or CD8⁺ T cells in the spleen or the lymph nodes. Results are indicative of 2 experiments using 2 MAPC cell donors (n = 10).

Thus, the frequency of Ki67 expressing CD4⁺ and CD8⁺ T cells in the spleen and lymph nodes was examined in ATG groups following MAPC cell therapy. Surprisingly, both MAPC cells IP and MAPC cells IV failed to suppress T cell proliferation in the spleen and lymph nodes. While MAPC cells IP did slightly reduce Ki67 expression by CD8⁺ T cells, this effect was not significant (Fig. 5.5). Thus, despite MAPC cells having a robust suppressive effect on IL-7 driven T cell proliferation as seen in chapter 4, this is not reproducible in the ATG model.

5.6 MAPC cells IP enhance the frequency of Treg in the lymph nodes following lymphodepletion.

In the context of allograft rejection, the outcome of the immune reaction depends on the ratio of pro-inflammatory T cells to Treg. The expansion of regulatory and memory T cells following ATG treatment is extensively reported (Ruzek *et al.*, 2009; Xia *et al.*, 2012; Boenisch *et al.*, 2012; Broady, Yu & Levings, 2009; Feng *et al.*, 2008; Meyer *et al.*, 2015; Valdez-Ortiz *et al.*, 2015). Furthermore, MSC have been shown to expand Treg populations both *in vitro* and *in vivo* (Luz-Crawford *et al.*, 2013; Cahill *et al.*, 2015; English *et al.*, 2009). Therefore, I sought to examine if MAPC cell therapy promoted Treg in the ATG model. The ATG model was set up as previously described. Splenocytes and lymph nodes were processed and stained for CD4 and CD25 before being stained intracellularly for FoxP3.

In the spleen, administration of ATG slightly increased the frequency of CD25⁺, FoxP3⁺ cells within the CD4⁺ compartment from 12.46%±0.5971 to 15.34%±1.334 (n = 12), however MAPC cells had no further effect (Fig. 5.5A). In the lymph nodes, ATG administration significantly increased the frequency of Treg from 9.342%±0.7697 to 14.83%±0.4843 (n = 12). MAPC cells further increased this population, however this was only significant when MAPC cells were administered IP, and when these groups were compared using the student's t test (Fig. 5.5B). Therefore, in contrast to the IL-7 model, MAPC cells can promote natural Treg in the ATG model, however this is only seen when MAPC cells are injected IP.

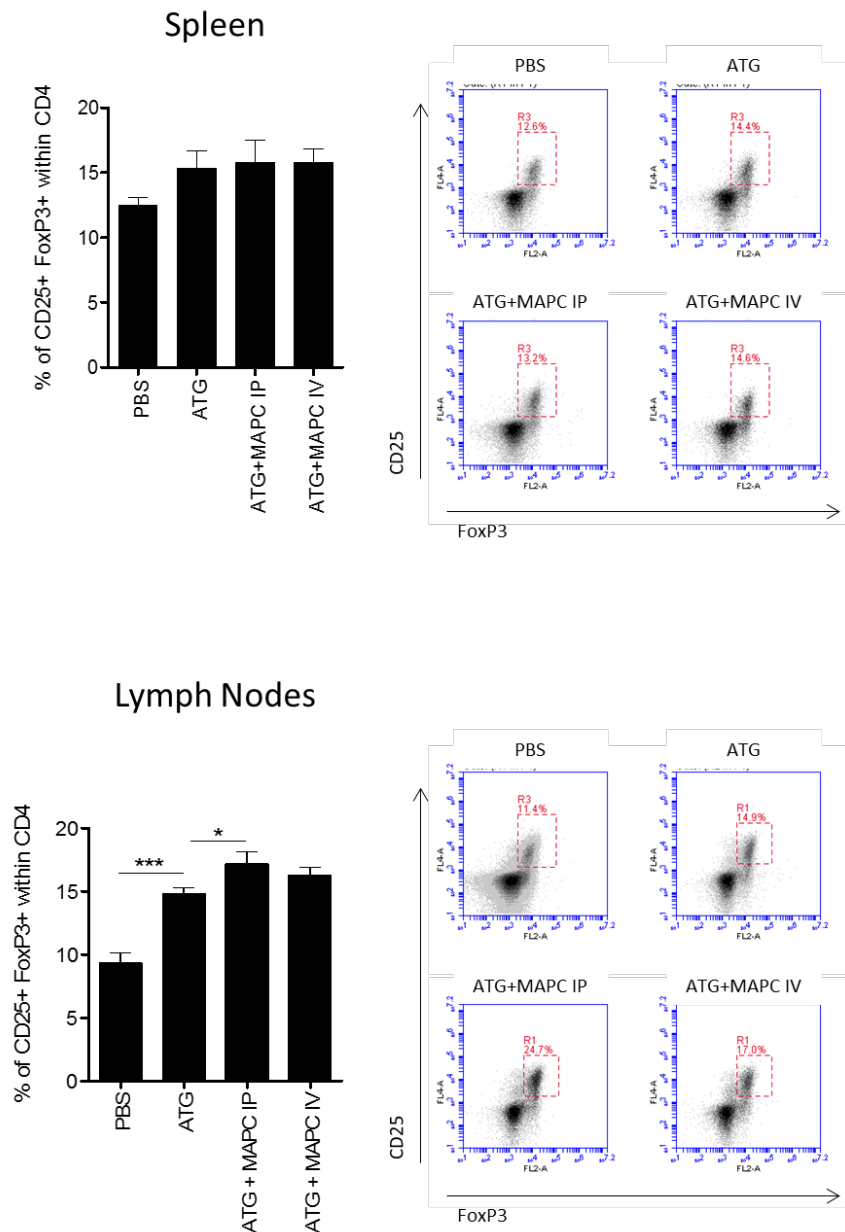
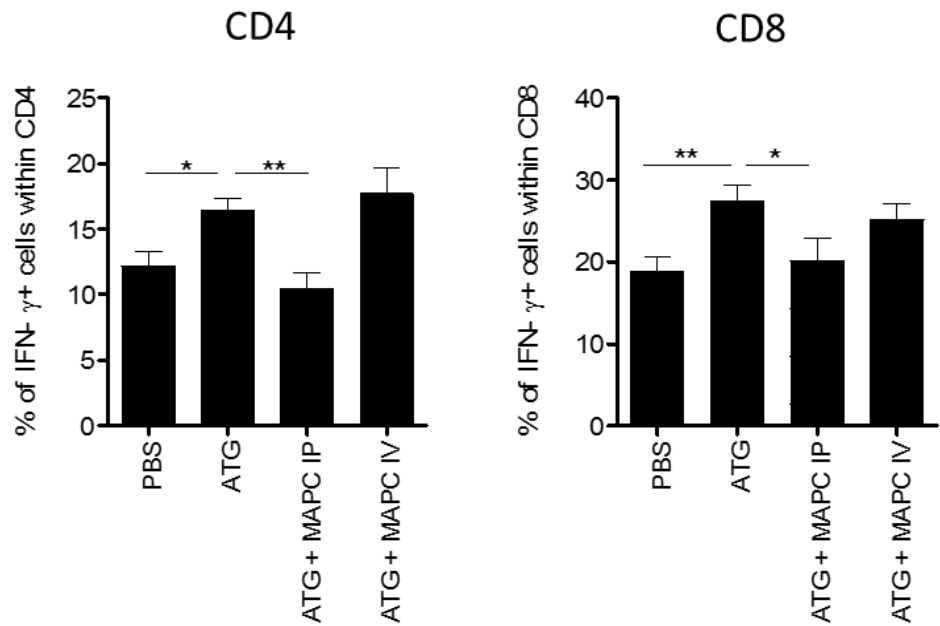


Figure 5.6 MAPC cells IP promote the frequency of Treg in the lymph nodes. The ATG model was set up as described in figure legend 5.4 and spleens and lymph nodes were harvested for flow cytometry on day 7. Cells were surface stained for CD4 and CD25 before being stained intracellularly for FoxP3. ATG increased the frequency of CD4⁺, CD25⁺, FoxP3⁺ T cells in the spleen and lymph nodes. In the spleen MAPC cells had no effect on Treg frequency, however, MAPC cells IP further increased Treg frequency in the lymph nodes. Results are indicative of 2 independent experiments using 2 MAPC cell donors. Statistical analysis was carried out using Kruskal-Wallis analysis with the original FDR method of Benjamini and Hochberg to correct for multiple comparisons where * ≤ 0.05 , ** ≤ 0.01 , and *** ≤ 0.001

Spleen:



Lymph Nodes:

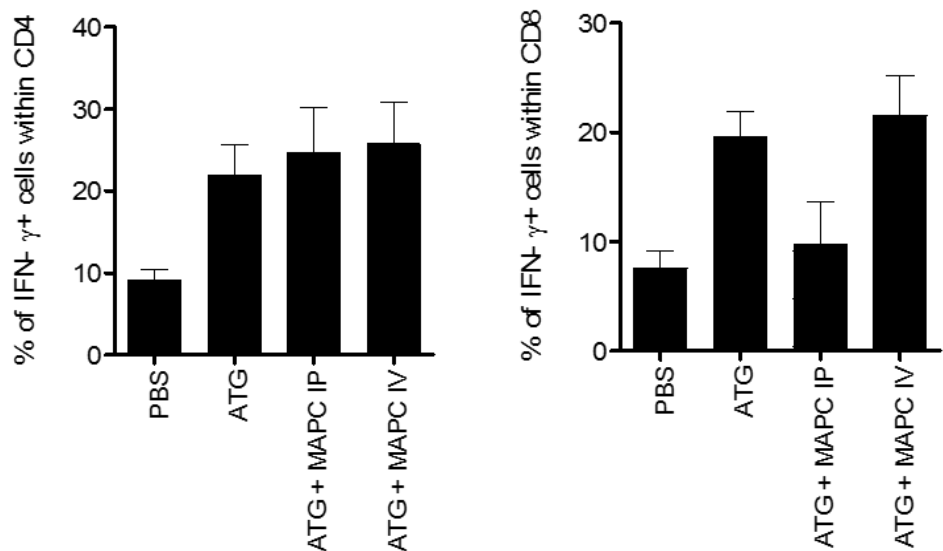


Figure 5.7 MAPC cells IP suppress IFN- γ production by T cells following ATG administration. The ATG model was set up as described in section 2.8.3. Spleens and lymph nodes were examined for IFN- γ by flow cytometry. MAPC cells IP reduced the frequency of IFN- γ producing CD4⁺ and CD8⁺ T cells in the spleen, and the frequency of IFN- γ producing CD8⁺ T cells but not CD4⁺ T cells in the lymph nodes. MAPC cells IV had no effect on the frequency of IFN γ producing T cells in either organ. Results are indicative of 2 independent experiments using 2 MAPC cell donors. Statistical analysis was carried out using Kruskal-Wallis analysis with the original FDR method of Benjamini and Hochberg to correct for multiple comparisons where * ≤ 0.05 , ** ≤ 0.01 .

5.7 MAPC cells suppress the frequency of CD8⁺ IFN- γ producing cells in the spleen and lymph nodes following lympho-depletion.

Under lymphopenic conditions, the increased availability of homeostatic stimuli causes the skew of remaining T cells towards a Th1 phenotype. Since MAPC cells suppressed IFN- γ production by T cells in the IL-7 model, it was hypothesised that they would show similar efficacy following lymphodepletion. Splenocytes and lymph nodes were harvested from the ATG model and prepared for intracellular cytokine staining as described in section 2.10.4. The frequency of IFN- γ ⁺ cells was significantly increased in both the CD4⁺ and CD8⁺ compartments in the spleen and lymph nodes. MAPC cells IP significantly reduced the frequency of IFN- γ ⁺ CD4⁺ and CD8⁺ splenocytes, however MAPC cells IV had no such effect. In the lymph nodes MAPC cells had no effect on IFN- γ production by CD4⁺ cells, however MAPC cells IP reduced the percentage of IFN- γ producing cells within the CD8⁺ population (Fig. 5.7). Thus, similar to the IL-7 model, MAPC cells IP show superior efficacy to MAPC cells IV in the ATG model.

5.8 Suppression of IFN- γ production by CD8⁺ T cells by MAPC cells is dependent on PGE2

PGE2 has been shown to be an important contributor to MSC and MAPC cells mediated immunosuppression in a number of *in vivo* settings (Auletta *et al.*, 2015; Highfill *et al.*, 2010). Furthermore, we have previously shown that suppression of IL-7 activated T cells by MAPC cells *in vitro* requires PGE2 (Reading *et al.*, 2015). Thus, it was hypothesised that the suppression observed by MAPC cells *in vivo* would be mediated by the same mode of action. To test this hypothesis, the COX inhibitor indomethacin was administered to the ATG model along with MAPC cells IP on day 4. Indomethacin was injected again on days 5 and 6, followed by harvest of the spleens and lymph nodes on day 7. Indomethacin injected alone to ATG mice had no effect on IFN- γ production by CD8⁺ T cells (Fig. 5.8). As expected, the frequency of IFN- γ producing CD8⁺ cells in both the spleen and lymph nodes of the ATG group was increased compared to the PBS group (n = 6 and n = 4 respectively). MAPC cells

IP reduced the frequency of IFN- γ producing T cells in the spleen from 27.40% \pm 2.379 to 17.35% \pm 2.056 (n = 6), while in the lymph nodes, MAPC cells reduced this frequency from 18.13% \pm 2.241 to 6.225% \pm 2.099 (n = 4). Administration of indomethacin reversed the effects of MAPC cells IP, suggesting that PGE2 is required for immunosuppressive effects of MAPC cells in this model (Fig. 5.9).

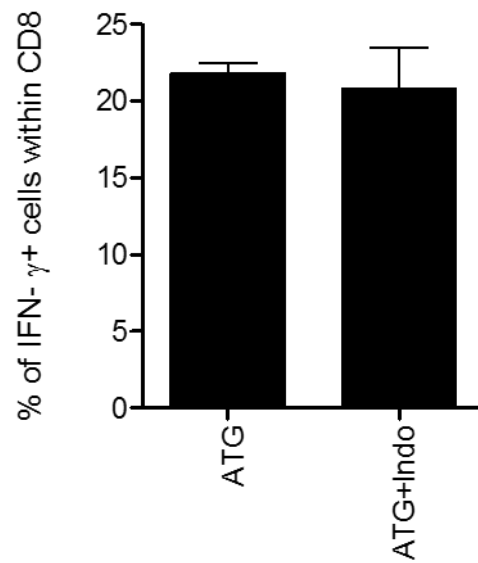


Figure 5.8 Indomethacin does not impair IFN- γ production by T cells following ATG administration. ATG was administered on days 0 and 3 followed by IP injection of 30 μ g Indomethacin (Indo) on days 4, 5 and 6. Spleens were harvested on day 7 and examined for production of IFN- γ . Indomethacin had no effect on the production of IFN- γ by splenic CD8⁺ T cells (n = 5).

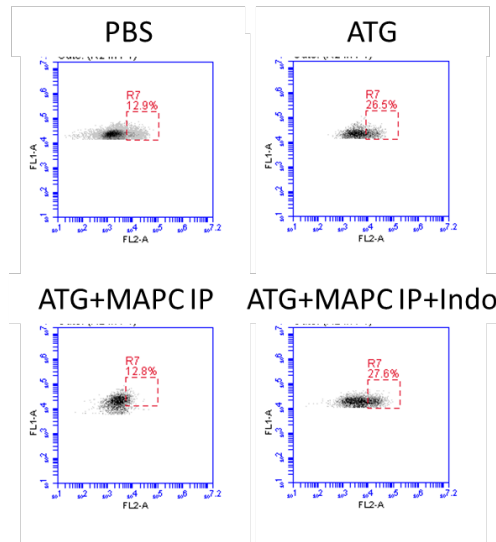
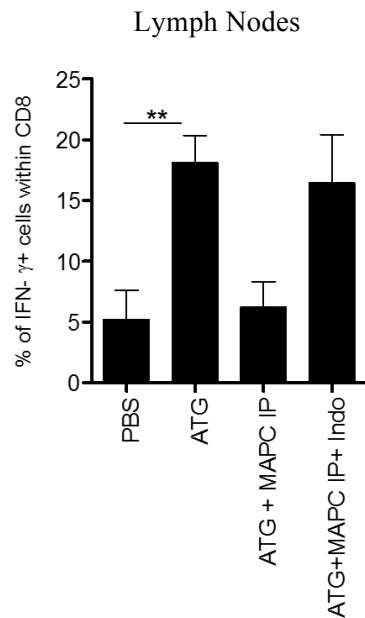
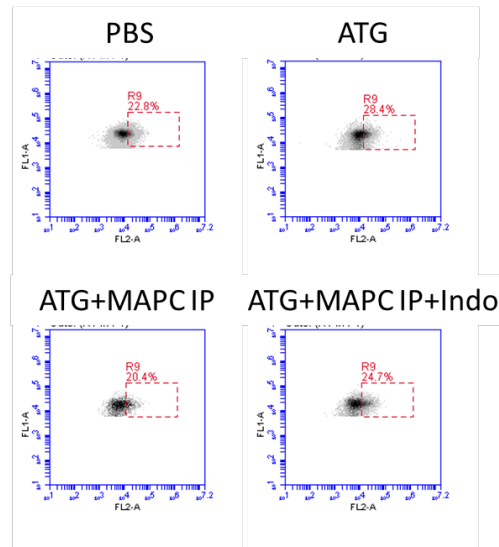
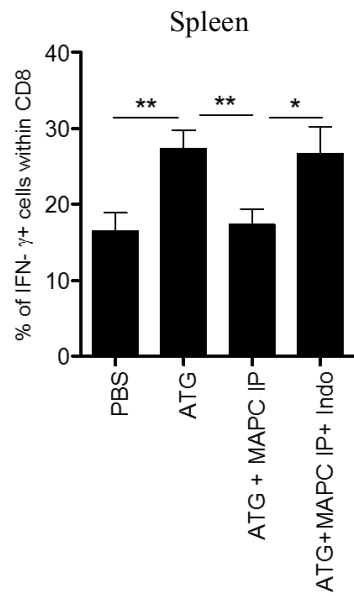


Figure 5.9 MAPC cells IP suppress IFN- γ production by T cells following ATG administration in a COX2 dependent manner. ATG was administered on days 0 and 3 followed by MAPC cells IP on day 4, IP injection of 30 μ g Indomethacin (Indo) on days 4, 5 and 6. Spleens and lymph nodes were harvested on day 7 and examined for production of IFN- γ by flow cytometry. MAPC cells suppressed the production of IFN- γ by CD8⁺ T cells in both the spleen and the lymph nodes, and indomethacin reversed this. Results are indicative of 2 independent experiments using 2 MAPC cell donors. Statistical analysis was carried out using Kruskal-Wallis analysis where * ≤ 0.05 , and ** ≤ 0.01 .

5.9 Summary

The IL-7 model was a first step to examine the effects of MAPC cells on IL-7 driven stimulation of T cells. However, in the clinic the abundant levels of IL-7 are due to decreased competition for homeostatic stimuli following the use of lymphodepleting drugs. Thus, the aim of this chapter was to build on the data collected in Chapter 4 using the more clinically relevant model of HP following lymphodepletion rather than following administration of recombinant IL-7. First, a model of HP following ATG administration was set up. A number of doses of ATG and routes of administration were tested following a dosing timeline outlined in a number of studies wherein two doses of ATG are administered 3 days apart (Ruzek *et al.*, 2009; Xia *et al.*, 2012; Ayasoufi *et al.*, 2016). Using this dosing schedule, it was decided that a dose of 100 mg/kg ATG administered IP over two doses was the most robust method of depleting T cells in the lymph nodes and spleen. Depletion was shown to be more robust with CD8⁺ than CD4⁺ cells as expected, and ATG administration affected T cells within the spleen more rapidly than the lymph nodes. Although the timing of depletion and subsequent proliferation was slightly different between the spleen and lymph nodes, overall depletion was evident at day 4 and proliferation was measurable on day 7. Therefore, MAPC cells were introduced to the model either IP or IV on day 4, and spleens and lymph nodes were harvested on day 7 to look at the effects of MAPC cells on T cell HP.

Similar to the IL-7 model, ATG administration increased the proliferation and IFN- γ production by T cells. In this case however, neither MAPC cells administered IP or IV had an effect on T cell proliferation at either site. On the other hand, MAPC cells IP did suppress IFN- γ production by CD8⁺ T cells in both the spleen and the lymph nodes, while MAPC cells IV failed to have this effect. Treg were also examined in this model, using just the traditional panel of CD25 and FoxP3 co-expression. It is well known that ATG increases Treg populations (Feng *et al.*, 2008; Boenisch *et al.*, 2012; Valdez-Ortiz *et al.*, 2015), and this was also demonstrated in our model. Similar to the IL-7 model, MAPC cells had no effect on Treg in the spleen, however MAPC cells IP did further enhance the frequency of Treg in the lymph

nodes. Thus, overall, the data obtained using the ATG model was quite similar to that of the IL-7 model, in that MAPC cells can prevent the skew of T cells towards Th1 populations during HP, and MAPC cells IP are more proficient in doing this than MAPC cells IV.

Finally, the mode of action of MAPC cells IP in the ATG model was examined. We have previously shown *in vitro* that the effects of MAPC on IL-7 activation of T cells is dependent on PGE2 production by MAPC cells (Reading *et al.*, 2015), and others have shown that suppression of murine GvHD by MAPC cells is PGE2 dependent (Highfill *et al.*, 2009). Furthermore, in Chapter 3 we speculate that the improved efficacy of PPAR(-) MAPC cells in the GvHD model is due to an increase in COX-2 expression by PPAR(-) MAPC cells following IFN- γ stimulation. Therefore, it was hypothesised that MAPC cells would require PGE2 for their function in this model, and the COX inhibitory indomethacin was introduced *in vivo* to block PGE2 production by MAPC cells. PGE2 inhibition prevented MAPC cells IP from suppressing IFN- γ production by T cells following lymphodepletion. Thus, this chapter demonstrates that MAPC cells are unable to suppress proliferation of T cells during lymphodepletion, however MAPC cells IP can prevent the skew of T cells towards pro-inflammatory profiles and promote Treg during HP. Furthermore, the anti-inflammatory effects of MAPC cells IP in this model are likely dependent on PGE2.

Chapter 6

Discussion

In 2004, Le Blanc *et al.* published a landmark study reporting the successful use of haploidentical MSC in a young patient with steroid refractory GvHD (Le Blanc *et al.*, 2004). Since then, investigators have been excited about the potential of using ‘off the shelf’ MSC and MAPC cells as a prophylaxis to prevent or treat GvHD and SOT rejection. Preclinical and small scale clinical studies have reported promising safety and efficacy data using these therapies in both instances, with MSC and MAPC cells being shown to suppress T cell proliferation, promote regulatory cell populations and protect damaged tissue (Auletta *et al.*, 2015; Highfill *et al.*, 2009; Maziarz *et al.*, 2012; Ringden *et al.*, 2006; Soeder *et al.*, 2015). However, in a larger industry sponsored clinical trial using clinical grade MSC to treat steroid refractory GvHD, MSC performed poorly compared to the placebo (Phinney *et al.*, 2013). It is clear from this, and disappointing efficacy data derived from other clinical trials, that the facets of MSC and MAPC cell biology that are misunderstood require clarification in order to maximise the therapeutic potential of these cells. The main problems that commonly arise regarding the use of MSC and MAPC cells in the clinic usually lead to questions surrounding the timing or schedule of their administration, routes of cell delivery, expansion methods and donor variation (Phinney *et al.*, 2013). This study sought to increase our understanding on the efficacy, biodistribution and modes of action of MAPC cells in murine models of transplantation. Knowledge gained from this study could then be used to optimise the use of MAPC cells in the future.

The first part of Chapter 3 focused on ensuring the characteristics and potency of MAPC cells used for this study were sufficient prior to advancing to *in vivo* experiments. These tests are important for a number of reasons. Firstly, since a number of cell types can be isolated from the BM, it is important to examine the characteristics of the MSC and MAPC cells used for this study using standardised methods. Secondly, for both ethical and practical reasons, *in vitro* potency assays should be used to validate the functional capacities of MAPC cells before introducing these cells to animal models (Lehman *et al.*, 2012; Roobrouck *et al.*, 2011). In the early 2000s the number of investigators interested in MSC and MAPC cells in

both academic and industrial settings increased dramatically. Unsurprisingly, the sources and methods of cell isolation and expansion varied between different groups, which lead to many inconsistencies within the field. In 2006 the ISCT addressed these inconsistencies by proposing that MSC must fit the following criteria; adherence to plastic *in vitro*, surface expression of CD105, CD73, and CD90, negative expression of CD45, CD34, and HLA DR, and finally, the ability to undergo multipotent differentiation into osteocytes, adipocytes and chondrocytes (Dominici *et al.*, 2006). MAPC cells also meet these criteria, with the primary difference between the MSC and MAPC cell phenotype being that MAPC cells express lower levels of HLA ABC (Roobrouck *et al.*, 2011). The initial experiments outlined in Chapter 3 demonstrate that the MAPC cells used herein adhere to these criteria outlined by the ISCT; MAPC cells adhered to plastic and maintained the small spindly phenotype expected, expressed the required surface antigens, and differentiated into osteocytes and adipocytes under controlled *in vitro* conditions.

In recent years, the increased use of MSC and MAPC cells in the clinic has highlighted the need to further standardise the consistency and quality of these therapies. The complex nature of cellular therapies means that subtle differences in cell source or preparation can have significant effects on their therapeutic efficacy. Thus, it is not enough to merely identify cells using the criteria outlined by the ISCT, but potency assays should also be used to ensure that cells are fit for purpose before being introduced to clinical studies (Bravery *et al.*, 2013). For ethical and practical reasons, these potency assays were also used prior to animal studies during this project. By ensuring that MAPC cells were of good quality before being used *in vivo*, we could avoid unnecessary use of animals with potentially poor-quality cells. Potency assays used by different groups varies depending on the condition MSC or MAPC cells are being used for. For example, to indicate the efficacy of MSC to treat GvHD, Osiris Therapeutics Inc. measure TNFR1 secretion by MSC and link this to potency (Danilkovitch, 2006), while Athersys Inc. measure the levels of VEGF, CXCL5 and IL-8 to predict the pro-angiogenic capacity of MAPC cells in myocardial infarction (Lehman *et al.*, 2012).

For this study, we chose to predict the immunosuppressive capacity of MAPC cells using a T cell suppression assay, and the pro-angiogenic capacity of MAPC cells using a tube formation assay. These two characteristics of MAPC cell function were particularly important for this project, as MAPC cells were expected to suppress T cell proliferation and protect damaged tissue in the murine models of inflammation used herein. MAPC cells are known to carry out these functions in a range of *in vitro* and *in vivo* assays using soluble factors such as IDO, PGE2, VEGF and CXCL5, and the efficacy of MAPC cells in these assays has been previously demonstrated by others (Reading *et al.*, 2013, 2015; Lehman *et al.*, 2012). Thus, these robust assays were chosen as reliable indicators of MAPC cell quality. MAPC cells were demonstrated to suppress the proliferation of T cells in response to stimulation with anti-CD3/CD28 beads in a dose dependent manner. This was expected based on previous studies using MAPC cells in this type of assay (Reading *et al.*, 2013). Similarly, MAPC cells had the capacity to promote tube formation by HUVEC cultured in Matrigel. MAPC cells have previously been reported to be superior promoters of angiogenesis compared to MSC in a murine model of stroke, and this difference between the two cell types was reproduced in the potency assay used herein (Mora-Lee *et al.*, 2012). Thus, the clinical grade MAPC cells used in this study were of good quality and carried out their expected functionality in these *in vitro* assays.

The use of characterisation and potency assays are not always entirely predictive of the efficacy of MSC or MAPC cells *in vivo*, and this should be borne in mind when moving cells into *in vivo* models. Cellular therapies are extremely complex, and they function through multiple modes of action. Furthermore, the environment *in vivo* is very different to that *in vitro*, and so the efficacy of MAPC cells in the previously mentioned assays does not guarantee that the cells would be effective at suppressing inflammatory conditions *in vivo*. Nevertheless, these assays do act as a guide to the operator, and when cells are ineffective *in vivo* these tests can be used to show that it is not due to poor quality cells, but may be due to other factors such as timing of administration, cell number infused etc. Furthermore, these tests can identify differences in potency between cells cultured using varying conditions, or

between different donors. Differences in the potency among donors is a major concern regarding the use of MSC and MAPC cells, as it is well known that not all donor cells possess the same therapeutic capacities (Kuci *et al.*, 2016). Thus, these assays are also valuable for predicting the efficacy of various MSC or MAPC cell donors *in vivo*.

Once the characteristics and functionality of MAPC cells were demonstrated, Chapter 3 moved on to focus on improving the efficacy and biodistribution of MAPC cells in a humanised model of aGvHD. Both MSC and MAPC cells have previously been shown to treat GvHD in murine models (Auletta *et al.*, 2015; Highfill *et al.*, 2009), and our group have reported the efficacy of MSC in a humanised model (Tobin *et al.*, 2013). In the humanised aGvHD model, human BM-MSC have no effect on IL-2 or IFN- γ production by T cells, but they do inhibit TNF- α production. Surprisingly, total IFN- γ levels in the sera of aGvHD mice are actually increased when MSC are administered, demonstrating the complex interactions between MSC/MAPC cells and the environment *in vivo* (M. Healy, 2015, PhD thesis). These preclinical studies and many others have provided both efficacy and mechanistic data regarding the use of MSC and MAPC cells to prevent or treat GvHD, and have highlighted a number of concerns which may explain the disappointing phase III Prochymal[®] trial. These rodent studies have both advanced our understanding of MSC or MAPC cell biology, while simultaneously reinforcing the reality that we need to understand exactly how these cell types work in order to maximise their full therapeutic potential in the clinic. Without fully understanding the exact mechanisms by which these cells alleviate GvHD in animal models, it is extremely difficult to determine the optimal conditions which should be used when administering MSC or MAPC cells in the clinic.

One such concern surrounding the use of MSC or MAPC cells in the clinic is at what point should cells be administered. Murine models have shed some light on this issue. For example, Highfill *et al.* (2009) found that murine MAPC cells had no effect on GvHD prevention when infused systemically on the same day as BMT, however intrasplenic delivery of MAPC cells was beneficial. Similarly, Tobin *et al.* (2013), and Jeon *et al.* (2010) found that human MSC administered IV on day 0 were ineffective at alleviating GvHD symptoms. In

traditional xenogeneic models, early administration of two doses of MSC has been beneficial. For example, administration of MSC to murine models of GvHD on days 1 and 3 or 4 post BMT has been shown to be effective by a number of groups (Auletta *et al.*, 2015, M. Healy, 2015, PhD thesis), while administration of human MSC to a similar model on day 7 failed to alleviate the disease (Jeon *et al.*, 2010). On the other hand, when administered to a humanised GvHD model on day 7, MSC are effective at delaying aGvHD onset (Tobin *et al.* 2013, M. Healy, 2015, PhD thesis). The differences in efficacy of MSC in these models is probably due to differences in the inflammatory state *in vivo*, as GvHD would not develop along identical time courses in each model.

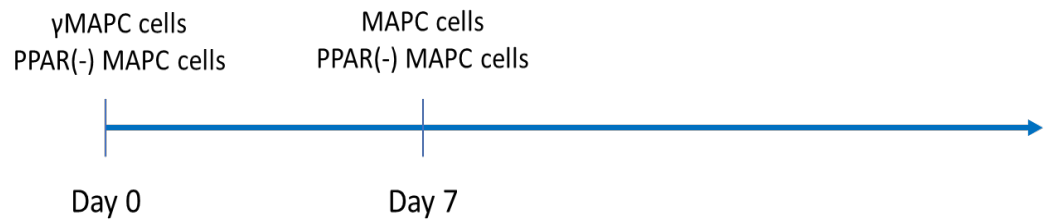
For this study, the first step was to test the efficacy of MAPC cells at either preventing or treating aGvHD using a humanised model. While the above studies suggest that MAPC cells should be therapeutic in this system, it has not yet been tested using a humanised model. The humanised aGvHD model is established following the administration of human PBMC to irradiated NSG mice. Human immune cells engraft and are activated following the recognition of xenogeneic MHC molecules expressed by the host. aGvHD then develops and manifests itself through symptoms such as weight loss, hair loss and reduced activity. The humanised model is particularly valuable, as it allows for the interactions between human MAPC cells and the human immune cells which are driving the disease. The study by Highfill *et al.* examined the effects of murine MAPC cells in a murine model of GvHD, however there may be discrepancies between the modes of action of rodent and human MAPC cells. For example, murine MSC are thought to modulate T cell function through the production of iNOS, while human MSC use IDO for this purpose (Ren *et al.*, 2008; Meisel *et al.*, 2004). While this problem can be overcome by administering human MAPC cells to murine models, this type of xenogeneic setup has some limitations. For example, cross-species activity between human and murine IFN- γ is low (Fitzgerald *et al.*, 2001), which is particularly problematic for these studies where IFN- γ is such a potent activator of MAPC cell activity. Furthermore, xenogeneic (human) MAPC cells may be cleared earlier by murine immune cells than human

immune cells. Thus, the humanised model allows for a more accurate depiction of how exactly MAPC cells would act in patients compared to a normal murine model.

Of course, the humanised model of aGvHD is not an exact replica of clinical GvHD. In clinical GvHD, host DC can present antigen to donor T cells, contributing to disease development (Markey, Macdonald & Hill, 2014). In contrast, NSG mice lack DC, thus the humanised model is driven only by donor DC activating donor T cells, and human T cells cannot directly recognise murine MHC molecules. Thus, this aGvHD model is predominantly driven by CD4⁺ T cells. CD8⁺ T cells can contribute, but must be supported by CD4⁺ cells (Ito *et al.*, 2017). Therefore, this model is not ideal, however, humanised models are as close to the clinical scenario as is currently possible in the lab setting.

MAPC cells were administered to the humanised aGvHD model on either day 0 or day 7 to examine the capacity of MAPC cells to either prevent or treat aGvHD. Cells were administered IV since this is the most relevant route of delivery in the clinic, and MSC administered IV have previously been shown to be effective in this model (Tobin *et al.*, 2013). Mice were monitored daily for the presentation of aGvHD traits, and assigned disease scores which correlated to symptom severity. Once animals reached a disease score of 5, or lost 20% of their original weight they were humanely sacrificed. GvHD is known to cause systemic tissue destruction, particularly in the lung, liver, small intestine, and colon, thus these tissues were harvested to determine whether MAPC cells could alleviate tissue damage. Overall, MAPC cells administered on day 7 significantly improved the disease score, survival time, and tissue pathology of aGvHD animals, while MAPC cells administered on day 0 only slightly improved survival of aGvHD mice from a median survival time of day 13.5 to day 15 (Fig. 6.1). While MAPC cells were more potent at alleviating cellular infiltration and tissue damage in the lung and GI tract when administered on day 7 compared to day 0, surprisingly MAPC cells delivered on day 0 were superior at reducing signs of GvHD in the liver. MSC and MAPC cells are known to distribute to the liver following IV injection (Schmuck *et al.*, 2016), and cause a transient inflammatory response (Hoogduijn *et al.*, 2013). Tissue from all experimental groups was harvested on day 12. Thus, the reduced cellular infiltration observed

Effective MAPC treatments



Ineffective MAPC treatments

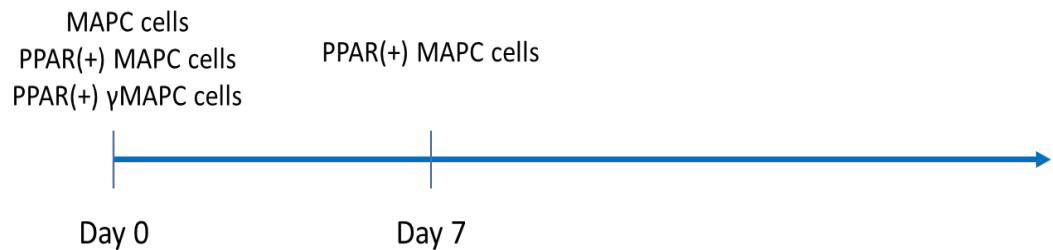


Figure 6.1 Schematic timeline of effective and ineffective MAPC therapies administered to the humanised aGvHD model. MAPC cells were effective at day 0 when pre-treated with IFN- γ (γ MAPC cells) or the PPAR δ antagonist (PPAR(-) MAPC cells). When administered on day 7, untreated MAPC cells, and PPAR(-) MAPC cells were effective. Untreated MAPC cells and PPAR(+) γ MAPC cells were ineffective on day 0, while PPAR(+) MAPC cells administered on both day 0 and day 7 failed to alleviate aGvHD. Effective MAPC treatments are defined as the capacity to significantly prolong survival in the aGvHD model. Ineffective MAPC treatments are defined as failure to significantly prolong survival in the aGvHD model

in tissue from animals treated with MAPC cells on day 0 compared to those treated with MAPC cells on day 7 may be due to the resolution of this inflammatory response to MAPC cells by day 12 in the group treated on day 0, while this could still be ongoing in the group treated with MAPC cells on day 7. This could be clarified by harvesting tissue at a range of time points.

Overall, this data aligns well with previous work by our group demonstrating that MSC can treat, but not prevent, the development of aGvHD using this model (Tobin *et al.*, 2013). Furthermore, the tissue pathology data aligned well with that of previous studies where MSC therapy is not equally protective in every tissue. In line with other studies using MSC, MAPC cells demonstrated superior therapeutic effects in the liver and gut compared to the lung (Martin *et al.*, 2010; Tobin *et al.*, 2013, M. Healy, 2015, PhD thesis). It is unclear why damage in the lung is not resolved as potently as other tissues, and is surprising given that the majority of MAPC cells administered IV would be expected to accumulate in the lung (Schrepfer *et al.*, 2007). This could be explained by the fact that IV administration of MSC is known to cause damage in the lung by forming microemboli (Choi *et al.*, 2011). Thus, this negative effect of MSC or MAPC cells in the lung could counteract the therapeutic effect of MSC and MAPC cells in pulmonary tissue.

This study did not examine the effects of MAPC cells on aGvHD at the cellular level, however previous studies by our group have demonstrated that MSC reduce TNF- α production by T cells and expand Treg in this model (M. Healy, 2015, PhD thesis, J. Corbett, 2016, PhD thesis). Therefore, it is likely that MAPC cells are mediating their therapeutic effect in a similar manner, however this would require further investigation. TNF- α contributes to tissue destruction and is part of a positive feedback loop of DC and T cell activation in GvHD (Henden & Hill, 2015), and both TNF- α blockade, and adoptive transfer of Treg have been shown to be therapeutic in GvHD (McDonald-Hyman, Turka & Blazar, 2015). Thus, it is likely that MAPC cells are partially alleviating GvHD symptoms in this manner. As mentioned previously, *in vitro* potency assays are commonly used to predict the ability of MSC to suppress T cell activity and expand Treg in in GvHD (Bravery *et al.*, 2013), however

the modes of action of MSC and MAPC cells are extremely complex, thus it is likely that other factors contribute to their immunomodulatory effects *in vivo*. It is unclear whether the observed effects of MSC on TNF- α production or Treg expansion are actually vital for their suppressive capacities, or whether other effects are more important. The investigation of this would be important in order to elucidate the mechanisms involved in MSC or MAPC cell therapeutic efficacy in aGvHD, and would assist researchers and clinicians in designing the correct processes and protocols surrounding culture conditions, potency assay development, and donor selection.

As mentioned previously, Highfill *et al.* found that murine MAPC cells could prevent GvHD following intrasplenic administration, suggesting that the spleen is an important site of activity for MAPC cells, while Auletta *et al.* (2015) have shown that human MSC administered IV to a murine model of GvHD on days 1 and 4 post BM transplant can be detected in the spleen 24 hours post administration. Furthermore, Auletta *et al.* elegantly showed that MSC suppressed T cell proliferation within the spleen, while Highfill *et al.* showed that MAPC cells in the spleen produce PGE₂. Thus, MSC have been shown to be present at this major allo-priming site following IV administration, however, since few studies compare the biodistribution between aGvHD and healthy mice, it is unknown whether biodistribution of MSC to this location is a passive process. One of the aims of this chapter was to improve our understanding of MAPC cell migration in the humanised model of aGvHD. Therefore, I sought to determine whether MAPC cells were responding to inflammatory cues *in vivo*, and migrating to target organs accordingly, or whether the detection of MSC in the spleen of GvHD mice by Auletta *et al.* was merely due to a passive systemic biodistribution of MSC *in vivo*. Commonly used tracking methods such as PCR or MRI do not accurately quantify the number of cells detected *in vivo* which makes subtle differences in biodistribution difficult to interpret. Furthermore, some tracking methods have been subject to criticism as labels detected *in vivo* can represent dead cells or phagocytes that have engulfed MSC (Eggenhofer *et al.*, 2012). This study used novel CryoViz™ imaging equipment, which allows for the improved detection and quantification of fluorescently labelled cells. Moreover,

the Qtracker[®] labelling kit used for this study requires the fluorescent beads to be tightly packed together within the cell to be detected by the CryoViz[™] (Luk *et al.*, 2016). Thus, the cells detected in this study are intact, and have not been phagocytosed.

There are cons to the use of CryoViz[™] technology, perhaps the main one being that animals must be sacrificed prior to imaging. Therefore, unlike live animal imaging where the distribution of MAPC cells could be traced in the same mouse over a range of time points, here each time point requires a separate animal. This restricted the time points which could be observed due to the costs associated with using large numbers of mice. Secondly, using the CryoViz[™] is quite costly and time consuming, particularly when imaging whole mice. The main costs associated with the use of the machine, are the Qtracker[®] labelling kit, and the blade used to section samples. Replacement blades are required more frequently when sectioning whole mice compared to tissue samples. Secondly, to section and image a whole mouse takes roughly three full days, and to process the images using the software can take roughly two weeks. Thus, whole mouse imaging was used sparingly during this project. Thirdly, a limiting feature of this technology is the need to use fluorescent labelling, which makes cells difficult to detect in auto-fluorescent regions. This was particularly problematic when imaging the gut, as the gut and its contents are extremely auto-fluorescent. While the CryoViz[™] quantification software did detect fluorescent signals in the GI tract, it was impossible to discriminate between Qtracker[®] labelled MAPC cells and background autofluorescence. Thus, the GI tract wasn't examined for MAPC cell biodistribution, and for whole mice experiments all fluorescent cells detected in the GI tract were dismissed. This was unfortunate as the GI tract is an important target organ in GvHD, and future studies should use alternative methods to examine the distribution of MAPC cells to this organ. Finally, since the CryoViz[™] is such a novel piece of machinery, its technology is being developed and improved constantly. The machine in Maynooth is the first in Europe, and some features of the machine required substantial refinement (freezer and quantification software) in order to use the machine regularly. These issues contributed to the length of time required to obtain biodistribution

data, and demonstrate the need to refine experiments to minimise costs and improve productivity.

Using CryoViz™ technology, it was observed that MAPC cells administered on day 7 to mice that received PBMC after irradiation exhibited increased biodistribution to GvHD target organs at 4 and 24 hours post infusion, compared to MAPC cells administered to mice that received PBS after irradiation. At 4 hours post infusion, the number of MAPC cells detected in each of the lung, liver, and spleen was higher in PBMC mice than PBS mice. Interestingly, at 24 hours post administration the number of cells in the lung was lower in PBMC mice compared to PBS mice, suggesting that MAPC cells were responding to systemic inflammation and escaping entrapment in the lungs. In the spleen, the number of MAPC cells detected was further increased at 24 hours in PBMC mice compared to PBS mice, while interestingly, the number of cells detected in the liver at 24 hours was the same in each group. Overall this data aligns well with other studies which show that the majority of MSC are trapped in the lung following IV administration, followed by the liver and spleen (Eggenhofer *et al.*, 2014), and demonstrates that MAPC cells respond to inflammatory cues *in vivo* and migrate accordingly.

Most researchers agree that MSC are cleared in the first few days after administration (Leibacher & Henschler, 2016). Whole mice were imaged to examine whether there was a difference in the clearance of MAPC cells depending on whether they were delivered to PBS or PBMC mice. For the reasons outlined above, only one time point was chosen for imaging of whole mice. It was hypothesised that imaging at 48 hours would generate relevant data, as MAPC cells would have started to be cleared at this point, but not so much so that no cells would be detected. Roughly 6% of MAPC cells administered to PBS mice were detected at 48 hours, while roughly 10% of administered MAPC cells were detected in PBMC mice at this point. This data aligns with that of others showing that the vast majority of cells are cleared quickly (Leibacher *et al.*, 2017; Eggenhofer *et al.*, 2012) and furthermore, this data suggests that there is not a huge difference in the persistence of MAPC cells regardless of whether the host has aGvHD or not. Only one mouse per group was analysed for this experiment, for the

reasons previously mentioned. Thus, it is unclear whether this slight increase in cell number in PBMC mice is reproducible. Nevertheless, it shows that MAPC cells are not being cleared faster in mice with PBMC compared to PBS, and that the reduced number of cells detected in the lungs of PBMC mice is not just due to an overall decrease in MAPC cell persistence in these animals. This data is similar to data collected by Toupet *et al.* (2015) wherein human AT-MSC exhibited similar persistence rates one day after injection to normal mice or mice with collagen induced arthritis, and suggests that the inflammatory environment does not accelerate MSC or MAPC cell death *in vivo*.

It could be suggested that the presence of PBMC would result in faster clearance of MAPC, however this is not the case, and MAPC cells can be cleared even in irradiated immunodeficient mice from which there should be no allogeneic response. Thus, the clearance of MAPC cells in this model is probably due to the hostile conditions encountered *in vivo* regardless of the inflammatory milieu. Leibacher *et al.* (2017) recently published an interesting study examining the survival of human MSC administered IV to normal immunocompetent mice. Within 30 minutes of administration more than half of the MSC administered expressed phagocytic markers, while 2 hours after infusion the majority of MSC lost their nuclei as shown by Hoescht staining. Furthermore, MSC showed a rapid decrease in mitochondrial membrane potential and a high propidium iodide signal within 5 minutes of injection. Thus, it is likely that the clearance of MAPC cells in this model is not due to allo-recognition by host immune cells, but is due to death and subsequent phagocytosis. Since NSG do not have functional macrophages, MAPC cells in PBS mice in this model are probably cleared by granulocytes, monocytes or non-professional phagocytes.

This PhD thesis and others have shown that IV delivered MAPC cells and MSC are ineffective at preventing aGvHD following injection on day 0, however when these therapies are administered at later time points they are effective (Polchert *et al.*, 2008; Tobin *et al.*, 2013). The differences in the efficacy of MSC and MAPC cells depending on the timing of delivery is more than likely due to the level of inflammation *in vivo*. IFN- γ is an important activator of MSC and MAPC cells, and in studies where IFN- γ signalling is blocked, MSC

have failed to be immunomodulatory (Vigo *et al.*, 2016; Mounayar *et al.*, 2015; Meisel *et al.*, 2004; Krampera *et al.*, 2006). The recognition of the host by donor T cells is not instantaneous, thus the levels of pro-inflammatory cytokines *in vivo* at early time points are probably not high enough to activate MSC or MAPC cells. Since MSC and MAPC cells are cleared quickly, and have a short window of opportunity to produce immunomodulatory mediators, it is imperative that MSC and MAPC cells are activated as soon as possible once infused. This may explain why MSC have not been as successful in clinical trials as originally hoped. In animal models of GvHD, timing of disease onset can be predicted, and this can be used to choose the most appropriate time to administer MSC or MAPC cells. This however is not as straight-forward in the clinic, as it is not clear if a patient will develop GvHD until they present with symptoms. Standard practice employs administration of other therapies before MSC or MAPC cells. When symptoms have already developed, it may be too late for MSC or MAPC cells to be effective, as demonstrated by failure of UC-MSC to protect against GvHD (humanised mouse model) when administered after disease onset (Tisato *et al.* 2007).

Pre-stimulation with IFN- γ before administration improves the therapeutic effect of MSC delivered to GvHD animals at early time points (Polchert *et al.*, 2008; Tobin *et al.*, 2013), and IFN- γ stimulation of human BM-MSC improves their ability to ameliorate colitis in both DSS and TNBS murine models (Duijvestein *et al.*, 2011). On the other hand, IFN- γ stimulation neither hinders nor improves the efficacy of MSC delivered on day 7 to the humanised aGvHD model (M. Healy, 2015, PhD thesis), probably because there is sufficient IFN- γ present *in vivo* at this point to stimulate the cells. Notably, IFN- γ levels *in vivo* can be reduced by ISDs, and this may interfere with MSC or MAPC cell activation if the two therapies are used together. Co-therapy of ISDs and MSC in the humanised aGvHD model has been investigated by the English lab, and IFN- γ stimulation improves the effect of MSC administered on day 6 in this case (J. Corbett, 2016, PhD thesis). Thus, it may be advantageous to stimulate MSC or MAPC cells with IFN- γ prior to administration to ensure that they can carry out immunomodulatory effects even when endogenous IFN- γ

concentrations are low. Thus, I sought to determine if IFN- γ stimulation of MAPC cells would improve their ability to prevent GvHD development.

First the immunosuppressive capacity of MAPC cells following IFN- γ stimulation was examined using the *in vitro* T cell proliferation assay previously described. MAPC cells were cultured with or without 50 ng/ml IFN- γ for 24 hours before PBMC and anti-CD3/CD28 beads were added to the co-culture. This time the assay was only done using a high ratio of PBMC to MAPC cells (1:80), as a difference between the immunosuppressive capacities of MAPC cells and γ MAPC cells would only be detected at a point where MAPC cells did not have a rigorous inhibitory effect on T cell proliferation. As expected, γ MAPC cells were more potent suppressors of T cell proliferation than MAPC cells at this ratio, which strengthened our hypothesis that IFN- γ stimulation would improve the efficacy of MAPC cells administered to the GvHD model on day 0. Next, γ MAPC cells or unstimulated MAPC cells were administered alongside PBMC to irradiated NSG mice. Overall, γ MAPC cells delivered to the aGvHD model on day 0 were superior at alleviating the disease score, prolonging survival, and reducing tissue damage than unstimulated MAPC cells (Fig. 6.1). However, in line with the study where MAPC cell administration on days 0 and 7 were compared, mice that received unstimulated MAPC cells exhibited less signs of GvHD in the liver than those that received γ MAPC cells. Again, this may be explained by an accumulation of cells in the liver in response to γ MAPC cells in the liver, as γ MAPC cells are found in the liver in higher numbers than unstimulated MAPC cells, and may persist longer. Overall, this data aligns well with the previously mentioned studies by Tobin *et al.* (2013) and Polchert *et al.* (2008). Furthermore, this data supports the proposal that stimulation of MSC or MAPC cells with IFN- γ prior to administration may safeguard these therapies from being ineffective when delivered at suboptimal time points.

Next, I sought to examine whether γ MAPC cells would show increased migration towards GvHD target tissues compared to unstimulated MAPC cells. MSC stimulated with IFN- γ show increased expression of adhesion molecules, migratory, and chemotactic mediators such as CXCL9, ICAM1, and CXCL12 (K. English, unpublished data) and both

MSC and MAPC cells stimulated with IFN- γ are less susceptible to NK cell lysis (Jacobs *et al.*, 2014; Noone *et al.*, 2013). Therefore, it was hypothesised that γ MAPC cells would demonstrate increased migration towards GvHD target organs or persist for longer compared to unstimulated MAPC cells. Based on the previously obtained data, 24 hours was chosen as the most appropriate time point to measure differences in biodistribution patterns. At 24 hours post administration, the number of γ MAPC cells detected in the spleen and liver of aGvHD mice was significantly higher than the number of unstimulated MAPC cells detected. The number of cells detected in the lung was unchanged, which suggests that γ MAPC cells were not persisting longer than unstimulated MAPC cells, but were specifically migrating towards target tissues. Of course, whole animal imaging would be required to confirm this point, however the previous data demonstrated that differences between the persistence of MAPC cells in different inflammatory milieu is quite subtle. It was hypothesised that similar subtle differences would be observed between the persistence of MAPC cells and γ MAPC cells, however, time constraints did not allow for imaging in whole mice, thus it is unclear if MAPC cells are undergoing accelerated clearance compared to γ MAPC cells in this model.

This data aligns well with a recent study by Martin Hoogduijn's group where UC-MSC stimulated with a cocktail of TGF- β , IFN- γ and retinoic acid showed improved migration towards the liver in a murine model of liver injury. Interestingly, in this model cells stimulated with IFN- γ alone did not show enhanced migrative capacity, demonstrating that migration of MSC and MAPC cells may be altered depending on cell source and the inflammatory condition being treated. Our data suggests that improved migration of MAPC cells towards target tissue contributes to improved therapeutic efficacy. However, despite their improved migratory capacity, MSC treated with the cytokine cocktail did not alleviate disease severity compared to untreated MSC. This surprising observation may be due to the read outs used, as serum levels of the cytokines MCP-1, IP-10 and the liver damage marker ALT were the only proteins measured and no analysis was performed on liver tissue. Since aGvHD is such a severe model, differences in efficacy are clearly observed in survival time followed by disease score and tissue damage. However, since this liver damage model is not as severe, more

thorough examinations than serum protein levels might need to be done to observe differences in MSC efficacy (de Witte *et al.*, 2017).

The data collected thus far in Chapter 3 demonstrates that MAPC cells can delay the development of aGvHD using the humanised model, however their efficacy is dependent on the timing of administration, as MAPC cells administered on day 0 were unable to alleviate aGvHD symptoms. IFN- γ stimulation of MAPC cells can improve their efficacy when administered on day 0, and so it is reasonable to suggest that pre-treatment of MAPC cells with IFN- γ may improve their efficacy in the clinic. Stimulating or pre-treating cells prior to administration may not be entirely convenient in the clinical environment as cells are generally infused immediately after thawing, and culture of the cells prior to administration would disregard the importance of the ‘off the shelf’ aspect of MAPC cell therapy. The fact that MSC and MAPC cells are infused straight after thawing in the clinic has been subject to criticism, and some investigators believe that this may be the reason for poor efficacy in clinical trials. These concerns are justified based on the findings that cryopreserved MSC show impaired immunomodulatory capacities compared to MSC from culture (Moll *et al.*, 2014; François *et al.*, 2012a). Chinnadurai *et al.* (2016), recently reported that IFN- γ stimulation of MSC prior to cryopreservation improved their immunomodulatory capacity post thaw. Thus, this method of stimulating cells prior to cryopreservation may be a realistic approach to improving the potential of MAPC cell therapy using IFN- γ stimulation, without sacrificing the convenience or reproducibility associated with infusing cells straight after thawing. Unfortunately, MSC stimulated with IFN- γ prior to thaw did not display superior efficacy compared to MSC from culture, thus some of the benefit of IFN- γ stimulation is certainly lost when cells are cryopreserved. Nevertheless, this method might be a practical compromise between improving the efficacy of MAPC cell therapy, while still maintaining the features of a reproducible and conveniently infused ‘off the shelf’ product.

Without the assurance of IFN- γ stimulation before administration, the effects of endogenous IFN- γ or other inflammatory cues are imperative for the activation of MAPC cells. To ensure that MAPC cells are used to their maximum benefit, the effects of inflammatory

cues on MAPC cells need to be fully elucidated. It is important that the inflammatory environment to which the cells are being introduced is understood, as a certain level of inflammatory stimuli may be required to activate MAPC cells. For example, MAPC cells require close contact with IL-1 β producing monocytes *in vitro* in order to produce PGE2 (Reading *et al.*, 2015). The makeup of the inflammatory environment is extremely complex, particularly in the clinic where levels of each and every cytokine will differ from condition to condition, and patient to patient. This is then further complicated by the fact that MAPC cells generate different responses depending on the stimuli encountered. The differential responses of MAPC cells depending on their environment has been highlighted by Reading *et al.* (2013,2015) in alternate T cell proliferation assays. When MAPC cells are co-cultured with CD3/CD28 activated T cells, IDO is required for their suppressive activity. On the other hand, PGE2 is required for the suppressive effects of MAPC cells in a T cell proliferation assay where IL-7 is the stimulus. Thus, the complexity of cellular therapies, and their response to inflammatory cues makes it extremely difficult to pinpoint a time at which MAPC cell delivery is appropriate to ensure optimal activation of MAPC cells *in vivo*. Furthermore, the activity of MAPC cells can vary from donor to donor.

Of course, the ability of MAPC cells to generate different responses depending on the cytokine milieu is beneficial, however it is also perplexing. It is unrealistic to expect each and every patient to receive MAPC therapy at the optimal time point, and to attain the maximum potential from each MAPC cell dose. However, by improving our understanding surrounding the effects of important stimuli on MAPC cells, the number of patients who respond to MAPC cell therapy could certainly increase. Therefore, it is imperative that we advance our knowledge regarding the effects of pro-inflammatory cytokines on MAPC cells at the molecular level. A recent study by Luz-Crawford *et al.* (2016) made progress on this front, by investigating the role of the nuclear transcription factor PPAR δ in the NF- κ B pathway in MSC. Murine MSC lacking PPAR δ demonstrated increased efficacy in a murine model of arthritis, and responded to cytokine stimulation with enhanced expression of immunomodulatory factors such as VCAM1, ICAM1 and NOS due to increased NF- κ B activity. Little else is known

about the role of PPAR δ in MSC, however, in macrophages PPAR δ activation inhibits STAT1 and NF- κ B activation (Kang *et al.*, 2008; Odegaard *et al.*, 2008; Diaz-Gandarilla *et al.*, 2013; Adhikary *et al.*, 2015). Since STAT1 and NF- κ B activation are required for the therapeutic efficacy of MSC (Vigo *et al.*, 2016; Dorronsoro *et al.*, 2014), I sought to further understand the role of PPAR δ activation or inhibition on the immunomodulatory capacity of MAPC cells in the aGvHD model.

First the effects of PPAR δ activation or inhibition on the efficacy of MAPC cells administered to the aGvHD model on day 7 was explored. Activation of PPAR δ using a selective PPAR δ agonist significantly impaired the ability of MAPC cells administered at this time point to prolong survival and reduce disease score compared to normal MAPC cells (Fig. 6.1). Furthermore, PPAR δ activation of MAPC cells reduced their ability to alleviate tissue damage as shown using H&E staining. Inhibition of PPAR δ in this case had no additive effect on the efficacy of MAPC cells. The hampering effect of PPAR δ agonism on MAPC cells suggests that PPAR δ blocks the activation of MAPC cells by pro-inflammatory cytokines, in line with the study by Luz-Crawford *et al.* While PPAR δ inhibition increased the response of MAPC cells to pro-inflammatory cytokines (Luz-Crawford *et al.* 2016), the inhibition of PPAR δ here was probably redundant, as MAPC cells are already mounting a robust response to the inflammatory milieu. This is comparable to data obtained previously by the English group, where IFN- γ stimulation had no additive effect on the potency of MSC administered to the aGvHD model on day 7 (M. Healy, 2015, PhD thesis).

Since PPAR δ ^{-/-} MSC demonstrated increased expression of ICAM1 and VCAM1 when stimulated with IFN- γ and TNF- α (Luz-Crawford *et al.*, 2016b), and PPAR δ activation hindered the immunosuppressive capacity of MAPC cells in the aGvHD model, it was hypothesised that PPAR(+) MAPC cells would show impaired biodistribution compared to normal MAPC cells. The number of PPAR δ agonist activated MAPC cells detected in the lungs 24 hours following administration was slightly higher than the number of normal MAPC cells detected, however the number of PPAR(+) MAPC cells detected in the liver and spleen was significantly lower than normal MAPC cells. This data suggests that PPAR δ agonism

hinders the ability of MAPC cells to escape entrapment in the lung, and migrate to GvHD target organs, and this shortfall may contribute to the impaired efficacy of PPAR(+) MAPC cells *in vivo*. As mentioned above PPAR $\delta^{-/-}$ MSC expressed higher levels of VCAM1 and ICAM1 in response to cytokine stimulation compared to wildtype MSC (Luz-Crawford *et al.*, 2016b), while Adhikary *et al.* (2015) found that PPAR δ activation of human macrophages lead to reduced mRNA expression of a number of chemokines including CXCL9, CXCL10 and CXCL11. Thus, it is possible that PPAR δ activation of MAPC cells may impair their ability to express these adhesive and chemotactic molecules, reducing their ability to egress from the lung.

Next the effects of PPAR δ agonism or PPAR δ inhibition on MAPC cells delivered to the aGvHD model on day 0 was examined. Since PPAR δ inhibits STAT1 activity in macrophages (Adhikary *et al.*, 2015), and MSC require STAT1 to respond to IFN- γ (Vigo *et al.*, 2016), it was hypothesised that PPAR δ agonism would diminish the beneficial effect of IFN- γ stimulation on MAPC cells. Furthermore, it was hypothesised that PPAR(-) MAPC cells would demonstrate superior efficacy in this set up compared to normal MAPC cells, as PPAR δ inhibition may reduce the level of pro-inflammatory stimuli required by MAPC cells to generate an immunomodulatory response. MAPC cells were treated with a PPAR δ agonist prior to IFN- γ stimulation based on the observations made in earlier studies where PPAR δ agonism prior to delivery to the GvHD model impaired MAPC cell efficacy. In those experiments MAPC cells were treated with the agonist or antagonist before being exposed to inflammatory stimuli *in vivo*. Alternative sequences of stimulation such as treatment with the PPAR δ alongside or after IFN- γ stimulation were not explored herein due to time and animal constraints, however it would be interesting to investigate this in future studies.

PPAR(+) MAPC cells increased the survival of aGvHD mice from a median time of 17.5 to 25.5 days. This increase was not significant, nevertheless it is an interesting observation which may spur further study. When administered on day 7, PPAR(+) MAPC cells are presumably exposed to high levels of pro-inflammatory cytokines immediately, however when administered on day 0 this is not the case. By the time PPAR(+) MAPC cells

administered on day 0 are exposed to stimulatory levels of cytokine it is possible that PPAR δ activation has returned to basal or below basal levels. Thus, it would be interesting to measure PPAR δ activity in MAPC cells at varying time points following agonism, as this may explain the data observed. As the difference in efficacy between PPAR(+) MAPC cells and untreated MAPC cells is not significant it is difficult to know if this disparity is robust. The PPAR(+) MAPC cells in this instance is only representative of 6 animals, as later experiments were refined to reduce animal numbers, and the effects of PPAR δ agonism on γ MAPC cells was the main focus of future experiments. Furthermore, the PBMC donors used for these experiments did not induce aGvHD as potently as usual, with mice in the PBMC only group surviving until day 21. Thus, it is possible that in a more acute model with higher numbers of replicates that PPAR(+) MAPC cells would not have been as protective.

PPAR(-) MAPC cells significantly alleviated disease severity comparable to that of γ MAPC cells as expected. It is likely that PPAR δ antagonism and IFN- γ stimulation may cumulatively improve MAPC cell efficacy, however this group was excluded as PPAR(-) MAPC cells did not show increased efficacy compared to MAPC cells when administered on day 7. Since MAPC cells administered on day 7, and γ MAPC cells administered on day 0 are already effective in this model, it is difficult to determine if PPAR δ antagonism is improving their potency. To examine this robustly the experiments should be extended past the 28 day end-point. This type of modification to animal experiments requires approval from governing bodies, which unfortunately would not have been obtained within the time available for this project.

In order to investigate the effects of PPAR δ agonism on γ MAPC cells, MAPC cells were treated with the PPAR δ agonist for 24 hours before stimulation with IFN- γ . The efficacy of γ MAPC cells was y impaired by PPAR δ activation, as shown by disease score and survival data (Fig. 6.1). Based on this data, and the fact that PPAR δ activation impaired the migration of MAPC cells administered on day 7, it was hypothesised that PPAR δ activation would inhibit the migration of γ MAPC cells towards GvHD target organs. In this case, PPAR δ activation caused a significant reduction in the number of γ MAPC cells detected in each of the

lung, liver, and spleen. This may suggest that in this instance PPAR δ activation increases the clearance of γ MAPC cells *in vivo*. This wasn't examined for the reasons outlined previously, but it would be interesting to elucidate the differences observed depending on the time point of cell delivery. The day 7 data suggests that PPAR(+) MAPC cells do not die earlier than untreated MAPC cells, and PPAR δ is anti-apoptotic in murine keratinocytes and human T cells (Tan *et al.*, 2001; al Yacoub *et al.*, 2008). Thus, it is unlikely that the increased clearance of PPAR(+) γ MAPC cells is due to PPAR δ mediated apoptosis. The differences in the clearance rates of PPAR(+) MAPC cells delivered on day 7 compared to PPAR(+) γ MAPC cells delivered on day 0 may be due to the the predominant cell populations *in vivo* at the time of administration. For example, early in the aGvHD model NK cells may be active and may target PPAR(+) γ MAPC cells more potently than γ MAPC cells. HLA ABC expression by PPAR(+) γ MAPC and γ MAPC cells was not compared, however it is unlikely that this was changed as other IFN- γ target genes were unaffected by PPAR δ agonism. γ MAPC cells may avoid clearance by NK cells by producing anti-inflammatory mediators (Jacobs *et al.*, 2014), thus it is possible that PPAR(+) MAPC cells failed to suppress NK cell activity in a similar manner, and this would be an interesting point for further study. By day 7 T cells are activated within the aGvHD model, and their presence combined with an increase in pro-inflammatory signals may negate the differential effects of NK cells on the two cell types. Nevertheless, there is a clear correlation between the efficacy and biodistribution of PPAR δ activated MAPC cells and γ MAPC cells in both experiments. It would also be interesting to examine the biodistribution of PPAR(-) MAPC cells as these cells showed increased efficacy compared to normal MAPC cells when administered to the model on day 0. Again, this wasn't examined due to the budget and time constraints.

PPAR $\delta^{-/-}$ murine MSC show increased expression of VCAM1, ICAM1 and NOS in response to stimulation with IFN- γ and TNF- α stimulation compared to wildtype MSC (Luz-Crawford *et al.*, 2016b). Since PPAR δ activation hindered the immunosuppressive capacity of γ MAPC cells, it was hypothesised that PPAR δ agonism would inhibit the stimulatory effects of IFN- γ on MAPC cells. The first step in elucidating the effects of PPAR δ on IFN- γ

activation of MAPC cells was to look at STAT1 phosphorylation. STAT1 is the main mediator of IFN- γ signalling in most cell types, and has been shown to be crucial for the anti-inflammatory response of MSC to IFN- γ stimulation (Vigo *et al.*, 2016). Here, it was observed that PPAR(+) γ MAPC cells expressed slightly lower protein levels of STAT1 and pSTAT1 compared to γ MAPC cells. Similar data has also been reported for human macrophages (Adhikary *et al.*, 2015). Once phosphorylated, STAT1 translocates to the nucleus, forms homodimers or heterodimers with STAT-3, and then binds to the GAS promoter element, leading to the induction of IFN- γ induced proteins (Platanias, 2005). Thus, I sought to determine if the observed STAT1 inhibition was having a negative effect on the induction of the IFN- γ induced proteins ICAM1, VCAM1, IDO or COX-2. Despite the slightly inhibitory effects of PPAR δ activation on STAT1 expression, neither PPAR δ agonism or PPAR δ antagonism affected ICAM1, VCAM1, or IDO expression in response to IFN- γ . COX-2 expression in response to IFN- γ stimulation however was blocked following PPAR δ agonism, and amplified following PPAR δ antagonism.

Since PPAR δ agonism slightly reduced STAT1 phosphorylation, it was hypothesised that this might lead to reduced protein levels of STAT1 target genes, however this was not the case. The alteration of COX-2 expression here probably STAT1 independent, as COX-2 is generally considered to be an NF- κ B target gene, and NF- κ B can be activated by IFN- γ independent of STAT1 (Gough *et al.*, 2008). This data may also be explained by the fact that STAT3 is also phosphorylated following IFN- γ stimulation in MSC (Vigo *et al.*, 2016), and COX-2 is a STAT3 target gene in some cell types (Gong *et al.*, 2014; Xiong *et al.*, 2014; Lo *et al.*, 2010). Since PPAR δ is known to interfere with NF- κ B activity (Daynes & Jones, 2002) and PPAR δ agonism suppresses STAT3 target gene expression in human macrophages (Adhikary *et al.*, 2015) the effects seen in MAPC cells here may be due to impaired NF- κ B or STAT3 rather than STAT1 signalling following IFN- γ stimulation (Fig. 6.2). The slight reduction in STAT1 activity following PPAR δ agonism may not be sufficient to affect target protein induction.

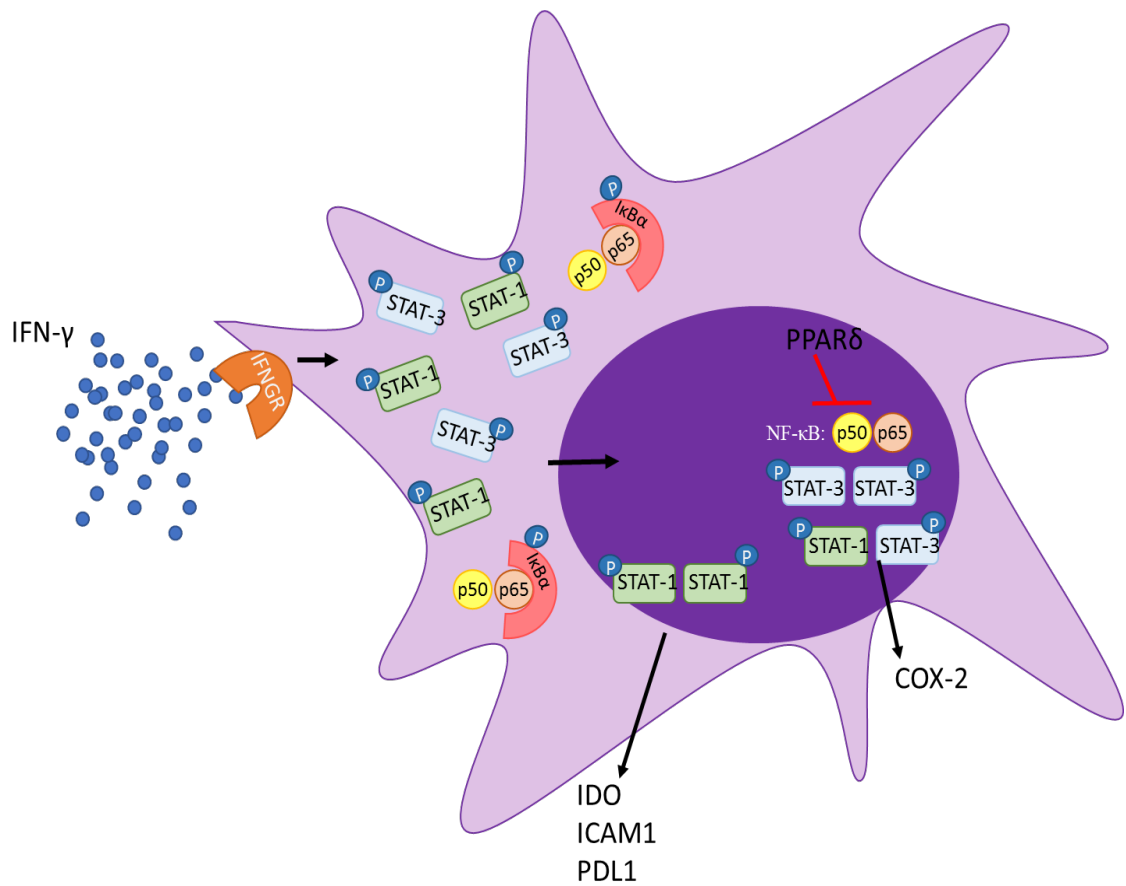


Figure 6.2 Proposed model of the effects of PPAR δ on IFN- γ signalling in MAPC cells. IFN- γ stimulation leads to phosphorylation of STAT1 and STAT-3 and activation of NF- κ B. STAT1 target genes (IDO, ICAM1, PDL1) are unaffected by PPAR δ activation in MAPC cells. COX-2 expression is inhibited by PPAR δ , which is known to suppress NF- κ B and STAT-3 signalling. PPAR δ : Peroxisome proliferator activated receptor δ IFN- γ : interferon- γ , IFNGR: IFN- γ receptor, STAT: signal transducer and activator of transcription, NF- κ B: Nuclear factor- κ B, IDO: indoleamine-pyrrole 2,3-dioxygenase, ICAM1: intercellular adhesion molecule 1, PDL1: programmed death ligand 1, COX-2: cyclooxygenase 2

COX-2 is the first step in the pathway which converts endogenous arachidonic acid to PGE2 (Zhang *et al.*, 2015). The COX-2 data suggests that the effects of PPAR δ agonism on the potency of MAPC cells in our model may be due to impaired production of PGE2 in response to inflammation, while the increase in potency of PPAR(-) MAPC cells administered on day 0 of the model may be due to enhanced PGE2 production *in vivo*. Unfortunately, PGE2 production was not measured in this study due to financial constraints, however it would be an important step going forward. Moreover, to prove that COX-2 induction is the reason for enhanced potency of PPAR(-) MAPC cells *in vivo*, future studies where COX-2 expression in PPAR- MAPC is inhibited could be carried out. Overall, this data shows that PPAR δ activation hinders the immunosuppressive capacity of MAPC cells, while PPAR δ inhibition has the opposite effect. This aligns with the study by Luz Crawford *et al.* (2016b) who found that PPAR $\delta^{-/-}$ murine MSC showed increased therapeutic efficacy in an experimental arthritis model. Interestingly, Luz Crawford *et al.* also showed that human MSC derived from different sites expressed differential levels of PPAR δ mRNA, and expression levels inversely correlated with their immunosuppressive capacity in an *in vitro* T cell proliferation assay. For example, menstrual blood derived MSC expressed higher levels of PPAR δ mRNA than BM-MSC and were not as inhibitory *in vitro*. Thus, it is possible PPAR δ expression could be used as a marker to predict the potency of MSC or MAPC cells derived from different tissues or different donors, however this would require further investigation.

Another important consideration to make would be the presence of PPAR δ ligands in cell culture reagents or *in vivo*. For example, linoleic acid is a potent PPAR δ agonist in macrophages, and this is present in the growth media used to expand MAPC cells (Schumann *et al.*, 2015). This may explain why MAPC cells express higher mRNA levels of the PPAR δ target gene ANGPTL4 than MSC, which are not cultured in the presence of linoleic acid (Roobrouck *et al.*, 2011). It would be interesting to compare MAPC cells cultured with or without linoleic acid to examine if linoleic acid in this instance is activating PPAR δ , or hindering the potency of MAPC cells.

Similarly, endogenous PPAR δ ligands may affect MAPC cell efficacy. For example, PGD2 is highly expressed in the bronchoalveolar fluid during asthmatic episodes, and PGI2 is expressed by endothelial cells during acute inflammation (Ricciotti & Fitzgerald, 2011). Furthermore, dietary administration of linoleic acid enhances PPAR δ activity in the GI tract (Hollingshead *et al.*, 2007). Thus, these lipids may activate PPAR δ in MAPC *in vivo*. Furthermore, TNF- α and IFN- γ increase PPAR δ expression in murine keratinocytes (Tan *et al.*, 2001), while TNF- α and IFN- α (but not IFN- γ) have a similar effect on human T cells (Yacoub *et al.*, 2008). Thus, these agents may modulate PPAR δ activity in MAPC cells *in vivo*, and augment their therapeutic potential. This may also explain the site specific effects of MAPC cells administered at different time points, for example there may be more PPAR δ ligands present in the liver than the gut, which might sequester IFN- γ signalling in already activated cells (day 7 MAPC cells, and γ MAPC cells). The activity levels of PPAR δ in MSC or MAPC cells following pro-inflammatory cytokine or ligand stimulation is unclear, however it would be an important area of future study and might explain donor to donor variation with regards to cytokine responsiveness.

Chapter 4 focused on the effects of MAPC cells on IL-7 driven T cell stimulation. T cell depletive therapies are commonly used in the clinic to prevent or delay allograft rejection, however one of the consequences of this type of therapy is the development of a pro-inflammatory T cell pool due to HP (Zwang & Turka, 2014). HP is driven by the gamma chain cytokine IL-7 which has limited availability in the 'full' T cell pool. When T cells are depleted however, the cells which escape depletion are exposed to much higher levels of IL-7 than usual, and this causes accelerated T cell proliferation, and the skew of the T cell pool towards a Th1 population which contributes to graft rejection (Wu *et al.*, 2004). While maintenance immunosuppression is used to inhibit the proliferation of T cells following induction therapy, none of the therapies currently on the market target the IL-7 axis, despite its known role in the homeostatic expansion of T cells during lymphopenia (Mai *et al.*, 2014; Chung, Dudl & Min, 2007). MAPC cells have previously been shown to be therapeutic in experimental models of GvHD and SOT (Highfill *et al.*, 2009; Eggenhofer *et al.*, 2013), however

their effect on HP has never been examined *in vivo*. We have previously shown that human MAPC cells suppress IL-7 driven proliferation and activation of T cells *in vitro* (Reading *et al.*, 2015), and so this study sought to build on that data, by translating the findings to an *in vivo*, translationally relevant setting.

An *in vivo* model of IL-7 driven HP was developed based on a system previously described by Boyman *et al.* (2008). This model requires the incubation of recombinant IL-7 to an anti-IL-7 antibody for 30 minutes prior to administration, and this IL-7 complex is then administered IP three times on alternate days. The anti-IL-7 antibody improves the stability of IL-7 *in vivo*, and reduces the amount of IL-7 required to generate a HP response. The first read out of this experiment was to ensure that T cells were proliferating in response to IL-7 treatment, and so two methods of measuring T cell proliferation were compared. Cells which are undergoing proliferation can be identified using an intracellular antibody for Ki67 which is a nuclear antigen expressed by cells during each active stage of the cell cycle, but not when cells are in their resting state. This is a convenient method of measuring the proliferation of endogenous cells, however it only provides a snapshot of the proliferative state of cells, and does not indicate the division history of cells. In comparison, proliferation dyes are taken up by cells *ex vivo* and the amount of dye in each cell is diluted with every division, allowing the number of times each cell has proliferated to be counted. The drawback to this method is that cells must be labelled *ex vivo* and adoptively transferred, thus CD4⁺ T cells from a congenic strain to the host were labelled with the proliferation dye and adoptively transferred. The adoptive transfer using a proliferation dye was unsuccessful as the number of adoptively transferred cells acquired after harvest was too low to produce meaningful data. Thus, the Ki67 method of measuring endogenous T cell proliferation was used in further experiments, which unfortunately meant that only the cells which were proliferating at the time of harvest could be measured.

As mentioned previously, IL-7 stimulates the proliferation and activation of T cells, and this contributes to graft rejection. Since MAPC cells can modulate T cell function *in vitro*, and MAPC cells IV alleviate aGvHD, it was hypothesised that MAPC cells IV would suppress

T cell HP following IL-7 administration. Using the IL-7 model, it was demonstrated that MAPC cells IV suppressed IL-7 driven T cell proliferation in the spleen, but not the lymph nodes. Since Highfill *et al.* (2009) had reported that MAPC cells must be administered locally to sites of allo-priming in order to be therapeutic in a murine model of GvHD, MAPC cells IP were administered with the hypothesis that this route of delivery would put MAPC cells in closer proximity to the lymph nodes. As expected, MAPC cells IP had the capacity to suppress IL-7 stimulation of T cell proliferation in the lymph nodes. Furthermore, MAPC cells IP showed similar efficacy to MAPC cells IV in the spleen. This data was promising as it demonstrated that MAPC cells can suppress IL-7 driven HP, and next I sought to examine the effects of MAPC cells on the skew of the T cell pool following IL-7 treatment. IL-7 can stimulate T cells to produce pro-inflammatory cytokines such as IFN- γ , TNF- α , and IL-17 (Reading *et al.*, 2015), thus production of IFN- γ and TNF- α by T cells was examined following IL-7 and MAPC cell administration. As expected, the production of these cytokines was increased following IL-7 administration in both the spleen and the lymph nodes. Furthermore, both MAPC cells IV and MAPC cells IP suppressed this cytokine production in the spleen, and only MAPC cells IP suppressed this in the lymph nodes.

In the context of allograft rejection, the outcome of the immune reaction depends on the ratio of pro-inflammatory T cells to Treg (Neujahr *et al.*, 2006; Moxham *et al.*, 2008). The effect of IL-7 on Treg is unclear, however, *in vitro* studies have shown that IL-7 can abrogate Treg suppressive function, and memory Treg treated with IL-7 can acquire a Th17 phenotype (Younas *et al.*, 2013; Heninger *et al.*, 2012). MSC and MAPC cells are known to expand Treg populations in some circumstances (Cahill *et al.*, 2015; Eggenhofer *et al.*, 2013; M. Healy, 2015, PhD Thesis), and so it was hypothesized that MAPC cells would also promote Treg in this model.

The immunophenotyping study carried out in collaboration with the 3i team did not include intracellular staining, thus FoxP3 was replaced with GITR, while the experiment was then repeated in Maynooth using a CD25 and FoxP3 panel. IL-7 had no effect on the frequency of CD25⁺ GITR⁺ cells, but MAPC cells IP expanded this population. Using the more tradi-

tional panel however, IL-7 was shown to significantly increase the frequency of CD4⁺ cells expressing CD25 and FoxP3, and both MAPC cells IV and IP slightly reduced this. The Treg data found here shows the importance of choosing appropriate markers for each cell type, and cautions against over-interpretation of data. In mice co-expression of CD25 and FoxP3 is the most commonly used method to identify CD4⁺ Treg (Morikawa & Sakaguchi, 2014). This is an accurate method of identification for thymic derived Treg, however peripheral Treg can include heterogeneous subsets of induced Treg which may not always express FoxP3. GITR is a TNF receptor related protein with co-stimulatory functions, and is expressed by suppressive T cells such as Tr1 and Th3 cells (Ronchetti *et al.*, 2015). This data suggests that MAPC cells may expand peripheral FoxP3⁻ Treg, but hinder the expansion of thymus derived FoxP3⁺ Treg.

The percentage of terminally differentiated CD25⁺ GITR⁺ Treg (identified by expression of KLRG1) was enhanced following administration of MAPC cells IP, suggesting that MAPC cells IP might drive the proliferation of this population. Previous *in vitro* work by the English lab however, suggests that MSC do not expand Treg populations, but promote their survival (M. Healy, 2015, PhD thesis), thus it may also be possible that MAPC cells IP are protecting CD4⁺ CD25⁺ GITR⁺ cells from undergoing apoptosis. It is difficult to explain why CD4⁺ CD25⁺ FoxP3⁺ T cells are not promoted by MAPC cells, considering that CD4⁺ CD25⁺ GITR⁺ cells are, and CD4⁺ CD25⁺ FoxP3⁺ T cells are expanded by MSC and MAPC cells in other models. The lymph nodes were not examined for this panel due to the limited number of cells isolated, and so it is possible that CD4⁺ CD25⁺ FoxP3⁺ populations were expanded there. Another explanation may be that the increase in activated T cells in the spleen following IL-7 administration may have caused the mobilization of FoxP3⁺ Treg towards the spleen, or the induction of FoxP3 expression in FoxP3⁻ T cells. This promotion of Treg would not have been necessary following the administration of MAPC cells, as their suppression of inflammatory T cells would remove the need for the presence of increased numbers of Treg in the spleen. Due to the complexities associated with identifying Treg populations, functional assays are required to truly understand the suppressive activity of different regulatory cell types. Thus, assays

whereby Treg are isolated and used in suppressor assays following MAPC cell administration would provide further knowledge on the exact effects of MAPC cells on Treg.

Overall this data suggests that MAPC cells can inhibit the skew of the T cell pool towards a pro-inflammatory profile in response to abundant levels of IL-7 (Table 6.1). This data aligns well with that of Reading *et al.* as it shows that MAPC cells do have the capacity to suppress T cell activation in response to IL-7, however similar to the report by Highfill *et al.* their efficacy at different sites depends on their route of administration. It is unclear whether MAPC cells are having direct effects on T cells or whether their effects on the T cell pool are modulated through intermediate cell populations, which may account for the differences observed following IV and IP administration. For example, in a murine model of cardiac allotransplantation MAPC cells induce Treg in a myeloid derived suppressor cell (MDSC) dependent fashion (Eggenhofer *et al.*, 2013), while our group have shown that murine BM-MSCs promote tolerogenic DC *in vitro* which can go on to expand Treg populations (Cahill *et al.*, 2015). Moreover, in murine models of corneal allotransplantation and OVA induced asthma, the therapeutic effects of IV administered MSC are lost when pulmonary monocytes and macrophages are depleted (Ko *et al.*, 2016; Mathias *et al.*, 2013). Thus, in this model MAPC cells may be augmenting the HP of T cells by altering other immune compartments.

The effects of MAPC cells and IL-7 on the wider immune compartment within the spleen were examined using a 12-colour immunophenotyping study. While the effects of IL-7 on the HP of T cells has been widely documented (Monti & Piemonti, 2013), the effects of IL-7 on myeloid cells has not been well studied. Due to the role of APC as providers of self MHC/peptide complexes, I sought to understand the effects of both IL-7 and MAPC cells on the myeloid populations. Since MSC are known to modulate innate immune cells (Le Blanc & Davies, 2015), it was hypothesised that MAPC cells may reduce the number of APC *in vivo*, limiting the abundance of homeostatic stimuli available to T cells in this model. IL-7 increased the size of the overall myeloid pool, and MAPC cells administered both IV and IP reduced this. Within the myeloid compartment, IL-7 increased the number and frequency of eosinophils and both MAPC IP and MAPC cells IV returned these figures to basal levels. IL-7

had no significant effect on monocytes or granulocytes, however MAPC cells IP reduced both the number and frequency of these populations to levels below those found in the PBS group. Interestingly, IL-7 significantly reduced both the number and frequency of macrophages in the spleen, and while MAPC cells had no considerable impact on this, MAPC cells IP did reduce the expression of MHC II by macrophages.

Since the spleen was the only organ examined here it is unclear whether the effects of IL-7 or MAPC cells is due to an overall suppression or expansion of each population, or whether the location or migration of each cell type is being altered. For example, MAPC cells IP reduced the frequency of monocytes and granulocytes in the spleen, however these populations may have migrated to other sites such as the lymph nodes or peritoneal cavity. The effects of IL-7 and MAPC cells on eosinophils is particularly interesting. Little is known about the effects of IL-7 on eosinophils, apart from one study which demonstrates that IL-7 can promote the survival of human eosinophils *in vitro* through the induction of GM-CSF (Kelly *et al.*, 2009). On the other hand, IL-7 stimulates GM-CSF production by T cells (Sheng *et al.*, 2014), and so it is likely that this effect could expand the eosinophil population indirectly through T cells. Since the effects of IL-7 and MAPC cells on eosinophils mimics that of the T cell data previously described, it could be possible that GM-CSF production is enhanced by T cells in response to IL-7 and that this is suppressed by MAPC which would consequently block eosinophil expansion (Fig. 6.3). While the effects of MAPC cells on eosinophils has not previously been reported, this study aligns well with an *in vivo* study which showed that IV administered MSC suppress eosinophilia in a murine model of OVA induced asthma (Kavanagh & Mahon, 2011). Unfortunately, GM-CSF production by either eosinophils or T cells was not measured in this study, however it would be interesting to investigate this in future studies.

The effects of IL-7 on macrophages is not well studied, and it is unclear why IL-7 administration reduced the number and frequency of macrophages in the spleen. On the other hand, the effects of MSC and MAPC cells on macrophages has been an intense area of research, and both cell types are known to skew macrophages towards an anti-inflammatory profile (Carty, Mahon & English, 2017). The markers required to determine whether macrophages adopt the

M1 or M2 phenotype were not included in this study, however, it was shown that MAPC cells IP decrease MHC II expression by splenic macrophages. This aligns with a previous study wherein murine BM-MSC suppressed MHC II expression by LPS stimulated macrophages *in vitro* (Maggini *et al.*, 2010). In this particular study by Maggini *et al.*, MHC II suppression by MSC was accompanied by reduced expression of CD86, TNF- α , IL-6, and IFN- γ and increased production of IL-10. Thus, reduced MHC II expression by macrophages may indicate that the population is skewing towards an M2 profile following MAPC cell administration, however, a full panel of M2 markers would be required to determine if this is the case.

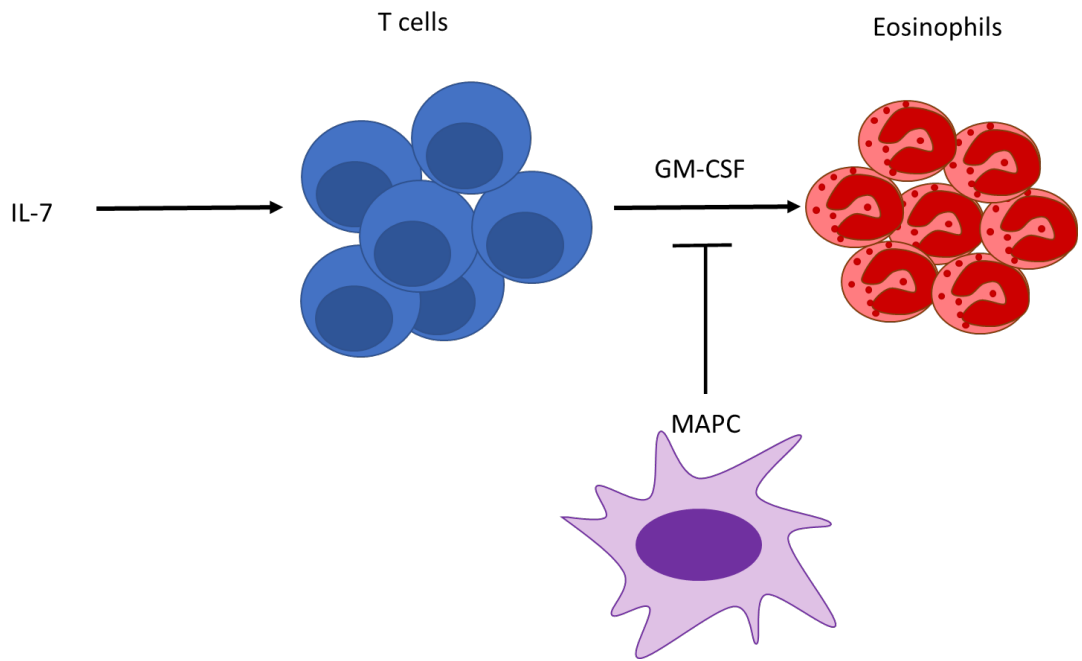


Figure 6.3 Proposed model of the mechanism by which IL-7 and MAPC cells modulate the eosinophil pool. T cells produce GM-CSF upon IL-7 stimulation, which induces eosinophil proliferation. MAPC cells suppress the activation state of T cells following IL-7 administration, thus, limiting the availability of GM-CSF to eosinophils, and preventing their proliferation. IL-7: Interleukin 7, GM-CSF: Granulocyte macrophage colony stimulating factor

DC are the main APC involved in T cell HP, and it is well known that MSC suppress their maturation and antigen presentation capacities (English, Barry & Mahon, 2008; Cahill *et al.*, 2015). Thus, it was hypothesized that MAPC cells may act similarly in this model, and that suppression of T cell HP by MAPC cells might partially be due to the decreased stimulatory capacity of DC. DC are divided into two compartments: conventional DC and plasmacytoid DC (cDC and pDC). In general, cDC are considered to be potent stimulatory APC, while pDC are thought to have poor co-stimulatory capacities, and tend to skew T cells towards regulatory populations (Rogers, Isenberg & Thomson, 2013). IL-7 slightly enhanced the frequency of cDC, while the frequency of pDC was reduced. MAPC cells IP, but not MAPC cells IV returned both of these populations to basal levels, suggesting that MAPC cells IP could modulate the antigen presentation capacity of the DC pool. Within the cDC compartment, DC can be further divided into CD8⁺ and CD8⁻ populations. CD8⁺ cDC are a particularly interesting population, as they are thought to have a role in the maintenance of T cell tolerance to self-antigen, and host CD8⁺ DC are protective in murine models of GvHD (Hey & O'Neill, 2012; Weber *et al.*, 2014; Toubai *et al.*, 2015). IL-7 enhanced the frequency and number of CD11b⁺ CD8⁻ cells and MAPC cells IP returned these to normal levels, while IL-7 decreased the number and frequency of CD8⁺ CD11b⁻ dendritic cells and MAPC cells IP again returned these to normal levels. Overall, this body of DC data suggests that MAPC cells may suppress antigen presentation by DC, and promote tolerogenic DC with inhibitory functions. This aligns well with previous work by our group which demonstrates that murine BM-MSc can induce tolerogenic DC that have the capacity to suppress T cell proliferation and expand Treg *in vitro*. Furthermore, we have shown that the effects of MSC in this context are dependent on contact signaling via the Notch signaling pathway, and knockdown of Jagged 1 reduced the efficacy of MSC in a murine model OVA induced airway inflammation. (Cahill *et al.*, 2015). Thus, the differential effects of MAPC cells on DC depending on their administration may be due to juxtacrine effects, as MAPC cells IV accumulating in the lung would not be in contact with the same populations as MAPC cells IP.

Overall, the data obtained using the myeloid panel suggests that suppression of T cell HP by MAPC cells may be due in part to their modulation of APC (Table 6.2). It was not possible to examine the lymph nodes for this study as an insufficient number of cells were harvested. Many APC move between the spleen and lymph nodes depending on their activation state, thus it would have been beneficial to compare the effects of MAPC cells on the myeloid cells at both sites. Nonetheless, the data generated does provide valuable insight, demonstrating that MAPC cells may have the capacity to skew innate cells towards tolerogenic populations. It is impossible to conclude that this is true based on this body of data, however, this work does provide a starting point for others to further investigate the effects of MAPC cells on these populations. In particular, further studies looking at the effects of MAPC cells on eosinophils, macrophages and DC would be interesting, and this data could be developed by analyzing the cytokine profile of these populations in this model. Furthermore, these cell types could be harvested and introduced into functional assays *ex vivo* to determine whether MAPC cell administration affects the ability of these populations to activate T cells.

Next the effects of IL-7 and MAPC cells on B cells was determined. Pre B cells require IL-7 for their development, and abundant IL-7 levels is associated with the expansion of pre-B cells and immature or transitional B cells (Malaspina *et al.*, 2006; Komschlies *et al.*, 1994). Upon maturation however, IL-7R expression is lost, and reconstitution of B cells in lymphopenic hosts is independent of IL-7 (Mackall, Fry & Gress, 2011; Tchao & Turka, 2012). Mature B cell populations may however be modified by IL-7 in this model indirectly, by signals derived from other cell populations. Most studies regarding the effects of IL-7 on B cells focus on B cell development or homeostasis under normal conditions, rather than the effects of IL-7 on B cells in the context of transplantation. Thus, it was unclear what effects IL-7 administration would have on B cells in this model. Nevertheless, B cells can contribute to HP by either supporting or inhibiting T cell activation, thus the effects of both IL-7 and MAPC cells on B cell populations is of interest.

The effects of MSC on B cells is a topic of controversy, with some groups including our own reporting that MSC promote B cell survival and proliferation (Healy *et al.*, 2015), while

others have found that MSC suppress B cell proliferation (Corcione *et al.*, 2006; Franquesa *et al.*, 2015; Rosado *et al.*, 2015). In a clinical study, cGvHD patients who had a complete or partial response to MSC therapy maintained consistent B cell numbers in the peripheral blood, while those that had no response to MSC therapy experienced a decrease in B cell numbers. In those that responded to MSC therapy, there was an increase in memory B cells and pre GC B cells (Peng *et al.*, 2014a). With regards to regulatory populations, MSC have been shown to promote IL-10 producing CD38⁺ CD24⁺ B cells *in vitro* (Franquesa *et al.*, 2015) and peripheral CD5⁺ IL-10⁺ B cells in human cGvHD patients (Peng *et al.*, 2014b). Similarly, IP delivered UC-MSCs increase the frequency of CD5⁺ B Cells in the spleen, lymph nodes and peritoneal cavity in an experimental model of colitis (Chao *et al.*, 2016). Therefore, it is possible that MSC and MAPC cells may promote B cells *in vivo*, and the effects of MAPC cells on regulatory B cell subsets is particularly interesting.

As expected based on the fact that mature B cells do not express IL-7R, IL-7 had no effect on the total number of B cells within the spleen. On the other hand, MAPC cells delivered both IV and IP did increase the size of the B cell pool, in line with the above-mentioned publications by Healy *et al.* (2015) and Peng *et al.* (2014a). Within the B cell pool both IL-7 and MAPC cells altered the frequency of some populations. IL-7 increased the frequency of B1a, transitional-1 and transitional-2 B cells, which is unsurprising given that these B cell subsets are increased in lymphopenic conditions (Malaspina *et al.*, 2006; Drexler *et al.*, 1987). In contrast, administration of IL-7 reduced the percentage of marginal zone B cells within the spleen by half. This result is misleading however, as the total number of marginal zone B cells was not dramatically changed (data not shown), and this reduction is reflected by the increase in the transitional subsets. Thus, it is important when interpreting this type of data, that both the number and frequency of subsets are considered. The effects of MAPC cells on B cell subsets was largely dependent on their route of administration, as MAPC cells IV increased GC, B1a, and plasma cells, while MAPC cells IP promoted transitional-1 B cells (Table 6.3). Interestingly each of these subsets have been associated with positive outcomes in transplantation. As previously mentioned, cGvHD patients who respond to MSC therapy show increased levels of

Table 6.1 Effects of MAPC cells on T cells in the IL-7 model

	IL-7	MAPC IV	MAPC IP
Spleen			
Ki67⁺ T cells	↑	↓	↓
IFN-γ⁺ Treg	↑	↓	↓
GITR⁺ Treg	-	-	↑
FoxP3⁺ Treg	↑	↓	↓
Lymph Nodes			
Ki67⁺ T cells	↑	-	↓
IFN-γ⁺ Treg	↑	-	↓

Comparison of the IL-7 group is to the PBS group, and MAPC groups to IL-7 group

Table 6.2 Effects of MAPC cells on splenic myeloid cells in the IL-7 model

	IL-7	MAPC IV	MAPC IP
Monocytes	-	-	↓
Eosinophils	↑	↓	↓
Granulocytes	-	-	↓
Macrophages	↓	-	-
MHCII⁺ Macrophages	-	-	↓
cDC	↑	-	↓
pDC	↓	-	↑
CD8⁺ cDC	↑	-	↓
CD8⁻ cDC	↓	-	↑

Comparison of the IL-7 group is to the PBS group, and MAPC groups to IL-7 group

Table 6.3 Effects of MAPC cells on splenic B cells in the IL-7 model

	IL-7	MAPC IV	MAPC IP
B1a cells	↑	↑	-
Plasma cells	-	↑	-
B2 cells	-	↑	↑
Follicular B cells	↓	-	↑
GC B cells	-	↑	-
MZ B cells	-	-	-
Transitional 1 B cells	↑	-	↑
Transitional 2 B cells	↑	-	-

Comparison of the IL-7 group is to the PBS group, and MAPC groups to IL-7 group

peripheral pre GC B cells and B1a cells (Peng *et al.*, 2014a, 2014b). Similarly, both transitional B cells and B1a cells are associated with improved outcomes in transplantation (Shabir *et al.*, 2015; Durand & Chiffolleau, 2015; Rosser & Mauri, 2015).

While the literature regarding the effects of MSC on B cells is confusing, this data presented herein best aligns with that of Healy *et al.* and Peng *et al.* who demonstrate that MSC promote B cell survival. The mechanism by which MAPC cells are having this effect *in vivo* is unknown, however Healy *et al.* demonstrated that MSC derived VEGF promotes B cell survival *in vitro*. MSC required cell contact with B cells to produce VEGF, thus the differential effects of MAPC cells IV and IP may be due to the cells with which they come into contact at their respective sites of distribution. The data generated here also suggests that MAPC cells promote regulatory B cell populations *in vivo*. As previously mentioned, the absence of cytokine measurement in this study made it impossible to analyse IL-10 production by B cells in response to IL-7, thus it isn't clear whether these populations expanded by MAPC cells are truly suppressive. Nevertheless, this study is a starting point and may spur further investigations into the effects of MAPC cells on regulatory B cell populations. Many B cell subsets can adopt regulatory functions, and MSC have been shown to promote IL-10 producing immature B cells *in vitro* (Franquesa *et al.*, 2015) and B1a cells in humans (Peng *et al.*, 2014b). To the best of our knowledge, the effects of MSC or MAPC cells on the regulatory potential of other B cell subsets has not been characterized, thus future studies focusing on the cross-talk between these populations would be beneficial.

Overall, this immunophenotyping study was a valuable guide to suggest possible intermediate cell types that MAPC cells may require interaction with in order to carry out their suppressive functions *in vivo*. Suppression of eosinophils and APC, along with the expansion of Breg may contribute to the suppressive effects of MAPC cells on T cell activation in response to IL-7, however this would certainly require further study. Intracellular staining to measure cytokine production by each cell type following administration of MAPC cells would elucidate the inflammatory profile of each population, while *ex vivo* assays could be used to determine the suppressive or antigen presentation capacities of the cell types of interest. *In vivo* depletion of

particular cell types could also further clarify the modes of action of MAPC cells in this model. Each of these methods are costly and time consuming and unfortunately were not possible to carry out within this project. While the initial T cell data generated in Maynooth indicated that the route of delivery impacts MAPC cell function, this immunophenotyping study further reinforced this idea. The differences in the effects of MAPC cells IP and MAPC cells IV were striking and this lead us to investigate the biodistribution patterns of MAPC cells following these two routes of administration.

It is well known that MAPC cells are found primarily in the lung following IV administration, with a small number of cells eventually migrating to distal organs such as the liver and spleen (Leibacher & Henschler, 2016). The biodistribution of IP delivered MSC or MAPC cells is not as well documented, however it has been shown that MSC administered IP form aggregates with macrophages and B cells in the peritoneal cavity (Bazhanov *et al.*, 2016). It was hypothesised that the superior efficacy of MAPC cells IP in the lymph nodes may be due to their ability to migrate there compared to MAPC cells IV, thus CryoViz™ technology was used to investigate this. The IL-7 model is very short, thus we opted to harvest organs as close to the usual harvest time as possible. It was thought that waiting until 96 hours post MAPC cell administration (the usual harvest time) would be too late to detect MAPC cells, however since MAPC cells could still be detected in the GvHD model at 48 hours, it was decided that some MAPC cells would probably still be detected at 72 hours post administration. Imaging experiments revealed that while MAPC cells IP did not gain access to the spleen or lymph nodes, they were retained in the omental tissue surrounding these tissues. On the contrary, some MAPC cells IV did gain access to the spleen, however access to the spleen did not correlate to the improved therapeutic efficacy of MAPC cells. This supports the hypothesis that MAPC cells mediate their effects on HP through the production of soluble factors (Reading *et al.*, 2015), as MAPC cells IP cannot come into contact with splenic T cells. Whole animal imaging revealed that 72 hours following administration very few MAPC cells IV could be detected, however more than 20-fold the number of MAPC cells were detected following IP injection. Thus, the reason for the differing effects of MAPC cells IV and MAPC cells IP could

be due not just to alternative sites of distribution, but also due to prolonged persistence of MAPC cells IP.

These differential biodistribution patterns explains the differences in the observed data for various reasons. Firstly, it is hypothesised that the effects of MAPC cells on T cell HP is due to PGE2. PGE2 has a short half live *in vivo*, and it is thought that PGE2 producing MAPC cells may need to be in close proximity to the cells on which they have an effect (Highfill *et al.*, 2009). MAPC cells IP are in closer proximity to the harvested lymph nodes than MAPC cells IV, thus PGE2 produced by MAPC cells IP would be more likely to affect T cells within the lymph nodes compared to PGE2 produced by MAPC cells IV. Furthermore, the whole mouse data demonstrated that MAPC cells IP persist in the IL-7 model for longer than MAPC cells IV. Thus, MAPC cells IP could be producing PGE2 continuously for a longer period of time than MAPC cells IV. Secondly, the superior efficacy of MAPC cells IP compared to MAPC cells IV might be due to the activation state of MAPC cells at different sites. *In vitro*, MAPC cells require contact with monocytes to produce PGE2 (Reading *et al.*, 2015). MAPC cells IP may be more likely to be activated by monocytes or other cell types in the omentum than MAPC cells IV would be in the lung.

Another explanation for the differences in the functionality of MAPC cells IP and MAPC cells IV would be the cells with which they come into contact at their respective sites of distribution. MAPC cells IP were restricted to the omental tissue, which is a rich source of immune cells such as macrophages, B cells and natural killer T (NKT) cells. Interestingly, the omentum contains high numbers of regulatory cells including B1 cells, NKT cells and Treg (Meza-Perez & Randall, 2017). MSC form aggregates with peritoneal immune cells following IP administration (Bazhanov *et al.*, 2016; Sala *et al.*, 2015), thus, it is likely that MAPC cells IP may interact with, and promote, these regulatory populations in the omentum (Fig. 6.4). Some T cells and B2 cells can also circulate from the spleen and lymph nodes to the omentum and vice-versa (Meza-Perez & Randall, 2017), thus some of the cells in the lymph nodes and spleen at the time of harvest may have been in contact with MAPC cells in the omentum at one point. Apart from the studies by Bazhanov *et al.* and Sala *et al.* very little has been published

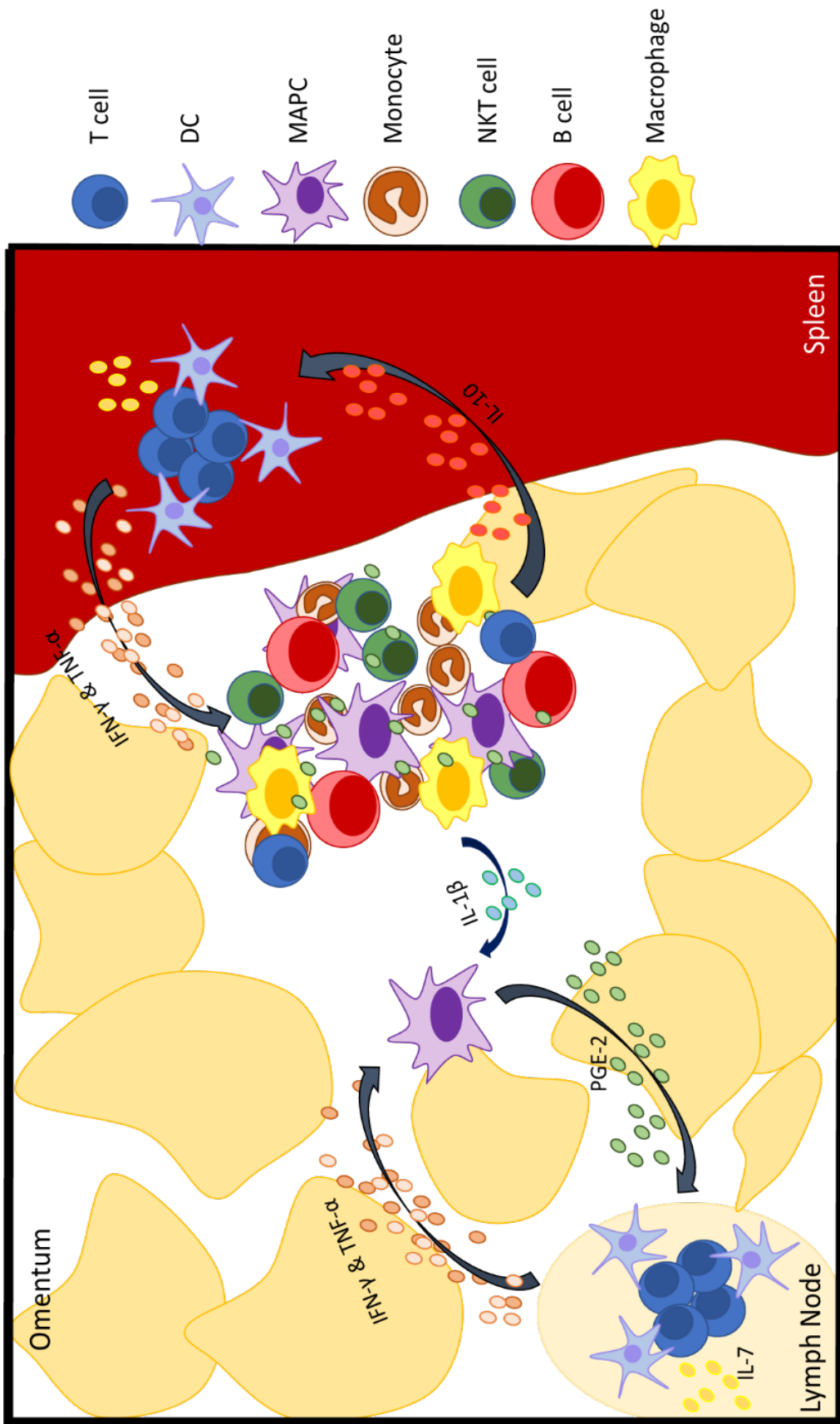


Figure 6.4 Proposed model of MAPC cell activity in the omentum. T cells in the spleen and lymph nodes produce IFN- γ and TNF- α during HP. These cytokines may activate MAPC cells in the omentum directly, resulting in the production of PGE2. MAPC cells in the omentum may also be activated by innate cells (such as IL-1 β producing monocytes) to produce PGE2 which could then disseminate to the SLO's and suppress T cell activation. MAPC cells may also form aggregates with cell populations in the omentum and promote regulatory cells through the production of PGE2. These cells may then regulate the T cell response during HP by production of IL-10 or other mediators. DC: Dendritic cell, NKT cell: Natural killer T cell, IL: Interleukin, IFN- γ : Interferon- γ , TNF- α : Tumour necrosis factor- α , PGE2: Prostaglandin E2.

regarding the effects of MSC or MAPC cells on peritoneal or omental immune cells. While these studies demonstrate interactions between MSC and peritoneal or omental macrophages, B cells and T cells, the effector function of these cells is unclear. Thus, it is difficult to predict what exactly may be happening between MAPC cells and omental populations in the HP models.

On the other hand, interactions between tumours and omental tissue are quite well studied. Many immunomodulatory mechanisms are shared by MAPC cells and tumour cells, thus MAPC cells may operate in a similar manner. Implantation of tumour cells into the omentum causes an increase in the production of VEGF by mesothelial cells, and this drives the recruitment of MDSC (Meza-Perez & Randall, 2017). If MAPC cells were to have similar effects, VEGF might affect B cell survival in a similar manner to MSC in the study by Healy *et al.* (2015). Moreover, in a murine model of cardiac allo-transplantation MAPC require MDSC for the induction of Treg (Eggenhofer *et al.*, 2013). Thus, increased VEGF levels *in vivo* following the administration of MAPC cells IP might explain the differences observed depending on the route of delivery, and would be interesting to investigate in further detail.

It is probable that the differences observed following the different routes of administration of MAPC cells is due to multiple factors including those suggested above. The cross-talk between MAPC cells and omental leukocytes has not previously been studied, and examination of this would likely explain the differences between MAPC cells IP and IV. Omental tissue was harvested in an attempt to elucidate the effects of IL-7 and MAPC cells on omental Treg and NKT cells. Unfortunately, despite multiple attempts, flow cytometric analysis of the omentum was unsuccessful. The omentum is mainly comprised of adipocytes which need to be digested prior to antibody staining, thus the protocol to process the tissue for flow cytometry is quite laborious. In addition to this, approximately 20-30 mice were used for these experiments, and spleens and lymph nodes were harvested at the same time as the omentum. The combination of the digestion step, and the overall time taken from tissue dissections to acquisition on the flow cytometer affected cell viability, and samples were of too poor quality to extract meaningful data. I was advised that 10 omentums at most should be

harvested in the one day to streamline the process and improve the data obtained (A. Hogan, personal communication), however unfortunately this was not conducive to these experiments.

The IL-7 model was a valuable first step to examine the effects of MAPC cells on IL-7 driven stimulation of T cells. However, in the clinic the increase in IL-7 availability is due to the use of lymphodepleting drugs. ATG is a T cell depleting agent commonly used as a conditioning regimen prior to HSCT or as an induction agent prior to SOT (Hardinger, Brennan & Klein, 2013). T cells which escape depletion by ATG are exposed to higher levels of homeostatic stimuli than normal, which allows for the reconstitution of the T cell pool. Unfortunately, under these lymphopenic conditions T cells adopt a pro-inflammatory profile which can contribute to graft rejection and autoimmune disease (Tchao & Turka, 2012). To examine the effects of MAPC cells on HP following lymphodepletion is more translationally relevant than the IL-7 model for a number of reasons. The IL-7 model measures the effect of increased IL-7 availability on a 'full' T cell pool, which would not occur under physiological conditions. Next, the IL-7 model does not take into account that other factors play a role in HP. Thus, despite IL-7 levels being increased, the number of APC and other homeostatic cytokines such as IL-15 presumably remain at normal levels. Thirdly, the IL-7 model looked at the effects of HP on a normal, diverse T cell pool. Induction therapies have varying depletive effects on different subsets. Thus, the T cell pool that undergoes HP in the clinic would not have the composition of a normal T cell pool, with some subsets being overrepresented compared to others. Thus, I moved on to look at the effects of MAPC cells on HP following lymphodepletion.

A model of HP following ATG administration was set up, and this was the focus of chapter 5. Similar to IL-7 administration, ATG administration increased the proliferation and IFN- γ production by T cells in the spleen and lymph nodes. In this case however, MAPC cells administered either IP or IV had no effect on T cell proliferation at either site. This was surprising given that MAPC cells could inhibit T cell proliferation in the IL-7 model. MAPC cells IP did however suppress IFN- γ production in both the spleen and the lymph nodes, while MAPC cells IV failed to have this effect. Treg were also examined in this model, this time

using just the traditional panel of CD25 and FoxP3 co-expression. It is well known that ATG expands Treg populations (Feng *et al.*, 2008; Boenisch *et al.*, 2012; Valdez-Ortiz *et al.*, 2015), and this was also demonstrated in our model in the spleen, and more so in the lymph nodes. Similar to the IL-7 model, MAPC cells had no effect on Treg in the spleen, however MAPC cells IP did further enhance the frequency of Treg in the lymph nodes. Thus, the same might be true in the IL-7 model.

It is unclear why MAPC cells are unable to suppress T cell proliferation in this case, however it is probably because the increase in proliferation is not as dramatic as in the IL-7 model. This supports our theory that the IL-7 model is not entirely relevant to HP following lymphodepletion, and probably presents an exaggerated case of HP. The inability of MAPC cells to suppress proliferation is not a cause for concern, as reconstitution of the immune system following lymphodepletion is required. One of the main problems associated with the use of blanket immunosuppressants such as CsA is that the entire T cell pool is inhibited, and patients are unable to establish an immune response to infections and malignancies. Thus, the aim here is not to totally extinguish HP, but to prevent the generation of a problematic pro-inflammatory pool. The hypothesis that MAPC cells might prevent the skew of the T cell pool towards the Th1 phenotype was demonstrated as MAPC cells can suppress IFN- γ production by T cells, and promote Treg in the lymph nodes. The Treg data is similar to that in the IL-7 model in that MAPC cells have little effect on FoxP3⁺ Treg in the spleen. In the ATG model however, MAPC cells IP do increase the frequency of Treg in the lymph nodes. The GITR panel was not examined in this model, but it would be beneficial to examine this in future studies, along with suppressive capacity or cytokine profile of Treg.

Similar to the proliferation data, the increase in IFN- γ production is not as dramatic in the ATG model as the IL-7 model. This may explain why MAPC cells IV had no effect in this model, as the amount of inflammatory cytokines produced in the spleen and lymph nodes may not be sufficient to activate MAPC cells accumulating in the lung. MAPC cells IP on the other hand would be closer to the spleen and lymph nodes, and thus, closer to the sites of pro-inflammatory cytokine production, and more likely to be activated. Extrapolation of data

concerning the activation and mode of action of MAPC cells in these murine models should be carefully interpreted, as human MAPC cells may not be activated as potently, or in the same way by murine cells as they would by human cells. As previously mentioned, human cells are not sensitive to murine IFN- γ (Hemmi, Merlin & Aguet, 1992), so while IFN- γ is a crucial activator of MSC and MAPC cells in allogeneic or humanised settings, other cytokines are likely to activate MAPC cells in the xenogeneic experiments used to generate this HP data. The development of humanised models of SOT are underway in the English lab, and these will improve the relevance of this data regarding the effects of MAPC cells on HP, and the subsequent effects on transplant rejection.

Finally, the mode of action of MAPC cells IP in the ATG model was examined. We have previously shown *in vitro* that the effects of MAPC cells on IL-7 activation of T cells is dependent on the production of PGE2 by MAPC cells (Reading *et al.*, 2015), and suppression of GvHD by intrasplenically delivered MAPC cells has been shown to be PGE2 dependent (Highfill *et al.*, 2009). Many other studies have attributed the therapeutic effects of MSC to PGE2 in a range of *in vitro* and *in vivo* settings (English *et al.*, 2009; Chiossone *et al.*, 2016; Kota *et al.*, 2017; Duffy *et al.*, 2011; Vasandan *et al.*, 2016; Hsu *et al.*, 2013). Furthermore, it was speculated that the improved efficacy of PPAR(-) MAPC cells in the aGvHD model is due to an increase in COX-2 expression following IFN- γ stimulation. In the ATG model, inhibition of PGE2 *in vivo* using the COX inhibitor indomethacin ablated the suppressive effects of MAPC cells IP following lymphodepletion. PGE2 has a half short life *in vivo*, and acts in a local manner (Zhang *et al.*, 2015), thus it is possible that MAPC cells IP are more effective in both the IL-7 and ATG models due to being in closer proximity to the sites of interest in this model than MAPC cells IV. Furthermore, IP injected MSC have previously been shown to form aggregates with macrophages (Bazhanov *et al.*, 2016), which can be modulated by MSC derived PGE2 (Chiossone *et al.*, 2016; Vasandan *et al.*, 2016). Therefore, the superior therapeutic efficacy of MAPC cells IP in this study may be due to the interaction of MAPC cells with macrophages at this site. This might also explain why MAPC cells IP but not MAPC cells IV suppressed MHC II expression by macrophages in the IL-7 model. On the

other hand, our previous study demonstrated that MAPC cells require IL-1 β stimulation from monocytes to produce PGE2 (Reading *et al.*, 2015), thus monocytes or macrophages in the omental tissue may provide these signals, inducing PGE2 production by MAPC cells administered IP (Fig. 6.4). As shown using the GvHD model, the efficacy of MAPC cells can be improved following cytokine stimulation. Thus, if the poor efficacy of MAPC cells IV is due to the low availability of inflammatory stimuli, pre-stimulation with cytokines may improve their therapeutic capacity. As previously mentioned, this may not be required in a human model where activation by cytokines would be more robust, however, in this system, activation of MAPC cells with IFN- γ or IL-1 β might certainly improve their efficacy. Moreover, this emphasises the value obtained from humanized models.

While other studies have demonstrated therapeutic efficacy of MAPC in models of allo-transplantation (Highfill *et al.*, 2009; Eggenhofer *et al.*, 2013), the effect of MAPC cells on HP has only been studied previously *in vitro* (Reading *et al.*, 2015). This study suggests that MAPC cells may prevent allograft rejection in part by modulating the T cell pool during HP, however, the effect of MAPC cells on long term immune reconstitution and how it would impact graft survival remains to be shown. These investigations are currently underway in the English lab using skin and islet transplantation. Furthermore, the route of administration or dosing of cells requires optimisation. While this study and others show that MAPC cells require close proximity to the spleen for therapeutic efficacy in transplant models (Highfill *et al.*, 2009; Eggenhofer *et al.*, 2013), IP and intrasplenic delivery routes may not be feasible in the clinic. A recent study has demonstrated that MAPC cells improve islet graft survival when the two cell types are co-transplanted in a composite pellet (Cunha *et al.*, 2016). Thus, co-transplantation of MAPC cells along with allografts at the time of transplantation may be an effective and more practical approach where systemic administration is not sufficient. Otherwise, adjustments to timing or administration, or pre-stimulation with pro-inflammatory cytokines may improve the efficacy of MAPC cells IV, as shown in chapter 3.

Overall, the aim of this thesis was to demonstrate the efficacy and elucidate the modes of action of MAPC cells in various *in vivo* models of transplant rejection. This is the first

study to prove the efficacy of MAPC cells IV in a humanised model of aGvHD, and provides knowledge regarding appropriate dosing schedules and strategies to improve MAPC cell potency. Murine MAPC cells were previously shown to suppress murine GvHD, but only when delivered intrasplenically (Highfill *et al.*, 2009). Intrasplenic administration of MAPC cells is unlikely to be used in the clinic, and this thesis demonstrates that this delivery route is not necessary when MAPC cells are administered at an appropriate time point. The appropriate time to administer MAPC cells is difficult to predict in the clinic, however, the data herein suggests that pre-stimulation of MAPC cells with IFN- γ improves the prospects of achieving effective MAPC cell therapy at early time points. Thus, this thesis provides knowledge which could be used to improve the therapeutic potential of MAPC cells in the clinic. The biodistribution of MAPC cells following administration is important to advance our understanding of exactly how these cells operate *in vivo*, and studies using rodent MAPC cells demonstrate that access to the spleen is important for therapeutic efficacy in models of transplantation (Eggenhofer *et al.*, 2013; Highfill *et al.*, 2009). This thesis demonstrates for the first time that MAPC cells administered IV have the ability to migrate towards the spleen in the aGvHD model. Furthermore, the improved potency of γ MAPC cells corresponds to increased lung clearance and enhanced migration towards the liver and spleen compared to unstimulated MAPC cells.

This thesis and many other studies highlight the importance of IFN- γ signalling for the activation of MSC and MAPC cells. In order to improve the efficacy of MAPC cells in inflammatory conditions, it is imperative that we understand the molecular mechanisms which leads to their IFN- γ response. Luz-Crawford *et al.* (2016b) recently published an interesting study which implicated PPAR δ as a modulator of NF- κ B activation in murine MSC. This study built on that data by demonstrating that PPAR δ agonism and antagonism modulates the response of MAPC cells to IFN- γ stimulation. For the first time, this thesis shows that PPAR δ agonism destroys the efficacy of MAPC cells in the aGvHD model, while PPAR δ antagonism has the opposite effect. We speculate that this may be due to the inhibition or promotion of COX-2 expression by PPAR δ activation or inhibition respectively. This requires further

investigation, which is currently in progress by other members of the English lab. This data provides further insight into the molecular mechanisms behind the immunomodulatory effects of MAPC cells, and this information could be used to develop potency assays or adjust the conditions used for MAPC cell expansion.

Finally, the capacity of MAPC cells to modulate IL-7 and lymphopenia driven T cell HP was demonstrated. There were differences observed in the effects of MAPC cells depending on the model used, however overall the data suggests that MAPC cells suppress IFN- γ production and promote Treg during HP through the production of PGE₂. This might prevent graft rejection, and this theory is currently being investigated by the English lab. It is unclear whether MAPC cells work directly on T cells in this model, or whether intermediate cell types play a role. The effects of MAPC cells on APC and B cells was particularly interesting, and future studies might further investigate the relationships between these cell types. MAPC cells IV were not as effective as MAPC cells IP in these models of HP, which may be problematic in the clinic, as IP infusion is rarely used. The biodistribution data suggests that MAPC cells IP might interact with regulatory cells within the omentum, or may merely be superior as they are in closer contact to the secondary lymphoid organs harvested in these models. The differences between MAPC cells IV and MAPC cells IP highlight the complex nature of these cells, and their ability to adjust their response depending on their environment. This study might spur others to investigate the effects of MAPC cells on omental cell populations, which could generate meaningful knowledge regarding the relationship between MAPC cells and regulatory cell types.

In conclusion, this thesis has provided further knowledge into the mechanisms by which MAPC cell therapy mediate their effects in murine models of transplantation. The main findings presented herein are: IFN- γ improves MAPC cell efficacy and biodistribution in a humanised GvHD model, PPAR δ interferes with the therapeutic effect of MAPC cells, MAPC cells suppress *in vivo* T cell function during HP through the production of PGE₂, and MAPC cells have differential effects depending on their route of administration. The knowledge gained from this project can be used to optimise MAPC cell therapy, and provides a basis for

future studies regarding the effects of MAPC cells on the immune response during transplant rejection.

Chapter 7

Bibliography

- Adams, D.H., Sanchez-Fueyo, A. & Samuel, D. (2015) From immunosuppression to tolerance. *Journal of Hepatology*. 62 (1), S170–S185.
- Adhikary, T., Wortmann, A., Schumann, T., Finkernagel, F., Lieber, S., Roth, K., Toth, P.M., Diederich, W.E., Nist, A., Stiewe, T., Kleinesudeik, L., Reinartz, S., Muler-Brusselbach, S. & Muller, R. (2015) The transcriptional PPARbeta/delta network in human macrophages defines a unique agonist-induced activation state. *Nucleic Acids Research*. 43 (10), 5033–5051.
- Afzali, B., Lombardi, G. & Lechler, R.I. (2013) Pathways of major histocompatibility complex allorecognition. *Current opinion in organ transplantation*. 13 (4), 1–12.
- Aggarwal, S. & Pittenger, M.F. (2005) Human mesenchymal stem cells modulate allogeneic immune cell responses. *Blood*. 105 (4), 1815–1822.
- Ahern, A.T., Artruc, S.B., DellaPelle, P., Cosimi, A.B., Russell, P.S., Colvin, R.B. & Fuller, T.C. (1982) Hyperacute rejection of HLA-AB-identical renal allografts associated with B lymphocyte and endothelial reactive antibodies. *Transplantation*. 33 (1) pp.103–106.
- Allison, M. (2009) Genzyme backs Osiris, despite Prochymal flop. *Nature Biotechnology*. 27 (11), 966–967.
- Amarnath, S., Foley, J.E., Farthing, D.E., Gress, R.E., Laurence, A., Eckhaus, M.A., Metais, J.Y., Rose, J.J., Hakim, F.T., Felizardo, T.C., Cheng, A. V., Robey, P.G., Stroncek, D.E., Sabatino, M., Battiwalla, M., Ito, S., Fowler, D.H. & Barrett, A.J. (2015) Bone Marrow Derived Mesenchymal Stromal Cells Harness Purinergic Signalling to Tolerize Human Th1 Cells In Vivo. *Stem Cells*. 73 (4), 389–400.
- Anderson, B.E., McNiff, J.M., Jain, D., Blazar, B.R., Shlomchik, W.D. & Shlomchik, M.J. (2005) Distinct roles for donor- and host-derived antigen-presenting cells and costimulatory molecules in murine chronic graft-versus-host disease: Requirements depend on target organ. *Blood*. 105 (5), 2227–2234.

- Ankrum, J.A., Ong, J.F. & Karp, J.M. (2014) Mesenchymal stem cells: immune evasive, not immune privileged. *Nature biotechnology*. 32 (3), 252–260.
- Arbelaez, C.A., Glatigny, S., Duhon, R., Eberl, G., Oukka, M. & Bettelli, E. (2015) IL-7/IL-7R signaling differentially affects effector CD4⁺ T cell subsets involved in experimental autoimmune encephalomyelitis 1. *Journal of Immunology*. 195 (5), 1974–1983.
- Archbold, J.K., Ely, L.K., Kjer-Nielsen, L., Burrows, S.R., Rossjohn, J., McCluskey, J. & Macdonald, W.A. (2008a) T cell allorecognition and MHC restriction-A case of Jekyll and Hyde? *Molecular immunology*. 45 (3), 583–598.
- Archbold, J.K., Macdonald, W.A., Burrows, S.R., Rossjohn, J. & McCluskey, J. (2008b) T-cell allorecognition: a case of mistaken identity or déjà vu? *Trends in immunology*. 29 (5), 220–226.
- Athersys Inc. (2014) *Athersys Announces Results From Phase 2 Study of MultiStem (R) Cell Therapy for Ulcerative Colitis MultiStem Demonstrates Good Tolerability and Safety Profile But Fails to Show Efficacy Over 8 Weeks in Patients With Chronic , Advanced Ulcerative Colitis*. 2014. Athersys.com.
- Auletta, J.J., Eid, S.K., Wuttisarnwattana, P., Silva, I., Metheny, L., Keller, M.D., Guardia-Wolff, R., Liu, C., Wang, F., Bowen, T., Lee, Z., Solchaga, L.A., Ganguly, S., Tyler, M., Wilson, D.L. & Cooke, K.R. (2015) Human mesenchymal stromal cells attenuate graft-versus-host disease and maintain graft-versus-leukemia activity following experimental allogeneic bone marrow transplantation. *Stem Cells*. 33 (2), 601–614.
- Ayasoufi, K., Fan, R., Fairchild, R.L. & Valujskikh, A. (2016) CD4 T Cell Help via B Cells Is Required for Lymphopenia-Induced CD8 T Cell Proliferation. *Journal of Immunology*. 196 (7), 3180–3190.
- Azzi, J.R., Sayegh, M.H. & Mallat, S.G. (2013) Calcineurin inhibitors: 40 years later, can't live without ... *Journal of immunology*. 191 (12), 5785–5791.
- Ball, L.M., Bernardo, M.E., Roelofs, H., van Tol, M.J.D., Contoli, B., Zwaginga, J.J.,

- Avanzini, M.A., Conforti, A., Bertaina, A., Giorgiani, G., Jol-van der Zijde, C.M., Zecca, M., Le Blanc, K., Frassoni, F., Egeler, R.M., Fibbe, W.E., Lankester, A.C. & Locatelli, F. (2013) Multiple infusions of mesenchymal stromal cells induce sustained remission in children with steroid-refractory, grade III-IV acute graft-versus-host disease. *British Journal of Haematology*. 163 (4), 501–509.
- Barbash, I.M., Chouraqui, P., Baron, J., Feinberg, M.S., Etzion, S., Tessone, A., Miller, L., Guetta, E., Zipori, D., Kedes, L.H., Kloner, R.A. & Leor, J. (2003) Systemic delivery of bone marrow-derived mesenchymal stem cells to the infarcted myocardium: feasibility, cell migration, and body distribution. *Circulation*. 108 (7), 863–868.
- Bartosh, T.J., Ylostalo, J.H., Bazhanov, N., Kuhlman, J. & Prockop, D.J. (2013) Dynamic compaction of human mesenchymal stem/precursor cells (MSC) into spheres self-activates caspase-dependent IL1 signaling to enhance secretion of modulators of inflammation and immunity (PGE2, TSG6 and STC1). *Stem Cells*. 100 (2), 130–134.
- Bazhanov, N., Ylostalo, J.H., Bartosh, T.J., Tiblow, A., Mohammadipoor, A., Foskett, A. & Prockop, D.J. (2016) Intraperitoneally infused human mesenchymal stem cells form aggregates with mouse immune cells and attach to peritoneal organs. *Stem cell research & therapy*. 7 (1), 1.
- Benichou, G., Gonzalez, B., Marino, J., Ayasoufi, K. & Valujskikh, A. (2017) Role of memory T cells in allograft rejection and tolerance. *Frontiers in Immunology*. 8 (170), 1–9.
- Bernardo, M.E. & Fibbe, W.E. (2013) Mesenchymal stromal cells: Sensors and switchers of inflammation. *Cell Stem Cell*. 13 (4), 392–402.
- Le Blanc, K. & Davies, L.C. (2015) Mesenchymal stromal cells and the innate immune response. *Immunology Letters*. 168 (2), 140–146.
- Le Blanc, K., Rasmusson, I., Sundberg, B., Hassan, M. & Uzunel, M. (2004) Treatment of severe acute graft-versus-host disease with third party haploidentical mesenchymal stem cells. *The Lancet*. 363, 1439–1442.

- Le Blanc, K., Tammki, L., Sundberg, B., Haynesworth, S.E. & Ringden, O. (2003) Mesenchymal stem cells inhibit and stimulate mixed lymphocyte cultures and mitogenic response independently of the major histocompatibility complex. *Scand J Immunol.* 57, 11–20.
- Bleakley, M. & Riddell, S.R. (2004) Molecules and mechanisms of the graft-versus-leukaemia effect. *Nature Reviews Cancer.* 4 (5), 371–380.
- Boardman, D.A., Jacob, J., Smyth, L.A., Lombardi, G. & Lechler, R.I. (2016) What Is Direct Allorecognition? *Current Transplantation Reports.* 3 (4), 275–283.
- Boenisch, O., Lopez, M., Elyaman, W., Magee, C.N., Ahmad, U. & Najafian, N. (2012) Ex vivo expansion of human Tregs by rabbit ATG is dependent on intact STAT3-signaling in CD4 + T cells and requires the presence of monocytes. *American Journal of Transplantation.* 12 (4), 856–866.
- Bokkelen, G. Van (2011) Company Profile Athersys. *Regen. Med.* 6 (1), 39–43.
- Boyman, O., Ramsey, C., Kim, D.M., Sprent, J. & Surh, C.D. (2008) IL-7/anti-IL-7 mAb complexes restore T cell development and induce homeostatic T Cell expansion without lymphopenia. *Journal of immunology.* 180 (11), 7265–7275.
- Bravery, C.A., Carmen, J., Fong, T., Oprea, W., Hoogendoorn, K.H., Woda, J., Burger, S.R., Rowley, J.A., Bonyhadi, M.L. & Van't Hof, W. (2013) Potency assay development for cellular therapy products: an ISCT review of the requirements and experiences in the industry. *Cytotherapy.* 15 (1), 9–19.
- Braza, F., Dirou, S., Forest, V., Sauzeau, V. & Hassoun, D. (2016) Mesenchymal stem cells induce suppressive macrophages through phagocytosis in a mouse model of asthma. *Stem Cells.* 34, 1836–1845.
- van den Brink, M.R.M., Alpdogan, Ö. & Boyd, R.L. (2004) Strategies to enhance T-cell reconstitution in immunocompromised patients. *Nature Reviews Immunology.* 4 (11), 856–867.

- Broady, R., Yu, J. & Levings, M.K. (2009) ATG-induced expression of FOXP3 in human CD4⁺ T cells in vitro is associated with T-cell activation and not the induction of FOXP3⁺ T regulatory cells. *Blood*. 114 (24), 5003–5006.
- Bruck, F., Belle, L., Lechanteur, C., De Leval, L., Hannon, M., Dubois, S., Castermans, E., Humblet-Baron, S., Rahmouni, S., Beguin, Y., Briquet, A. & Baron, F. (2013) Impact of bone marrow-derived mesenchymal stromal cells on experimental xenogeneic graft-versus-host disease. *Cytotherapy*. 15 (3), 267–279.
- Burman, A.C., Banovic, T., Kuns, R.D., Clouston, A.D., Stanley, A.C., Morris, E.S., Rowe, V., Bofinger, H., Skoczylas, R., Raffelt, N., Fahy, O., McColl, S.R., Engwerda, C.R., McDonald, K.P.A. & Hill, G.R. (2007) IFN γ differentially controls the development of idiopathic pneumonia syndrome and GVHD of the gastrointestinal tract. *Blood*. 110 (3), 1064–1072.
- Busch, S.A., Hamilton, J.A., Horn, K.P., Cuascut, F.X., Cutrone, R., Lehman, N., Deans, R.J., Ting, A.E., Mays, R.W. & Silver, J. (2011) Multipotent Adult Progenitor Cells Prevent Macrophage-Mediated Axonal Dieback and Promote Regrowth after Spinal Cord Injury. *Journal of Neuroscience*. 31 (3), 944–953.
- Cahill, E.F., Kennelly, H., Carty, F., Mahon, B.P. & English, K. (2016) Hepatocyte Growth Factor Is Required for Mesenchymal Stromal Cell Protection Against Bleomycin-Induced Pulmonary Fibrosis. *Stem cells translational medicine*. 5, 1307–1318.
- Cahill, E.F., Tobin, L.M., Carty, F., Mahon, B.P. & English, K. (2015) Jagged-1 is required for the expansion of CD4⁺ CD25⁺ FoxP3⁺ regulatory T cells and tolerogenic dendritic cells by murine mesenchymal stromal cells. *Stem Cell Research & Therapy*. 6 (1), 1–13.
- Caplan, A.I. (2009) Why are MSCs therapeutic? New data: new insight. *The Journal of pathology*. 217, 318–324.
- Caplan, A.I., Mason, C. & Reeve, B. (2017) The 3Rs of Cell Therapy. *Stem Cells Transl Med*. 6, 17–21.

- Carty, F., Mahon, B.P. & English, K. (2017) The influence of macrophages on mesenchymal stromal cell therapy: Passive or aggressive agents? *Clinical & Experimental Immunology*. 5, 1–11.
- Casiraghi, F., Azzollini, N., Cassis, P., Imberti, B., Morigi, M., Cugini, D., Cavinato, R.A., Todeschini, M., Solini, S., Sonzogni, A., Perico, N., Remuzzi, G. & Noris, M. (2008) Pretransplant Infusion of Mesenchymal Stem Cells Prolongs the Survival of a Semiallogeneic Heart Transplant through the Generation of Regulatory T Cells. *The Journal of Immunology*. 181 (6), 3933–3946.
- Casiraghi, F., Azzollini, N., Todeschini, M., Cavinato, R. a., Cassis, P., Solini, S., Rota, C., Morigi, M., Introna, M., Maranta, R., Perico, N., Remuzzi, G. & Noris, M. (2012) Localization of mesenchymal stromal cells dictates their immune or proinflammatory effects in kidney transplantation. *American Journal of Transplantation*. 12 (9), 2373–2383.
- Chao, K., Zhang, S., Qiu, Y., Chen, X., Zhang, X., Cai, C., Peng, Y., Mao, R., Pevsner-fischer, M., Ben-horin, S., Elinav, E., Zeng, Z., Chen, B., He, Y., Xiang, A.P. & Chen, M. (2016) Human umbilical cord-derived mesenchymal stem cells protect against experimental colitis via CD5 + B regulatory cells. *Stem Cell Research & Therapy*. 1–12.
- Chapel, A., Bertho, J.M., Bensidhoum, M., Fouillard, L., Young, R.G., Frick, J., Demarquay, C., Cuvelier, F., Mathieu, E., Trompier, F., Dudoignon, N., Germain, C., Mazurier, C., Aigueperse, J., Borneman, J., Gorin, N.C., Gourmelon, P. & Thierry, D. (2003) Mesenchymal stem cells home to injured tissues when co-infused with hematopoietic cells to treat a radiation-induced multi-organ failure syndrome. *Journal of Gene Medicine*. 5 (12), 1028–1038.
- Chapman, J.R., Webster, A.C. & Wong, G. (2013) Cancer in the transplant recipient. *Cold Spring Harbor Perspectives in Medicine*. 3 (7), 1–16.
- Chaudhry, M.S., Velardi, E., Malard, F. & van den Brink, M.R.M. (2017) Immune

Reconstitution after Allogeneic Hematopoietic Stem Cell Transplantation: Time To T Up the Thymus. *The Journal of Immunology*. 198 (1), 40–46.

Cheng, G., Yuan, X., Tsai, M.S., Podack, E.R., Yu, a & Malek, T.R. (2012) IL-2 receptor signaling is essential for the development of Klrp1+ terminally differentiated T regulatory cells. *J Immunol*. 189 (4), 1780–1791.

Cheng, P., Liu, X.C., Ma, P.F., Gao, C., Li, J.L., Lin, Y.Y., Shao, W., Han, S., Zhao, B., Wang, L.M., Fu, J.Z., Meng, L.X., Li, Q., Lian, Q.Z., Xia, J.J. & Qi, Z.Q. (2015) iPSC-MSCs Combined with Low-Dose Rapamycin Induced Islet Allograft Tolerance Through Suppressing Th1 and Enhancing Regulatory T-Cell Differentiation. *Stem Cells and Development*. 24 (15), 1793–1804.

Chiesa, S., Morbelli, S., Morando, S., Massollo, M., Marini, C., Bertoni, a., Frassoni, F., Bartolome, S.T., Sambuceti, G., Traggiai, E. & Uccelli, a. (2011) Mesenchymal stem cells impair in vivo T-cell priming by dendritic cells. *Proceedings of the National Academy of Sciences*. 108 (42), 17384–17389.

Chinnadurai, R., Copland, I.B., Ng, S., Garcia, M., Prasad, M., Arafat, D., Gibson, G., Kugathasan, S. & Galipeau, J. (2015) Mesenchymal Stromal Cells Derived From Crohn's Patients Deploy Indoleamine 2,3-dioxygenase-mediated Immune Suppression, Independent of Autophagy. *Mol Ther*. 23 (7), 1248–1261.

Chinnadurai, R., Copland, I.B., Patel, S.R. & Galipeau, J. (2014) IDO-Independent Suppression of T Cell Effector Function by IFN- γ – Licensed Human Mesenchymal Stromal Cells. *The Journal of Immunology*. 192, 1491–1501.

Chiossone, L., Conte, R., Spaggiari, G.M., Serra, M., Romei, C., Bellora, F., Becchetti, F., Andaloro, A., Moretta, L. & Bottino, C. (2016) Mesenchymal Stromal Cells Induce Peculiar Alternatively Activated Macrophages Capable of Dampening Both Innate and Adaptive Immune Responses. *Stem Cells*. 34, 1909–1921.

Choi, H., Lee, R.H., Bazhanov, N., Oh, J.Y. & Prockop, D.J. (2011) Anti-inflammatory protein

- TSG-6 secreted by activated MSCs attenuates zymosan-induced mouse peritonitis by decreasing TLR2/NF- κ B signaling in resident macrophages. *Blood*. 118 (2), 330–338.
- Chong, A.S. & Sciammas, R. (2015) Memory B cells in transplantation. *Transplantation*. 99 (1), 21–28.
- Chu, Y.W. & Gress, R.E. (2008) Murine Models of Chronic Graft-versus-Host Disease: Insights and Unresolved Issues. *Biology of Blood and Marrow Transplantation*. 14 (4), 365–378.
- Chung, B., Dudl, E. & Min, D. (2007) Prevention of graft-versus-host disease by anti-IL-7R alpha antibody. *Blood*. 110 (8), 2803–2810.
- Corcione, A., Benvenuto, F., Ferretti, E., Giunti, D., Cappiello, V., Cazzanti, F., Risso, M., Gualandi, F., Mancardi, G.L., Pistoia, V. & Uccelli, A. (2006) Human mesenchymal stem cells modulate B-cell functions. *Multiple Sclerosis*. 107 (1), 367–372.
- Cornelissen, A.S., Maijenburg, M.W., Nolte, M.A. & Voermans, C. (2015) Organ-specific migration of mesenchymal stromal cells: Who, when, where and why? *Immunology Letters*. 168 (2), 159–169.
- Crabbe, M.A.E., Gijbels, K., Visser, A., Craeye, D., Walbers, S., Pinxteren, J., Deans, R.J., Annaert, W. & Vaes, B.L.T. (2016) Using miRNA-mRNA Interaction Analysis to Link Biologically Relevant miRNAs to Stem Cell Identity Testing for Next-Generation Culturing Development. *Stem cells translational medicine*. 5, 709–722.
- Cravedi, P. & Heeger, P.S. (2014) Complement as a multifaceted modulator of kidney transplant injury. *Journal of Clinical Investigation*. 124 (6).
- Creane, M., Howard, L., O'Brien, T. & Coleman, C.M. (2017) Biodistribution and retention of locally administered human mesenchymal stromal cells: Quantitative polymerase chain reaction-based detection of human DNA in murine organs. *Cytotherapy*. 19 (3), 384–394.
- Crepin, T., Carron, C., Roubiou, C., Gaugler, B., Gaiffe, E., Simula-Faivre, D., Ferrand, C.,

- Tiberghien, P., Chalopin, J.M., Moulin, B., Frimat, L., Rieu, P., Saas, P., Ducloux, D. & Bamoulid, J. (2015) ATG-Induced Accelerated Immune Senescence: Clinical Implications in Renal Transplant Recipients. *American Journal of Transplantation*. 15 (4), 1028–1038.
- Crespo, M., Pascual, M., Tolkoff-Rubin, N., Mauiyyedi, S., Collins, A.B., Fitzpatrick, D., Farrell, M.L., Williams, W.W., Delmonico, F.L., Cosimi, A.B., Colvin, R.B. & Saidman, S.L. (2001) Acute humoral rejection in renal allograft recipients: I. Incidence, serology and clinical characteristics. *Transplantation*. 71 (5), 652–658.
- Cunha, J.P.M.C.M., Leuckx, G., Sterkendries, P., Korf, H., Bomfim-Ferreira, G., Overbergh, L., Vaes, B., Heimberg, H., Gysemans, C. & Mathieu, C. (2016) Human multipotent adult progenitor cells enhance islet function and revascularisation when co-transplanted as a composite pellet in a mouse model of diabetes. *Diabetologia*. 1–9.
- Danilkovitch, A. (2006) *Potency Assay Development for a Novel Cell Therapy Product: Prochymal Adult Mesenchymal Stem Cells*. 2006. Meeting of: Cellular, Tissue and Gene Therapies Advisory Committee.
- Darlington, P.J., Boivin, M.N., Renoux, C., François, M., Galipeau, J., Freedman, M.S., Atkins, H.L., Cohen, J.A., Solchaga, L. & Bar-Or, A. (2010) Reciprocal Th1 and Th17 regulation by mesenchymal stem cells: Implication for multiple sclerosis. *Annals of Neurology*. 68 (4), 540–545.
- Davies, L.C., Heldring, N., Kadri, N. & Le Blanc, K. (2016) Mesenchymal Stromal Cell Secretion of Programmed Death-1 Ligands Regulates T Cell Mediated Immunosuppression. *Stem cells*. 766–776.
- Daynes, R.A. & Jones, D.C. (2002) Emerging roles of ppar α in inflammation and immunity. *Nature Reviews Immunology*. 2 (10), 748–759.
- Deeg, H.J. (2007) How I treat How I treat refractory acute GVHD. *Blood*. 109 (10), 4119–4126.

- Deng, J., Wang, X., Chen, Q., Sun, X., Xiao, F., Ko, K., Zhang, M. & Lu, L. (2016) *B1a cells play a pathogenic role in the development of autoimmune arthritis*. 7 (15).
- DePaul, M.A., Palmer, M., Lang, B.T., Cutrone, R., Tran, A.P., Madalena, K.M., Bogaerts, A., Hamilton, J.A., Deans, R.J., Mays, R.W., Busch, S.A. & Silver, J. (2015) Intravenous multipotent adult progenitor cell treatment decreases inflammation leading to functional recovery following spinal cord injury. *Scientific Reports*. 5 (October), 16795.
- Detry, O., Vandermeulen, M., Delbouille, M.H., Somja, J., Bletard, N., Briquet, A., Lechanteur, C., Giet, O., Baudoux, E., Hannon, M., Baron, F. & Beguin, Y. (2017) Infusion of mesenchymal stromal cells after deceased liver transplantation: A phase I-II, open-label, clinical study. *Journal of Hepatology*. 67 (1), 47–55.
- Diaz-Gandarilla, J.A., Osorio-Trujillo, C., Hernandez-Ramirez, V.I. & Talamas-Rohana, P. (2013) PPAR Activation Induces M1 Macrophage Polarization via cPLA 2 -COX-2 Inhibition, Activating ROS Production against *Leishmania mexicana*. *BioMed research international*. 2013, 215283.
- Djouad, F., Charbonnier, L.M., Bouffi, C., Louis-Pence, P., Bony, C., Apparailly, F., Cantos, C., Jorgensen, C. & Noël, D. (2007) Mesenchymal Stem Cells Inhibit the Differentiation of Dendritic Cells Through an Interleukin-6-Dependent Mechanism. *Stem Cells*. 25 (8), 2025–2032.
- Dodson, B.P. & Levine, A.D. (2015) Challenges in the translation and commercialization of cell therapies. *BMC Biotechnology*. 15 (1), 70.
- Dominici, M., Le Blanc, K., Mueller, I., Slaper-Cortenbach, I., Marini, F., Krause, D., Deans, R., Keating, a, Prockop, D. & Horwitz, E. (2006) Minimal criteria for defining multipotent mesenchymal stromal cells. The International Society for Cellular Therapy position statement. *Cytotherapy*. 8 (4), 315–317.
- Dorransoro, A., Ferrin, I., Salcedo, J.M., Jakobsson, E., Fernández-Rueda, J., Lang, V., Sepulveda, P., Fechter, K., Pennington, D. & Trigueros, C. (2014) Human mesenchymal

stromal cells modulate T-cell responses through TNF- α -mediated activation of NF- κ B. *European Journal of Immunology*. 44 (2), 480–488.

Drexler, H.G., Brenner, M.K., Wimperis, J.Z., Gignac, S.M., Janossy, G., Prentice, H.G. & Hoffbrand, A.V. (1987) CD5-positive B cells after T cell depleted bone marrow transplantation. *Clinical and experimental immunology*. 68 (3), 662–668.

Duffy, M.M., Pindjakova, J., Hanley, S.A., McCarthy, C., Weidhofer, G.A., Sweeney, E.M., English, K., Shaw, G., Murphy, J.M., Barry, F.P., Mahon, B.P., Belton, O., Ceredig, R. & Griffin, M.D. (2011) Mesenchymal stem cell inhibition of T-helper 17 cell-differentiation is triggered by cell-cell contact and mediated by prostaglandin E2 via the EP4 receptor. *European Journal of Immunology*. 41 (10), 2840–2851.

Duijvestein, M., Wildenberg, M.E., Welling, M.M., Hennink, S., Molendijk, I., Van Zuylen, V.L., Bosse, T., Vos, A.C.W., De Jonge-Muller, E.S.M., Roelofs, H., Van Der Weerd, L., Verspaget, H.W., Fibbe, W.E., Te Velde, A.A., Van Den Brink, G.R. & Hommes, D.W. (2011) Pretreatment with interferon- γ enhances the therapeutic activity of mesenchymal stromal cells in animal models of colitis. *Stem Cells*. 29 (10), 1549–1558.

Durand, J. & Chiffolleau, E. (2015) B cells with regulatory properties in transplantation tolerance. *World J Transplant*. 5 (4), 196–208.

Durand, J., Huchet, V., Merieau, E., Usal, C., Chesneau, M., Remy, S., Heslan, M., Anegon, I., Cuturi, M.C., Brouard, S. & Chiffolleau, E. (2015) Regulatory B Cells with a Partial Defect in CD40 Signaling and Overexpressing Granzyme B Transfer Allograft Tolerance in Rodents. *The Journal of Immunology*. 195 (10), 5035–5044.

Eggenhofer, E., Benseler, V., Kroemer, A., Popp, F.C., Geissler, E.K., Schlitt, H.J., Baan, C.C., Dahlke, M.H. & Hoogduijn, M.J. (2012) Mesenchymal stem cells are short-lived and do not migrate beyond the lungs after intravenous infusion. *Frontiers in Immunology*. 3 (SEP), 1–8.

Eggenhofer, E., Luk, F., Dahlke, M.H. & Hoogduijn, M.J. (2014) The life and fate of

mesenchymal stem cells. *Frontiers in Immunology*. 5 (148), 1–6.

Eggenhofer, E., Popp, F.C., Mendicino, M., Silber, P., Van't Hof, W., Renner, P., Hoogduijn, M.J., Pinxteren, J., van Rooijen, N., Geissler, E.K., Deans, R., Schlitt, H.J. & Dahlke, M.H. (2013) Heart Grafts Tolerized Through Third Party Multipotent Adult Progenitor Cells Can Be Reimplanted to Secondary Hosts With No Immunosuppression. *Stem cells translational medicine*. 2, 595–606.

Eggenhofer, E., Steinmann, J.F., Renner, P., Slowik, P., Piso, P., Geissler, E.K., Schlitt, H.J., Dahlke, M.H. & Popp, F.C. (2011) Mesenchymal stem cells together with mycophenolate mofetil inhibit antigen presenting cell and T cell infiltration into allogeneic heart grafts. *Transplant Immunology*. 24 (3), 157–163.

Eltzschig, H.K. & Eckle, T. (2011) Ischemia and reperfusion—from mechanism to translation. *Nature medicine*. 17 (11), 1391–1401.

English, K. (2013) Mechanisms of mesenchymal stromal cell immunomodulation. *Immunology and Cell Biology*. 91 (1), 19–26.

English, K., Barry, F.P., Field-Corbett, C.P. & Mahon, B.P. (2007a) IFN- γ and TNF- α differentially regulate immunomodulation by murine mesenchymal stem cells. *Immunology letters*. 110 (2), 91–100.

English, K., Barry, F.P., Field-Corbett, C.P. & Mahon, B.P. (2007b) IFN- γ and TNF- α differentially regulate immunomodulation by murine mesenchymal stem cells. *Immunology Letters*. 110 (2), 91–100.

English, K., Barry, F.P. & Mahon, B.P. (2008) Murine mesenchymal stem cells suppress dendritic cell migration, maturation and antigen presentation. *Immunology Letters*. 115 (1), 50–58.

English, K. & Mahon, B.P. (2011) Allogeneic mesenchymal stem cells: Agents of immune modulation. *Journal of Cellular Biochemistry*. 112 (8), 1963–1968.

- English, K., Ryan, J.M., Tobin, L., Murphy, M.J., Barry, F.P. & Mahon, B.P. (2009) Cell contact, prostaglandin E2 and transforming growth factor beta 1 play non-redundant roles in human mesenchymal stem cell induction of CD4+CD25Highforkhead box P3+ regulatory T cells. *Clinical and Experimental Immunology*. 156 (1), 149–160.
- English, K. & Wood, K.J. (2013) Mesenchymal Stromal Cells in Transplantation Rejection and Tolerance. *Cold Spring Harbor perspectives in medicine*. 3, a015560.
- Fábrega, E., López-Hoyos, M., San Segundo, D., Casafont, F., Benito, M.J. & Pons-Romero, F. (2009) Effect of Immunosuppressant Blood Levels on Serum Concentration of Interleukin-17 and -23 in Stable Liver Transplant Recipients. *Transplantation Proceedings*. 41 (3), 1025–1027.
- Fábrega, E., López-Hoyos, M., San Segundo, D., Casafont, F. & Pons-Romero, F. (2007) Changes in the serum levels of interleukin-17/interleukin-23 during acute rejection in liver transplantation. *Liver Transplantation*. 13 (3), 465–466.
- Feng, X., Kajigaya, S., Solomou, E.E., Keyvanfar, K., Xu, X., Munson, P.J., Herndon, T.M., Chen, J., Young, N.S. & Raghavachari, N. (2008) Rabbit ATG but not horse ATG promotes expansion of functional CD4 + Rabbit ATG but not horse ATG promotes expansion of functional CD4+ CD25 high FOXP3+ regulatory T cells in vitro. *Blood*. 111, 3675–3683.
- Ferrara (2009) Mouse models of graft-versus-host disease. *StemBook*. 1–23.
- Ferrara, J., Levine, J., Reddy, P. & Holler, E. (2009) Graft-versus-host disease. *The Lancet*. 373 (9674), 1550–1561.
- Fischer, U.M., Harting, M.T., Jimenez, F., Monzon-Posadas, W.O., Xue, H., Savitz, S.I., Laine, G.A. & Cox, C.S. (2009) Pulmonary passage is a major obstacle for intravenous stem cell delivery: the pulmonary first-pass effect. *Stem cells and development*. 18 (5), 683–692.
- Fishman, J.A., Sacks, S.H., Page, E., Kwun, J., Oh, B., Anderson, D.J., Kirk, A.D., Orlando,

- G., Soker, S., Stratta, R.J., Chapman, J.R., Webster, A.C., English, K. & Wood, K.J. (2013) Opportunistic Infections — Coming to the Limits. *Cold Spring Harbor perspectives in medicine*. 3, a015669.
- Fitzgerald, K., O'Neill, L.A.J., Gearing, A.J.H. & Callard, R.E. (2001) *The Cytokine FactsBook*. Second. San Diego, Academic Press.
- Flowers, M.E.D. & Martin, P.J. (2015) How we treat chronic graft-versus-host disease. *Blood*. 125 (4), 606–615.
- Forman, B.M., Chen, J. & Evans, R.M. (1997) Hypolipidemic drugs, polyunsaturated fatty acids, and eicosanoids are ligands for peroxisome proliferator-activated receptors alpha and delta. *Proceedings of the National Academy of Sciences*. 94 (9), 4312–4317.
- Franchimont, D. (2004) Overview of the actions of glucocorticoids on the immune response: A good model to characterize new pathways of immunosuppression for new treatment strategies. *Annals of the New York Academy of Sciences*. 1024, 124–137.
- François, M., Copland, I.B., Yuan, S., Romieu-Mourez, R., Waller, E.K. & Galipeau, J. (2012a) Cryopreserved mesenchymal stromal cells display impaired immunosuppressive properties as a result of heat-shock response and impaired interferon- γ licensing. *Cytotherapy*. 14 (2), 147–152.
- François, M., Romieu-Mourez, R., Li, M. & Galipeau, J. (2012b) Human MSC Suppression Correlates With Cytokine Induction of Indoleamine 2,3-Dioxygenase and Bystander M2 Macrophage Differentiation. *Molecular Therapy*. 20 (1), 187–195.
- François, S., Usunier, B., Douay, L., Benderitter, M. & Chapel, A. (2014) Long-term quantitative biodistribution and side effects of human mesenchymal stem cells (hMSCs) engraftment in NOD/SCID mice following irradiation. *Stem Cells International*. 2014 (939275), 1–13.
- Franquesa, M., Mensah, F.K., Huizinga, R., Strini, T., Boon, L. & Lombardo, E. (2015) Human Adipose Tissue-Derived Mesenchymal Stem Cells Abrogate Plasmablast

- Formation and Induce Regulatory B Cells Independently of T Helper Cells. *Stem Cells*. 33, 880–891.
- Fry, T.J. & Mackall, C.L. (2009) Interleukin-7 : from bench to clinic. *Blood*. 99 (11), 3892–3904.
- Fujii, H., Luo, Z.J., Kim, H.J., Newbigging, S., Gassas, A., Keating, A. & Egeler, R.M. (2015) Humanized chronic graft-versus-host disease in NOD-SCID il2 γ ^{-/-} (NSG) mice with G-CSF-mobilized peripheral blood mononuclear cells following cyclophosphamide and total body irradiation. *PLoS ONE*. 10 (7), 1–16.
- Galipeau, J. (2013) The mesenchymal stromal cells dilemma-does a negative phase III trial of random donor mesenchymal stromal cells in steroid-resistant graft-versus-host disease represent a death knell or a bump in the road? *Cytotherapy*. 15 (1), 2–8.
- Gallon, L., Gagliardini, E., Benigni, A., Kaufman, D., Waheed, A., Noris, M. & Remuzzi, G. (2006) Immunophenotypic analysis of cellular infiltrate of renal allograft biopsies in patients with acute rejection after induction with alemtuzumab (Campath-1H). *Clinical journal of the American Society of Nephrology*. 1 (3), 539–545.
- Gallon, L., Traitanon, O., Yu, Y., Shi, B., Leventhal, J.R., Miller, J., Mas, V., L, X. & Mathew, J.M. (2015) Differential Effects of Calcineurin and Mammalian Target of Rapamycin Inhibitors on Alloreactive Th1, Th17, and Regulatory T Cells. *Transplantation*. 99 (9), 1774–1784.
- Gao, L., Zhang, Y., Hu, B., Liu, J., Kong, P., Lou, S., Su, Y., Yang, T., Li, H., Liu, Y., Zhang, C., Gao, L., Zhu, L., Wen, Q., Wang, P., Chen, X., Zhong, J. & Zhang, X. (2016) Phase II Multicenter, Randomized, Double-Blind Controlled Study of Efficacy and Safety of Umbilical Cord-Derived Mesenchymal Stromal Cells in the Prophylaxis of Chronic Graft-Versus-Host Disease After HLA-Haploidentical Stem-Cell Transplantation. *Journal of Clinical Oncology*. 34 (24).
- Ge, W., Jiang, J., Arp, J., Liu, W., Garcia, B. & Wang, H. (2010) Regulatory T-cell generation

and kidney allograft tolerance induced by mesenchymal stem cells associated with indoleamine 2,3-dioxygenase expression. *Transplantation*. 90 (12), 1312–1320.

Ge, W., Jiang, J., Baroja, M.L., Arp, J., Zassoko, R., Liu, W., Bartholomew, a., Garcia, B. & Wang, H. (2009) Infusion of mesenchymal stem cells and rapamycin synergize to attenuate alloimmune responses and promote cardiac allograft tolerance. *American Journal of Transplantation*. 9 (8), 1760–1772.

Ghannam, S., Pène, J., Torcy-Moquet, G., Jorgensen, C. & Yssel, H. (2010) Mesenchymal stem cells inhibit human Th17 cell differentiation and function and induce a T regulatory cell phenotype. *Journal of immunology*. 185, 302–312.

Giaretta, F., Bussolino, S., Beltramo, S., Fop, F., Rossetti, M., Messina, M., Cantaluppi, V., Ranghino, A., Basso, E., Camussi, G., Segoloni, G.P. & Biancone, L. (2013) Different regulatory and cytotoxic CD4⁺ T lymphocyte profiles in renal transplants with antibody-mediated chronic rejection or long-term good graft function. *Transplant immunology*. 28 (1), 48–56.

Glauzy, S., Soret, J., Fournier, I., Douay, C., Moins-Teisserenc, H., Peffault de Latour, R., Maki, G., Robin, M., Socié, G., Toubert, A. & Clave, E. (2014) Impact of acute and chronic graft-versus-host disease on human B-cell generation and replication. *Blood*. 124 (15), 2459–2463.

Gong, J., Xie, J., Bedolla, R., Rivas, P., Chakravarthy, D., Freeman, J.W., Reddick, R., Kopetz, S., Peterson, A., Wang, H., Fischer, S. & Kumar, A. (2014) Combined targeting of Stat3/NFkB/Cox-2/EP4 for effective management of pancreatic cancer. *Clinical Cancer Research*. 20 (5), 1259–1273.

Gough, D.J., Levy, D.E., Johnstone, R.W. & Clarke, C.J. (2008) IFN γ signaling-Does it mean JAK-STAT? *Cytokine and Growth Factor Reviews*. 19 (5–6), 383–394.

Grazia, T.J., Plenter, R.J., Weber, S.M., Lepper, H.M., Victorino, F., Zamora, M.R., Pietra, B.A. & Gill, R.G. (2010) Acute Cardiac Allograft Rejection by Directly Cytotoxic CD4

- T Cells: Parallel Requirements for Fas and Perforin. *Transplantation*. 89 (1), 33–39.
- Griffin, M.D., Elliman, S.J., Cahill, E., English, K., Ceredig, R. & Ritter, T. (2013) Concise review: adult mesenchymal stromal cell therapy for inflammatory diseases: how well are we joining the dots? *Stem cells*. 31 (10), 2033–2041.
- Grimaldi, F., Potter, V., Perez-Abellan, P., Veluchamy, J.P., Atif, M., Grain, R., Sen, M., Best, S., Lea, N., Rice, C., Pagliuca, A., Mufti, G.J., Marsh, J.C.W. & Barber, L.D. (2016) Mixed T-Cell Chimerism after Allogeneic Hematopoietic Stem Cell Transplantation for Severe Aplastic Anemia Using an Alemtuzumab-Containing Regimen is Shaped by Persistence of Recipient CD8 T Cells. *Biology of blood and marrow transplantation*. 23 (2), 293–299.
- Gurkan, S., Luan, Y., Dhillon, N., Allam, S.R., Montague, T., Bromberg, J.S., Ames, S., Lerner, S., Ebcioğlu, Z., Nair, V., Dinavahi, R., Sehgal, V., Heeger, P., Schroppe, B. & Murphy, B. (2010) Immune Reconstitution Following Rabbit Antithymocyte Globulin. *American journal of physiology. Renal physiology*. 10 (9), 2132–2141.
- Hardinger, K.L., Brennan, D.C. & Klein, C.L. (2013) Selection of induction therapy in kidney transplantation. *Transplant International*. 26 (7), 662–672.
- Harmon, C., Sanchez-Fueyo, a., O’Farrelly, C. & Houlihan, D.D. (2016) Natural Killer Cells and Liver Transplantation: Orchestrators of Rejection or Tolerance? *American Journal of Transplantation*. 16 (3), 751–757.
- Harper, S.J.F., Ali, J.M., Wlodek, E., Negus, M.C., Harper, I.G., Chhabra, M., Qureshi, M.S., Mallik, M., Bolton, E., Bradley, J.A. & Pettigrew, G.J. (2015) CD8 T-cell recognition of acquired alloantigen promotes acute allograft rejection. *Proceedings of the National Academy of Sciences*. 112 (41), 12788–12793.
- Havari, E., Turner, M.J., Campos-Rivera, J., Shankara, S., Nguyen, T.H., Roberts, B., Siders, W. & Kaplan, J.M. (2014) Impact of alemtuzumab treatment on the survival and function of human regulatory T cells in vitro. *Immunology*. 141 (1), 123–131.

- Healy, M.E., Bergin, R., Mahon, B.P. & English, K. (2015) Mesenchymal stromal cells protect against caspase 3 mediated apoptosis of CD19+ peripheral B cells through contact dependent up-regulation of VEGF. *Stem cells and development*. 24 (20), 2391–2402.
- Hemmi, S., Merlin, G. & Aguet, M. (1992) Functional characterization of a hybrid human-mouse interferon gamma receptor: evidence for species-specific interaction of the extracellular receptor domain with a putative signal transducer. *Proceedings of the National Academy of Sciences of the United States of America*. 89 (7), 2737–2741.
- Henden, A.S. & Hill, G.R. (2015) Cytokines in Graft-versus-Host Disease. *The Journal of Immunology*. 194 (10), 4604–4612.
- Heninger, A.K., Theil, A., Wilhelm, C., Petzold, C., Huebel, N., Kretschmer, K., Bonifacio, E. & Monti, P. (2012) IL-7 abrogates suppressive activity of human CD4+CD25+FOXP3+ regulatory T cells and allows expansion of alloreactive and autoreactive T cells. *Journal of immunology*. 189 (12), 5649–5658.
- Hermankova, B., Zajicova, A., Javorkova, E., Chudickova, M., Trosan, P., Hajkova, M., Krulova, M. & Holan, V. (2016) Suppression of IL-10 production by activated B cells via a cell contact-dependent cyclooxygenase-2 pathway upregulated in IFN- γ -treated mesenchymal stem cells. *Immunobiology*. 221 (2), 129–136.
- Hernandez, M.D.P., Martin, P. & Simkins, J. (2015) Infectious Complications After Liver Transplantation. *Gastroenterology & hepatology*. 11 (11), 741–753.
- Hey, Y.Y. & O'Neill, H.C. (2012) Murine spleen contains a diversity of myeloid and dendritic cells distinct in antigen presenting function. *Journal of Cellular and Molecular Medicine*. 16 (11), 2611–2619.
- Highfill, S.L., Kelly, R.M., Shaughnessy, M.J.O., Zhou, Q., Xia, L., Taylor, P.A., Tolar, J., Blazar, B.R., Dc, W. & Panoskaltsis-mortari, A. (2009) Multipotent adult progenitor cells can suppress graft-versus-host disease via prostaglandin E 2 synthesis and only if localized to sites of allopriming Multipotent adult progenitor cells can suppress graft-

versus-host disease via prostaglandin E₂ synthesis. *Blood*. 114 (3), 693–701.

Hildner, K., Edelson, B.T., Purtha, W.E., Diamond, M., Matsushita, H., Kohyama, M., Calderon, B., Schraml, B.U., Unanue, E.R., Diamond, M.S., Schreiber, R.D., Murphy, T.L. & Murphy, K.M. (2008) Batf3 deficiency reveals a critical role for CD8 α ⁺ dendritic cells in cytotoxic T cell immunity. *Science (New York, N.Y.)*. 322 (5904), 1097–1100.

Hoffmann-Fezer, G., Gall, C., Zengerle, U., Kranz, B. & Thierfelder, S. (1993) Immunohistology and immunocytology of human T-cell chimerism and graft-versus-host disease in SCID mice. *Blood*. 81 (12), 3440–3448.

Hollingshead, H.E., Morimura, K., Adachi, M., Kennett, M.J., Billin, A.N., Willson, T.M., Gonzalez, F.J. & Peters, J.M. (2007) PPAR β / δ protects against experimental colitis through a ligand-independent mechanism. *Digestive Diseases and Sciences*. 52 (11), 2912–2919.

Hoogduijn, M.J., Roemeling-van Rhijn, M., Engela, A.U., Korevaar, S.S., Mensah, F.K.F., Franquesa, M., de Bruin, R.W.F., Betjes, M.G.H., Weimar, W. & Baan, C.C. (2013) Mesenchymal stem cells induce an inflammatory response after intravenous infusion. *Stem cells and development*. 22 (21), 2825–2835.

van den Hoogen, M.W.F., Hoitsma, A.J. & Hilbrands, L.B. (2012) Anti-T-cell antibodies for the treatment of acute rejection after renal transplantation. *Expert opinion on biological therapy*. 12 (8), 1031–1042.

Horwitz, E.M., Gordon, P.L., Koo, W.K.K., Marx, J.C., Neel, M.D., McNall, R.Y., Muul, L. & Hofmann, T. (2002) Isolated allogeneic bone marrow-derived mesenchymal cells engraft and stimulate growth in children with osteogenesis imperfecta: Implications for cell therapy of bone. *Proceedings of the National Academy of Sciences of the United States of America*. 99 (13), 8932–8937.

Horwitz, E.M., Prockop, D.J., Fitzpatrick, L.A., Koo, W.W., Gordon, P.L., Neel, M., Sussman,

- M., Orchard, P., Marx, J.C., Pyeritz, R.E. & Brenner, M.K. (1999) Transplantability and therapeutic effects of bone marrow-derived mesenchymal cells in children with osteogenesis imperfecta. *Nature medicine*. 5 (3), 309–313.
- Hsu, W.T., Lin, C.H., Chiang, B.L., Jui, H.Y., Wu, K.K.Y. & Lee, C.M. (2013) Prostaglandin E2 Potentiates Mesenchymal Stem Cell-Induced IL-10+IFN- +CD4+ Regulatory T Cells To Control Transplant Arteriosclerosis. *The Journal of Immunology*. 190 (5), 2372–2380.
- Ito, R., Katano, I., Kawai, K., Hirata, H., Ogura, T., Kamisako, T., Eto, T. & Ito, M. (2009) Highly Sensitive Model for Xenogenic GVHD Using Severe Immunodeficient NOG Mice. *Transplantation*. 87 (11), 1654–1658.
- Ito, R., Katano, I., Kawai, K., Yagoto, M., Takahashi, T., Ka, Y., Ogura, T., Takahashi, R. & Ito, M. (2017) A Novel Xenogeneic Graft-Versus-Host Disease Model for Investigating the Pathological Role of Human CD4 + or CD8 + T Cells Using Immunodeficient NOG Mice. *American Journal of Transplantation*. 17, 1216–1228.
- Itoh, S., Nakae, S., Axtell, R.C., Velotta, J.B., Kimura, N., Kajiwara, N., Iwakura, Y., Saito, H., Adachi, H., Steinman, L., Robbins, R.C. & Fischbein, M.P. (2010) IL-17 contributes to the development of chronic rejection in a murine heart transplant model. *Journal of clinical immunology*. 30 (2), 235–240.
- Jackson, J.S., Golding, J.P., Chapon, C., Jones, W.A. & Bhakoo, K.K. (2010) Homing of stem cells to sites of inflammatory brain injury after intracerebral and intravenous administration: a longitudinal imaging study. *Stem Cell Research & Therapy*. 1 (2), 17.
- Jacobs, S.A., Pinxteren, J., Roobrouck, V.D., Luyckx, A., van't Hof, W., Deans, R., Verfaillie, C.M., Waer, M., Billiau, A.D. & Van Gool, S.W. (2013) Human multipotent adult progenitor cells are nonimmunogenic and exert potent immunomodulatory effects on alloreactive T-cell responses. *Cell transplantation*. 22 (10), 1915–1928.
- Jacobs, S.A., Plessers, J., Pinxteren, J., Roobrouck, V.D., Verfaillie, C.M. & Van Gool, S.W. (2014) Mutual interaction between human multipotent adult progenitor cells and NK

- cells. *Cell Transplantation*. 23 (9), 1099–1110.
- Jaglowski, S.M. & Devine, S.M. (2014) Graft-versus-Host Disease : Why Haven't We Made More Progress. *Curr Opin Hematol*. 21 (2), 141–147.
- Jenq, R.R. & van den Brink, M.R.M. (2010) Allogeneic haematopoietic stem cell transplantation: individualized stem cell and immune therapy of cancer. *Nature Reviews Cancer*. 10 (3), 213–221.
- Jeon, M.S., Lim, H.J., Yi, T.G., Im, M.W., Yoo, H.S., Choi, J.H., Choi, E.Y. & Song, S.U. (2010) Xenoreactivity of human clonal mesenchymal stem cells in a major histocompatibility complex-matched allogeneic graft-versus-host disease mouse model. *Cellular Immunology*. 261 (1), 57–63.
- Jiang, D., Muschhammer, J., Qi, Y., Kugler, A., de Vries, J.C., Saffarzadeh, M., Sindrilaru, A., Vander Beken, S., Wlaschek, M., Kluth, M.A., Ganss, C., Frank, N.Y., Frank, M.H., Preissner, K.T. & Scharffetter-Kochanek, K. (2016) Suppression of Neutrophil-Mediated Tissue Damage-A Novel Skill of Mesenchymal Stem Cells. *Stem Cells*. 34, 2393–2406.
- Jiang, S., Herrera, O. & Lechler, R.I. (2004) New spectrum of allorecognition pathways: implications for graft rejection and transplantation tolerance. *Current opinion in immunology*. 16 (5), 550–557.
- Kang, K., Reilly, S.M., Karabacak, V., Gangl, M.R., Fitzgerald, K., Hatano, B. & Lee, C.H. (2008) Adipocyte-Derived Th2 Cytokines and Myeloid PPARdelta Regulate Macrophage Polarization and Insulin Sensitivity. *Cell Metabolism*. 7 (6), 485–495.
- Karp, J.M. & Leng Teo, G.S. (2009) Mesenchymal stem cell homing: the devil is in the details. *Cell stem cell*. 4 (3), 206–216.
- Kavanagh, H. & Mahon, B.P. (2011) Allogeneic mesenchymal stem cells prevent allergic airway inflammation by inducing murine regulatory T cells. *Allergy*. 66 (4), 523–531.
- Kebriaei, P., Isola, L., Bahceci, E., Holland, K., Rowley, S., McGuirk, J., Devetten, M.,

- Jansen, J., Herzig, R., Schuster, M., Monroy, R. & Uberti, J. (2009) Adult Human Mesenchymal Stem Cells Added to Corticosteroid Therapy for the Treatment of Acute Graft-versus-Host Disease. *Biology of Blood and Marrow Transplantation*. 15 (7), 804–811.
- Kekre, N. & Antin, J.H. (2017) ATG in allogeneic stem cell transplantation: standard of care in 2017? Counterpoint. *Blood Advances*. 1 (9), 573–576.
- Kelly, E.A.B., Koziol-White, C.J.C., Clay, K.J., Liu, L.Y., Bates, M.E., Bertics, P.J. & Jarjour, N.N. (2009) Potential contribution of IL-7 to allergen-induced eosinophilic airway inflammation in asthma. *The Journal of Immunology*. 182 (3), 1404–1410.
- Kennelly, H., Mahon, B.P. & English, K. (2016) Human mesenchymal stromal cells exert HGF dependent cytoprotective effects in a human relevant pre-clinical model of COPD. *Scientific Reports*. 6 (April), 38207.
- Kerkela, E., Hakkarainen, T., Makela, T., Raki, M., Kambur, O., Kilpinen, L., Nikkila, J., Lehtonen, S., Ritamo, I., Pernu, R., Pietila, M., Takalo, R., Juvonen, T., Bergstrom, K., Kalso, E., Valmu, L., Laitinen, S., Lehenkari, P. & Nystedt, J. (2013) Transient proteolytic modification of mesenchymal stromal cells increases lung clearance rate and targeting to injured tissue. *Stem Cells Transl Med*. 2 (7), 510–520.
- Kim, J. & Hematti, P. (2009) Mesenchymal stem cell-educated macrophages: A novel type of alternatively activated macrophages. *Experimental Hematology*. 37 (12), 1445–1453.
- Kimura, M., Pobeziński, L., Guintier, T., Thomas, J., Adams, A., Park, J.H., Tai, X. & Singer, A. (2013) IL-7 signaling must be intermittent, not continuous, during CD8 T cell homeostasis to promote cell survival instead of cell death. *Nat Immunol*. 14 (2), 143–151.
- King, M.A., Covassin, L., Brehm, M.A., Racki, W., Pearson, T., Leif, J., Laning, J., Fodor, W., Foreman, O., Burzenski, L., Chase, T.H., Gott, B., Rossini, A.A., Bortell, R., Shultz, L.D. & Greiner, D.L. (2009) Human peripheral blood leucocyte non-obese diabetic-severe combined immunodeficiency interleukin-2 receptor gamma chain gene mouse model of

xenogeneic graft-versus-host-like disease and the role of host major histocompatibility complex. *Clinical and Experimental Immunology*. 157 (1), 104–118.

Kinnear, G., Jones, N.D. & Wood, K.J. (2013) Costimulation blockade : Current perspectives and implications for therapy. *Transplantation*. 95 (4), 527–535.

Ko, J.H., Lee, H.J., Jeong, H.J., Kim, M.K., Wee, W.R., Yoon, S., Choi, H., Prockop, D.J. & Oh, J.Y. (2016) Mesenchymal stem/stromal cells precondition lung monocytes/macrophages to produce tolerance against allo- and autoimmunity in the eye. *Proceedings of the National Academy of Sciences*. 113 (1), 158–163.

Komschlies, K.L., Gregorio, T.A., Gruys, M.E., Back, T.C., Faltynek, C.R. & Wiltout, R.H. (1994) Administration of recombinant human IL-7 to mice alters the composition of B-lineage cells and T cell subsets, enhances T cell function, and induces regression of established metastases. *The Journal of Immunology*. 152, 5776–5784.

Kota, D.J., Prabhakara, K.S., Toledano-Furman, N., Bhattarai, D., Chen, Q., DiCarlo, B., Smith, P., Triolo, F., Wenzel, P.L., Cox Jr, C.S. & Olson, S.D. (2017) Prostaglandin E2 Indicates Therapeutic Efficacy Of Mesenchymal Stem Cells In Experimental Traumatic Brain Injury. *Stem Cells*. 35 (5), 1416–1430.

Kovacsovics-Bankowski, M., Mauch, K., Raber, a, Streeter, P.R., Deans, R.J., Maziarz, R.T. & Van't Hof, W. (2008) Pre-clinical safety testing supporting clinical use of allogeneic multipotent adult progenitor cells. *Cytotherapy*. 10 (7), 730–742.

Kovacsovics-Bankowski, M., Streeter, P.R., Mauch, K.A., Frey, M.R., Raber, A., van't Hof, W., Deans, R. & Maziarz, R.T. (2009) Clinical scale expanded adult pluripotent stem cells prevent graft-versus-host disease. *Cellular immunology*. 255 (1–2), 55–60.

Koyama, M., Cheong, M., Markey, K.A., Gartlan, K.H., Kuns, R.D., Locke, K.R., Lineburg, K.E., Teal, B.E., Leveque-El mouttie, L., Bunting, M.D., Vuckovic, S., Zhang, P., Teng, M.W.L., Varelias, A., Tey, S.K., Wockner, L.F., Engwerda, C.R., Smyth, M.J., Belz, G.T., McColl, S.R., MacDonald, K.P.A. & Hill, G.R. (2015) Donor colonic CD103+

dendritic cells determine the severity of acute graft-versus-host disease. *Journal of Experimental Medicine*. 212 (8), 1–19.

Koyama, M. & Hill, G.R. (2017) *Review Article Alloantigen presentation and graft-versus-host disease : fuel for the fi re*. 127 (24), 2963–2971.

Koyama, M., Kuns, R.D., Olver, S.D., Raffelt, N.C., Wilson, Y.A., Don, A.L.J., Lineburg, K.E., Cheong, M., Robb, R.J., Markey, K.A., Varelias, A., Malissen, B., Hämmerling, G.J., Clouston, A.D., Engwerda, C.R., Bhat, P., MacDonald, K.P. a & Hill, G.R. (2011) Recipient nonhematopoietic antigen-presenting cells are sufficient to induce lethal acute graft-versus-host disease. *Nature Medicine*. 18 (1), 135–142.

Krampera, M., Cosmi, L., Angeli, R., Pasini, A., Liotta, F., Andreini, A., Santarlaschi, V., Mazzinghi, B., Pizzolo, G., Vinante, F., Romagnani, P., Maggi, E., Romagnani, S. & Annunziato, F. (2006) Role for interferon-gamma in the immunomodulatory activity of human bone marrow mesenchymal stem cells. *Stem cells*. 24 (2), 386–398.

Kuci, Z., Bonig, H., Kreyenberg, H., Bunos, M., Jauch, A., Janssen, J.W.G., Skific, M., Michel, K., Eising, B., Lucchini, G., Bakhtiar, S., Greil, J., Lang, P., Basu, O., von Luettichau, I., Schulz, A., Sykora, K.W., Jarisch, A., Soerensen, J., Salzmann-Manrique, E., Seifried, E., Klingebiel, T., Bader, P. & Kuci, S. (2016) Mesenchymal stromal cells from pooled mononuclear cells of multiple bone marrow donors as rescue therapy in pediatric severe steroid-refractory graft-versus-host disease: A multicenter survey. *Haematologica*. 101 (8), 985–994.

Kurtzberg, J., Prockop, S., Teira, P., Bittencourt, H., Lewis, V., Chan, K.W., Horn, B., Yu, L., Talano, J.A., Nemecek, E., Mills, C.R. & Chaudhury, S. (2014) Allogeneic human mesenchymal stem cell therapy (Remestemcel-L, Prochymal) as a rescue agent for severe refractory acute graft-versus-host disease in pediatric patients. *Biology of Blood and Marrow Transplantation*. 20 (2), 229–235.

Lechler, R.I. & Batchelor, J. (1982) Restoration of Immunogenicity To Passenger Addition of

Donor. *Journal of experimental medicine*. 155, 31–41.

- Lee, R.H., Pulin, A.A., Seo, M.J., Kota, D.J., Ylostalo, J., Larson, B.L., Semprun-Prieto, L., Delafontaine, P. & Prockop, D.J. (2014) Intravenous hMSCs Improve Myocardial Infarction in Mice because Cells Emobilized in Lung Are Activated to Secrete the Anti-inflammatory Protein TSG-6. *Cell Stem Cell*. 5 (1), 54–63.
- Lee, R.H., Seo, M.J., Pulin, A.A., Gregory, C.A., Ylostalo, J. & Prockop, D.J. (2009) The CD34-like protein PODXL and alpha6-integrin (CD49f) identify early progenitor MSCs with increased clonogenicity and migration to infarcted heart in mice. *Blood*. 113 (4), 816–826.
- Lehman, N., Cutrone, R., Raber, A., Perry, R., Van't Hof, W., Deans, R., Ting, A.E. & Woda, J. (2012) Development of a surrogate angiogenic potency assay for clinical-grade stem cell production. *Cytherapy*. 14, 994–1004.
- Leibacher, J., Dauber, K., Ehser, S., Brixner, V., Kollar, K., Vogel, A., Spohn, G., Sch??fer, R., Seifried, E. & Henschler, R. (2017) Human mesenchymal stromal cells undergo apoptosis and fragmentation after intravenous application in immune-competent mice. *Cytherapy*. 19 (1), 61–74.
- Leibacher, J. & Henschler, R. (2016) Biodistribution, migration and homing of systemically applied mesenchymal stem/stromal cells. *Stem Cell Research & Therapy*. 7 (1), 7.
- Li, D., Han, Y., Zhuang, Y., Fu, J., Liu, H., Shi, Q. & Ju, X. (2015) Overexpression of COX-2 but not indoleamine 2,3-dioxygenase-1 enhances the immunosuppressive ability of human umbilical cord-derived mesenchymal stem cells. *International Journal of Molecular Medicine*. 35 (5), 1309–1316.
- Li, F.R., Wang, X.G., Deng, C.Y., Qi, H., Ren, L.L. & Zhou, H.X. (2010a) Immune modulation of co-transplantation mesenchymal stem cells with islet on T and dendritic cells. *Clinical and Experimental Immunology*. 161 (2), 357–363.
- Li, H., Demetris, A.J., McNiff, J., Matte-Martone, C., Tan, H.S., Rothstein, D.M., Lakkis, F.G.

- & Shlomchik, W.D. (2012) Profound Depletion of Host Conventional Dendritic Cells, Plasmacytoid Dendritic Cells, and B Cells Does Not Prevent Graft-versus-Host Disease Induction. *The Journal of Immunology*. 188 (8), 3804–3811.
- Li, L., Huang, L., Vergis, A.L., Ye, H., Bajwa, A., Narayan, V., Strieter, R.M., Rosin, D.L. & Okusa, M.D. (2010b) IL-17 produced by neutrophils regulates IFN- γ – mediated neutrophil migration in mouse kidney ischemia-reperfusion injury. *Journal of clinical investigation*. 120, 331–342.
- Li, Y.P., Paczesny, S., Lauret, E., Poirault, S., Bordigoni, P., Mekhloufi, F., Hequet, O., Bertrand, Y., Ou-Yang, J.P., Stolz, J.F., Miossec, P. & Eljaafari, A. (2008) Human Mesenchymal Stem Cells License Adult CD34+ Hemopoietic Progenitor Cells to Differentiate into Regulatory Dendritic Cells through Activation of the Notch Pathway. *The Journal of Immunology*. 180, 1598–1608.
- Lionaki, S., Panagiotellis, K., Iniotaki, A. & Boletis, J.N. (2013) Incidence and clinical significance of de novo donor specific antibodies after kidney transplantation. *Clinical & developmental immunology*. 2013, 849835.
- Liu, W., Zhang, S., Gu, S., Sang, L. & Dai, C. (2015) Mesenchymal stem cells recruit macrophages to alleviate experimental colitis through TGF β 1. *Cellular Physiology and Biochemistry*. 35 (3), 858–865.
- Liu, Y., Wang, L., Kikuri, T., Akiyama, K., Chen, C., Xu, X., Yang, R., Chen, W., Wang, S. & Shi, S. (2012) Mesenchymal Stem Cell-Based Tissue Regeneration is Governed by Recipient T Lymphocyte via IFN- γ and TNF- α . *Nature medicine*. 17 (12), 1594–1601.
- Liu, Z., Fan, H. & Jiang, S. (2013) CD4(+) T-cell subsets in transplantation. *Immunological reviews*. 252 (1), 183–191.
- Lo, H.W., Cao, X., Zhu, H. & Ali-Osman, F. (2010) Cyclooxygenase-2 Is a Novel Transcriptional Target of the Nuclear EGFR-STAT3 and EGFRvIII-STAT3 Signaling Axes. *Molecular Cancer Research*. 8 (2), 232–245.

- Lockridge, J.L., Zhou, Y., Becker, Y.A., Ma, S., Kenney, S.C., Hematti, P., Capitini, C.M., Burlingham, W.J., Gendron-Fitzpatrick, A. & Gumperz, J.E. (2013) Mice engrafted with human fetal thymic tissue and hematopoietic stem cells develop pathology resembling chronic graft-versus-host disease. *Biology of Blood and Marrow Transplantation*. 19 (9), 1310–1322.
- Lowenstein, H., Shah, A., Chant, A. & Khan, A. (2006) Different mechanisms of Campath-1H-mediated depletion for CD4 and CD8 T cells in peripheral blood. *Transplant international*. 19 (11), 927–936.
- Luk, F., de Witte, S., Korevaar, S.S., Roemeling-van Rhijn, M., Franquesa, M., Strini, T., van den Engel, S., Gargasha, M., Roy, D., Dor, F.J., Horwitz, E.M., de Bruin, R.W., Betjes, M.G., Baan, C.C. & Hoogduijn, M.J. (2016) Inactivated mesenchymal stem cells maintain immunomodulatory capacity. *Stem cells and development*. 25 (18), 1342–1354.
- Lundstrom, W., Highfill, S., Walsh, S.T.R., Beq, S., Morse, E., Kockum, I., Alfredsson, L., Olsson, T., Hillert, J. & Mackall, C.L. (2013) Soluble IL7R potentiates IL-7 bioactivity and promotes autoimmunity. *Proceedings of the National Academy of Sciences*. 110 (19), E1761–E1770.
- Luz-Crawford, P., Djouad, F., Toupet, K., Bony, C., Franquesa, M., Hoogduijn, M.J., Jorgensen, C. & Noel, D. (2016a) Mesenchymal Stem Cell-Derived Interleukin 1 Receptor Antagonist Promotes Macrophage Polarization and Inhibits B Cell Differentiation. *Stem Cells*. 483–492.
- Luz-Crawford, P., Ipseiz, N., Espinosa-Carrasco, G., Caicedo, A., Tejedor, G., Toupet, K., Loriau, J., Scholtysek, C., Stoll, C., Khoury, M., Noël, D., Jorgensen, C., Krönke, G. & Djouad, F. (2016b) PPAR β/δ directs the therapeutic potential of mesenchymal stem cells in arthritis. *Annals of the Rheumatic Diseases*. 75 (12), 2166–2174.
- Luz-Crawford, P., Kurte, M., Bravo-Alegría, J., Contreras, R., Nova-Lamperti, E., Tejedor, G., Noël, D., Jorgensen, C., Figueroa, F., Djouad, F. & Carrión, F. (2013) Mesenchymal

- stem cells generate a CD4⁺CD25⁺Foxp3⁺ regulatory T cell population during the differentiation process of Th1 and Th17 cells. *Stem cell research & therapy*. 4 (65), 1–12.
- Luz-Crawford, P., Noël, D., Fernandez, X., Khoury, M., Figueroa, F., Carrión, F., Jorgensen, C. & Djouad, F. (2012) Mesenchymal Stem Cells Repress Th17 Molecular Program through the PD-1 Pathway. *PLoS ONE*. 7 (9), e45272.
- Luz-Crawford, P., Torres, M.J., Noel, D., Fernandez, A., Toupet, K., Alcayaga-Miranda, F., Tejedor, G., Jorgensen, C., Illanes, S.E., Figueroa, F.E., Djouad, F. & Khoury, M. (2016c) Immunosuppressive Signature of Menstrual Blood Mesenchymal Stem Cells Entails Opposite Effects on Experimental Arthritis and Graft Versus Host Diseases. *Stem Cells*. 34, 456–469.
- Macedo, C., Walters, J.T., Orkis, E.A., Isse, K., Elinoff, B.D., Fedorek, S.P., McMichael, J.M., Chalasani, G., Randhawa, P., Demetris, A.J., Zeevi, A., Tan, H., Shapiro, R., Landsittel, D., Lakkis, F.G. & Metes, D. (2012) Long-Term Effects of Alemtuzumab on Regulatory and Memory T-Cell Subsets in Kidney Transplantation. *Transplantation*. 93 (8), 813–821.
- Mackall, C.L., Fry, T.J. & Gress, R.E. (2011) Harnessing the biology of IL-7 for therapeutic application. *Nature reviews. Immunology*. 11 (5), 330–342.
- Maggini, J., Mirkin, G., Bognanni, I., Holmberg, J., Piazzón, I.M., Nepomnaschy, I., Costa, H., Cañones, C., Raiden, S., Vermeulen, M. & Geffner, J.R. (2010) Mouse bone marrow-derived mesenchymal stromal cells turn activated macrophages into a regulatory-like profile. *PLoS ONE*. 5 (2), e9252.
- Mai, H. Le, Boeffard, F., Longis, J., Danger, R., Martinet, B., Haspot, F., Vanhove, B., Brouard, S. & Soulillou, J.P. (2014) IL-7 receptor blockade following T cell depletion promotes long-term allograft survival. *Journal of Clinical Investigation*. 124 (4), 1723–1733.
- Malaspina, A., Moir, S., Ho, J., Wang, W., Howell, M.L., O’Shea, M.A., Roby, G.A., Rehm,

- C.A., Mican, J.M., Chun, T.W. & Fauci, A.S. (2006) Appearance of immature/transitional B cells in HIV-infected individuals with advanced disease: Correlation with increased IL-7. *Proceedings of the National Academy of Sciences*. 103 (7), 2262–2267.
- Marco, M.R., Dons, E., van der Windt, D., Bhama, J.K., Lu, L.T., Zahorchak, A.F., Lakkis, F.G., Cooper, D.K.C., Ezzelarab, M.B. & Thomson, A.W. (2013) Post-transplant repopulation of naive and memory T cells in blood and lymphoid tissue after alemtuzumab-mediated depletion in heart-transplanted cynomolgus monkeys. *Transplant Immunology*. 29, 88–98.
- Marino, J., Babiker-Mohamed, M.H., Crosby-Bertorini, P., Paster, J.T., LeGuern, C., Germana, S., Abdi, R., Uehara, M., Kim, J.I., Markmann, J.F., Tocco, G. & Benichou, G. (2016) Donor exosomes rather than passenger leukocytes initiate alloreactive T cell responses after transplantation. *Science Immunology*. 1 (1), 1–21.
- Marino, J., Paster, J. & Benichou, G. (2016) Allorecognition by T lymphocytes and allograft rejection. *Frontiers in Immunology*. 7 (DEC), 1–9.
- Markey, K.A., Banovic, T., Kuns, R.D., Olver, S.D., Don, A.L.J., Raffelt, N.C., Wilson, Y.A., Raggatt, L.J., Pettit, A.R., Bromberg, J.S., Hill, G.R. & MacDonald, K.P.A. (2009) Conventional dendritic cells are the critical donor APC presenting alloantigen after experimental bone marrow transplantation. *Blood*. 113 (22), 5644–5649.
- Markey, K.A., Koyama, M., Gartlan, K.H., Leveque, L., Kuns, R.D., Lineburg, K.E., Teal, B.E., MacDonald, K.P. a. & Hill, G.R. (2014) Cross-Dressing by Donor Dendritic Cells after Allogeneic Bone Marrow Transplantation Contributes to Formation of the Immunological Synapse and Maximizes Responses to Indirectly Presented Antigen. *The Journal of Immunology*. 192 (11), 5426–5433.
- Markey, K.A., Macdonald, K.P. a & Hill, G.R. (2014) The biology of graft-versus-host disease : experimental systems instructing clinical practice. *Blood*. 124 (3), 354–363.

- Martin, C.E., van Leeuwen, E.M.M., Im, S.J., Roopenian, D.C., Sung, Y.C. & Surh, C.D. (2013) IL-7/anti-IL-7 mAb complexes augment cytokine potency in mice through association with IgG-Fc and by competition with IL-7R. *Blood*. 121 (22), 4484–4492.
- Martin, P.J., Lee, S.J., Przepiorka, D., Horowitz, M.M., Koreth, J., Vogelsang, G.B., Walker, I., Carpenter, P.A., Griffith, L.M., Mohty, M., Wolff, D., Pavletic, S.Z. & Cutler, C.S. (2015) National Institutes of Health Consensus Development Project on Criteria for Clinical Trials in Chronic Graft-versus-Host Disease: VI. The 2014 Clinical Trial Design Working Group Report. *Biol Blood Marrow Transplant*. 21 (8), 1343–1359.
- Martin, P.J., Uberti, J.P., Soiffer, R.J., Klingemann, H., Waller, E.K., Daly, A.S., Herrmann, R.P. & Kebriaei, P. (2010) Prochymal Improves Response Rates In Patients With Steroid-Refractory Acute Graft Versus Host Disease (SR-GVHD) Involving The Liver And Gut: Results Of A Randomized, Placebo-Controlled, Multicenter Phase III Trial In GVHD. *Biology of Blood and Marrow Transplantation*. 16 (2), S169–S170.
- Masson, D.A., Bouaziz, J. david, Buanec, L.H., Robin, M., Meara, A.O., Parquet, N., Rybojad, M., Hau, E., Monfort, J.B., Branchtein, M., Michonneau, D., Dessirier, V., Fontbrune, F.S. De, Bergeron, A., Itzykson, R., Dhedin, N., Bengoufa, D., Peffault de Latour, R., Xhaard, A., Bagot, M., Bensussan, A. & Socié, G. (2015) CD24 hi CD27 1 and plasmablast-like regulatory B cells in human chronic graft-versus-host disease. *Transplantation*. 125 (11), 1830–1840.
- Mathias, L.J., Khong, S.M.L., Spyroglou, L., Payne, N.L., Siatskas, C., Thorburn, A.N., Boyd, R.L. & Heng, T.S.P. (2013) Alveolar macrophages are critical for the inhibition of allergic asthma by mesenchymal stromal cells. *Journal of immunology*. 191 (12), 5914–5924.
- Matthews, K., Lim, Z., Afzali, B., Pearce, L., Abdallah, A., Kordasti, S., Pagliuca, A., Lombardi, G., Madrigal, J.A., Mufti, G.J. & Barber, L.D. (2009) Imbalance of effector and regulatory CD4 T cells is associated with graft-versus-host disease after hematopoietic stem cell transplantation using a reduced intensity conditioning regimen

and alemtuzumab. *Haematologica*. 94 (7), 956–966.

Mauiyyedi, S., Pelle, P.D., Saidman, S., Collins, A.B., Pascual, M., Tolkoff-Rubin, N.E., Williams, W.W., Cosimi, A.A., Schneeberger, E.E. & Colvin, R.B. (2001) Chronic humoral rejection: identification of antibody-mediated chronic renal allograft rejection by C4d deposits in peritubular capillaries. *Journal of the American Society of Nephrology*. 12 (3), 574–582.

Mays, R. & Deans, R. (2016) Adult adherent cell therapy for ischemic stroke: Clinical results and development experience using MultiStem. *Transfusion*. 56 (4), 6S–8S.

Maziarz, R.T., Devos, T., Bachier, C., Goldstein, S.C., Leis, J., Cooke, K.R., Perry, R., Deans, R.J., Van't Hof, W.J. & Lazarus, H.M. (2012) Prophylaxis of Acute GVHD Using Multistem® Stromal Cell Therapy: Preliminary Results After Administration of Single or Multiple Doses in a Phase 1 Trial. *Biology of Blood and Marrow Transplantation*. 18 (2), S264–S265.

Maziarz, R.T., Devos, T., Bachier, C.R., Goldstein, S.C., Leis, J.F., Devine, S.M., Meyers, G., Gajewski, J.L., Maertens, J., Deans, R.J., Van't Hof, W. & Lazarus, H.M. (2015) Single and Multiple Dose MultiStem (Multipotent Adult Progenitor Cell) Therapy Prophylaxis of Acute Graft-versus-Host Disease in Myeloablative Allogeneic Hematopoietic Cell Transplantation: A Phase 1 Trial. *Biology of Blood and Marrow Transplantation*. 21 (4), 720–728.

Mazzucchelli, R. & Durum, S.K. (2007) Interleukin-7 receptor expression: intelligent design. *Nature reviews. Immunology*. 7 (2), 144–154.

Mcdonald-Hyman, C., Turka, L.A. & Blazar, B.R. (2015) Advances and Challenges in Immunotherapy for Solid Organ and Bone Marrow Transplantation. *Science Translational Medicine*. 7 (280).

Mcdonald, G.B. (2016) How I Treat How I treat acute graft-versus-host disease of the gastrointestinal tract and the liver. *Blood*. 127 (12), 1544–1551.

- Meisel, R., Zibert, A., Laryea, M., Gobel, U., Daubener, W. & Dilloo, D. (2004) Human bone marrow stromal cells inhibit allogeneic T cell responses by indoleamine 2,3-dioxygenase-mediated tryptophan degradations. *Blood*. 103 (12), 4619–4621.
- Melief, S.M., Schrama, E., Brugman, M.H., Tiemessen, M.M., Hoogduijn, M.J., Fibbe, W.E. & Roelofs, H. (2013) Multipotent stromal cells induce human regulatory T cells through a novel pathway involving skewing of monocytes toward anti-inflammatory macrophages. *Stem Cells*. 31 (9), 1980–1991.
- Mertsching, E., Burdet, C. & Ceredig, R. (1995) IL-7 transgenic mice: Analysis of the role of IL-7 in the differentiation of thymocytes in vivo and in vitro. *International Immunology*. 7 (3), 401–414.
- Meyer, C., Walker, J., Dewane, J., Engelmann, F., Laub, W., Pillai, S., Thomas Jr., C.R. & Messaoudi, I. (2015) Impact of irradiation and immunosuppressive agents on immune system homeostasis in rhesus macaques. *Clinical and experimental immunology*. 181 (3), 491–510.
- Meza-Perez, S. & Randall, T.D. (2017) Immunological Functions of the Omentum. *Trends in Immunology*. 21 (0), E182–E189.
- Mills, E.L. & O'Neill, L.A. (2016) Reprogramming mitochondrial metabolism in macrophages as an anti-inflammatory signal. *European Journal of Immunology*. 46 (1), 13–21.
- Miroux, C., Moralès, O., Carpentier, A., Dharancy, S., Conti, F., Boleslawski, E., Podevin, P., Auriault, C., Pancré, V. & Delhem, N. (2009) Inhibitory Effects of Cyclosporine on Human Regulatory T Cells In Vitro. *Transplantation Proceedings*. 41 (8), 3371–3374.
- Miroux, C., Morales, O., Ghazal, K., Othman, S. Ben, de Launoit, Y., Pancré, V., Conti, F. & Delhem, N. (2012) In Vitro Effects of Cyclosporine A and Tacrolimus on Regulatory T-Cell Proliferation and Function. *Transplantation*. 94 (2), 123–131.
- Mohty, M. (2007) Mechanisms of action of antithymocyte globulin: T-cell depletion and beyond. *Leukemia*. 21 (7), 1387–1394.

- Moll, G., Alm, J.J., Davies, L.C., von Bahr, L., Heldring, N., Stenbeck-Funke, L., Hamad, O.A., Hinsch, R., Ignatowicz, L., Locke, M., Lonnie, H., Lambris, J.D., Teramura, Y., Nilsson-Ekdahl, K., Nilsson, B. & Le Blanc, K. (2014) Do Cryopreserved Mesenchymal Stromal Cells Display Impaired Immunomodulatory and Therapeutic Properties? *Stem Cells*. 32 (9), 2430–2442.
- Moll, G. & Blanc, K. Le (2015) Engineering more efficient multipotent mesenchymal stromal (stem) cells for systemic delivery as cellular therapy. *ISBT Science Series*. 10 (1), 357–365.
- Monti, P. & Piemonti, L. (2013) Homeostatic T cell proliferation after islet transplantation. *Clinical and Developmental Immunology*. 2013.
- Mora-Lee, S., Sirerol-Piquer, M.S., Gutiérrez-Pérez, M., Gomez-Pinedo, U., Roobrouck, V.D., López, T., Casado-Nieto, M., Abizanda, G., Rabena, M.T., Verfaillie, C., Prósper, F. & García-Verdugo, J.M. (2012) Therapeutic Effects of hMAPC and hMSC Transplantation after Stroke in Mice. *PLoS ONE*. 7 (8), 1–11.
- Morikawa, H. & Sakaguchi, S. (2014) Genetic and epigenetic basis of Treg cell development and function: From a FoxP3-centered view to an epigenome-defined view of natural Treg cells. *Immunological Reviews*. 259 (1), 192–205.
- Morrissey, P.J., Conlon, P., Braddy, S., Williams, D.E., Namen, A.E. & Mochizuki, D.Y. (1991a) Administration of IL-7 to mice with cyclophosphamide-induced lymphopenia accelerates lymphocyte repopulation. *Journal of Immunology*. 146, 1547–1552.
- Morrissey, P.J., Conlon, P., Charrier, K., Braddy, S., Alpert, A., Namen, a E., Mochizuki, D., Namen, E., Williams, D., Braddy, S., Alpert, A. & Mochizuki, D. (1991b) Administration of IL-7 to normal mice stimulates B-lymphopoiesis and peripheral lymphadenopathy. *The Journal of Immunology*. 147, 561–568.
- Mounayar, M., Kefaloyianni, E., Smith, B., Solhjoui, Z., Maarouf, O.H., Azzi, J., Chabtini, L., Fiorina, P., Kraus, M., Briddell, R., Fodor, W., Herrlich, A. & Abdi, R. (2015) PI3ka and

- STAT1 interplay regulates human mesenchymal stem cell immune polarization. *Stem Cells*. 33 (6), 1892–1901.
- Moxham, V.F., Karegli, J., Phillips, R.E., Brown, K.L., Tapmeier, T.T., Hangartner, R., Sacks, S.H. & Wong, W. (2008) Homeostatic Proliferation of Lymphocytes Results in Augmented Memory-Like Function and Accelerated Allograft Rejection. *The Journal of Immunology*. 180 (6), 3910–3918.
- Mudrabettu, C., Kumar, V., Rakha, A., Yadav, A.K., Ramachandran, R., Kanwar, D.B., Nada, R., Minz, M., Sakhuja, V., Marwaha, N. & Jha, V. (2015) Safety and efficacy of autologous mesenchymal stromal cells transplantation in patients undergoing living donor kidney transplantation: A pilot study. *Nephrology*. 20 (1), 25–33.
- Munir, H., Luu, N.T., Clarke, L.S.C., Nash, G.B. & McGettrick, H.M. (2016) Comparative ability of mesenchymal stromal cells from different tissues to limit neutrophil recruitment to inflamed endothelium. *PLoS ONE*. 11 (5), 1–18.
- Murphy, W.J. (2000) Revisiting graft-versus-host disease models of autoimmunity: New insights in immune regulatory processes. *Journal of Clinical Investigation*. 106 (6), 745–747.
- Najar, M., Raicevic, G., Fayyad-Kazan, H., Bron, D., Toungouz, M. & Lagneaux, L. (2016) Mesenchymal stromal cells and immunomodulation: A gathering of regulatory immune cells. *Cytotherapy*. 18 (2), 160–171.
- Nakanishi, M. & Rosenberg, D.W. (2013) Multifaceted roles of PGE2 in inflammation and cancer. *Seminars in Immunopathology*. 35 (2), 123–137.
- Ben Nasr, M., Vergani, A., Avruch, J., Liu, L., Kefaloyianni, E., D’Addio, F., Tezza, S., Corradi, D., Bassi, R., Valderrama-Vasquez, A., Usuelli, V., Kim, J., Azzi, J., El Essawy, B., Markmann, J., Abdi, R. & Fiorina, P. (2015) Co-transplantation of autologous MSCs delays islet allograft rejection and generates a local immunoprivileged site. *Acta Diabetologica*. 52 (5), 917–927.

- Németh, K., Leelahavanichkul, A., Yuen, P.S.T., Mayer, B., Doi, K., Robey, P.G., Leelahavanichkul, K., Koller, B.H., Brown, J.M., Hu, X., Jelinek, I., Star, R.A. & Mezey, É. (2009) Bone marrow stromal cells attenuate sepsis via prostaglandin E₂-dependent reprogramming of host macrophages to increase their interleukin-10 production. *Nature medicine*. 15 (1), 42–49.
- Neujahr, D.C., Chen, C., Huang, X., Markmann, J.F., Cobbold, S., Waldmann, H., Sayegh, M.H., Hancock, W.W. & Turka, L.A. (2006) Accelerated Memory Cell Homeostasis during T Cell Depletion and Approaches to Overcome It. *The Journal of Immunology*. 176 (8), 4632–4639.
- Ng, K.S., Kunczewicz, T.M. & Karp, J.M. (2015) Beyond hit-and-run: Stem cells leave a lasting memory. *Cell Metabolism*. 22 (4), 541–543.
- Nguyen, M.T.J.P., Fryml, E., Sahakian, S.K., Liu, S., Michel, R.P., Lipman, M.L., Mucsi, I., Cantarovich, M., Tchervenkov, J.I. & Paraskevas, S. (2014) Pretransplantation recipient regulatory T cell suppressive function predicts delayed and slow graft function after kidney transplantation. *Transplantation*. 98 (7), 745–753.
- Nguyen, P.K., Riegler, J. & Wu, J.C. (2014) Stem cell imaging: From bench to bedside. *Cell Stem Cell*. 14 (4), 431–444.
- Nikolic, B., Lee, S., Bronson, R.T., Grusby, M.J. & Sykes, M. (2000) Th1 and Th2 mediate acute graft-versus-host disease, each with distinct end-organ targets. *Journal of Clinical Investigation*. 105 (9), 1289–1298.
- Noh, M.Y., Lim, S.M., Oh, K.W., Cho, K.A., Park, J., Kim, K.S., Lee, S.J., Kwon, M.S. & Kim, S.H. (2016) Mesenchymal Stem Cells Modulate the Functional Properties of Microglia via TGF- β Secretion. *Stem cells translational medicine*. 5, 1538–1549.
- Noone, C., Kihm, A., English, K., O’Dea, S. & Mahon, B.P. (2013) IFN- γ stimulated human umbilical-tissue-derived cells potently suppress NK activation and resist NK-mediated cytotoxicity in vitro. *Stem cells and development*. 22 (22), 3003–3014.

- Noorchashm, H., Reed, A.J., Rostami, S.Y., Mozaffari, R., Zekavat, G., Koeberlein, B., Caton, A.J. & Najj, A. (2006) B cell-mediated antigen presentation is required for the pathogenesis of acute cardiac allograft rejection. *The Journal of Immunology*. 177 (11), 7715–7722.
- Noris, M., Casiraghi, F., Todeschini, M., Cravedi, P., Cugini, D., Monteferrante, G., Aiello, S., Cassis, L., Gotti, E., Gaspari, F., Cattaneo, D., Perico, N. & Remuzzi, G. (2007) Regulatory T cells and T cell depletion: role of immunosuppressive drugs. *Journal of the American Society of Nephrology*. 18 (3), 1007–1018.
- Obermajer, N., Popp, F.C., Soeder, Y., Haarer, J., Geissler, E., Schlitt, H.J. & Dahlke, M.H. (2014a) Conversion of Th17 into IL-17A(neg) regulatory T cells: a novel mechanism in prolonged allograft survival promoted by mesenchymal stem cell-supported minimized immunosuppressive therapy. *Journal of immunology*. 193 (10), 4988–4999.
- Obermajer, N., Popp, F.C., Soeder, Y., Haarer, J., Geissler, E.K., Schlitt, H.J. & Dahlke, M.H. (2014b) Conversion of Th17 into IL-17A^{neg} Regulatory T Cells: A Novel Mechanism in Prolonged Allograft Survival Promoted by Mesenchymal Stem Cell-Supported Minimized Immunosuppressive Therapy. *The Journal of Immunology*. 193 (10), 4988–4999.
- Odegaard, J.I., Ricardo-Gonzalez, R.R., Red Eagle, A., Vats, D., Morel, C.R., Goforth, M.H., Subramanian, V., Mukundan, L., Ferrante, A.W. & Chawla, A. (2008) Alternative M2 Activation of Kupffer Cells by PPAR delta Ameliorates Obesity-Induced Insulin Resistance. *Cell Metabolism*. 7 (6), 496–507.
- Pan, G., Chen, Z., Xu, L., Zhu, J., Xiang, P., Ma, J., Peng, Y., Li, G., Chen, X., Fang, J., Guo, Y., Zhang, L. & Liu, L. (2016) Low-dose tacrolimus combined with donor-derived mesenchymal stem cells after renal transplantation: a prospective, non-randomized study. *Oncotarget*. 5 (11), 12089–12101.
- Parmar, S., Liu, X., Tung, S.S., Robinson, S.N., Rodriguez, G., Cooper, L.J.N., Yang, H.,

- Shah, N., Yang, H., Konopleva, M., Molldrem, J.J., Garcia-Manero, G., Najjar, A., Yvon, E., McNiece, I., Rezvani, K., Savoldo, B., Bollard, C.M. & Shpall, E.J. (2014) Third Party Umbilical Cord Blood-Derived Regulatory T cells Prevent Xenogenic Graft-versus-Host Disease. *Cytotherapy*. 16 (1), 90–100.
- Patel, R. & Paya, C. V (1997) Infections in solid-organ transplant recipients. *Clin Microbiol Rev*. 10 (1), 86–124.
- Pearson, T., Greiner, D.L. & Shultz, L.D. (2008) Creation of Humanized’’ Mice to Study Human Immunity. *Current Protocols in Immunology*. 81 (15.21).
- Peng, Y., Chen, X., Liu, Q., Xu, D., Zheng, H., Liu, L., Liu, Q., Liu, M., Fan, Z., Sun, J., Li, X., Zou, R. & Xiang, A.P. (2014a) Alteration of Naïve and Memory B-Cell Subset in Chronic Graft-Versus-Host Disease Patients After Treatment With Mesenchymal Stromal Cells. *STEM CELLS Translational Medicine*. 3 (9), 1023–1031.
- Peng, Y., Chen, X., Liu, Q., Zhang, X., Huang, K., Liu, L., Li, H., Zhou, M., Huang, F., Fan, Z., Sun, J., Ke, M., Li, X., Zhang, Q. & Xiang, A. (2014b) Mesenchymal stromal cells infusions improve refractory chronic graft versus host disease through an increase of CD5+ regulatory B cells producing interleukin 10. *Leukemia*. (January), 636–646.
- Perico, N., Casiraghi, F., Inrona, M., Gotti, E., Todeschini, M., Cavinato, R.A., Capelli, C., Rambaldi, A., Cassis, P., Rizzo, P., Cortinovis, M., Marasa, M., Golay, J., Noris, M. & Remuzzi, G. (2011) Autologous Mesenchymal Stromal Cells and Kidney Transplantation: A Pilot Study of Safety and Clinical Feasibility. *Clinical Journal of the American Society of Nephrology*. 6 (2), 412–422.
- Phinney, D.G., Galipeau, J., Krampera, M., Martin, I., Shi, Y. & Sensebe, L. (2013) MSCs: Science and Trials. *Nature Medicine*. 19 (7), 812–812.
- Phinney, D.G., Di Giuseppe, M., Njah, J., Sala, E., Shiva, S., St Croix, C.M., Stolz, D.B., Watkins, S.C., Di, Y.P., Leikauf, G.D., Kolls, J., Riches, D.W.H., Deiuliis, G., Kaminski, N., Boregowda, S. V, McKenna, D.H. & Ortiz, L.A. (2015) Mesenchymal stem cells use

- extracellular vesicles to outsource mitophagy and shuttle microRNAs. *Nature communications*. 6, 8472.
- Plas, D.R., Rathmell, J.C. & Thompson, C.B. (2002) Homeostatic control of lymphocyte survival: potential origins and implications. *Nat Immunol*. 3 (6), 515–521.
- Platanias, L.C. (2005) Mechanisms of type-I- and type-II-interferon-mediated signalling. *Nature Reviews Immunology*. 5 (5), 375–386.
- Plessers, J., Dekimpe, E., Van Woensel, M., Roobrouck, V.D., Bullens, D.M., Pinxteren, J., Verfaillie, C.M. & Van Gool, S.W. (2016) Clinical-Grade Human Multipotent Adult Progenitor Cells Block CD8+ Cytotoxic T Lymphocytes. *Stem Cells Translational Medicine*. 5, 1607–1619.
- Polchert, D., Sobinsky, J., Douglas, G.W., Kidd, M., Moadsiri, A., Reina, E., Genrich, K., Mehrotra, S., Setty, S., Smith, B. & Bartholomew, A. (2008) IFN- γ activation of mesenchymal stem cells for treatment and prevention of graft versus host disease. *European Journal of Immunology*. 38 (6), 1745–1755.
- Ponticelli, C. (2014) Ischaemia-reperfusion injury: a major protagonist in kidney transplantation. *Nephrology, dialysis, transplantation*. 29 (6), 1134–1140.
- Popp, F.C., Eggenhofer, E., Renner, P., Slowik, P., Lang, S.A., Kaspar, H., Geissler, E.K., Piso, P., Schlitt, H.J. & Dahlke, M.H. (2008) Mesenchymal stem cells can induce long-term acceptance of solid organ allografts in synergy with low-dose mycophenolate. *Transplant Immunology*. 20 (1–2), 55–60.
- Popp, F.C., Fillenberg, B., Eggenhofer, E., Renner, P., Dillmann, J., Benseler, V., Schnitzbauer, A.A., Hutchinson, J., Deans, R., Ladenheim, D., Graveen, C.A., Zeman, F., Koller, M., Hoogduijn, M.J., Geissler, E.K., Schlitt, H.J. & Dahlke, M.H. (2011) Safety and feasibility of third-party multipotent adult progenitor cells for immunomodulation therapy after liver transplantation--a phase I study (MISOT-I). *Journal of translational medicine*. 9 (1), 124.

- Prockop, D.J. & Olson, S.D. (2009) Clinical trials with adult stem / progenitor cells for tissue repair : let ' s not overlook some essential precautions. *Blood*. 109 (8), 3147–3151.
- Racusen, L.C. & Haas, M. (2006) Antibody-mediated rejection in renal allografts: lessons from pathology. *Clinical journal of the American Society of Nephrology*. 1 (3), 415–420.
- Rasmusson, I., Ringden, O., Sundberg, B. & Le Blanc, K. (2003) Mesenchymal stem cells inhibit the formation of cytotoxic T lymphocytes, but not activated cytotoxic T lymphocytes or natural killer cells. *Transplantation*. 76 (8), 1208–1213.
- Rauch, P.J., Chudnovskiy, A., Robbins, C.S., Weber, G.F., Etzrodt, M., Hilgendorf, I., Tiglaio, E., Figueiredo, J., Theurl, I., Gorbатов, R., Waring, M.T., Chicoine, A.T., Pittet, M.J., Nahrendorf, M., Weissleder, R. & Filip, K. (2012) Innate Response Activator B Cells Protect Against Microbial Sepsis. *Science*. 335 (6068), 597–601.
- Reading, J.L., Vaes, B., Hull, C., Sabbah, S., Hayday, T., Wang, N.S., DiPiero, A., Lehman, N.A., Taggart, J.M., Carty, F., English, K., Pinxteren, J., Deans, R., Ting, A.E. & Tree, T.I.M. (2015) Suppression of IL-7-dependent Effector T-cell Expansion by Multipotent Adult Progenitor Cells and PGE2. *Molecular therapy*. 23, 1783–1793.
- Reading, J.L., Yang, J.H.M., Sabbah, S., Skowera, A., Knight, R.R., Pinxteren, J., Vaes, B., Allsopp, T., Ting, A.E., Busch, S., Raber, A., Deans, R. & Tree, T.I.M. (2013) Clinical-grade multipotent adult progenitor cells durably control pathogenic T cell responses in human models of transplantation and autoimmunity. *Journal of immunology*. 190 (9), 4542–4552.
- Reddy, P., Negrin, R. & Hill, G.R. (2008) Mouse Models of Bone Marrow Transplantation. *Biology of Blood and Marrow Transplantation*. 14 (1), 129–135.
- Ren, G., Zhang, L., Zhao, X., Xu, G., Zhang, Y., Roberts, A.I., Zhao, R.C. & Shi, Y. (2008) Mesenchymal Stem Cell-Mediated Immunosuppression Occurs via Concerted Action of Chemokines and Nitric Oxide. *Cell Stem Cell*. 2 (2), 141–150.
- Ren, G., Zhao, X., Zhang, L., Zhang, J., L'Huillier, A., Ling, W., Roberts, A.I., Le, A.D., Shi,

- S., Shao, C. & Shi, Y. (2010) Inflammatory Cytokine-Induced Intercellular Adhesion Molecule-1 and Vascular Cell Adhesion Molecule-1 in Mesenchymal Stem Cells Are Critical for Immunosuppression. *The Journal of Immunology*. 184 (5), 2321–2328.
- Reyes, M. & Verfaillie, C.M. (2001) Characterization of multipotent adult progenitor cells, a subpopulation of mesenchymal stem cells. *Annals of the New York Academy of Sciences*. 938, 231-233-235.
- Ricciotti, E. & Fitzgerald, G.A. (2011) Prostaglandins and inflammation. *Arteriosclerosis, Thrombosis, and Vascular Biology*. 31 (5), 986–1000.
- Riesner, K., Kalupa, M., Shi, Y., Elezkurtaj, S. & Penack, O. (2016) A preclinical acute GVHD mouse model based on chemotherapy conditioning and MHC-matched transplantation. *Bone Marrow Transplantation*. 51 (3), 410–417.
- Ringden, O., Uzunel, M., Rasmusson, I., Remberger, M., Sundberg, B., Lonnies, H., Marschall, H.U., Dlugosz, A., Szakos, A., Hassan, Z., Omazic, B., Aschan, J., Barkholt, L. & Le Blanc, K. (2006) Mesenchymal Stem Cells for Treatment of Therapy-Resistant Graft-versus-Host Disease. *Transplantation*. 81 (10), 1390–1397.
- Robb, R.J. & Hill, G.R. (2012) The interferon-dependent orchestration of innate and adaptive immunity after transplantation. *Blood*. 119 (23), 5351–5358.
- Rogers, N.M., Isenberg, J.S. & Thomson, A.W. (2013) Plasmacytoid dendritic cells: no longer an enigma and now key to transplant tolerance. *Am J Transplant*. 13 (5), 1125–1133.
- Ronchetti, S., Ricci, E., Petrillo, M.G., Cari, L., Migliorati, G., Nocentini, G. & Riccardi, C. (2015) Glucocorticoid-induced tumour necrosis factor receptor-related protein: A key marker of functional regulatory T cells. *Journal of Immunology Research*. 2015.
- Roobrouck, V.D., Clavel, C., Jacobs, S.A., Ulloa-Montoya, F., Crippa, S., Sohni, A., Roberts, S.J., Luyten, F.P., Van Gool, S.W., Sampaolesi, M., Delforge, M., Luttun, A. & Verfaillie, C.M. (2011) Differentiation potential of human postnatal mesenchymal stem cells, mesoangioblasts, and multipotent adult progenitor cells reflected in their

transcriptome and partially influenced by the culture conditions. *Stem cells*. 29 (5), 871–882.

Rosado, M.M., Bernardo, M.E., Scarsella, M., Conforti, A., Biagini, S., Cascioli, S., Rossi, F., Guzzo, I., Strologo, L. Dello, Emma, F., Locatelli, F. & Carsetti, R. (2015) Inhibition of B-cell proliferation and antibody production by mesenchymal stromal cells is mediated by T cells. *Stem cells and development*. 24 (1), 93–103.

Rosser, E.C. & Mauri, C. (2015) Regulatory B Cells: Origin, Phenotype, and Function. *Immunity*. 42 (4), 607–612.

Rowe, V., Banovic, T., Macdonald, K.P., Kuns, R., Don, A.L., Morris, E.S., Burman, A.C., Bofinger, H.M., Clouston, A.D. & Hill, G.R. (2006) Host B cells produce IL-10 following TBI and attenuate acute GVHD after allogeneic bone marrow transplantation. Host B cells produce IL-10 following TBI and attenuate acute GVHD after allogeneic bone marrow transplantation. *Blood*. 108 (7), 2485–2492.

Rozenberg, A., Rezk, A., Boivin, M.N., Darlington, P.J., Nyirenda, M., Li, R., Jalili, F., Winer, R., Artsy, E.A., Uccelli, A., Reese, J.S., Planchon, S.M., Cohen, J.A. & Bar-Or, A. (2016) Human Mesenchymal Stem Cells Impact Th17 and Th1 Responses Through a Prostaglandin E2 and Myeloid-Dependent Mechanism. *Stem cells translational medicine*. 5, 1–9.

Ruzek, M.C., Neff, K.S., Luong, M., Smith, K.A., Culm-Merdek, K., Richards, S.M., Williams, J.M., Perricone, M. & Garman, R.D. (2009) In vivo characterization of rabbit anti-mouse thymocyte globulin: a surrogate for rabbit anti-human thymocyte globulin. *Transplantation*. 88 (2), 170–179.

Ruzek, M.C., Waire, J.S., Hopkins, D., Lacorcchia, G., Sullivan, J., Roberts, B.L., Richards, S.M., Nahill, S.R., Williams, J.M., Scaria, A., Dzuris, J., Shankara, S. & Garman, R.D. (2008) Characterization of in vitro antimurine thymocyte globulin – induced regulatory T cells that inhibit graft-versus-host disease in vivo. *Blood*. 111 (3), 1726–1734.

- Ryan, J.M., Barry, F.P., Murphy, J.M. & Mahon, B.P. (2005) Mesenchymal stem cells avoid allogeneic rejection. *Journal of inflammation*. 2 (8).
- Saat, T.C., Van Den Engel, S., Bijman-Lachger, W., Korevaar, S.S., Hoogduijn, M.J., Ijzermans, J.N.M. & De Bruin, R.W.F. (2016) Fate and Effect of Intravenously Infused Mesenchymal Stem Cells in a Mouse Model of Hepatic Ischemia Reperfusion Injury and Resection. *Stem Cells International*. 2016 (5761487).
- Sad, S., Marcotte, R. & Mosmann, T.R. (1995) Cytokine-induced differentiation of precursor mouse CD8⁺ T cells into cytotoxic CD8⁺ T cells secreting Th1 or Th2 cytokines. *Immunity*. 2 (3), 271–279.
- Sadeghi, B., Aghdami, N., Hassan, Z., Forouzanfar, M., Rozell, B., Abedi-Valugerdi, M. & Hassan, M. (2008) GVHD after chemotherapy conditioning in allogeneic transplanted mice. *Bone Marrow Transplantation*. 42 (12), 807–818.
- Safinia, N., Afzali, B., Atalar, K., Lombardi, G. & Lechler, R.I. (2010) T-cell alloimmunity and chronic allograft dysfunction. *Kidney International Suppl*. 78 (119), S2-12.
- Sala, E., Genua, M., Petti, L., Anselmo, A., Arena, V., Cibella, J., Zanotti, L., D'Alessio, S., Scaldaferrri, F., Luca, G., Arato, I., Calafiore, R., Sgambato, A., Rutella, S., Locati, M., Danese, S. & Vetrano, S. (2015) Mesenchymal Stem Cells Reduce Colitis in Mice via Release of TSG6, Independently of Their Localization to the Intestine. *Gastroenterology*. 149 (1), 163–176.
- Sarantopoulos, S., Blazar, B.R., Cutler, C. & Ritz, J. (2014) B Cells in Chronic Graft-versus-Host Disease. *Biology of blood and marrow transplantation*. 21 (2), 1–8.
- Sasaki, M., Abe, R., Fujita, Y., Ando, S., Inokuma, D. & Shimizu, H. (2008) Mesenchymal Stem Cells Are Recruited into Wounded Skin and Contribute to Wound Repair by Transdifferentiation into Multiple Skin Cell Types. *The Journal of Immunology*. 180, 2581–2587.
- Schmuck, E.G., Koch, J.M., Centanni, J.M., Hacker, T.A., Braun, R.K., Eldridge, M., Hei,

- D.J., Hematti, P. & Raval, A.N. (2016) Biodistribution and Clearance of Human Mesenchymal Stem Cells by Quantitative Three-Dimensional Cryo-Imaging After Intravenous Infusion in a Rat Lung Injury Model. *Stem Cells Transl Med.* 5, 1–8.
- Schrepfer, S., Deuse, T., Reichenspurner, H., Fischbein, M.P., Robbins, R.C. & Pelletier, M.P. (2007) Stem cell transplantation: the lung barrier. *Transplantation proceedings.* 39, 573–576.
- Schumann, T., Adhikary, T., Wortmann, A., Finkernagel, F., Lieber, S., Schnitzer, E., Legrand, N., Schober, Y., Nockher, W.A., Toth, P.M., Diederich, W.E., Nist, A., Stiewe, T., Wagner, U., Reinartz, S., Müller-Brüsselbach, S. & Müller, R. (2015) Deregulation of PPAR β/δ target genes in tumor-associated macrophages by fatty acid ligands in the ovarian cancer microenvironment. *Oncotarget.* 6 (15), 13416–13433.
- Selleri, S., Bifsha, P., Civini, S., Pacelli, C., Massar, M., Lemieux, W., Jin, P., Bazin, R., Patey, N., Marincola, M., Moldovan, F., Zaouter, C., Trudeau, L., Benabdhalla, B., Louis, I., Beauséjour, C. & Stroncek, D. (2016) Human mesenchymal stromal cell-secreted lactate induces M2- macrophage differentiation by metabolic reprogramming. *Oncotarget.* 7 (21), 30193–30210.
- Shabir, S., Girdlestone, J., Briggs, D., Kaul, B., Smith, H., Daga, S., Chand, S., Jham, S., Navarrete, C., Harper, L., Ball, S. & Borrow, R. (2015) Transitional B Lymphocytes Are Associated With Protection From Kidney Allograft Rejection: A Prospective Study. *American Journal of Transplantation.* n/a-n/a.
- Shan, J., Feng, L., Li, Y., Sun, G., Chen, X. & Chen, P. (2015) The effects of rapamycin on regulatory T cells: Its potential time-dependent role in inducing transplant tolerance. *Immunology Letters.* 162 (1), 74–86.
- Shen, B., Li, J. & Yang, B. (2013) NKG2D blockade significantly attenuates ischemia-reperfusion injury in a cardiac transplantation model. *Transplantation proceedings.* 45 (6), 2513–2516.

- Sheng, W., Yang, F., Zhou, Y., Yang, H., Low, P.Y., Kemeny, D.M., Tan, P., Moh, A., Kaplan, M.H., Zhang, Y. & Fu, X.Y. (2014) STAT5 programs a distinct subset of GM-CSF-producing T helper cells that is essential for autoimmune neuroinflammation. *Cell Research*. 24 (12), 1387–1402.
- Shimabukuro-Vornhagen, A., Hallek, M., Storb, R. & Bergwelt-Baildon, M. (2009) The role of B cells in the pathogenesis of graft-versus-host disease. *Blood*. 114 (24), 4919–4927.
- Shiu, K.Y., McLaughlin, L., Rebollo-Mesa, I., Zhao, J., Semik, V., Cook, H.T., Roufosse, C., Brookes, P., Bowers, R.W., Galliford, J., Taube, D., Lechler, R.I., Hernandez-Fuentes, M.P. & Dorling, A. (2015) B-lymphocytes support and regulate indirect T-cell alloreactivity in individual patients with chronic antibody-mediated rejection. *Kidney International*. 88 (3), 560–568.
- Shlomchik, W.D., Couzens, M.S., Tang, C.B., McNiff, J., Robert, M.E., Liu, J., Shlomchik, M.J., Emerson, S.G., Cells, A., Shlomchik, W.D., Couzens, M.S., Tang, B., McNiff, J., Robert, M.E., Liu, J., Shlomchik, M.J. & Emerson, S.G. (1999) Prevention of Graft Versus Host Disease by Inactivation of Host Antigen-Presenting Cells. *Science*. 285 (5426), 412–415.
- Shultz, L.D., Lyons, B.L., Burzenski, L.M., Gott, B., Chen, X., Chaleff, S., Kotb, M., Gillies, S.D., King, M., Mangada, J., Greiner, D.L. & Handgretinger, R. (2005) Human Lymphoid and Myeloid Cell Development in NOD/LtSz-scid IL2R null Mice Engrafted with Mobilized Human Hemopoietic Stem Cells. *The Journal of Immunology*. 174 (10), 6477–6489.
- Simonetta, F., Gestermann, N., Martinet, K.Z., Boniotto, M., Tissières, P., Seddon, B. & Bourgeois, C. (2012) Interleukin-7 influences FOXP3+CD4+ regulatory T cells peripheral homeostasis. *PLoS ONE*. 7 (5), 1–9.
- Singh, N.J. & Schwartz, R.H. (2006) The Lymphopenic Mouse in Immunology: From Patron to Pariah. *Immunity*. 25 (6), 851–855.

- Sivanathan, K.N., Gronthos, S., Rojas-Canales, D., Thierry, B. & Coates, P.T. (2014) Interferon-gamma modification of mesenchymal stem cells: implications of autologous and allogeneic mesenchymal stem cell therapy in allotransplantation. *Stem cell reviews*. 10 (3), 351–375.
- Sleater, M., Diamond, a. S. & Gill, R.G. (2007) Islet allograft rejection by contact-dependent CD8+ T cells: Perforin and FasL play alternate but obligatory roles. *American Journal of Transplantation*. 7 (8), 1927–1933.
- Smyth, L.A., Lechler, R.I. & Lombardi, G. (2017) Continuous Acquisition of MHC:Peptide Complexes by Recipient Cells Contributes to the Generation of Anti-Graft CD8+ T Cell Immunity. *American Journal of Transplantation*. 17 (1), 60–68.
- Socie, G. & Blazar, B.R. (2009) Review article Acute graft-versus-host disease : from the bench to the bedside. *Blood*. 114 (20), 4327–4336.
- Soeder, Y., Loss, M., Johnson, C.L., Hutchinson, J.A., Haarer, J., Ahrens, N., Offner, R., Deans, R.J., Van Bokkelen, G., Geissler, E.K., Schlitt, H.J. & Dahlke, M.H. (2015) First-in-Human Case Study: Multipotent Adult Progenitor Cells for Immunomodulation After Liver Transplantation. *Stem cells translational medicine*. 4, 1–6.
- Sohni, A. & Verfaillie, C.M. (2013) Mesenchymal Stem Cells Migration Homing and Tracking. *Stem cells international*. 2013 (130763).
- Sonntag, K., Eckert, F., Welker, C., Müller, H., Müller, F., Zips, D., Sipos, B., Klein, R., Blank, G., Feuchtinger, T., Schumm, M., Handgretinger, R. & Schilbach, K. (2015) Chronic graft-versus-host-disease in CD34⁺-humanized NSG mice is associated with human susceptibility HLA haplotypes for autoimmune disease. *Journal of Autoimmunity*. 62, 55–66.
- Spaggiari, G.M., Abdelrazik, H., Becchetti, F. & Moretta, L. (2009) MSCs inhibit monocyte-derived DC maturation and function by selectively interfering with the generation of immature DCs: Central role of MSC-derived prostaglandin E2. *Blood*. 113 (26), 6576–

- Spaggiari, G.M., Capobianco, A., Abdelrazik, H., Becchetti, F., Mingari, M.C. & Moretta, L. (2008) Mesenchymal stem cells inhibit natural killer cell proliferation, cytotoxicity, and cytokine production: role of indoleamine 2, 3-dioxygenase and prostaglandin E2. *Blood*. 111 (3), 1327–1333.
- Spaggiari, G.M., Capobianco, A., Becchetti, S., Mingari, M.C. & Moretta, L. (2006) Mesenchymal stem cell – natural killer cell interactions: evidence that activated NK cells are capable of killing MSCs, whereas MSCs can inhibit IL-2 – induced NK-cell proliferation. *Blood*. 107 (4), 1484–1490.
- Sudres, M., Norol, F., Trenado, A., Gregoire, S., Charlotte, F., Levacher, B., Lataillade, J.J., Bourin, P., Holy, X., Vernant, J.P., Klatzmann, D. & Cohen, J.L. (2006) Bone Marrow Mesenchymal Stem Cells Suppress Lymphocyte Proliferation In Vitro but Fail to Prevent Graft-versus-Host Disease in Mice. *The Journal of Immunology*. 176 (12), 7761–7767.
- Sullivan, J.A., Adams, A.B. & Burlingham, W.J. (2014) The emerging role of TH17 cells in organ transplantation. *Transplantation*. 97 (5), 483–489.
- Sung, A.D. & Chao, N.J. (2013) Concise Review: Acute Graft-Versus-Host Disease: Immunobiology, Prevention, and Treatment. *Stem Cells Transl Med*. 2 (1), 25–32.
- Tan, J., Wu, W., Xu, X., Liao, L., Zheng, F., Messinger, S., Sun, X., Chen, J., Yang, S., Cai, J., Gao, X., Pileggi, A. & Ricordi, C. (2012) Induction Therapy With Autologous Mesenchymal Stem Cells in Living-Related Kidney Transplants. *JAMA*. 307 (11), 1169–1177.
- Tan, N.S., Michalik, L., Noy, N., Yasmin, R., Pacot, C., Heim, M., Flühmann, B., Desvergne, B. & Wahli, W. (2001) Critical roles of PPAR β/δ in keratinocyte response to inflammation. *Genes and Development*. 15 (24), 3263–3277.
- Taylor, A.L., Negus, S.L., Negus, M., Bolton, E.M., Bradley, J.A. & Pettigrew, G.J. (2007) Pathways of helper CD4 T cell allorecognition in generating alloantibody and CD8 T cell

alloimmunity. *Transplantation*. 83 (7), 931–937.

Tchao, N.K. & Turka, L.A. (2012) Lymphodepletion and homeostatic proliferation: Implications for transplantation. *American Journal of Transplantation*. 12 (5), 1079–1090.

Tisato, V., Naresh, K., Girdlestone, J., Navarrete, C. & Dazzi, F. (2007) Mesenchymal stem cells of cord blood origin are effective at preventing but not treating graft-versus-host disease. *Leukemia*. 21 (9), 1992–1999.

Tobin, L.M., Healy, M.E., English, K. & Mahon, B.P. (2013) Human mesenchymal stem cells suppress donor CD4+ T cell proliferation and reduce pathology in a humanized mouse model of acute graft-versus-host disease. *Clinical and Experimental Immunology*. 172 (2), 333–348.

Tolar, J., Shaughnessy, M.J.O., Panoskaltsis-mortari, A., Mcelmurry, R.T., Bell, S., Riddle, M., Mcivor, R.S., Yant, S.R., Kay, M.A., Krause, D., Verfaillie, C.M. & Blazar, B.R. (2011) Host factors that impact the biodistribution and persistence of multipotent adult progenitor cells Host factors that impact the biodistribution and persistence of multipotent adult progenitor cells. *Blood*. 107 (10), 4182–4188.

Tomasoni, S., Longaretti, L., Rota, C., Morigi, M., Conti, S., Gotti, E., Capelli, C., Introna, M., Remuzzi, G. & Benigni, A. (2013) Transfer of Growth Factor Receptor mRNA Via Exosomes Unravels the Regenerative Effect of Mesenchymal Stem Cells. *Stem Cells and Development*. 22 (5), 772–780.

Tomblyn, M., Chiller, T., Einsele, H., Gress, R., Sepkowitz, K., Storek, J., Wingard, J.R., Young, J.H. & Boeckh, M.A.J.A. (2009) Guidelines for Preventing Infectious Complications among Hematopoietic Cell Transplant Recipients: A Global Perspective Recommendations. *Biology of blood and marrow transplantation*. 15 (10), 1143–1238.

Toubai, T., Mathewson, N., Oravec-Wilson, K. & Reddy, P. (2015) Host CD8 α +dendritic cells may be a key factor for separating graft-versus-host disease from graft-versus-

leukemia. *Biology of Blood and Marrow Transplantation*. 21 (4), 775–776.

Toubai, T., Mathewson, N.D., Magenau, J. & Reddy, P. (2016) Danger signals and graft-versus-host disease: Current understanding and future perspectives. *Frontiers in Immunology*. 7 (NOV), 1–15.

Toupet, K., Maumus, M., Luz-Crawford, P., Lombardo, E., Lopez-Belmonte, J., Van Lent, P., Garin, M.I., Van Den Berg, W., Dalemans, W., Jorgensen, C. & Noël, D. (2015) Survival and biodistribution of xenogenic adipose mesenchymal stem cells is not affected by the degree of inflammation in arthritis. *PLoS ONE*. 10 (1), 1–13.

Traitanon, O., Gorbachev, A., Bechtel, J.J., Keslar, K.S., Baldwin, W.M., Poggio, E.D. & Fairchild, R.L. (2014) IL-15 induces alloreactive CD28- Memory CD8 T cell proliferation and CTLA4-Ig resistant memory CD8 T cell activation. *American Journal of Transplantation*. 14 (6), 1277–1289.

Trpkov, K., Campbell, P., Pazderka, F., Cockfield, S., Solez, K. & Halloran, P.F. (1996) Pathologic features of acute renal allograft rejection associated with donor-specific antibody: analysis using the banff grading schema1. *Transplantation*. 61 (11), 1586–1592.

Vaes, B., Van't Hof, W., Deans, R. & Pinxteren, J. (2012) Application of MultiStem(®) Allogeneic Cells for Immunomodulatory Therapy: Clinical Progress and Pre-Clinical Challenges in Prophylaxis for Graft Versus Host Disease. *Frontiers in immunology*. 3 (November), 345.

Valdez-Ortiz, R., Bestard, O., Llaudó, I., Franquesa, M., Cerezo, G., Torras, J., Herrero-Fresneda, I., Correa-Rotter, R. & Grinyó, J.M. (2015) Induction of suppressive allogeneic regulatory T cells via rabbit antithymocyte polyclonal globulin during homeostatic proliferation in rat kidney transplantation. *Transplant international*. 28 (1), 108–119.

Vasandan, A.B., Jahnavi, S., Shashank, C., Prasad, P., Kumar, A. & Prasanna, S.J. (2016) Human Mesenchymal stem cells program macrophage plasticity by altering their

metabolic status via a PGE2-dependent mechanism. *Scientific Reports*. 6 (1), 38308.

Vignali, D., G rth, C.M., Pellegrini, S., Sordi, V., Sizzano, F., Piemonti, L. & Monti, P. (2016) IL-7 Mediated Homeostatic Expansion of Human CD4+CD25+FOXP3+ Regulatory T Cells After Depletion With Anti-CD25 Monoclonal Antibody. *Transplantation*. 100 (9), 1853–1861.

Vigo, T., Procaccini, C., Ferrara, G., Baranzini, S., Oksenberg, J.R., Matarese, G., Diaspro, A., Kerlero de Rosbo, N. & Uccelli, A. (2016) IFN- γ orchestrates mesenchymal stem cell plasticity through the signal transducer and activator of transcription 1 and 3 and mammalian target of rapamycin pathways. *Journal of Allergy and Clinical Immunology*. 139 (5), 1667–1676.

Walker, P.A., Bedi, S.S., Shah, S.K., Jimenez, F., Xue, H., Hamilton, J.A., Smith, P., Thomas, C.P., Mays, R.W., Pati, S. & Cox, C.S. (2012) Intravenous multipotent adult progenitor cell therapy after traumatic brain injury: modulation of the resident microglia population. *Journal of neuroinflammation*. 9 (1), 228.

Wang, D., Feng, X., Lu, L., Konkell, J.E., Zhang, H., Chen, Z., Li, X., Gao, X., Lu, L., Shi, S., Chen, W. & Sun, L. (2014) A CD8 T cell/indoleamine 2,3-dioxygenase axis is required for mesenchymal stem cell suppression of human systemic lupus erythematosus. *Arthritis and Rheumatology*. 66 (8), 2234–2245.

Wang, F., Eid, S., Cooke, K., Auletta, J. & Lee, Z. (2015a) Route of delivery influences biodistribution of human bone marrow-derived mesenchymal stromal cells following experimental bone marrow transplantation. *Journal of Stem Cells and Regenerative Medicine*. 11 (2), 34.

Wang, S., Guo, L., Ge, J., Yu, L., Cai, T., Tian, R., Jiang, Y., Zhao, R.C.H. & Wu, Y. (2015b) Excess Integrins Cause Lung Entrapment of Mesenchymal Stem Cells. *Stem Cells*. 33, 3315–3326.

Weber, M., Rudolph, B., Stein, P., Yogeve, N., Bosmann, M., Schild, H. & Radsak, M.P.

(2014) Host-Derived CD8+ Dendritic Cells Protect Against Acute Graft-versus-Host Disease after Experimental Allogeneic Bone Marrow Transplantation. *Biology of Blood and Marrow Transplantation*. 20 (11), 1696–1704.

Westin, J.R., Saliba, R.M., De Lima, M., Alousi, A., Hosing, C., Qazilbash, M.H., Khouri, I.F., Shpall, E.J., Anderlini, P., Rondon, G., Andersson, B.S., Champlin, R. & Couriel, D.R. (2011) Steroid-refractory acute GVHD: Predictors and outcomes. *Advances in Hematology*. 2011 (September 2002).

de Witte, S.F.H., Merino, A.M., Franquesa, M., Strini, T., van Zoggel, J.A.A., Korevaar, S.S., Luk, F., Gargsha, M., O'Flynn, L., Roy, D., Elliman, S.J., Newsome, P.N., Baan, C.C. & Hoogduijn, M.J. (2017) Cytokine treatment optimises the immunotherapeutic effects of umbilical cord-derived MSC for treatment of inflammatory liver disease. *Stem Cell Research & Therapy*. 8 (140).

Wong, Y.C., McCaughan, G.W., Bowen, D.G. & Bertolino, P. (2016) The CD8 T-cell response during tolerance induction in liver transplantation. *Clinical & Translational Immunology*. 5 (e102).

Wood, K.J. (2005) Is B Cell Tolerance Essential for Transplantation Tolerance? *Transplantation*. 79, S40–S42.

Wood, K.J., Bushell, A. & Hester, J. (2012) Regulatory immune cells in transplantation. *Nature reviews. Immunology*. 12 (6), 417–430.

Wood, K.J. & Goto, R. (2012) Mechanisms of rejection: current perspectives. *Transplantation*. 93 (1), 1–10.

Wu, Z., Bensinger, S.J., Zhang, J., Chen, C., Yuan, X., Huang, X., Markmann, J.F., Kassaei, A., Rosengard, B.R., Hancock, W.W., Sayegh, M.H. & Turka, L.A. (2004) Homeostatic proliferation is a barrier to transplantation tolerance. *Nature medicine*. 10 (1), 87–92.

Xia, C.Q., Chernatynskaya, A. V, Wasserfall, C.H., Wan, S., Looney, B.M., Eisenbeis, S., Williams, J., Clare-Salzler, M.J. & Atkinson, M.A. (2012) Anti-thymocyte globulin

- (ATG) differentially depletes naïve and memory T cells and permits memory-type regulatory T cells in nonobese diabetic mice. *BMC immunology*. 13, 70.
- Xie, Z., Hao, H., Tong, C., Cheng, Y., Liu, J., Pang, Y., Si, Y., Guo, Y., Zang, L., Mu, Y. & Han, W. (2016) Human umbilical cord-derived mesenchymal stem cells elicit macrophages into an anti-inflammatory phenotype to alleviate insulin resistance in type 2 diabetic rats. *Stem Cells*. 34 (3), 627–639.
- Xiong, H., Du, W., Sun, T.T., Lin, Y.W., Wang, J.L., Hong, J. & Fang, J.Y. (2014) A positive feedback loop between STAT3 and cyclooxygenase-2 gene may contribute to Helicobacter pylori-associated human gastric tumorigenesis. *International Journal of Cancer*. 134 (9), 2030–2040.
- al Yacoub, N., Romanowska, M., Krauss, S., Schweiger, S. & Foerster, J. (2008) PPAR δ Is a Type 1 IFN Target Gene and Inhibits Apoptosis in T Cells. *Journal of Investigative Dermatology*. 128 (8), 1940–1949.
- Yang, Z., Concannon, J., Ng, K.S., Seyb, K., Mortensen, L.J., Ranganath, S., Gu, F., Levy, O., Tong, Z., Martyn, K., Zhao, W., Lin, C.P., Glicksman, M.A. & Karp, J.M. (2016) Tetrandrine identified in a small molecule screen to activate mesenchymal stem cells for enhanced immunomodulation. *Scientific Reports*. 6 (1), 30263.
- Younas, M., Hue, S., Lacabartz, C., Guguin, A., Wiedemann, A., Surenaud, M., Beq, S., Croughs, T., Lelievre, J.D. & Levy, Y. (2013) IL-7 Modulates In Vitro and In Vivo Human Memory T Regulatory Cell Functions through the CD39/ATP Axis. *The Journal of Immunology*. 191 (6), 3161–3168.
- Zeiser, R., Socié, G. & Blazar, B.R. (2016) Pathogenesis of acute graft-versus-host disease: from intestinal microbiota alterations to donor T cell activation. *British Journal of Haematology*. 175 (2), 191–207.
- Zhang, B., Liu, R., Shi, D., Liu, X., Chen, Y., Dou, X., Zhu, X., Lu, C., Liang, W., Liao, L., Zenke, M. & Zhao, R.C.H. (2009) Mesenchymal stem cells induce mature dendritic cells

into a novel Jagged-2 dependent regulatory dendritic cell population. *Blood*. 113 (1), 46–57.

Zhang, F., Wang, C., Wang, H., Lu, M., Li, Y., Feng, H., Lin, J., Yuan, Z. & Wang, X. (2013) Ox-LDL promotes migration and adhesion of bone marrow-derived mesenchymal stem cells via regulation of MCP-1 expression. *Mediators of inflammation*. 2013, 691023.

Zhang, Y., Desai, A., Yang, S.Y., Bae, K.B., Antczak, M.I., Fink, S.P., Tiwari, S., Willis, J.E., Williams, N.S., Dawson, D.M., Wald, D., Chen, W.D., Wang, Z., Kasturi, L., Larusch, G.A., He, L., Cominelli, F., Di Martino, L., Djuric, Z., Milne, G.L., Chance, M., Sanabria, J., Dealwis, C., Mikkola, D., Naidoo, J., Wei, S., Tai, H.H., Gerson, S.L., Ready, J.M., Posner, B., Willson, J.K. V. & Markowitz, S.D. (2015) Inhibition of the prostaglandin-degrading enzyme 15-PGDH potentiates tissue regeneration. *Science*. 348 (6240), 1223-.

Zhang, Z.X., Wang, S., Huang, X., Min, W.P., Sun, H., Liu, W., Garcia, B. & Jevnikar, A.M. (2008) NK Cells Induce Apoptosis in Tubular Epithelial Cells and Contribute to Renal Ischemia-Reperfusion Injury. *The Journal of Immunology*. 181 (11), 7489–7498.

Zhao, Z.G., Xu, W., Sun, L., You, Y., Li, F., Li, Q.B. & Zou, P. (2012) Immunomodulatory Function of Regulatory Dendritic Cells Induced by Mesenchymal Stem Cells. *Immunological Investigations*. 41 (2), 183–198.

Zwang, N.A. & Turka, L.A. (2014) Homeostatic Expansion as a Barrier to Lymphocyte Depletion Strategies. *Current Opinion in Organ Transplantation*. 19 (4), 357–362.